



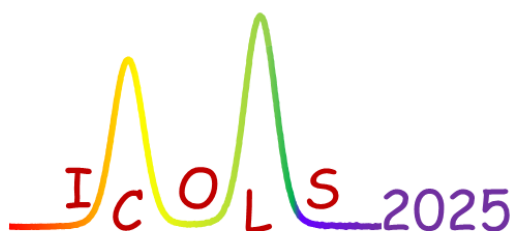
# ICOLS 2025

26<sup>th</sup> International Conference on Laser Spectroscopy



## Book of Abstracts

Edited by Stefania Gravina



# ICOLS 2025

26<sup>TH</sup> INTERNATIONAL CONFERENCE ON LASER SPECTROSCOPY

---

## Book of Abstracts

Updated on May 21, 2025

June 2–7, 2025

Elba Island, Tuscany, Italy

<https://www.icols2025.it>



# Contents

<a href="#">Program at a glance</a>	3
<a href="#">Partner Institutions and Sponsors</a>	4
<a href="#">Invited talks</a>	5
<a href="#">Hot topic talks</a>	35
<a href="#">Poster session 1</a>	45
<a href="#">Poster session 2</a>	106
<a href="#">Poster session 3</a>	166
<a href="#">Authors index</a>	215

# Program at a glance

	Monday 2 <sup>nd</sup>	Tuesday 3 <sup>rd</sup>	Wednesday 4 <sup>th</sup>	Thursday 5 <sup>th</sup>	Friday 6 <sup>th</sup>	Saturday 7 <sup>th</sup>
		Breakfast	Breakfast	Breakfast	Breakfast	Departure
08:30		Opening Session				
09:00		E. Cornell	J. Ye	W. Ketterle	D. Wineland	
09:30		D. DeMille	E. Peik	C. Koch	A. Safavi-Naini	
10:00		T. Mehlstäubler	K. Elkema	S. Will	A.M. Rey	
10:30		Coffee break	Coffee break	Coffee break	Coffee break	
11:00		H. Müller	J. Hangst	S. Cornish	S. Nascimbene	
11:30		M.-S. Zhan	K. Yoshioka	L. Cheuk	Y. Xingcan	
12:00		M. Arndt	F. Merkt	F. Martin	G. Roati	
12:30						
13:00	Arrival	Lunch	Lunch	Lunch	Lunch	
13:30						
14:00						
14:30		Poster Session 1	Poster Session 2	Excursion (Optional)	Poster Session 3	Firenze Lab Visit (Optional)
15:00						
15:30		Coffee break	Coffee break		Coffee break	
16:00	Registration	N. Picqué	P. Senellart-Mardon		B. Zhao	
16:30		D. Lisak	S. Franke-Arnold		L. Gacciapuoti K. van Druen L. Holberg	
17:00		D. Aude Craik E. Bohr N. Bouloufa-Maafa	U. Rapol C. Politi S. Wright		Closing Session	
17:30	Welcome Reception					
18:00						
18:30						
19:00	Dinner	Dinner	Dinner	Social Dinner	Dinner	
19:30						
20:00						

# Partner Institutions and Sponsors

---



UNIVERSITÀ  
DEGLI STUDI  
FIRENZE

Dipartimento  
di Fisica e  
Astronomia



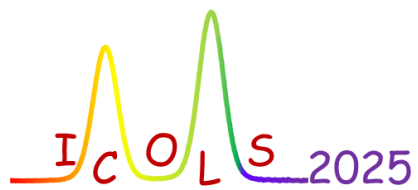
Gold sponsor:



Silver sponsors:



*Invited talks*  
*Abstracts*



Abstract number: I1  
Tuesday 09:00-09:30

## Bose-Einstein Condensation: Exactly as I planned and not at all as I thought

Cornell E.<sup>†</sup>

*JILA and University of Colorado, USA*

<sup>†</sup>cornell@jila.colorado.edu

This talk will not be a comprehensive survey of 30 years of Bose-Einstein Condensation, but instead a personal reflection on BEC: some aspects which turned out much as I expected, others which exceeded all my expectations, and a single aspect which has been something of a disappointment. I will conclude this loosely organized presentation with a few observations on precision metrology and particle physics.

Abstract number: I2  
 Tuesday 09:30-10:00

## Searches for new CP-violating physics using cold and ultracold molecules

**DeMille D.**<sup>†1,2,3</sup>

<sup>1</sup>Johns Hopkins University, Baltimore, MD, USA

<sup>2</sup>Argonne National Laboratory, Lemont, IL, USA

<sup>3</sup>University of Chicago, Chicago, IL, USA

<sup>†</sup>david.demille@jhu.edu

From cosmological observations of the asymmetry between matter and antimatter, it is known that new physics that violates CP symmetry must appear at some high energy scale. In many theories of physics beyond the Standard Model that account for this fact, the new physics leads to electric dipole moments (EDMs) or related asymmetric charge distributions along the spins of quantized particles such as electrons, protons, and nuclei. These EDMs arise from virtual excitations of new quantum fields that carry CP-violating interactions, much like the electron's anomalous magnetic moment arises from virtual excitations of the electromagnetic field.

The CP violation in the Standard Model gives rise to nonzero but extremely small EDMs, some 6 orders of magnitude smaller than current experimental sensitivities. By contrast, in typical extensions to the Standard Model, EDMs can be much larger even if the mass of particles associated with the new quantum fields is extremely large. Recent EDM experiments already probe mass scales well above TeV range in many models, significantly beyond the direct reach of the Large Hadron Collider. Because the observed value of the Higgs boson mass is naturally associated with new physics in the 1-1000 TeV range, probing such high mass scales is at the forefront of modern particle physics.

This talk will describe three ongoing experiments aiming to detect EDMs with unprecedented sensitivity. All are based on the  $\sim 10^4$ -fold enhancement of energy shifts due to EDMs in polar molecules, relative to atoms. First, we will provide an update on the ongoing third generation of the ACME experiment,<sup>1</sup> which aims to detect the electron's EDM (eEDM) using metastable ThO molecules. The ACME III apparatus is fully assembled and operating routinely, with statistical uncertainty sufficient to surpass the current best limit on the eEDM by an order of magnitude. We will describe ongoing work to uncover and quantify possible systematic errors in ACME III. Next, we will discuss the CeNTREX experiment, which aims to detect the proton EDM (pEDM) using ground-state TlF molecules.<sup>2</sup> Like ACME, CeNTREX uses a high flux of molecules in a cryogenic beam to achieve good statistics. We will describe the status of CeNTREX, which is nearing the end of its construction phase.

Finally, we will discuss a new, long-term effort to search for the EDM-like nuclear Schiff moment, with potentially orders of magnitude higher sensitivity than current experiments. Here, we aim to employ two major new features. First, we will use octupole-deformed nuclei that enhance the Schiff moment by  $\sim 10^3$ -fold relative to ordinary spherical nuclei. Second, we will embed these nuclei in ultracold polar molecules, where much longer spin coherence times (and hence better energy resolution) is possible relative to beam experiments. In particular, we aim to measure the Schiff moment of  $^{223}\text{Fr}$  nuclei, in ultracold FrAg molecules, which have been calculated to have near-ideal sensitivity to the nuclear Schiff moment.<sup>3</sup> Both Fr and Ag atoms have been laser cooled, and calculations indicate that ultracold FrAg molecules should be amenable to assembly using the same methods used to produce quantum gases of bi-alkali molecules.<sup>4</sup> We will describe progress towards this goal.

<sup>1</sup>ACME Collaboration, *Nature* **562**, 355 (2018).

<sup>2</sup>O. Grasdjik *et al.*, *Quant. Sci. Technol.* **6**, 044007 (2021).

<sup>3</sup>A. Marc, M. Hubert, and T. Fleig, *Phys. Rev. A* **108**, 062815 (2023).

<sup>4</sup>J. Klos, H. Li, E. Tiesinga, and S. Kotochigova, *New J. Phys.* **24** 025005 (2022).

Abstract number: I3  
 Tuesday 10:00-10:30

## Precision Spectroscopy in Ion Coulomb Crystals and Search for New Physics

Mehlstäubler T. E.<sup>†1,2</sup>, Yeh C.-H.<sup>1</sup>, Dreissen L.<sup>1</sup>, Fürst H.<sup>2</sup>, Keller J.<sup>1</sup>, Hausser N.<sup>1</sup>

<sup>1</sup>Physikalisch-Technische Bundesanstalt, Bundesallee 100, Braunschweig, Germany

<sup>2</sup>Leipniz University of Hannover, Welfengarten 1, Hannover, Germany

<sup>†</sup>tanja.mehlstaebler@ptb.de

Trapped and laser-cooled ions allow for a high degree of control of atomic quantum systems. They are the basis for modern atomic clocks, quantum computers and quantum simulators. In our research we use ion Coulomb crystals, i.e. many-body systems with complex dynamics, for precision spectroscopy. This paves the way to novel optical ion frequency standards with ultra-high stability and accuracy for applications such as relativistic geodesy and quantum simulators in which complex dynamics become accessible with atomic resolution.

On the other hand, the high precision obtained in the spectroscopy of trapped cold ions enables sensitive tests of the Standard Model and the search for new physics. The long-lived F-state of the  $\text{Yb}^+$ -ion has a high sensitivity to both relativistic and nuclear effects. We use isotope-shift spectroscopy as a sensitive probe for nuclear structure and fifth forces mediated by a new boson that couples to electrons and neutrons<sup>1</sup>. Deviations from a linear relation in the King-plot analysis can indicate new physics or higher-order SM effects. This powerful technique revealed large King-plot nonlinearities in  $\text{Yb}$ <sup>2</sup>. We present two-orders-of-magnitude improved spectroscopic measurements in all five stable spinless isotopes of this element. The transition frequency of the forbidden  $^2\text{S}_{1/2}$  to  $^2\text{D}_{5/2}$  and  $^2\text{S}_{1/2}$  to  $^2\text{F}_{7/2}$  transitions are determined with an accuracy of 6 and 16 Hz, respectively, yielding isotope shifts with a relative precision as low as  $10^{-9}$ . We combine these spectroscopic results with new mass measurements with a relative precision of a few  $10^{-12}$ . With this, we can extract a new bound on the mass and coupling strength of the potential new bosons. The results are also used to investigate higher-order nuclear structure effects along a chain of Yb isotopes. In combination with ab initio nuclear structure calculations, this provides a window to nuclear deformation and nuclear charge distributions along isotopic chains towards exotic, neutron-rich nuclei.

<sup>1</sup>J. C. Berengut *et al.*, 413 *Phys. Rev. Lett.* **120**, 091801 (2018)

<sup>2</sup>J. Hur *et al.*, *Phys. Rev. Lett.* **128**, 163201 (2022)

Abstract number: I4  
Tuesday 11:00-11:30

## Cavity-based, lattice-hold atom interferometry as a new tool for precision measurement and inertial sensing.

**Müller H.**<sup>1, †</sup>, **Egelhoff, J.**<sup>1</sup>, **Louie, G.**<sup>1</sup>, **Tao, M.**<sup>1</sup>

<sup>1</sup>*University of California, Berkeley, California, USA*

<sup>†</sup>hm@berkeley.edu

Atom interferometers are powerful tools for investigating Earth's gravity,<sup>1</sup> the gravity gradient,<sup>2</sup> rotations<sup>3</sup> and fundamental constants<sup>4</sup>. In all the above examples, they use atoms in free fall in atomic fountains. However, this limits the time that the quantum state can interact with the quantity to be measured to less than 3 seconds even in 10-m tall atomic fountains. Even in microgravity, thermal expansion of the atom cloud severely limits interaction times. Even a cesium atom (which is heavy and thus has a low average thermal velocity at a given temperature) at 200 nK moves at about 3.5 mm/s. Consequently, it remains within the area of a 1-cm laser beam for no longer than about 3 seconds, on average. Alternate approaches to circumvent these limitations have been explored in the form of trapping atoms in optical lattices.

Atom interferometers suspended in an optical lattice<sup>5</sup> have observed coherent quantum spatial superposition states for a few seconds. Recently, it has been shown that the mode of a Fabry–Perot cavity strongly reduces optical lattice imperfections, and has led to the demonstration of interaction times on the one-minute scale<sup>6</sup> as well as robustness against environmental influences such as tilt, linear vibrations, and magnetic fields<sup>7</sup>. As a result, there are now broad efforts to develop them into compact, versatile quantum sensors for applications in the field, but also for applications in fundamental physics, such as testing whether the gravitational field can be in a superposition of states<sup>8</sup>.

<sup>1</sup>A. Peters *et al.*, Nature **400**, 849–52 (1999); T. Zhang *et al.* Phys. Rev. Applied **20**, 014067 (2023)

<sup>2</sup>M. Snadden *et al.*, Phys. Rev. Lett. **81**, 971–74 (1998)

<sup>3</sup>I. Dutta *et al.*, Phys. Rev. Lett. **116**, 183003 (2016)

<sup>4</sup>G. F. Rosi *et al.*, Nature **510**, 518–21 (2014); R. Parker *et al.*, Science **360**, 191–95 (2018); L. Morel *et al.*, Nature **588**, 61–65 (2020)

<sup>5</sup>P. Cladé *et al.*, EPL **71**, 730 (2005), R. Charriere *et al.*, Phys. Rev. A **85**, 013639 (2005); A. Hilico *et al.*, Phys. Rev. A **91**, (2015); X. Zhang *et al.*, Phys. Rev. A **94**, 043608 (2016)

<sup>6</sup>V. Xu *et al.*, Science **366**, 745–49 (2019); C. D. Panda *et al.*, Nature **631**, 515–520 (2024); C. D. Panda *et al.*, Nature Physics **20**, 1234–39 (2024)

<sup>7</sup>C. D. Panda *et al.*, Appl. Phys. Lett. **123**, 064001 (2023)

<sup>8</sup>D. Carney *et al.*, PRX Quantum **2**, 3, 030330 (2021)



Abstract number: I5  
Tuesday 11:30-12:00

## Cold atom interferometry in space

Zhan M.-S.<sup>1,2,3 †</sup>

<sup>1</sup>Wuhan Institute of Physics and Mathematics, Innovation Academy for Precision Measurement Science and Technology, Chinese Academy of Sciences, Wuhan 430071, China

<sup>2</sup>Wuhan Institute of Quantum Technology, Wuhan 430206, China

<sup>3</sup>Hefei National Laboratory, Hefei 230088, China

†mszhan@apm.ac.cn

Atom interferometry has been expected to exhibit unique advantages in space due to the microgravity and ultra-low-noise environment, enabling breakthroughs in precision and sensitivity. These advantages position space-based cold atom interferometers as transformative tools for quantum sensing, navigation, and frontier physics. Explicitly, the key benefits from space include longer interrogation time (microgravity allows atoms to free-fall continuously in a few seconds to tens of seconds, increasing the interferometer's baseline and boosting sensitivity by orders of magnitude), suppressed environmental noise (isolation from ground vibrations, thermal fluctuations, and electromagnetic interference), enhanced sensitivity for fundamental physics (tests of general relativity (e.g., frame-dragging, equivalence principle) achieve unprecedented precision) and for applications in planetary exploration and deep space navigation. However, due to complexity of the technology and the high time and capital cost, experiments of space atomic interference have only started recently.

At the end of 2022, we successfully developed the dual-species  $^{85}\text{Rb}$  -  $^{87}\text{Rb}$  cold atom interferometer and loaded it on the microgravity cabinet of the Tianhe core module of the Chinese Space Station (CSS) with the Tianzhou-5 cargo spacecraft. Microgravity atomic interference experiments have been conducted for more than two years. The two-component atomic interferometer was realized successively, by which the space cold atom gyro and acceleration sensing were performed, and the preliminary experiment of the equivalence principle test was carried out.

One example is the realization of a cold atom gyroscope<sup>1</sup> (as shown in Fig.1), which was demonstrated by the atom interferometer installed in CSS as a payload. By compensating for the CSS's high dynamic rotation rate using a built-in piezoelectric mirror, spatial interference fringes in the interferometer were successfully obtained. Then, the optimized ratio of the Raman laser's angles was derived, the coefficients of the piezoelectric mirror are self-calibrated in orbit, and various systemic effects were corrected. A rotation measurement resolution of  $50 \mu\text{rad/s}$  for a single shot and  $17 \mu\text{rad/s}$  for an average number of 32 was achieved. The measured rotation is  $-1142 \pm 29 \mu\text{rad/s}$  and is compatible with that recorded by the classical gyroscope of the CSS.

The successful application of cold atom interferometers in space inertial sensing marks the transition of quantum technologies from labs to engineering. Future integration with quantum entanglement and miniaturized designs will further push the boundaries of deep-space exploration and fundamental physics.

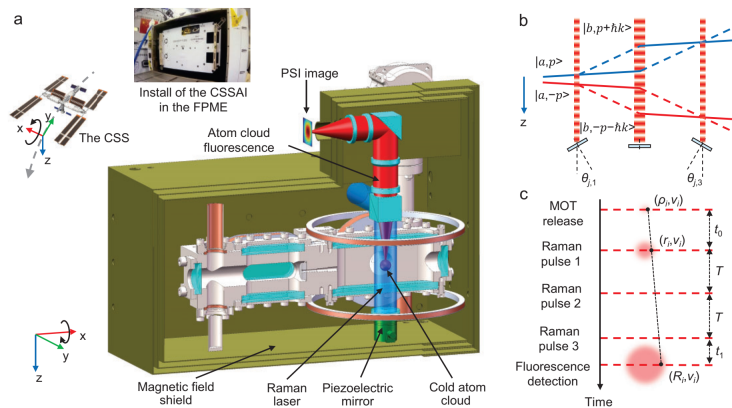


Figure 1: (from Fig.1 in Ref.[1]) The working principle of the China Space Station Atom Interferometer (CSSAI). (a) The installed CSSAI in the Free-floating Platform for Microgravity Experiment (FPME), and the CSSAI's physical system profile. The Raman laser for the point source interferometry (PSI) and the imaging of the fluorescence of the cold atom cloud are also illustrated in the physical system. (b) The double single diffraction Raman transition and Raman interference loop scheme for the  $^{85}\text{Rb}$  atom. (c) Atom position changes over time during the interference experiment.

<sup>1</sup>J.T. Li, X. Chen, D.F. Zhang, W.Z. Wang, Y. Zhou, M. He, J. Fang, L. Zhou, C. He, J.J. Jiang, H.Y. Sun, Q.F. Chen, L. Qin, X. Li, Y.B. Wang, X.W. Zhang, J.Q. Zhong, R.B. Li, M.Z. An, L. Zhang, S.Q. Wang, Z.F. Li, J. Wang, and M.S. Zhan, *Nat. Sci. Rev.* **12**, nwaf012(2025).

**Abstract number: I6****Tuesday 12:00-12:30**

## From Schrödinger kittens to UV spectroscopy

**Arndt M.**<sup>†</sup>*University of Vienna, Boltzmannngasse 5 A-1090 Vienna, Austria*<sup>†</sup>markus.arndt@univie.ac.at

When Erwin Schrödinger introduced his famous thought experiment of a cat being both dead and alive, he identified entanglement as a crucial ingredient.

However, entanglement is not a strict requirement for creating massive quantum superpositions of distinct states, even in warm, organic, or inorganic systems.

Over the years, our group in Vienna has developed a range of experiments that demonstrate the quantum delocalization of massive objects over distances hundreds of times their own diameter.

These objects range from carbonaceous molecules to polypeptides, tailored macromolecules to clusters of molecules — which may be well described as Schrödinger kittens.

I will review our recent efforts and advances in scaling up from “kittens” to more massive biological and metallic nanoparticles and discuss how such experiments both require and contribute to UV spectroscopy.

**Abstract number: I7**  
**Tuesday 16:00-16:30**

## Frequency comb interferometry

**Piqué N.**<sup>†1</sup>

*Humboldt University, Berlin, DE*

<sup>†</sup>Nathalie.Picque@mbi-berlin.de

Not available at time of printing.

Abstract number: I8  
Tuesday 16:30-17:00

## High-accuracy molecular spectroscopy exploiting resonant frequencies of an optical cavity

Lisak D.<sup>†</sup>

Institute of Physics, Faculty of Physics, Astronomy and Informatics, Nicolaus Copernicus University in Toruń,  
Grudziądzka 5, 87-100 Toruń, Poland

<sup>†</sup>dlsak@umk.pl

Laser spectroscopy applications for quantitatively detecting gas amount and composition are based on accurate measurements of reference line intensities and collisional line shapes. Exceptionally high accuracies of such data are required in atmospheric research focused on greenhouse gases where line intensities must be known at permille-level uncertainties. Similar or even lower uncertainties are needed for the realization of optical gas amount, concentration, and temperature standards, which, after the recent SI redefinition, allows greater flexibility in linking fundamental constants to measurable quantities.

We demonstrate low-uncertainty line intensities and line shapes of carbon monoxide<sup>1,2,3,4</sup> and hydrogen molecules<sup>3</sup> obtained through a combination of cavity-enhanced absorption and dispersion spectroscopies, interlaboratory comparison of independent measurements, and *ab initio* calculations. We also show that per mille uncertainties of line intensity for hydrogen molecules<sup>4</sup> require an advanced collisional line shape model<sup>5</sup> that goes beyond the standard description used in spectroscopic databases. Our experimental data were obtained using cavity mode-dispersion spectroscopy (CMDS)<sup>6</sup> and recently developed heterodyne cavity ring-down spectroscopy (HCRDS)<sup>3</sup> that exploit optical cavity resonant frequencies and enable high-resolution gas absorption and dispersion measurement with spectra fully linked to the primary frequency standard.

We also present the first primary spectroscopic thermometry leveraging optical cavity resonance frequencies and *ab initio* molecular line intensities<sup>7</sup>. Using CO rovibrational transitions, our frequency-based approach, achieving temperature uncertainty of 82 parts per million, is much more accurate than any reported spectroscopic thermometry at pressures above 1 kPa and applies to a tenfold broader pressure range. In particular, it enables fully optical, molecule-selective primary amount-of-substance measurements without contact sensors, achieving sub-permille uncertainty in gas concentration and pressure.

The research was supported by the state budget of Poland, allocated by the Minister of Education and Science under the "Polska Metrologia II" program, project no. PM-II/SP/0011/2024/02 and the European Partnership on Metrology project "22IEM03 PriSpecTemp".

<sup>1</sup>K. Bielska, *et al.*, *Phys. Rev. Lett.* **129**, 043002 (2022).

<sup>2</sup>A. A. Balashov, *et al.*, *J. Chem. Phys.* **158**, 234306 (2023).

<sup>3</sup>J. T. Hodges, *et al.*, *Metrologia* **62**, 08006 (2025).

<sup>4</sup>A. Cygan *et al.*, *Sci. Adv.* **11**, eadp8556 (2025).

<sup>5</sup>R. Ciuryło, *et al.*, *Phys. Rev. A* **65**, 012502 (2002).

<sup>6</sup>A. Cygan *et al.*, *Opt. Express* **23**, 14472 (2015).

<sup>7</sup>D. Lisak *et al.*, arXiv:2502.17660 [physics.optics] (2025).

Abstract number: I9  
Wednesday 09:00-09:30

## Scaling quantum systems for clock and fundamental physics

Ye J.<sup>†</sup>

*JILA, National Institute of Standards and Technology and University of Colorado Boulder, Colorado 80309-0440, USA*

<sup>†</sup>Ye@jila.colorado.edu

Scaling up quantum systems to increasingly large sizes promises to advance the performance of atomic clocks and bring opportunities for new discovery. Quantum technology has brought minute-long optical coherence to tens of thousands of atoms, enabling unprecedented measurement precision. The combination of stable laser, ultrafast optics, and precision metrology has provided new tools for nuclear physics, leading to quantum-state-resolved laser spectroscopy of thorium-229 nuclear transition. The permeation of quantum metrology to all corners of physics sparks new ideas for testing fundamental laws of nature and searching for new physics.

**Abstract number: I10**  
**Wednesday 09:30-10:00**

## Nuclear laser spectroscopy of the 8.4 eV transition in Th-229

**Peik E.**<sup>†</sup>

*Physikalisch-Technische Bundesanstalt, 38116 Braunschweig, Germany*

<sup>†</sup>ekkehard.peik@ptb.de

Recently, three experiments have obtained resonant laser excitation of a low-energy nuclear transition, from the ground state of Th-229 to its isomeric state at 8.4 eV, connected by a magnetic dipole transition with a natural linewidth in the range of 0.1 mHz. Table-top laser sources at a wavelength of 148 nm in the vacuum-ultraviolet have been used for the excitation<sup>1</sup>. The thorium nuclei have been prepared as dopant ions in VUV-transparent crystals like calcium fluoride. This opens a new field for experiments that connect nuclear physics with atomic physics, where a nuclear transition occurs in the energy range that is typical for transitions of atomic valence electrons. Among several possible applications, the development of an optical nuclear clock seems particularly attractive<sup>2</sup>. This clock would offer high accuracy, especially with laser cooled trapped Th-229 ions, high stability, because of the high number of nuclei that can be interrogated in Th-229-doped solids, and high sensitivity in clock-based tests of fundamental principles of physics, involving the strong interaction in addition to electromagnetism.

A range of activities on nuclear laser spectroscopy and towards such a clock is ongoing. I will present results of experiments at PTB using a laser system based on four-wave mixing in xenon and Th-229-doped calcium fluoride crystals grown at Technische Universität Wien, where we have recently observed a thermally activated laser-induced quenching, i.e. a shortening of the isomer lifetime under nonresonant laser radiation<sup>3</sup>. In an experiment with laser cooled <sup>229</sup>Th<sup>3+</sup> recoil ions from the  $\alpha$ -decay of U-233 we have studied the hyperfine structure to obtain information on nuclear properties like the magnetic moment and the charge distribution<sup>4</sup>.

<sup>1</sup>J. Tiedau *et al.*, *Phys. Rev. Lett.* **132**, 182501 (2024).

<sup>2</sup>K. Beeks, T. Sikorsky, T. Schumm, J. Thielking, M. V. Okhapkin, E. Peik, *Nature Reviews Phys.* **3**, 238 (2021).

<sup>3</sup>F. Schaden *et al.*, *arXiv:2412.12339* (2024).

<sup>4</sup>G. Zitzer, J. Tiedau, Ch. E. Düllmann, M. V. Okhapkin, E. Peik, *arXiv:2504.00974* (2025).

Abstract number: I11  
 Wednesday 10:00-10:30

## Alpha and helion particle charge radius difference determination with quantum-degenerate helium

Steinebach K.<sup>1</sup>, Van der Werf Y.<sup>1,2</sup>, Jannin R.<sup>1,3</sup>, Bethlem H. L.<sup>1</sup>, Eikema K.S.E.<sup>†1</sup>

<sup>1</sup>Vrije Universiteit Amsterdam, Netherlands

<sup>2</sup>Present address: Eindhoven University of Technology, Netherlands

<sup>3</sup>Present address: Laboratoire de Physique des Gaz et Plasmas, Université Paris Saclay, France

<sup>†</sup>k.s.e.eikema@vu.nl

Precision spectroscopy of atoms and molecules is widely used for tests of the Standard Model and determinations of fundamental constants. Nuclear charge and magnetic radii also play a vital part in the comparison between theory and experiment and can be measured by spectroscopy as well. Both neutral helium<sup>1</sup> and singly-ionized helium<sup>2</sup> spectroscopy are an interesting target for such an enterprise. In this presentation we mainly focus on precision spectroscopy of neutral <sup>3</sup>He and <sup>4</sup>He. In both isotopes we measure the doubly-forbidden  $2^3S_1 - 2^1S_0$  transition at 1557 nm with single-photon excitation. The isotope shift derived from this measurement enables an accurate determination of the nuclear charge radius difference.

We cool the helium atoms to quantum degeneracy to minimize the Doppler effect and confine them in an optical dipole trap at the magic wavelength of 320 nm. The resulting ultra-cold Fermi gas (<sup>3</sup>He) and Bose-Einstein condensate (<sup>4</sup>He) show widely different quantum behavior and spectroscopy<sup>3</sup>. In 2018 we reached<sup>4</sup> an accuracy of 200 Hz for the  $2^3S_1 - 2^1S_0$  transition in <sup>4</sup>He, and recently we improved the same determination<sup>1</sup> in <sup>3</sup>He to 170 Hz. Based on the resulting isotope shift, and theoretical calculations, we initially determined a charge radius difference  $\delta r^2 = r_h^2 - r_\alpha^2 = 1.0757(12)_{\text{exp}}(9)_{\text{theo}}$  fm<sup>2</sup> between the helion and alpha particle<sup>1</sup>. Interestingly, an evaluation by the CREMA collaboration of the same charge radius difference from muonic helium ion measurements<sup>5</sup> led to a value that deviates 3.6 combined sigma from ours. New theory evaluations of the hyperfine structure of <sup>3</sup>He by Qi et al.<sup>6</sup> and a full second-order calculation by Pachucki et al.<sup>7</sup> in 2024 has shown unexpectedly large contributions from higher-order effects that require a correction of the theoretical isotope shift (for point-like nuclei) by -1.77kHz. This leads to an updated  $\delta r^2$  (based on our isotope measurement) of  $1.0678(12)_{\text{exp}}(7)_{\text{theo}}$  fm<sup>2</sup>, which now agrees with that of the CREMA collaboration within 1.2 combined sigma<sup>1,5,7</sup>. These measurements serve as an interesting test of a wide range of physics, and it presents a benchmark for nuclear structure calculations.

We recently completed new spectroscopic measurements for <sup>4</sup>He on the  $2^3S_1 - 2^1S_0$  transition to improve the accuracy of the experimental isotope shift further, and therefore the accuracy of  $\delta r^2$ . We investigated and improved many aspects, such as the influence of magnetic fields, motion of the BEC in the dipole trap observed through time-resolved detection, the laser linewidth, BEC mean-field interaction, and the spectroscopy laser Stark shift. Preliminary evaluations indicate we can expect a <sup>4</sup>He transition frequency accuracy of a few parts in 10<sup>13</sup>. These aspects and the implications for improving  $\delta r^2$  will be presented.

<sup>1</sup>Y. van der Werf, K. Steinebach, R. Jannin, H.L. Bethlem, K.S.E. Eikema., arXiv:2306.02333, accepted 2025 for publication in Science

<sup>2</sup>E.L. Gründeman *et al.*, *Comm. Phys.* **7**, 414 (2024)

<sup>3</sup>R. Jannin, Y. van der Werf, K. Steinebach, H.L. Bethlem, K.S.E. Eikema, *Nat. Comm.* **13**, 6479 (2022)

<sup>4</sup>R.J. Rengelink *et al.*, *Nat. Phys.* **14**, 1132-1137 (2018)

<sup>5</sup>K. Schuhmann *et al.*, arXiv:2305.11679, accepted 2025 for publication in Science

<sup>6</sup>X-Q Qi et al., arXiv 2409.09279v1 (2024)

<sup>7</sup>K. Pachucki, V. Patkós, V.A. Yerokhin, *Phys. Rev. A* **110**, 062806 (2024)

Abstract number: I12  
 Wednesday 11:00-11:30

## Spectroscopy of Antihydrogen: The ALPHA experiment at CERN

Hangst J. S.<sup>†</sup>

*Department of Physics and Astronomy, Aarhus University, Denmark*

<sup>†</sup>jeffrey.hangst@cern.ch

The ALPHA experiment at CERN is unique in its demonstrated ability to study the internal structure of antihydrogen – the antimatter equivalent of the simplest atom. Such studies are motivated by the apparent absence of antimatter in the observable universe, and they probe the fundamental symmetries that underlie current theory. For example, the Standard Model requires that hydrogen and antihydrogen have the same spectrum. The possibility of applying the *precision* measurement and manipulation techniques of atomic physics to an antimatter atom makes antihydrogen a very compelling testbed for symmetries such as CPT and the Weak Equivalence Principle of General Relativity. To study antihydrogen, it must first be created, trapped, and then held for long enough to make a measurement – typically using very few anti-atoms. I will discuss the latest developments in antihydrogen physics, including the state-of-the art of spectroscopic studies using the ALPHA-2 machine. In ALPHA-2, we have studied several laser and microwave driven transitions and demonstrated laser cooling of trapped antihydrogen<sup>1</sup>. Very recently, we have shown that it is possible to accumulate more than  $10^4$  anti-atoms in a single day. I will illustrate the techniques necessary to achieve these many milestones and consider the future of antihydrogen studies, including gravitational measurements using antimatter<sup>2</sup>.

<sup>1</sup>Laser cooling of antihydrogen atoms (ALPHA Collaboration) *Nature* **592**, 35–42 (2021).

<sup>2</sup>Observation of the effect of gravity on the motion of antimatter (ALPHA Collaboration) *Nature* **621**, 716–722 (2023).



Abstract number: I13  
 Wednesday 11:30-12:00

## Laser cooling of positronium with a chirped laser pulse train

**Yoshioka K.**<sup>†1</sup>

<sup>1</sup>*The University of Tokyo, Japan*

<sup>†</sup>yoshioka@fs.t.u-tokyo.ac.jp

Positronium is a bound pair of an electron and its antiparticle, a positron. It is the simplest atom, consisting of only two elementary particles, and provides an important physical system for the rigorous verification of quantum electrodynamics. The stringent test of quantum electrodynamics may provide an important foundation for the recent trend of research that explores physics beyond the Standard Model through precision spectroscopy of atoms and molecules. It may also be useful in investigations of matter-antimatter asymmetry and investigations of gravity acting on antimatter. A typical experimental measurement is for the 1S-2S transition frequency<sup>1</sup> with a natural width of 1.26 MHz.

Uncertainties regarding the 1S-2S transition frequency of positronium are approximately five times worse experimentally than theoretically at this time. The fundamental causes of the difficulty in improving the experimental uncertainties are the large velocity due to the lightweight nature of positronium, the lack of statistics due to the insufficient number of atoms, and the short self-decay lifetime. Therefore, the realization of rapid cooling of positronium is essentially critical in precision spectroscopy. Heat exchange with low-temperature materials is inefficient, and the realization of laser cooling has been long awaited since the theoretical study in 1988<sup>2</sup>.

Laser cooling of positronium using the 1S-2P transition at a wavelength of 243 nm produces very large recoil velocities in a single cooling cycle, but the recoil-derived Doppler shift is on the order of several GHz. A special ultraviolet pulsed light source capable of maintaining the cooling cycle and accommodating a wide range of velocity distributions was needed. In this talk, we will present details of our demonstration of one-dimensional laser cooling of positronium<sup>3</sup>. The cooling is based on a pulse train that rapidly changes the central optical frequency during the lifetime of the positronium<sup>45</sup>: a portion of the dilute positronium gas at 600 K was cooled to approximately 1 K in 100 ns. This result marks the first laser cooling of positronium. It was demonstrated at the same time that the AEGIS collaboration<sup>6</sup>, which aims for highly efficient production of antihydrogen, performed positronium cooling with a broadband pulsed laser pulse. We will also discuss our ongoing extension to three-dimensional laser cooling and absolute measurement of 1S-2S transition frequency for slow positronium. We are also investigating highly efficient cooling using stimulated emission, which will also be the subject of this talk.

<sup>1</sup>M. S. Fee *et al.*, *Phys. Rev. Lett.* **70**, 1397 (1993).

<sup>2</sup>E. P. Liang and C. D. Dermer, *Opt. Commun.* **65**, 419 (1988).

<sup>3</sup>K. Shu *et al.*, *Nature* **633**, 793 (2024).

<sup>4</sup>K. Yamada *et al.*, *Phys. Rev. Appl.* **16**, 014009 (2021).

<sup>5</sup>K. Shu, N. Miyamoto, Y. Motohashi, R. Uozumi, Y. Tajima, and K. Yoshioka, *Phys. Rev. A* **109**, 043520 (2024).

<sup>6</sup>L. T. Glöggler *et al.*, *Phys. Rev. Lett.* **132**, 083402 (2024).

Abstract number: I14  
Wednesday 12:00-12:30

## Precision spectroscopy of few-body atoms and molecules

Clausen G.<sup>1</sup>, Scheidegger S.<sup>1, 2</sup>, Doran I.<sup>1</sup>, Merkt F.<sup>1</sup>

<sup>1</sup> ETH Zurich, Switzerland

<sup>2</sup> Present address: JILA, Boulder, Colorado, USA

High-resolution spectroscopic measurements in few-electron atoms and molecules are increasingly used as a means to test the foundations of the theory of atomic and molecular structure. Modern first-principles calculations of the energy-level structure of few-electron atomic and molecular systems consider all interactions in the realm of the standard model of particle physics.<sup>1,2,3,4</sup> Systematic comparisons of the results of such calculations with precise spectroscopic measurements in simple atoms and molecules such as H, He, H<sub>2</sub><sup>+</sup>, H<sub>2</sub> and He<sub>2</sub><sup>+</sup> aim at searching for effects not yet included in the theory (see, e.g., Refs.<sup>5,6</sup>) and at reducing the uncertainties of physical constants (see e.g., Refs.<sup>1,7,8</sup>).

This talk will present precision spectroscopic measurements of transitions to high Rydberg states of H, He, and H<sub>2</sub>, which we use to determine accurate values of their ionization energies and, in the case of H<sub>2</sub>, also of the spin-rovibrational energy-level structure of H<sub>2</sub><sup>+</sup>. The talk will describe our experimental strategy to overcome limitations in the precision and accuracy of the measurements originating from the Doppler effect, the Stark effect, and the laser-frequency calibration. The experimental results will then be compared with the results of first-principles calculations that include the treatment of finite-nuclear-size effects and relativistic and quantum-electrodynamics corrections up to high order in the fine-structure constant. Recent aspects of these investigations include a new determination of the Rydberg constant<sup>9</sup> as a contribution to the resolution of the proton-size puzzle<sup>10</sup>, a new method to record Doppler-free single-photon excitation spectra in the visible and UV spectral ranges<sup>11</sup> (see Figure 1), a “zero-quantum-defect” method to determine the energy-level structure of homonuclear diatomic molecular ions such as H<sub>2</sub><sup>+</sup>,<sup>12</sup> and a 9σ discrepancy between theory and experiment in the ionization energies of metastable (1s2s <sup>3</sup>S<sub>1</sub>) <sup>3</sup>He and <sup>4</sup>He.<sup>3,13</sup>

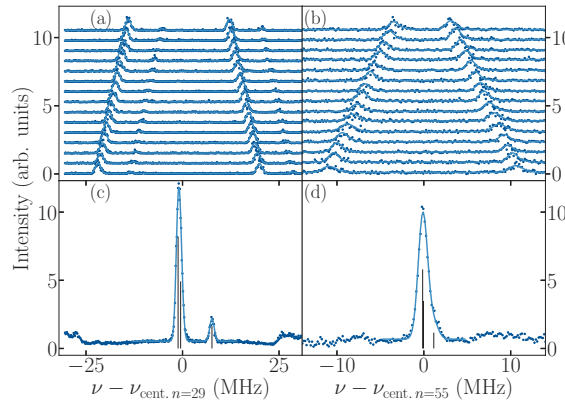


Figure 1: Imaging-assisted Doppler-free spectra of the (a)  $(1s)(29p) {}^3P_J \leftarrow (1s)(2s) {}^3S_1$  and (b)  $(1s)(55p) {}^3P_J \leftarrow (1s)(2s) {}^3S_1$  transitions in  ${}^4\text{He}$  in a supersonic beam, obtained by spatial imaging of atoms with different transverse-velocity components in the atomic beam (dots) and fits to the experimental spectra (solid lines). The photoexcitation laser beam is retroreflected so that each transition is recorded as a pair of lines with opposite Doppler shifts. (c) and (d): Sums of the corresponding cross-correlation spectra used to extract the first-order-Doppler-free line positions. The stick spectra give the positions of the  $J = 2, 1$  and  $0$  fine-structure components in order of increasing frequency and the full line represents the spectrum calculated using the line-shape parameters determined in the least-squares fits. From Ref.<sup>14</sup>

<sup>1</sup>E. Tiesinga, P. J. Mohr, D. B. Newell, and B. N. Taylor, *Rev. Mod. Phys.* **93**, 025010 (2021).

<sup>2</sup>V. Korobov, L. Hilico and J.-Ph. Karr, *Phys. Rev. Lett.* **118**, 233001 (2017).

<sup>3</sup>V. Patkos, V. A. Yerokhin, and K. Pachucki, *Phys. Rev. A* **103**, 042809 (2021).

<sup>4</sup>M. Puchalski, J. Komasa, P. Czachorowski, and K. Pachucki, *Phys. Rev. Lett.* **122**, 103003 (2019).

<sup>5</sup>C. Delaunay *et al.*, *Phys. Rev. Lett.* **130**, 121801 (2023).

<sup>6</sup>M. Germann *et al.*, *Phys. Rev. Res.* **3**, L022028 (2021).

<sup>7</sup>A. Grinin *et al.*, *Science* **370**(6520), 1061–1066 (2020).

<sup>8</sup>S. Schiller, J.-Ph. Karr, *Phys. Rev. A* **109**, 042825 (2024).

<sup>9</sup>S. Scheidegger, and F. Merkt, *Phys. Rev. Lett.* **132**, 113001 (2024).

<sup>10</sup>A. Antognini *et al.*, *Science* **339**(6118), 417–420 (2013).

<sup>11</sup>G. Clausen, S. Scheidegger, J. A. Agner, H. Schmutz, and F. Merkt, *Phys. Rev. Lett.* **131**, 103001 (2023).

<sup>12</sup>I. Doran, N. Hölsch, M. Beyer, and F. Merkt, *Phys. Rev. Lett.* **132**, 073001 (2024).

<sup>13</sup>G. Clausen, K. Gamlin, J. A. Agner, H. Schmutz, and F. Merkt, *Phys. Rev. A* **111**, 012817 (2025).

Abstract number: I15  
 Wednesday 16:00-16:30

## Revisiting and exploiting spontaneous emission with solid-state artificial atoms

**Senellart-Mardon P.<sup>†</sup>**

Center for Nanoscience and Nanotechnology, CNRS, University Paris Saclay.  
 11 Bd Thomas Gobert 91120 Palaiseau France

<sup>†</sup>pascale.senellart-mardon@universite-paris-saclay.f

A single atom coupled to a single mode of the electromagnetic fields is probably the most fundamental system to study light-matter interaction at the quantum level. It is also a fantastic resource for quantum technologies, allowing both the generation and manipulation of quantum light, with applications in quantum computation and networking. We investigate such atom-photon interface in the form of semiconductor quantum dots coupled to micropillar cavities<sup>1</sup>.

In this talk, I will first describe the high level of control we have gained on our artificial atoms, funneling their spontaneous emission into a single optical mode and isolating them from the fluctuations of their solid-state environment. We exploit them to generate highly indistinguishable single photons, now within plug-and-play fiber-pigtailed systems at unparalleled rates<sup>2</sup>, allowing small scale quantum information processing<sup>3</sup>. In a second part, we exploit the spin of a single electron trapped in a quantum dot and the optical selection rules to generate spin-multi-photon entangled states<sup>4,5</sup>, key resources for measurement based quantum protocols. Finally, we revisit the process of spontaneous emission itself and explore how it allows to generate more exotic states of light, such as the quantum superposition of zero and one photon<sup>6</sup> or the generation of entanglement in the photon number basis<sup>7</sup>.

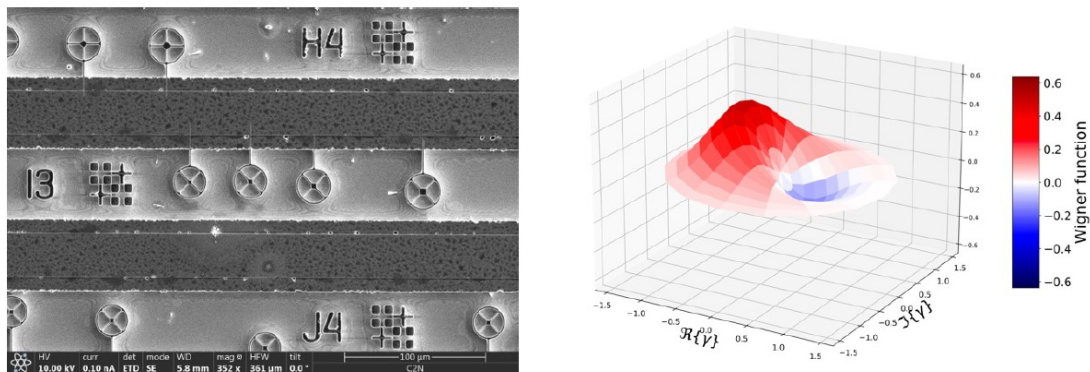


Figure 1: Left: SEM image. The wheel shaped structures are microcavities where a single quantum dot sits on the axis of the wheel. Right: measured Wigner function of a superposition of zero and one photon.

<sup>1</sup>N. Somaschi, V. Giesz *et al*, *Nature Photonics* **10**, 340 (2016)

<sup>2</sup>N. Margaria *et al*, arXiv:2410.07760

<sup>3</sup>N. Maring *et al.*, *Nature Photonics* **18** (6), 603-609 (2024)

<sup>4</sup>N. Coste *et al.*, *Nature Photonics* **17**, 582 (2023)

<sup>5</sup>H. Huet *et al*, arXiv:2410.23518

<sup>6</sup>J. Loredo *et al*, *Nature Photonics* **13** (11), 803-808 (2019)

<sup>7</sup>S.C. Wein *et al*, *Nature Photonics* **16** (5), 374-379 (2022)

Abstract number: I16  
Wednesday 16:30-17:00

## Polarisation textures of light and atoms

**Franke-Arnold S.**<sup>†1</sup>, **Svensson S.**<sup>1</sup>, **Samanta K.**<sup>1</sup>, **Westerberg, N.**<sup>1</sup>, **Wang Jinwen**<sup>2</sup>, **Clark T.**<sup>3</sup>

<sup>1</sup>University of Glasgow, School of Physics and Astronomy, Scotland

<sup>2</sup>Xi'an Jiaotong University, Xi'an, China

<sup>3</sup>Wigner Institute, Budapest, Hungary

<sup>†</sup>sonja.franke-arnold@glasgow.ac.uk

Polarisation - while invisible to the eye - has been recognized as an important feature of light since the days of Ptolemy. Over the last decades we have gained significant control in shaping light, allowing us to design phase and polarisation structures in 2D and 3D, to explore the associated topologies, and their interaction with matter. Optical  $\sigma_{\pm}$  transitions, excited by the right and left circular polarisation components of polarisation structured light, in conjunction with an external magnetic fields, can form an atomic state interferometer, rendering atomic interaction sensitive to the polarisation profile and allowing us to imprint optical polarisation textures onto atomic spin structures. Unlike optical polarisations, atomic spin alignments react to external fields and forces, promising applications in magnetometry,<sup>1</sup> and vice versa allowing us to sense properties of the structured light via atomic absorption patterns.<sup>2</sup> Structured light, when strongly focused, is shaped into highly confined vectorial electromagnetic field distributions, generally including a polarisation component along the optical axis. Manipulating and detecting such 3D light fields is challenging, as conventional optical elements and detectors do not interact with the axial polarisation component. Electric dipole transitions (specifically  $\pi$  transitions), however, are sensitive to the illustrious axial polarisation component. Working in the hyperfine Paschen-Back regime, where the electric dipole transitions are spectrally resolved, we demonstrate direct evidence of the axial polarisation component of strongly focused radial light. By measuring the spatially resolved absorption pattern at the  $\pi$  transition we retrieve the predicted distribution of the axially polarised light component, which corresponds to areas of radial polarisation in the input light (see Fig. 1).

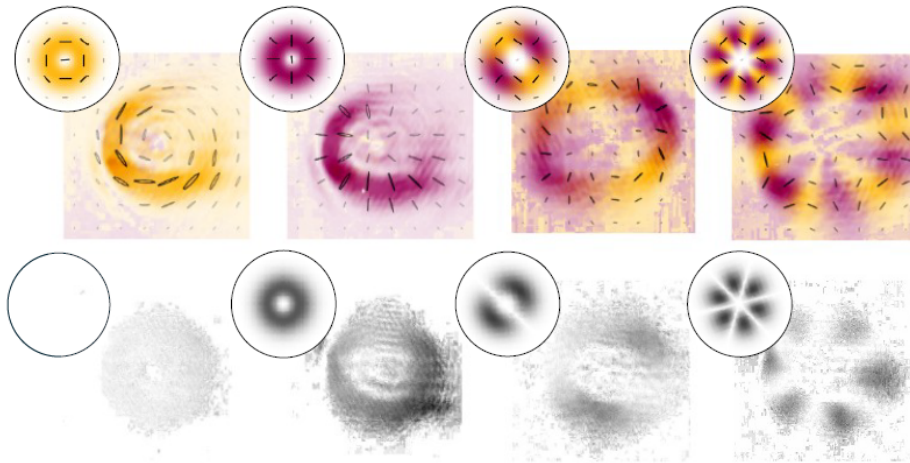


Figure 1: Visualizing the axial component of various strongly focused ( $NA = 0.4$ ) vector light beams (top row) via atomic optical densities at the  $\pi$  transition (bottom row). Radial polarisation components (which yield axial polarization when focused) are shown in purple, and azimuthal components in yellow. The disk insets show the corresponding theoretical predictions.

<sup>1</sup>F. Castellucci, T. W. Clark, A. Selyem, Jinwen Wang, and S. Franke-Arnold, *Phys. Rev. Lett.* **127** (2021).

<sup>2</sup>Jinwen Wang *et al*, *Phys. Rev. Lett.* **132**, 193803 (2024).

**Abstract number: I17**  
**Thursday 09:00-09:30**

## How one, two and many atoms scatter light

**Ketterle W.**<sup>†</sup>

*Massachusetts Institute of Technology, Cambridge, USA*

<sup>†</sup>ketterle@mit.edu

Scattering of light is one of the most elementary processes for atoms and is discussed in many textbooks. We have performed several light scattering experiments which reveal fundamental quantum aspects. At ultralow temperatures, light scattering is suppressed or enhanced by Pauli blocking and bosonic stimulation, respectively. Light scattering can distinguish a superfluid from a Mott insulator. We have experimentally investigated whether light is coherent and incoherent when scattered by single atoms. For two atoms confined to less than 50 nm, we have observed a novel stimulated dipole-dipole interaction, and large momentum transfers exceeding ten photon recoil when single photons are emitted.

Abstract number: I18

Thursday 09:30-10:00

## Quantum resonances in cold collisions

**Koch C.**<sup>†</sup>*Institut für Theoretische Physik, Freien Universität Berlin, Germany*<sup>†</sup>christiane.koch@fu-berlin.de

Quantum resonances in low-energy collisions are a sensitive probe of the intermolecular forces. They dominate the final quantum state distribution even for strong and highly anisotropic interactions, as recently observed for Feshbach resonances populated by Penning ionization of dihydrogen colliding with a metastable rare gas atom<sup>1</sup>. For such a small collision complex, full quantum scattering calculations can be carried out<sup>1</sup>. The theoretical predictions for the cross section involve then only the approximations made when constructing the potential energy surface (PES). Changes in the shape of the PES thus translate directly into modifications of the cross sections. This can be used to improve calculated PES, starting from the experimental data<sup>2</sup>. Conversely, one can also ask by how much the experimental resolution of measured cross sections must improve in order to unambiguously discriminate predictions derived from different levels of advanced ab initio electronic structure theory<sup>3</sup>. Such discrimination is equivalent to resolving the intermediate resonances governing the reaction dynamics, on top of the initial and final states.

---

<sup>1</sup>Margulis et al., *Science* **380**, 77 (2023)<sup>2</sup>Horn et al., *Science Advances* **10**, eadi6462 (2024)<sup>3</sup>Horn et al., arXiv:2408.13197

Abstract number: I19  
Thursday 10:00-10:30

## Bose-Einstein condensation of dipolar molecules

Will S.<sup>†</sup>

Department of Physics, Columbia University, New York, NY, USA

<sup>†</sup>sebastian.will@columbia.edu

We have created the first Bose-Einstein condensate (BEC) of dipolar molecules<sup>1</sup>, a deeply degenerate quantum system at temperatures as low as 5 nanokelvin. Using microwave dressing, we suppress inelastic losses by four orders of magnitude, dramatically improving evaporative cooling of molecules over previous efforts. Microwave dressing also provides us with an unprecedented level of control over the strength and anisotropy of dipole-dipole interactions, enabling continuous tuning from the weakly to the strongly interacting regime. Our latest results reveal intriguing quantum liquid behavior, including the observation of self-bound droplets and droplet arrays.

In this talk, I will discuss our approach to creating molecular BECs<sup>1,2,3</sup>, describe powerful new tools for controlling both s-wave and dipolar interactions<sup>4</sup>, and give an update on our latest results. Making connections with degenerate atomic gases, liquid helium, and quantum materials - degenerate molecular gases offer exciting prospects for new discoveries in many-body quantum physics.

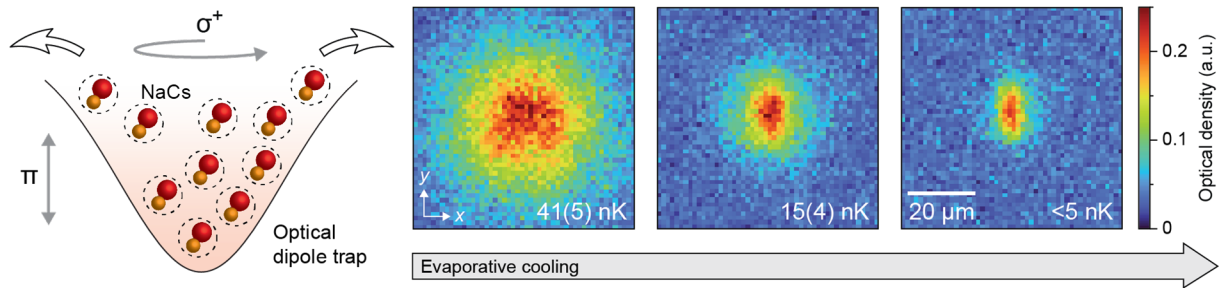


Figure 1: Evaporative cooling of NaCs molecules into a BEC.

<sup>1</sup>N. Bigagli, W. Yuan, S. Zhang, B. Bulatovic, T. Karman, I. Stevenson, S. Will, *Nature* **631**, 289-293 (2024).

<sup>2</sup>N. Bigagli, C. Warner, W. Yuan, S. Zhang, I. Stevenson, T. Karman, S. Will, *Nature Physics* **19**, 1579-1584 (2023).

<sup>3</sup>I. Stevenson, A. Z. Lam, N. Bigagli, C. Warner, W. Yuan, S. Zhang, S. Will, *Phys. Rev. Lett.* **130**, 113002 (2023).

<sup>4</sup>T. Karman, N. Bigagli, W. Yuan, S. Zhang, I. Stevenson, S. Will, arXiv:2501.08095 (2025).

Abstract number: I20

Thursday 11:00-11:30

## Dipolar interactions between ultracold RbCs molecules in magic-wavelength traps and optical tweezers

Ruttley D. K.<sup>1</sup>, Hepworth T. R.<sup>1</sup>, Gregory P. D.<sup>1</sup>, Guttridge A.<sup>1</sup>, **Cornish S. L.**<sup>†1</sup>  
<sup>1</sup>*Department of Physics, Durham University, South Road, Durham, DH1 3LE, United Kingdom*

<sup>†</sup>s.l.cornish@durham.ac.uk

Ultracold polar molecules are an exciting platform for quantum science and technology. The combination of rich internal structure of vibration and rotation, controllable long-range dipolar interactions and strong coupling to applied electric and microwave fields has inspired many applications. These include quantum simulation of strongly interacting many-body systems, the study of quantum magnetism, quantum metrology and molecular clocks, quantum computation, precision tests of fundamental physics and the exploration of ultracold chemistry. Many of these applications require full quantum control of both the internal and motional degrees of freedom of the molecule at the single particle level, combined with traps that support long coherence times for rotational-state superpositions.

Using ultracold RbCs molecules assembled from ultracold atoms, we demonstrate all these requirements. We present a novel magic-wavelength trap that supports second-scale rotational coherences in a gas of molecules and gives access to controllable dipole-dipole interactions<sup>1</sup>. We also report the efficient assembly of individual molecules in optical tweezers<sup>2</sup>. Using mid-sequence detection of molecule formation errors, we demonstrate rearrangement to produce small defect-free arrays. By transferring the molecules into magic-wavelength tweezers, we demonstrate long-lived rotational coherences. In the magic-wavelength tweezers we can resolve Hertz-scale dipolar interactions between pairs of molecules. We then use the dipolar interaction to engineer entanglement, both using a spin-exchange protocol and by direct microwave excitation<sup>3</sup>. Correcting for leakage errors, we measure an entanglement fidelity of  $0.976 \pm 0.015$ .

Finally, as an outlook, we demonstrate a new hybrid platform that combines single ultracold molecules with single Rydberg atoms<sup>4</sup>, opening up the prospect of non-destructive readout of the molecular state and fast entangling gates.

<sup>1</sup>P.D. Gregory *et al.*, *Nature Physics* **20**, 415–421 (2024).

<sup>2</sup>D.K. Ruttley *et al.*, *PRX Quantum* **5**, 020333 (2024).

<sup>3</sup>D.L. Ruttley, T.R. Hepworth, A. Guttridge and S.L. Cornish, *Nature* **637**, 827–832 (2025).

<sup>4</sup>A. Guttridge, D.K. Ruttley *et al.*, *Phys. Rev. Lett.* **131**, 013401 (2023).



Abstract number: I21

Thursday 11.30-12:00

## Quantum Many-Body Physics with Molecular Tweezer Arrays: From Magnon Dynamics to Spin-Squeezing

**Cheuk L.**<sup>†</sup>

*Princeton University, US*

<sup>†</sup>lcheuk@princeton.edu

Molecular tweezer arrays are an emerging platform for quantum science that combines the richness of molecules with the microscopic control of programmable optical tweezer traps. In the past few years, our group and others have significantly advanced the level of quantum control in this platform, establishing the building blocks required for quantum science. These include high-fidelity single molecule detection, high-fidelity state preparation, coherent control of interactions, and deterministic entanglement. These developments have opened the door to practical applications such as quantum simulation of interacting many-body systems, quantum information processing, and quantum-enhanced sensing.

In this talk, I will report recent work where we have entered, for the first time, the quantum many-body regime with molecular tweezer arrays. Using two new capabilities that we have developed - measurement-enhanced quantum state preparation and Floquet engineering, we have realized interacting dipolar quantum spin models with tunable XYZ interactions in mesoscopic 1D chains. I will report experiments exploring magnon dynamics in these systems, which include quantum walks of single spin excitations, dynamics of repulsive magnon bound states, and coherent pair creation and annihilation. If time permits, I will discuss our efforts to create metrologically useful entangled states via dynamical evolution under interacting spin Hamiltonians, and report on the first demonstration of spin-squeezing of molecules.

Abstract number: I22

Thursday 12:00-12:30

## Attosecond molecular science

**Martín F.**<sup>†1,2</sup><sup>1</sup>*Departamento de Química, Universidad Autónoma de Madrid, 28049 Madrid, Spain*<sup>2</sup>*Instituto Madrileño de Estudios Avanzados en Nanociencia (IMDEA-Nano), Cantoblanco, 28049 Madrid, Spain*<sup>†</sup>fernando.martin@uam.es

With the advent of attosecond light pulses at the dawn of the twenty first century, access to the time scale of electronic motion, i.e., the ultimate time scale responsible for chemical transformations, was finally at our reach. Since the first attosecond pump-probe experiments performed in molecules<sup>1,2</sup>, the field has grown exponentially<sup>3</sup>. As a result, it is nowadays possible to follow in real time the motion of the “fast” electronic motion in molecules, mostly in the gas phase, and understand how this motion affects the “slower” motion of atomic nuclei and vice versa. There are, however, new scenarios<sup>4</sup> that will allow one to extend the range of applications to more complex molecular systems, including the condensed phase, and to overcome some of the limitations of current attosecond technologies<sup>5,6,7,8,9</sup>, such as the low intensity of attosecond pulses produced by high harmonic generation, the impossibility to generate such pulses in the visible and UV spectral regions to avoid molecular ionization, or the difficulties to combine them with truly imaging methods for direct time-resolved observations of the electron density without the need for reconstruction from measured photoelectron, photoion or transient absorption spectra.

In this talk, I will describe current experimental and theoretical efforts aiming at overcoming the above-mentioned limitations, thus giving attosecond molecular science the necessary push to investigate problems of chemical interest

---

<sup>1</sup>G. Sansone *et al.*, *Nature* **465**, 763 (2010).<sup>2</sup>F. Calegari *et al.*, *Science* **346**, 336 (2014).<sup>3</sup>M. Nisoli, P. Decleva, F. Calegari, A. Palacios, and F. Martín, *Commun. Chem.* **6**, 184 (2023).<sup>4</sup>F. Calegari and F. Martín *Chem. Rev.* **117**, 10760 (2017).<sup>5</sup>A. Palacios and F. Martín, *WIREs Comput. Mol. Sci.* e1430 (2020).<sup>6</sup>G. Grell *et al.*, *Phys. Rev. Res.* **5**, 023092 (2023).<sup>7</sup>M. Galli *et al.*, *Optics Letters* **44**, 1308 (2019).<sup>8</sup>M. Reduzzi *et al.*, *Optics Express* **31**, 26854 (2023).<sup>9</sup>M. Garg, A. Martín-Jiménez, M. Pizarra, Y. Luo, F. Martín and K. Kern, *Nature Photonics* **16**, 196 (2022).

Abstract number: I23  
Friday 09:00-09:30

## Quantum Computers and Raising Schrödinger's Cat

Wineland D.<sup>†</sup>

*University of Oregon, Eugene, Oregon, US*

<sup>†</sup>djw34@uoregon.edu

Two energy levels of an atom can represent a binary bit of information. Quantum systems can also exist in “superposition states”, storing both states of the bit simultaneously, a quantum bit or “qubit.”  $N$  qubits could store  $2^N$  binary numbers yielding an exponential increase in memory and processing capacity. Qubit operations with trapped atomic ions are described, and could eventually lead to an analog of Schrödinger's famous cat.

Abstract number: I24  
Friday 09:30-10:00

## New pathway to universal quantum computing and entanglement generation

**Safavi-Naini A.**<sup>†</sup>

*University of Amsterdam, NL*

<sup>†</sup>a.safavinaini@uva.nl

Trapped-ions are one of the most mature platforms for quantum computation and quantum simulation. In trapped-ion quantum simulators the spin-spin interactions mediated by the collective motion of the ions in the crystal (phonons) are of the form  $r^{-a}$  where  $0 < a < 3$ . I will show that the addition of optical tweezers opens a new pathway for generating spin-dependent optical forces. The tweezers can be used to both enhance the programmability of the quantum simulator and to create new quantum computing architectures.

Next, I will discuss a new pathway to multi parameter sensing in trapped ion quantum simulators which can be readily implemented. Here, spin-dependent squeezing is used for the simultaneous sensing of  $x$  and  $p$ . I will discuss the advantages of this protocol compared to prior protocols which require phase-locking and/or two-mode squeezing.

Abstract number: I25

Friday 10:00-10:30

## New frontiers in quantum simulation and sensing via photon mediated interactions

**Rey A. M.<sup>†</sup>**

*JILA, NIST and University of Colorado, Boulder, CO 80309-0440, USA*

<sup>†</sup>arey@jilau1.colorado.edu

In this talk, I will discuss the potential of atomic systems loaded in optical cavities as a resource to enhance the energy scales needed to observe complex many-body behaviors by harnessing infinity range interactions mediated by photons that can couple a large set of internal levels. I will show how cavity systems can help us not only to shed light on behaviors of iconic Hamiltonians describing real materials but also to engineer broader classes of Hamiltonians with multi-body interactions too complex to emerge naturally. Furthermore, I will explain how they can facilitate the generation of quantum entanglement and overcome physical constraints currently limiting the performance of state-of-the-art atomic clocks and interferometers.

Abstract number: I26  
Friday 11:00-11:30

## Exploring quantum Hall physics with ultracold dysprosium atoms

**Nascimbene S.**<sup>†</sup>

*Laboratoire Kastler Brossel, Collège de France, CNRS, ENS-PSL University, Sorbonne Université,  
11 Place Marcelin Berthelot, 75005 Paris, France*

<sup>†</sup>sylvain.nascimbene@lkb.ens.fr

Ultracold atomic gases offer a versatile platform for exploring rich phenomena in quantum matter. In particular, topological states akin to those found in the quantum Hall effect can be engineered by simulating orbital magnetic fields—an approach greatly facilitated by the use of synthetic dimensions.

In this talk, I will present our experimental realization of a quantum Hall system using ultracold gases of dysprosium atoms. By leveraging the atom's large internal spin ( $J = 8$ ), we encode a synthetic dimension and couple it to atomic motion via two-photon optical transitions, which generates an effective magnetic field. We observe hallmark signatures of quantum Hall physics, including a quantized Hall response and gapless, chiral edge modes.

I will then describe a more intricate experiment designed to probe spatial entanglement by simulating the so-called entanglement Hamiltonian. Using the Bisognano-Wichmann theorem—which relates the entanglement Hamiltonian to a spatially deformed version of the original system—we implement this deformation along the synthetic dimension.

Lastly, I will discuss our recent investigation into a topological phase transition, induced by introducing an additional lattice potential. I will highlight the system's behavior in the critical regime and explore the emergent features associated with the transition.

Abstract number: I27  
Friday 11:30-12:00

## Correlations in homogeneous fermionic Hubbard gases: Coherence and Magnetism

Yao X. C.<sup>†1</sup>

<sup>1</sup>*Hefei National Research Center for Physical Sciences at the Microscale and School of Physical Sciences, University of Science and Technology of China, Hefei, 230026, China*

<sup>†</sup>yaoxing@ustc.edu.cn

The fermionic Hubbard model (FHM), which describes electron motion in a lattice, is considered one of the key models for understanding high-temperature superconductors. Yet, resolving its low-temperature phase diagram remains difficult, both theoretically and numerically. Ultracold Fermi atoms in optical lattices provide a clean and highly controllable platform for simulating the FHM. In this talk, I will present our recent progress in quantum simulations of the FHM. We have constructed a homogeneous fermionic Hubbard system with approximately 800,000 lattice sites at temperatures below the Neel temperature. By observing and quantitatively characterizing the interference patterns of fermions, we have precisely measured non-local correlation functions of the system, offering new insights into the many-body physics of the FHM. Furthermore, we have employed spin-sensitive Bragg scattering to measure the spin structure factor of the system. When interaction strength, temperature, and doping concentration are finely tuned to their respective critical values, we have observed a sharp increase in the spin structure factor. These observations can be well described by a power-law divergence, providing conclusive evidence for the realization of the antiferromagnetic phase transition.

Abstract number: I28  
 Tuesday 12:00-12:30

## Vortex dynamics in strongly interacting Fermi superfluids

**Roati G.**<sup>†1,2</sup>

<sup>1</sup>*National Institute of Optics, CNR, Firenze, Italy*

<sup>2</sup>*LENS, University of Florence, Italy*

<sup>†</sup>giacomo.roati@ino.cnr.it

Topological defects play a fundamental role in shaping the properties and structures of diverse out-of-equilibrium physical and biological systems across a wide range of scales. These include planetary atmospheres, turbulent flows in classical and quantum fluids, and electrical signaling in excitable biological media<sup>1</sup>. In superfluids and superconductors, the motion of quantized vortices is tied to the onset of dissipation, which limits the superflow<sup>2</sup>. Understanding vortex dynamics remains a challenge due to the complex interplay among vortices, disorder and system dimensionality. We address this challenge by exploring vortex matter in strongly interacting Fermi superfluids made of ultracold atoms<sup>3</sup>. By designing specific vortex configurations and tracking their trajectories with high spatial resolution, we transform our system into an ideal "quantum laboratory" for probing the fundamental nature of vortex-driven instabilities and dissipation<sup>4,5</sup>. Our research paves the way for deeper insights into vortex-matter phenomena in strongly correlated superfluids.

<sup>1</sup>Spiral and Vortices, K. Tsuji and S. C. Müller Editors, *Springer Nature* (2019).

<sup>2</sup>B. I. Halperin, G. Refael and E. Demler, *Int. J. Mod. Phys. B* **24**, 20n21 (2010)

<sup>3</sup>W. J. Kwon *et al.*, *Nature*, **600** (2021).

<sup>4</sup>D. Hernandez-Rajkov *et al.*, *Nat. Phys.* **20** (2024).

<sup>5</sup>N. Grani *et al.*, arXiv:2503.21628v1 (2025).



Abstract number: I29

Friday 16:00-16:30

## Creation of ultracold triatomic molecules

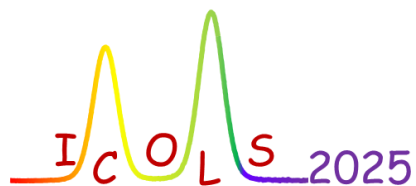
**Zhao B.**<sup>†</sup>*Hefei National Research Center for Physical Sciences at the Microscale and School of Physical Sciences, University of Science and Technology of China, Hefei, 230026, China*<sup>†</sup>bozhao@ustc.edu.cn

Ultracold assembly of diatomic molecules has enabled great advances in controlled chemistry, ultracold chemical physics, and quantum simulation with molecules. Extending the ultracold association to triatomic molecules will offer many new research opportunities and challenges in these fields. A possible approach is to form triatomic molecules in a mixture of ultracold atoms and diatomic molecules. I will talk about our recent work on the creation of ultracold triatomic molecules near the Feshbach resonance between  $^{23}\text{Na}^{40}\text{K}$  molecules in the rovibrational ground state and  $^{40}\text{K}$  atoms. We use radio-frequency association<sup>1</sup> and magnetoassociation<sup>2</sup> to form weakly bound triatomic Feshbach molecules. Moreover, we form deeply bound triatomic molecules in electronic excited states using Feshbach-enhanced photoassociation<sup>3</sup>. Our work contributes to the understanding of the complex spectroscopy of ultracold triatomic molecules and opens up an avenue toward bottom-up construction of ultracold polyatomic molecules.

---

<sup>1</sup>H. Yang *et al.*, *Nature* **602**, 229 (2022).<sup>2</sup>H. Yang *et al.*, *Science* **378**, 1009 (2022).<sup>3</sup>J. Cao *et al.*, *Phys. Rev. Lett.*, **132**, 093403 (2024).

*Hot topic talks*  
*Abstracts*



Abstract number: HT1  
Tuesday 17:00-17:20

## Searching for new physics by measuring isotope shifts and parity violation in trapped ions

Aude Craik D. P. L.<sup>†1</sup>, Huber L. I.<sup>1</sup>, Flannery J.<sup>1</sup>, Matt R.<sup>1</sup>, Stadler M.<sup>1</sup>, Oswald R.<sup>1</sup>, Schmid F.<sup>1</sup>, Kienzler D.<sup>1</sup>, Home J.<sup>1</sup>, Wilzewski A.<sup>2</sup>, Spieß L. J.<sup>2</sup>, Wehrheim M.<sup>2</sup>, Chen S.<sup>2</sup>, King S. A.<sup>2</sup>, Micke P.<sup>2</sup>, Filzinger M.<sup>2</sup>, Steinel M. R.<sup>2</sup>, Huntemann N.<sup>2</sup>, Benkler E.<sup>2</sup>, Schmidt P. O.<sup>2</sup>, Door M.<sup>3</sup>, Eliseev S.<sup>3</sup>, Filianin P.<sup>3</sup>, Herkenhoff J.<sup>3</sup>, Kromer K.<sup>3</sup>, Blaum K.<sup>3</sup>, Yerokhin V. A.<sup>3</sup>, Valuev I. A.<sup>3</sup>, Oreshkina N. S.<sup>3</sup>, Lyu C.<sup>3</sup>, Banerjee S.<sup>3</sup>, Keitel C. H.<sup>3</sup>, Harman Z.<sup>3</sup>, Berengut J. C.<sup>5</sup>, Viatkina A.<sup>2,6</sup>, Gilles J.<sup>2,6</sup>, Surzhykov A.<sup>2,6</sup>, Rosner M. K.<sup>3</sup>, Crespo López-Urrutia J. R.<sup>3</sup>, Richter J.<sup>4</sup>, Mariotti A.<sup>4</sup>, Fuchs E.<sup>2,4</sup>

<sup>1</sup>*Institute for Quantum Electronics, Department of Physics, Eidgenössische Technische Hochschule Zürich, Otto-Stern-Weg 1, 8093 Zürich, Switzerland*

<sup>2</sup>*Physikalisch-Technische Bundesanstalt, Bundesallee 100, 38116 Braunschweig, Germany*

<sup>3</sup>*Max-Planck-Institut für Kernphysik, Saupfercheckweg 1, 69117 Heidelberg, Germany*

<sup>4</sup>*Institut für Theoretische Physik, Leibniz Universität Hannover, Appelstraße 2, 30167 Hannover, Germany*

<sup>5</sup>*School of Physics, University of New South Wales, Sydney, NSW 2052, Australia*

<sup>6</sup>*Institut für Mathematische Physik, Technische Universität Braunschweig, D-38116 Braunschweig, Germany*

<sup>†</sup>dcaik@phys.ethz.ch

Isotope shift (IS) spectroscopy of atoms and ions has been proposed as a method to search for a fifth fundamental force mediated by a hypothetical new boson in the intermediate mass range (100eV to 10MeV). The existence of this force would cause neutron-number-dependent (and hence, isotope dependent) shifts in atomic transition frequencies. To distinguish these shifts from standard model (SM) shifts (relating, for example, to differences in the Coulomb potential of the nucleus between isotopes), one measures isotopes shifts on at least two transitions between three or more distinct pairs of isotopes. The data can then be plotted on a "King plot", which displays a nonlinearity if physics beyond first-order SM effects has contributed to the measured isotope shifts.

At the TIQI group at ETH, we measured isotope shifts on the 729nm electric quadrupole transition between pairs of co-trapped calcium ions at 100mHz precision, two orders of magnitude below the previous best measurement. We combined our measurements with IS measurements made by the group of Piet Schmidt on the 570nm transition in Ca14+ and improved nuclear mass measurements made by the group of Klaus Blaum, to produce the first sub-Hz King plot. King plots in calcium had previously remained linear up to the 10Hz level – our improved precision now reveals a large King non-linearity<sup>1</sup>. Whilst the second-order mass shift is an expected SM source of nonlinearity, a decomposition analysis of the nonlinearity pattern we observe reveals evidence for at least one other contributing source. I will discuss the implications of these results, combined with input from our theory collaborators, both to our understanding of nuclear structure and to the search for new physics. Finally, I will outline a new endeavor I am now starting in my new group at ETH to perform a stringent test of the electroweak sector of the Standard Model by measuring parity violation in barium ions using entanglement-enhanced spectroscopy<sup>2</sup>.

<sup>1</sup>A. Wilzewski et al., <https://arxiv.org/abs/2412.10277> (2024).

<sup>2</sup>D. P. L. Aude Craik, <https://arxiv.org/abs/2503.20003> (2025)

Abstract number: HT2  
Tuesday 17:20-17:40

## Observation of three and four-body interactions between momentum states in a high-finesse cavity

**Bohr E. A.<sup>†</sup>, Luo C., Zhang H., Maruko C., Rey A. M., Thompson J. K.**  
JILA, NIST, and Department of Physics, University of Colorado, Boulder, CO, USA

<sup>†</sup>eliot.bohr@colorado.edu

Spin Hamiltonians in quantum simulation and quantum sensing have traditionally relied on pairwise (two-body) interactions between system constituents. Here, we present an experimental realization of an effective three-body ( $n = 3$ ) Hamiltonian in a system of laser-cooled rubidium atoms in a high-finesse optical cavity<sup>1</sup>. The pseudo-spin-1/2 states are encoded in two atomic momentum states, and the interaction is achieved through two dressing tones that drive photon exchange via the cavity. This enables a virtual six-photon process while suppressing lower-order interactions through destructive interference. By tuning the desired process into resonance and detuning the unwanted processes, pure  $n$ -body interactions can be generated with the lower-order processes canceled via symmetry. The  $n$ -body interaction can be understood as  $n$  different atoms flipping their momentum states in concert from  $p_0 - \hbar k$  to  $p_0 + \hbar k$ . The  $n$ -body interactions are experimentally observed both via a spectroscopic signal and through mean-field dynamics measured over the Bloch sphere. The resulting interactions exhibit an all-to-all connectivity, making them suitable for rapid entanglement generation and the exploration of exotic quantum phases. The flexibility of our platform also allows for extension to multi-level systems and higher-order interactions, such as a four-body ( $n = 4$ ) interaction mediated by a virtual eight-photon process.

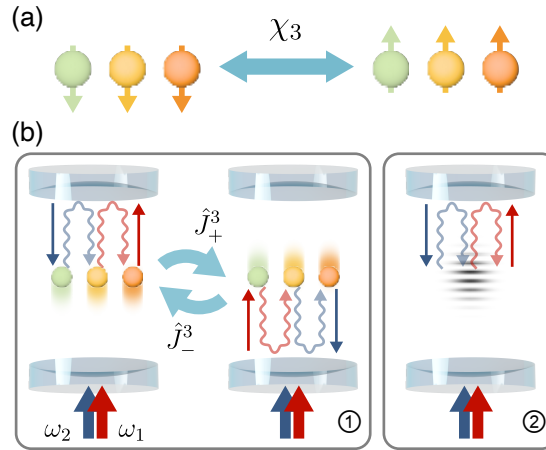


Figure 1: **(a)** A 3-body interaction with strength  $\chi_3$  causes a trio of spins to flip their spin states simultaneously. **(b)** Here, the pseudo-spin consists of two atomic momentum states  $|p_0 \pm \hbar k\rangle$  along the cavity axis, separated by  $2\hbar k$ . The atoms are driven by two dressing lasers (red and blue), and an all-to-all three-body interaction arises from photon exchange via the cavity. A density grating is formed when atoms are in superpositions of momentum states, enabling multiple light back-reflections that mediate the interaction.

<sup>1</sup>Chengyi Luo et al., *Science* **384**, 551-556 (2024).

Abstract number: HT3  
Tuesday 17:40-18:00

## Ionization threshold of $\text{Rb}_2$ molecule measured by the electric field-dependent Rydberg-state spectroscopy

**Bouloufa-Maafa N.**<sup>†1</sup>, **Lefrán Torres M.A.**<sup>2</sup>, **Rodriguez Fernández D.**<sup>2</sup>, **Borges Márquez J.J.**<sup>2</sup>, **Cardoso M.R.**<sup>2</sup>, **Pandey A.**<sup>1</sup>, **Vexiau R.**<sup>1</sup>, **Dulieu O.**<sup>1</sup>, **Marcassa L.G.**<sup>2</sup>

<sup>1</sup> Université Paris-Saclay, CNRS, Laboratoire Aimé Cotton, 91400 Orsay, France

<sup>2</sup> Instituto de Física de São Carlos, Universidade de São Paulo, Caixa Postal 369, 13560-970, São Carlos, SP, Brasil.

<sup>†</sup>nadia.bouloufa@universite-paris-saclay.fr

Recent experiments involving hybrid ion-atom systems in the ultracold domain ( $T < 1\mu\text{K}$ ), which is dominated by s-wave collisions, are expected to provide a rich experimental platform with new phenomena and applications<sup>1</sup>. For the specific case of Rb, weakly bound  $\text{Rb}_2^+$  ions have been observed after a single cold  $^{87}\text{Rb}^+$  ion was injected inside a  $^{87}\text{Rb}$  Bose-Einstein condensate<sup>2</sup>. Modeling of such experiments requires the precise knowledge of the ground state  $X^2\Sigma_g^+$  of the molecular ion<sup>3</sup> and thus the ionization threshold of  $\text{Rb}_2$

In this work we have measured the ionization threshold of the  $^{85}\text{Rb}_2$  molecule in a supersonic beam using resonantly enhanced 2-photon ionization (RE2PI) by applying two lasers of different wavelengths through a well chosen intermediate state. The first photon frequency is resonant with  $^{85}\text{Rb}_2 X^1\Sigma_g^+(v=0) - B^1\Pi_u(v_B=2)$  transition while the second photon frequency is swept allowing to address either different Rydberg levels of the molecule which could be ionized by a pulsed electric field, or vibrational levels of the molecular ion thus ionizing the molecule without an electric field.

Ionization spectra recorded at different electric field values (see Figure 1) exhibit several lines and an enhancement of the background of the signal which remain the same after a given frequency independent of the field intensity thus corresponding to the ionization threshold. The lines are identified as the pulsed field-ionized (PFI) Rydberg components of the spectra. In addition, we identify vibrational levels of  $\text{Rb}_2$  Rydberg states associated to vibrational levels of  $\text{Rb}_2^+$ ,  $v^+ = 0, 1, 2, 3, \dots$ . The ionization threshold energy of the  $^{85}\text{Rb}_2$  molecule is measured  $E_i = 31498(1) \text{ cm}^{-1}$  (with a dissociation energy of  $D_0 = 6158(1) \text{ cm}^{-1}$ ). This value is  $150 \text{ cm}^{-1}$  higher than the previous one measured by Bellos et al.<sup>4</sup> and is in better agreement with recent theoretical models.

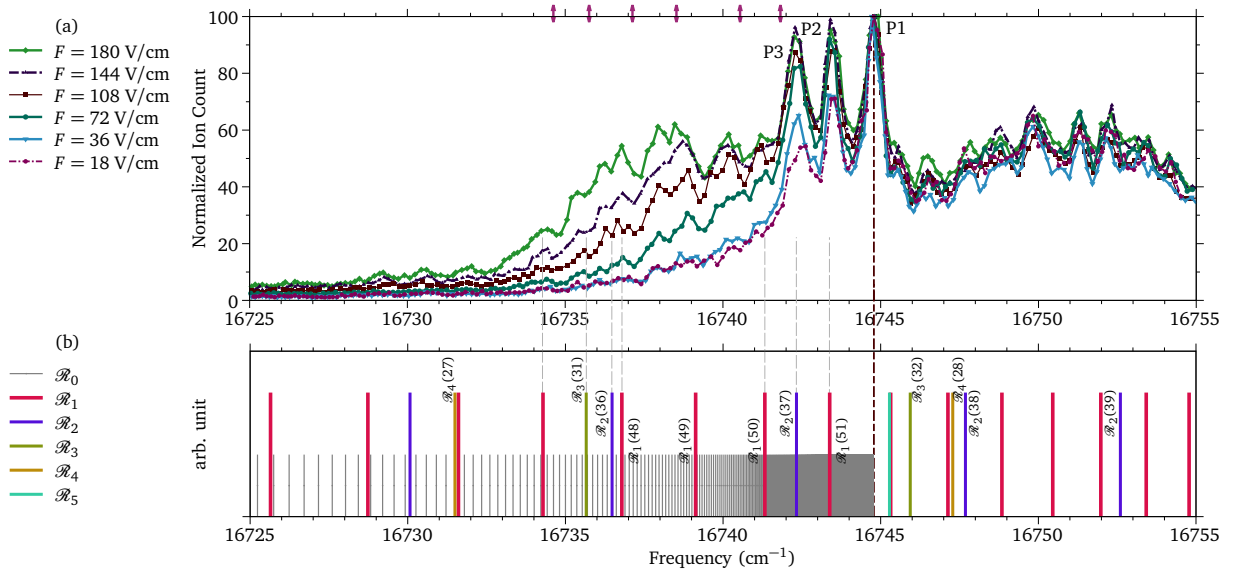


Figure 1: (a) Normalized  $\text{Rb}_2^+$  ion count as a function of the second photon frequency for several electrical fields ( $F=180, 144, 108, 72, 36$ , and  $18 \text{ V/cm}$ ). (b) Rydberg states associated with the vibrational levels of  $^{85}\text{Rb}_2^+, X^2\Sigma_g^+, v^+ = 0, 1, 2, \dots$  labeled as  $R_0, R_1, R_2, \dots$ , respectively.

Acknowledgement: This work is supported by Grants 2018/06835-0, 2022/16904-5, 2023/06732-5, and 2021/04107-0 from São Paulo Research Foundation (FAPESP), FA9550-23-1-0666 from the US Air Force Office of Scientific Research, 305257/2022-6 from CNPq, and ANR-21-CE30-0060-01 (COCOTRAMOS project) from Agence Nationale de la Recherche.

<sup>1</sup>T. Schmidet *et al.*, *Phys. Rev. Lett* **120**, 153401 (2018).

<sup>2</sup>A. Dieterle Härteret *et al.*, *Phys. Rev. Lett* **126**, 033401 (2021).

<sup>3</sup>A. Pandey *et al.*, *Phys. Rev. Res* **6**, 043010 (2024).

<sup>4</sup>M. Bellos *et al.*, *Phys. Rev. A* **109**, 012508 (2013).

Abstract number: HT4  
Wednesday 17:00-17:20

## Investigating Quantum Diffusion and Localization in Atom-Optics Kicked Rotor Systems

Rapol U. D.<sup>†1</sup>, Santhanam M. S.<sup>1</sup>, Mangaonkar J.<sup>1</sup>, Bharathi Kannan J.<sup>1</sup>, Paul S.<sup>2</sup>, Sagar Maurya S.<sup>3</sup>, Sarkar S.<sup>4</sup>

<sup>1</sup>Department of Physics, Indian Institute of Science Education and Research Pune Dr. Homi Bhabha Road, Pune 411008, India

<sup>2</sup>Department of Physics and Complex Systems, S. N. Bose National Centre for Basic Sciences, JD Block, Sector-III, Salt Lake City, Kolkata - 700 106, India

<sup>3</sup>Physikalisch-Technische Bundesanstalt, Bundesallee 100, 38116 Braunschweig, Germany

<sup>4</sup>Institute of Physics, University of Amsterdam, Science Park 904, 1090 GL Amsterdam, The Netherlands

<sup>†</sup>umakant.rapol@iiserpune.ac.in

The quantum kicked rotor (QKR) model serves as a fundamental platform for exploring dynamical localization due to quantum chaos and transport phenomena in quantum systems<sup>1</sup>. By subjecting particles to periodic, deterministic kicks, the QKR facilitates the study of transitions from diffusive to localized behaviour due to quantum interference effects. The quantum kicked rotor exhibits dynamical localization in momentum space, which is mathematically analogous to Anderson localization in disordered solids, where interference leads to the suppression of transport<sup>2</sup>. In our group, we implement cold atom kicked rotor systems that use laser-cooled atoms in optical lattices subjected to periodic kicks from pulsed laser fields to mimic the quantum kicked rotor<sup>3</sup>. In the first study<sup>4</sup>, we investigated the effects of nonstationary Lévy noise in the kick sequence of an atom-optics kicked rotor. We observed that the introduction of Lévy noise leads to slower-than-exponential decay of coherences, manifesting as quantum subdiffusion. This behavior is highly sensitive to the Lévy exponent, offering a tunable mechanism for controlling transport properties in quantum systems. Following up on this, In Ref<sup>5</sup>, we explored the dynamics of an atom-optics kicked rotor system by modifying the kick sequence. By flipping the sign of the kick sequence after every few kicks, achieved through half-Talbot time free evolution between kicks, we observed enhanced diffusion followed by asymptotic localization. This approach revealed localized yet nonexponential wave function profiles, suggesting a complex interplay between diffusion and localization mechanisms. Further, In Ref<sup>6</sup>, we used the kicked rotor setup to study asymmetric dynamical localization. The introduction of half-Talbot time free evolution between kicks resulted in an asymmetrically localized momentum distribution, dependent on the initial velocity of the BEC. This asymmetry enabled precise measurement of the micromotion of the BEC, detecting small initial velocities with high sensitivity<sup>6</sup>.

**Keywords:** Quantum kicked rotor, dynamical localization, quantum diffusion, Bose-Einstein condensate, micromotion measurement, Lévy noise.

<sup>1</sup>S. Wimberger, Quantum Chaos in the Atom-Optics Kicked Rotor, *Nonlinear Dynamics* **88**, 27–41 (2017).

<sup>2</sup>P. W. Anderson, Absence of Diffusion in Certain Random Lattices, *Physical Review* **109**, 1492 (1958).

<sup>3</sup>F. L. Moore, J. C. Robinson, C. F. Bharucha, B. Sundaram, and M. G. Raizen, Atom Optics Realization of the Quantum  $\delta$ -Kicked Rotor, *Physical Review Letters* **75**, 4598 (1995)

<sup>4</sup>S. Sarkar *et al.*, Nonexponential Decoherence and Subdiffusion in Atom-Optics Kicked Rotor, *Physical Review Letters* **118**, 174101 (2017).

<sup>5</sup>S. S. Maurya, J. B. Kannan, K. Patel, P. Dutta, K. Biswas, J. Mangaonkar, M. S. Santhanam, and U. D. Rapol, Interplay between quantum diffusion and localization in the atom-optics kicked rotor, *Physical Review E* **106**, 034207 (2022).

<sup>6</sup>S. S. Maurya, J. B. Kannan, K. Patel, P. Dutta, K. Biswas, M. S. Santhanam, and U. D. Rapol, Asymmetric dynamical localization and precision measurement of the micromotion of a Bose-Einstein condensate, *Phys. Rev. A* **110**, 053307 (2024).

Abstract number: HT5  
 Wednesday 17:20-17:40

## Two-photon cooling of calcium atoms

**Politi C.<sup>†</sup>, Adamczyk W., Koch S., Passagem H.F., Fischer C., Filippov P.,  
 Berterottière F., Kienzler D., Home J.P.**

<sup>1</sup>*Institute for Quantum Electronics, ETH Zürich, Otto-Stern-Weg 1, 8093 Zurich, Switzerland*

<sup>†</sup>cpoliti@phys.ethz.ch

Alkaline-earth(-like) atoms trapped in optical tweezers and excited to Rydberg states have emerged as a promising platform for quantum simulation and computation, owing to the high control and scalability of the system. In such systems, the long-lived metastable states can be used for motional ground state cooling, qubit readout and manipulation, as well as providing access to single-photon Rydberg excitation and quantum erasure conversion. To trap individual atoms in optical tweezers, temperatures as low as tens of microkelvin are desirable. The absence of hyperfine structure in alkaline-earth atoms precludes the use of standard sub-Doppler schemes developed for alkali atoms. In this work, we demonstrate two-photon cooling of calcium atoms using a two-photon transition from the  $^1S_0$  ground state to the upper  $4s5s\ ^1S_0$  state via the  $^1P_1$  intermediate state<sup>1</sup>. We achieve temperatures as low as  $260\mu\text{K}$  in a magneto-optical trap (MOT), well below the Doppler limit ( $T_D = 0.8\text{mK}$ ) of the  $^1P_1$  state. This scheme provides an alternative to the standard Doppler cooling applied to alkaline-earth atoms, based on a sequence of two magneto-optical traps, with the advantages of varying the effective linewidth of the  $^1P_1$  state, a higher transfer efficiency (close to 100%), and a more straightforward experimental implementation. Finally, we outline the progress towards optical trapping of ground and circular Rydberg states of calcium atoms in optical tweezers.

<sup>1</sup>W. Adamczyk *et al.*, *Phys. Rev. A* **111**, 043101 (2025).

Abstract number: HT6  
Wednesday 17:40-18:00

## Magneto-optical trapping of aluminium monofluoride

Wright S. C.<sup>1,†</sup>, Padilla-Castillo J. E.<sup>1</sup>, Cai J.<sup>1,2</sup>, Thomas R. S.<sup>1</sup>, Kray S.<sup>1</sup>, Sartakov B.<sup>1</sup>, Truppe S.<sup>2</sup>, Meijer G.<sup>1</sup>

<sup>1</sup>Fritz Haber Institute of the Max Planck Society, Berlin, Germany

<sup>2</sup>Centre for Cold Matter, Imperial College London, London, UK

<sup>†</sup>sidwright@fhi-berlin.mpg.de

Magneto-optical trapping of molecules has thus far been restricted to molecules with  $^2\Sigma$  or  $^2\Sigma$ -like electronic ground states. These species are normally chemically reactive and difficult to produce, and in the case of diatomic molecules with  $^2\Sigma^+$  ground states, a simple laser cooling scheme exists only for the first excited rotational level.

In this talk, I will present the first magneto-optical trap (MOT) for a  $^1\Sigma^+$  ground state molecule, the diatomic species aluminium monofluoride (AlF). The intense  $A^1\Pi \leftarrow X^1\Sigma^+$  transition in AlF enables efficient optical cycling on any Q(J) rotational line, and we take advantage of this fact by demonstrating a MOT for three different excited rotational levels. Our results represent the shortest wavelength magneto-optical trap for any atom or molecule to date, and pave the way to highly precise spectroscopy on the spin-forbidden  $a^3\Pi \leftarrow X^1\Sigma^+$  transition in AlF.

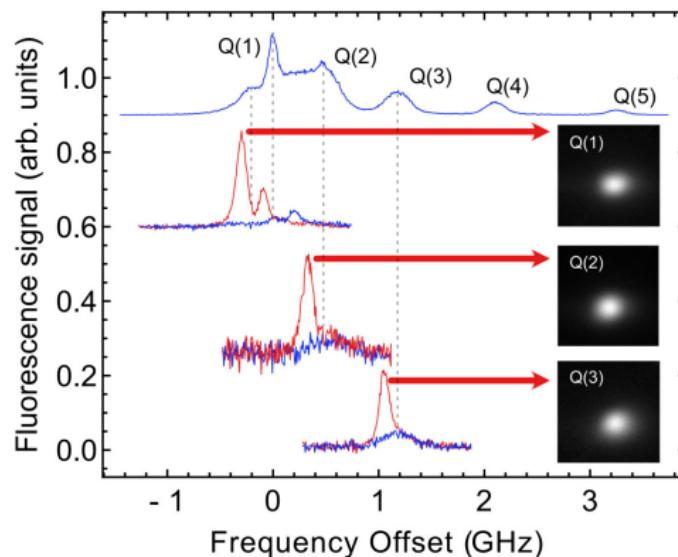


Figure 1: Magneto-optical trapping of AlF molecules. Upper spectrum: molecular beam fluorescence spectroscopy of the  $A^1\Pi, v = 0 \rightarrow X^1\Sigma^+, v = 0$  transition in AlF, showing the five lowest Q(J) lines. Lower spectra: fluorescence spectra of the MOT for three different rotational states. Red, solid lines: spectra with the circular polarisations of the trapping light configured for the MOT. Blue, solid lines: spectra with the circular polarisations of all trapping beams reversed. Dashed, grey lines show the position of resonance lines measured in the molecular beam. Insets show camera fluorescence images at the position of the fluorescence peak, for the MOT polarisation configuration.



Abstract number: HT7  
Friday 16:30-16:50

## ACES in orbit

Cacciapuoti L.<sup>†1</sup>, Pataria S.<sup>1</sup>, Peignier T.<sup>1</sup>, Plumaris M.<sup>1</sup>, Weinberg S.<sup>1</sup>, Bischoff U.<sup>2</sup>, Crescence P.<sup>2</sup>, Helm A.<sup>2</sup>, Kehr J.<sup>2</sup>, Lachaud R.<sup>2</sup>, Mitschke D.<sup>2</sup>, Niedermaier T.<sup>2</sup>, Esnault F. X.<sup>3</sup>, Léger B.<sup>3</sup>, Thulliez E.<sup>3</sup>, Massonnet D.<sup>3</sup>, Goujon D.<sup>4</sup>, Pittet J.<sup>4</sup>, Perri A.<sup>4</sup>, Wang Q.<sup>4</sup>, Liu S.<sup>5</sup>, Schaefer W.<sup>5</sup>, Schwall T.<sup>5</sup>, Prochazka I.<sup>6</sup>, Schlicht A.<sup>7</sup>, Schreiber U.<sup>7</sup>, Laurent P.<sup>8</sup>, Lilley M.<sup>8</sup>, Roze J.<sup>8</sup>, Wolf P.<sup>8</sup>, Gibble K.<sup>9</sup>, Salomon C.<sup>10</sup>

<sup>1</sup>European Space Agency, ESTEC, Noordwijk, The Netherlands

<sup>2</sup>Airbus Defence and Space, Friedrichshafen, Germany

<sup>3</sup>CNES, Toulouse, France

<sup>4</sup>Safran Timing Technologies SA, Neuchâtel, Switzerland

<sup>5</sup>Timetech, Stuttgart, Germany

<sup>6</sup>Czech Technical University in Prague, Prague, Czech Republic

<sup>7</sup>Technical University of Munich, Munich, Germany

<sup>8</sup>LTE, Observatoire de Paris-PSL, CNRS, LNE, Sorbonne Université, Université de Lille, Paris, France

<sup>9</sup>The Pennsylvania State University, University Park, USA

<sup>10</sup>Laboratoire Kastler Brossel, ENS, Paris, France

<sup>†</sup>Luigi.Cacciapuoti@esa.int

Atomic Clock Ensemble in Space (ACES) is an ESA (European Space Agency) mission that uses high performance clocks and links to test Einstein's theory of general relativity. From the International Space Station (ISS), the ACES payload will distribute a clock signal with fractional frequency instability and inaccuracy of  $1\text{-}2 \times 10^{-16}$  establishing a global network to compare clocks in space and on ground.

On 21 April 2025, ACES was launched to the ISS by a SpaceX Falcon 9 rocket and installed at the external payload facility of the Columbus module (see Fig. 1) using the robotic arm. From the ACES payload, the PHARAO clock, which uses laser cooled cesium atoms, and the active H-maser SHM will be compared to atomic clocks on ground using two time and frequency transfer systems, a link in the microwave domain (MWL) and a pulsed optical link (ELT). Connected to the ground terminals of the ACES MWL, the atomic clocks operated by LTE in France, PTB and Wettzell in Germany, NPL in the United Kingdom, JPL and NIST in the United States, and NICT in Japan are contributing to the ACES clock network. The ACES ground segment is then completed by satellite laser ranging stations (Wettzell, Graz, Herstmonceaux, Potsdam, Zimmerwald, etc.), which connect their clocks to ACES via the ELT optical link.



Figure 1: Figure 1: ACES installed at the external payload facility of the Columbus module and pointing towards the Earth (Credits: @ESA-NASA).

With a time instability of a few ps, the ACES microwave link will allow comparing clocks to  $1 \times 10^{-17}$ , opening unique opportunities to test general relativity and constrain dark matter models, but also to develop applications in relativistic geodesy, time & frequency metrology, and timescales distribution.

In this presentation, we will describe the progress on the ACES qualification and preliminary results in orbit.

Abstract number: HT8  
Friday 16:50-17:10

## Measurement of the $g$ factor of ground-state $^{87}\text{Sr}$ at the parts-per-million level using co-trapped ultracold atoms

Thekkepatt P.<sup>1</sup>, Digvijay<sup>1</sup>, Urech A.<sup>1,2</sup>, Schreck F.<sup>1,2</sup>, van Druten K.<sup>†1,2</sup>

<sup>1</sup>Van der Waals-Zeeman Institute, Institute of Physics, University of Amsterdam, The Netherlands

<sup>2</sup>QuSoft, Amsterdam, The Netherlands

<sup>†</sup>n.j.vandruten@uva.nl

We demonstrate nuclear magnetic resonance of optically trapped ground-state ultracold  $^{87}\text{Sr}$  atoms. Using a scheme in which a cloud of ultracold  $^{87}\text{Rb}$  is co-trapped nearby, see Fig. 1, we improve the determination of the nuclear  $g$  factor,  $g_I$ , of atomic  $^{87}\text{Sr}$  by more than two orders of magnitude, reaching accuracy at the part-per-million level. We achieve similar accuracy in the ratio of relevant  $g$  factors between Rb and Sr. This establishes ultracold  $^{87}\text{Sr}$  as an excellent linear in-vacuum magnetometer. These results are relevant for ongoing efforts towards quantum simulation, quantum computation and optical atomic clocks employing  $^{87}\text{Sr}$ , and these methods can also be applied to other alkaline-earth and alkaline-earth-like atoms.

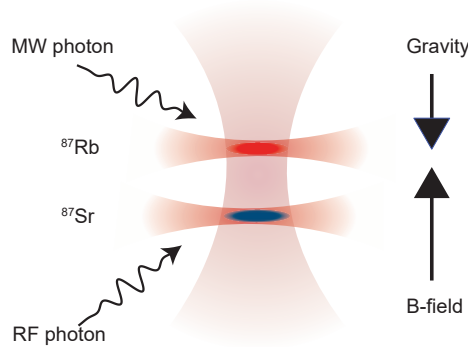


Figure 1: Schematic of the experimental setup used to measure  $g_I$  of  $^{87}\text{Sr}$  in the electronic ground state. Clouds of Rb and Sr atoms are confined in respective crossed optical dipole traps, where the (near-)vertical dipole trap beam is common to both traps. The microwave radiation is emitted using a dedicated microwave antenna, whereas the radio frequency radiation is emitted using coils carrying alternating current.

Abstract number: HT9  
Friday 17:10-17:30

## Dynamic Imaging Magnetic Fields with Yb Fluorescence

Hollberg L. H.<sup>†</sup>, Na Narong T., Li H., Tong J., Duenas, L.,  
Stanford University, Dept. of Physics and Dept. of Geophysics, Stanford, CA, USA

<sup>†</sup>leoh@stanford.edu

We observe unexpected dark stripes in bright green fluorescence from the  $^1S_0 - ^3P_1$  transition (556 nm) in a Yb atomic beam when excited by two (or more) resonant fields. This occurs when the two fields are resonant with Zeeman-split levels in the  $^3P_1$  state and both fields are “strong” relative to the saturation intensity (rather small  $I_{\text{sat}}=136 \mu\text{W}/\text{cm}^2$ ), Fig.1. In magnetic field gradients the dark-lines are contours of constant magnetic field. The  $^3P_1$  lifetime, 875 ns enables both good spatial resolution ( $\sim 100 \mu\text{m}$ ) and rapid ( $\sim 10 \mu\text{s}$ ) imaging of magnetic field dynamics with simple cameras. The dark stripes are reminiscent of the well-known CPT and EIT. But for Yb even isotopes in the V-configuration these dark lines result from different physics: predominantly the Autler-Townes AC-Stark splitting at all fields and at low fields the spatial Hanle effect.<sup>1,2</sup>

Experimental images guided our development of a theoretical model for the closed 4-level  $^1S_0 - ^3P_1$  transition that is driven by multiple “strong” optical fields, including the Zeeman structure and Doppler broadening. With the model and images, it’s possible to make scalar and vector magnetic field measurements at video frame rates over spatial dimensions of 5 cm (feasible up to meter) with 0.1 mm resolution. Two videos here<sup>3</sup> illustrate some unique capabilities of this Yb imaging magnetometer. This model allows direct computation of magnetic field tomography from images collected in experiments as well as generation of fluorescence images given B-field input. In principle, this Yb transition allows for  $\sim \mu\text{s}$  response times and a spatially imaging magnetic fields with a large dynamic range (from micro-tesla to many tesla).

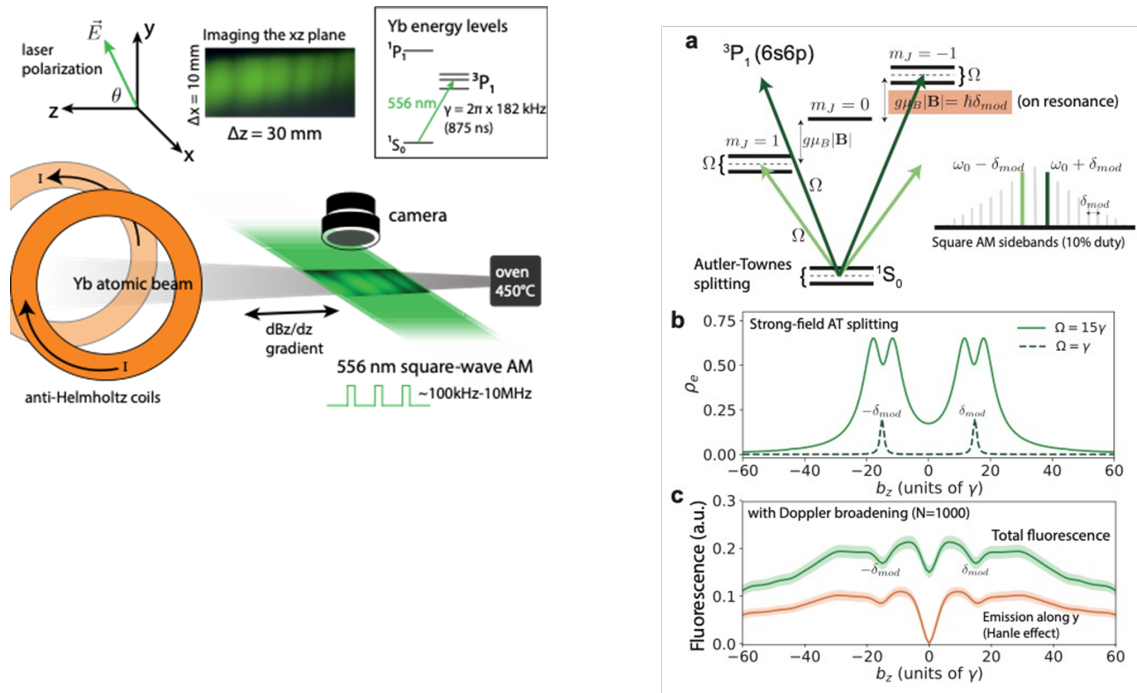


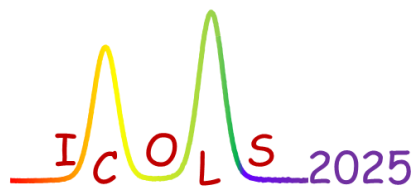
Figure 1: 1) Simple experimental system: Yb atomic beam, probed by a sheet of resonant laser modulated in time, camera, and magnetic field gradient. a)  $^3P_1$  levels split by Zeeman and Autler-Townes splitting on all three resonant V- levels. b) calculated fluorescence as function of  $|b_z|$  for two fixed frequency sidebands, both weak vs. strong, c) adding Doppler averaging. The central feature near  $|b_z|=0$  is due to the spatial Hanle effect.

<sup>1</sup>T. Na Narong, H.Li, J. Tong, M. Duenas, L. Hollberg, accepted for publication Phys Rev. Letts, (Apr. 2025), and <https://doi.org/10.48550/arXiv.2411.14426> . and videos ref. 3 below.

<sup>2</sup>Tanaporn Na Narong, PhD thesis, Stanford University (2023).

<sup>3</sup>[https://drive.google.com/drive/folders/12Kyw5\\_sI6B8Sh832fMSA5XTkmiKxQCqfN?usp=drive\\_link](https://drive.google.com/drive/folders/12Kyw5_sI6B8Sh832fMSA5XTkmiKxQCqfN?usp=drive_link)

*Poster session 1*  
*Abstracts*



Abstract number: P1  
Tuesday 14:00-15:30

## Exploring correlated hopping along a synthetic dimension in a strontium cavity QED system

Young D. J.<sup>1</sup>, Song E. Y.<sup>1</sup>, Chew S. H. P.<sup>1</sup>, Kwan J.<sup>1</sup>, Rey A. M.<sup>1, 2</sup>, Thompson J. K.<sup>†1</sup>

<sup>1</sup>JILA, NIST, and Department of Physics, University of Colorado, Boulder, CO, USA

<sup>2</sup>Center for Theory of Quantum Matter, University of Colorado, Boulder, CO, USA

<sup>†</sup>jkt@jila.colorado.edu

Cavity quantum electrodynamics (cavity QED) has emerged as a promising platform for quantum science, with a particular strength in engineering long-range correlations between atoms, leading to recent applications in quantum sensing, computing, and simulation. A recent theory proposal<sup>1</sup> discussed prospects for a new interaction for the cavity QED toolbox: correlated hopping of atoms within a manifold of hyperfine sublevels acting as a synthetic ladder of states. Extending previous demonstrations of pair creation in atom-cavity systems,<sup>2</sup> this proposed interaction induces atoms to coherently hop up or down several rungs of the ladder in pairs, fully exploring the multilevel synthetic dimension as shown in Fig. 1.

Here, we present progress towards engineering this physics in an ensemble of  $N = 2 \times 10^5$   $^{87}\text{Sr}$  atoms, which feature a ladder of 10 sublevels in the  $F = 9/2$  ground state manifold. By applying detuned drives and utilizing cavity-mediated photon exchange interactions, we aim to generate correlated hopping between sublevels while suppressing uncorrelated single-particle and collective Raman processes. Further, we plan to characterize correlations in sublevel populations through the use of nondestructive, state-dependent cavity readout techniques.

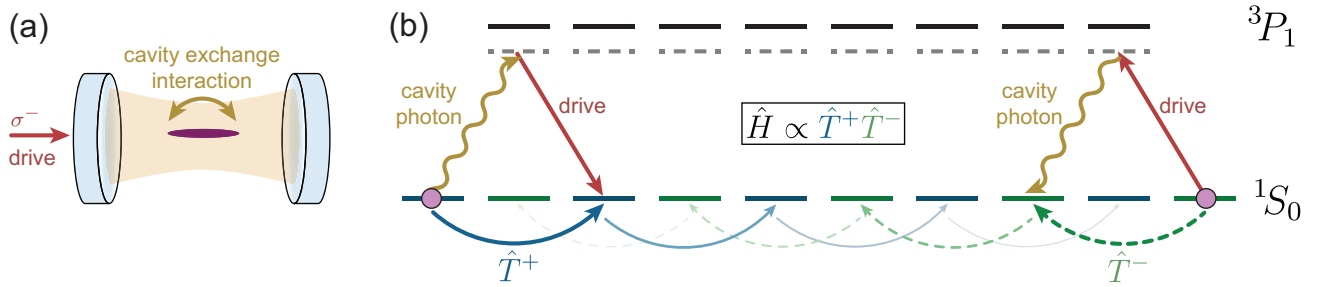


Figure 1: (a) We trap many  $^{87}\text{Sr}$  atoms in an optical cavity and shine a detuned  $\sigma^-$  polarized drive into the cavity. (b) This configuration induces a fourth order process where atoms undergo  $\Delta m = \pm 2$  hops in pairs by exchanging a photon through the cavity. This is analogous to pair creation physics at short times, but at longer times the dynamics is more complicated and explores the full manifold of states.

<sup>1</sup>A. Chu, A. Piñeiro Orioli, D. Barberena, J. K. Thompson, and A. M. Rey, *Phys. Rev. Res.* **5**, L022034 (2023)

<sup>2</sup>E. J. Davis, G. Bentsen, L. Homeier, T. Li, and M. H. Schleier-Smith, *Phys. Rev. Lett.* **122**, 010405 (2019)

Abstract number: P2  
Tuesday 14:00-15:30

## Towards continuous spectroscopy and superradiance

**Heizenreder B.**<sup>†1</sup>, **Famà F.**<sup>1</sup>, **Beli Silva C.**<sup>1</sup>, **Dubey S.**<sup>2</sup>, **Kazakov G. A.**<sup>2</sup>, **Zhou S.**<sup>1</sup>, **Jäger S. B.**<sup>3</sup>, **Schäffer S. A.**<sup>4</sup>, **Sitaram A.**<sup>1</sup>, **Schreck F.**<sup>1</sup>

<sup>1</sup>*Van der Waals-Zeeman Institute, Institute of Physics, University of Amsterdam, Science Park 904, 1098XH Amsterdam, Netherlands*

<sup>2</sup>*Atominstitut, TU Wien, Stadionallee 2, 1020 Vienna, Austria*

<sup>3</sup>*Physics Department and Research Center OPTIMAS, University of Kaiserslautern-Landau, 67663 Kaiserslautern, Germany*

<sup>4</sup>*Niels Bohr Institute, University of Copenhagen, Blegdamsvej 17, 2100 Copenhagen, Denmark*

<sup>†</sup>b.heizenreder@uva.nl

Superradiance, a collective phenomenon that enables lasing from narrow clock transitions, holds great promise for active optical clocks. We present two experimental setups designed for continuous superradiance.

In the first setup, we demonstrate collective strong coupling on the semi-forbidden  $^1S_0 \rightarrow ^3P_1$  transition of  $^{88}\text{Sr}$  using a collimated atomic beam and an optical single-mode cavity. Interrogation with an external drive reveals normal mode splitting for ground-state atoms<sup>1</sup> and up to 600% optical amplification for an inverted atomic sample, suggesting proximity to self-sustained lasing.

The second setup focuses on continuous superradiance with ultracold  $^{88}\text{Sr}$  atoms on the  $^1S_0 \rightarrow ^3P_0$  clock transition, achieved by opening the transition with a magnetic field. Superradiant emission is simulated using parameters inspired by our apparatus<sup>2</sup>. Experimentally, we aim to achieve continuous operation by spatially, rather than temporally, separating the laser cooling steps<sup>3</sup>. We also propose an advanced loading scheme for quasi-continuous, long-distance transport, based on a two-stage MOT combined with a Bloch accelerator technique. Towards this goal, we are exploring a new method of position-dependent spectroscopy with our second-stage MOT and combining it with a new generation of frequency comb to create a long-term stable 10 MHz source.

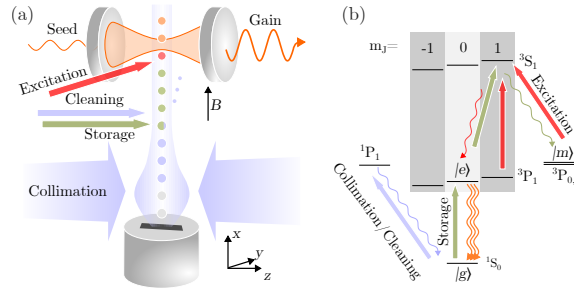


Figure 1: (a) Schematic of the first setup. An oven emits an atomic beam of  $^{88}\text{Sr}$  atoms through a nozzle. The beam is then collimated by an optical molasses. Next, the atoms are transferred from the ground state  $|g\rangle = ^1S_0$  to the upper lasing state  $|e\rangle = ^3P_{1,m_j=0}$  through a 3-step process: 1) storage, by optical pumping to the metastable states  $|m\rangle = ^3P_{2,0}$ ; 2) cleaning, by accelerating the remaining  $^1S_0$  atoms to velocities along the cavity axis at which they are irrelevant; and 3) excitation, by optically pumping atoms from  $|m\rangle$  to  $|e\rangle$ . Finally, the prepared sample traverses the TEM<sub>00</sub>-mode of a bad-cavity optical resonator. (b) Relevant level structure of the Sr atoms. We specify wavelengths and polarizations used in the collimation and 3-step sequence. For clarity, some optical pumping transitions are not shown.

<sup>1</sup>F. Famà *et al.*, Phys. Rev. A **110**, 063721 (2024).

<sup>2</sup>S. Dubey *et al.*, arXiv:2409.06575 (2024).

<sup>3</sup>C. Chun-Chia, *et al.*, Nature **606**, 683–687 (2022).

Abstract number: P3  
Tuesday 14:00-15:30

## Enhanced Sensitivity of Coherent Anti-Stokes Raman Spectroscopy via SU(1,1) Interferometry

Kumar T., Shukla G., Mishra D. K.<sup>†</sup>

Department of Physics, Institute of Science, Banaras Hindu University, Varanasi-221005, Uttar Pradesh, India.

<sup>†</sup>kndmishra@gmail.com

Quantum technologies like quantum sensors, quantum imaging, and chemical sensing require precise measurements. Quantum metrology achieves higher precision than classical methods by using quantum features of light. In particular, quantum optical interferometers such as the Mach-Zehnder interferometer (MZI) and SU(1,1) interferometers have become essential tools in quantum metrology. One field that got advantages from these progresses is Raman spectroscopy, which is a powerful tool for the identification of material by detecting its molecular vibrations. However, it is limited by weak signal intensity and non-resonant background noise caused by the surrounding molecules. To address these issues, coherent anti-Stokes Raman spectroscopy (CARS) was developed using nonlinear processes (four-wave mixing (FWM)) to increase signal intensity. However, it is also limited by the shot-noise limit (SNL) and struggles with non-resonant backgrounds (such as the solvent), when investigating diluted samples. Michael *et.al.*<sup>1</sup> have proposed a squeezing-enhanced CARS using an SU (1,1) interferometer to increase sensitivity by using single-intensity detection. We explored its performance under sum-intensity detection and homodyne detection schemes, aiming to find the possibility of further enhancement in sensitivity and suppression of non-resonant backgrounds. In addition, to provide the ultimate theoretical precision limit, we have calculated the quantum Cramér-Rao bound (QCRB).

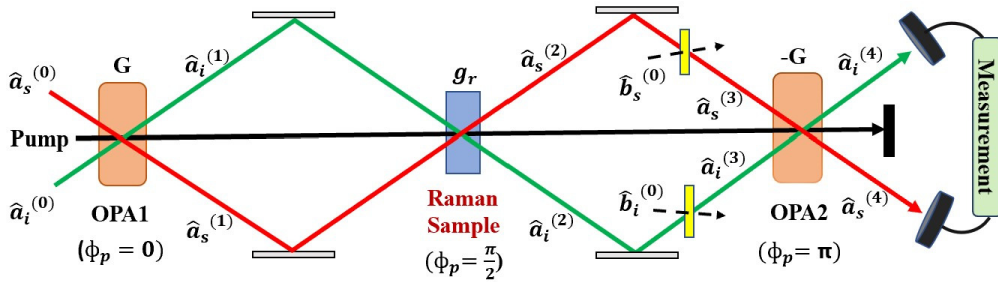


Figure 1: Squeezing-enhanced CARS with internal photon loss which is modeled by a fictitious beam splitter with reflection and transmission coefficients,  $|r|$  and  $|t|$ , respectively, in both arms.

The Raman sample (acting as a weak parametric amplifier via Raman-based FWM) is placed inside an SU(1,1) interferometer, seeded by a coherent idler in the presence of internal photon loss, as shown in the figure. When non-resonant light is produced by OPA1 and OPA2 (e.g., via photonic crystal fibers, etc.), the resonant Raman amplification of the sample occurs at  $90^\circ$  without requiring additional phase adjustment. The Raman sample can be considered as a mixture of infinitesimal parametric amplifiers that perform either resonant amplification from the target molecules or non-resonant amplification from background substances. The non-resonant contribution is eliminated through gain balancing. The transformation between field operators of the signal and idler through OPA1, Raman sample, and OPA2 can be described using the Bogoliubov transformation. We perform the sum-intensity detection and the homodyne detection at the signal port to determine the minimum detectable Raman gain  $g_{\min}$ , by using the error propagation formula, which is compared with that in the single-intensity detection scheme, SNL and QCRB.

Our analysis shows homodyne detection performs better than sum-intensity and known single-intensity detection scheme results. It also provides a broader working range and shows more robustness against internal photon losses and remarkably improved performance in the gain-imbalanced configuration of the SU(1,1) interferometer. In addition, sensitivity under homodyne detection approaches QCRB when both OPAs are exactly crossed. As a result, we expect that our findings will be useful in quantum sensing and imaging techniques. This work is based on our recent publication<sup>2</sup>.

<sup>1</sup>Michael Y, Bello L, Rosenbluh M, and Pe'er A., *npj Quantum Inf* **5**, 81 (2019).

<sup>2</sup>Kumar T, Shukla G, and Mishra DK *Applied Physics B* **131**, 25 (2025).



Abstract number: P4  
Tuesday 14:00-15:30

## 3D-Printed Optical Cavity for Laser Stabilization

**Mondal S.**<sup>1†</sup>, Wayland J.<sup>1</sup>, Hughes J.<sup>2</sup>, Kale Y.<sup>1</sup>, Coles L.A.<sup>3</sup>, Jerrard P.<sup>4</sup>, Clark C.<sup>5</sup>, Papastavrou M.<sup>3</sup>, Irvine F.<sup>5</sup>, Wallace G.<sup>5</sup>, Sharp J.<sup>5</sup>, Boudet A.<sup>5</sup>, Sun Q.<sup>6</sup>, Singh A. K.<sup>6</sup>, Gilks D.<sup>6</sup>, Singh Y.<sup>1</sup>

<sup>1</sup>School of Physics and Astronomy, University of Birmingham, Edgbaston, Birmingham, B15 2TT, UK

<sup>2</sup>M Squared Lasers Limited, 1 Kelvin Campus, West of Scotland Science Park, G20 0SP, Glasgow, UK

<sup>3</sup>Metamorphic Additive Manufacturing Ltd., Riverside Chambers, Derby, Derbyshire, DE1 3AF, UK

<sup>4</sup>3T Additive Manufacturing Ltd., Greenham Business Park, Unit 101, RG19 6HN, Warehouse Road, UK

<sup>5</sup>Helia Photonics Ltd, Rosebank Park, Livingston, West Lothian, EH54 7EJ, Scotland, UK

<sup>6</sup>British Telecommunications PLC, 1 Braham Street, London, E1 8EE, UK

†[s.mondal.1@bham.ac.uk](mailto:s.mondal.1@bham.ac.uk)

Stable and narrow-linewidth lasers are critical for high-precision applications in atomic physics, quantum metrology, and optical clocks. Optical cavities serve as high-fidelity frequency references, significantly improving laser frequency stability by providing a well-defined optical resonance. We demonstrated a novel 3D-printed<sup>1</sup> optical cavity shown in figure 1 using additive manufacturing (AM), optimized for laser stabilization. The cavity spacer is fabricated from low thermal expansion Invar, mitigating thermal fluctuations that typically degrade long-term frequency stability. The cavity achieves a finesse of 1000 and the cavity is well-suited for precision atomic clocks (Strontium at 689 nm),

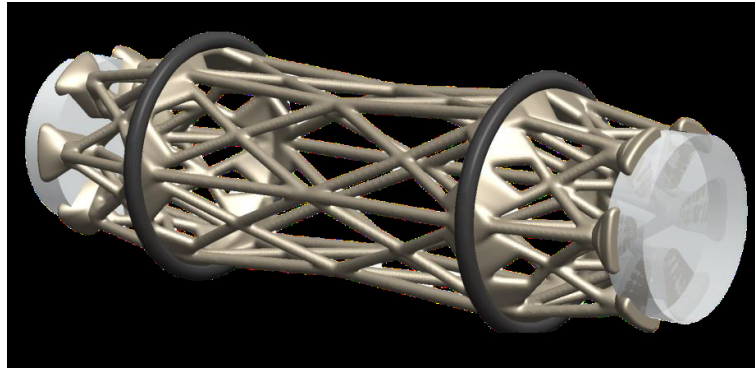


Figure 1: Design of 3D-printed optical cavity with mirrors

In laser stabilization, cavity locking offers several advantages over spectroscopy-based locking techniques. While spectroscopy locking relies on atomic or molecular resonances, it is often limited by Doppler broadening and requires complex frequency modulation schemes. In contrast, cavity locking provides a much narrower and more stable reference, enabling improved short-term and long-term frequency stability. The Pound-Drever-Hall (PDH)<sup>2</sup> technique is commonly employed to lock lasers to optical cavities, allowing suppression of frequency noise at levels required for precision metrology and quantum technologies<sup>3,4</sup>. Additionally, optical cavities enable stabilization at arbitrary frequencies, unlike atomic spectroscopy, which is constrained to discrete atomic transitions.

The use of AM in fabricating high-precision optical reference cavities presents a transformative approach to laser stabilization. Traditional cavity manufacturing processes involve expensive and labor-intensive machining, whereas 3D printing allows for rapid prototyping, complex geometries, and reduced costs. These advantages make this cavity a viable solution for developing compact, thermally stable, and cost-effective frequency-stabilization systems for emerging quantum technologies.

<sup>1</sup>Wang, F. et al., *Quantum Science and Technology* **10**, article number (2024).

<sup>2</sup>Idjadi, M.H., Aflatouni, F., *Nature Communications* **8**, article number (2017)

<sup>3</sup>Drever, R.W.P., et al. *Applied Physics* **31**, article number (1983)

<sup>4</sup>Young, B. C. et al., *Physical Review Letters* **82**, article number (1999)



Abstract number: P5  
Tuesday 14:00-15:30

# Quantum logic control of transition metal and molecular ions

Rehmer T.<sup>1,2</sup>, Zawierucha M. J.<sup>1,2</sup>, Dietze K.<sup>1,2</sup>, Schmidt P. O.<sup>1,2</sup>, Wolf F.<sup>†1</sup>  
<sup>1</sup>QUEST Institute, Physikalisch-Technische Bundesanstalt (PTB), Braunschweig, Germany  
<sup>2</sup>Institut für Quantenoptik, Leibniz Universität Hannover, Hannover, Germany  
<sup>†</sup>fabian.wolf@ptb.de

Extending quantum control to increasingly complex systems is essential for advancing quantum technologies and fundamental physics. In particular, laser cooling and manipulation have significantly enhanced precision spectroscopy, driving major developments in our understanding of fundamental physics. However, only a limited number of atomic and molecular species possess suitable transitions for laser cooling, restricting the range of accessible species. This limitation can be overcome in trapped-ion systems using quantum logic spectroscopy, a technique that exploits methods originally developed for quantum information processing. By coupling a spectroscopy ion, chosen for its favorable spectroscopic properties, with a logic ion that allows for precise control and readout, quantum logic spectroscopy enables high-precision measurements even for species that are inaccessible to direct laser cooling. This approach has already been successfully demonstrated in the aluminum optical clock<sup>1</sup> and the first clock based on a highly charged ion<sup>2</sup>.

Our primary research goal is to establish a quantum control toolbox for diatomic molecular ions, with applications in precision spectroscopy and tests of fundamental symmetries. In a first step, we have demonstrated non-destructive rotational state detection of a molecular ion<sup>3</sup>. Spontaneous Raman scattering – limiting state preparation in this scheme – can be overcome by replacing the near-detuned Raman laser with a far-detuned one<sup>4</sup>.

In our experiment, we use  $^{40}\text{Ca}^+$  as the logic ion and  $^{24}\text{MgH}^+$  as the spectroscopy ion. As we progress toward quantum logic spectroscopy of single molecular  $\text{MgH}^+$  ions, we are also exploring the applicability of these techniques to other ionic species. Recently, we have demonstrated quantum logic control of a single atomic titanium ion<sup>5</sup>, achieving state detection (see Fig. 1a and b) and coherent control (see Fig. 1c) of different Zeeman manifolds within the  $a^4\text{F}$  groundstate as well as precise measurements of the corresponding Landé g-factors. The universal applicability of the Raman laser approach facilitates the extension of these methods to other qubit systems, including a large variety of molecular and atomic ions. By enhancing control over these systems, our work paves the way for novel applications in quantum technology and fundamental physics, making an entirely new class of ions accessible to precision-spectroscopy.

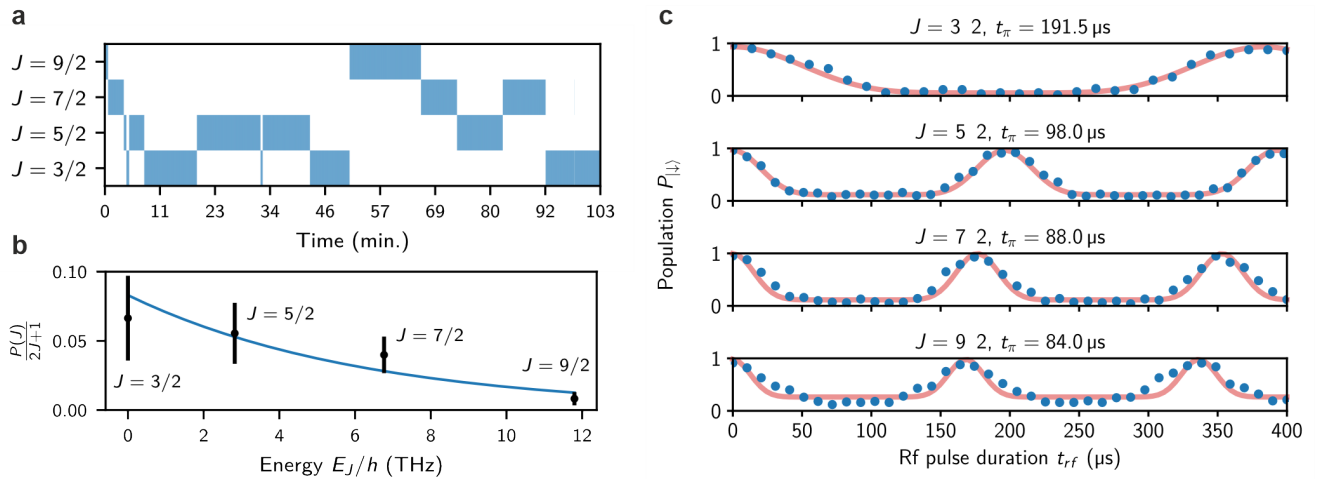


Figure 1: **a** Real-time state tracking of the finestructure state of a single  $^{48}\text{Ti}^+$  ion. **b** Measured dwell time  $P(J)$  in finestructure state  $|J\rangle$ , inversely weighted by the degeneracy factor  $2J + 1$  for a measurement time of around 16 h. The blue line shows a theoretical Boltzmann distributions for thermal equilibrium in a 300 K environment. **c** Coherent spin rotations of the four groundstate finestructure components.

<sup>1</sup>S. M. Brewer *et al.*, Physical Review Letters **123**, 033201 (2019).

<sup>2</sup>S. A. King *et al.*, Nature **611**, 43-47 (2022).

<sup>3</sup>F. Wolf, Y. Wan, J. C. Heip, F. Gebert, C. Shi, P. O. Schmidt, Nature **530**, 457-460 (2016).

<sup>4</sup>C. W. Chou, C. Kurz, D. B. Hume, P. N. Plessow, D. R. Leibbrandt, D. Leibfried, Nature **545**, 203-207 (2017).

<sup>5</sup>T. Rehmer, M. J. Zawierucha, K. Dietze, P. O. Schmidt, F. Wolf, arXiv:2410.07936 (2024)

Abstract number: P6  
Tuesday 14:00-15:30

## Cavity-enhanced spectroscopy of H<sub>2</sub> in a deep cryogenic regime

Stankiewicz K.<sup>1</sup>, Makowski M.<sup>1</sup>, Słowiński M.<sup>1</sup>, Sołtys K.L.<sup>1</sup>, Bednarski B.<sup>1</sup>, Józwiak H.<sup>1</sup>, Stolarczyk N.<sup>1</sup>, Narożnik M.<sup>1</sup>, Kierski D.<sup>1</sup>, Wójtewicz S.<sup>1</sup>, Cygan A.<sup>1</sup>, Kowzan G.<sup>1</sup>, Masłowski P.<sup>1</sup>, Piwiński M.<sup>1</sup>, Lisak D.<sup>1</sup>, Wcisło P.<sup>1</sup>

<sup>1</sup>*Institute of Physics, Faculty of Physics, Astronomy and Informatics, Nicolaus Copernicus University in Toruń, Toruń, Poland*

†503474@doktorant.umk.pl

We demonstrate the first cavity-enhanced spectrometer fully operating in a deep cryogenic regime down to 4 K. Not only the sample but the entire cavity, including the mirrors and cavity length actuator<sup>1</sup>, is uniformly cooled down ensuring the thermodynamic equilibrium of a gas sample. The setup is designed in a way that efficiently attenuates both external vibrations and those originating from the cryocooler itself ensuring stable operation of the optical cavity. Thermodynamic equilibrium and high tunability of pressure, temperature as well as high tunability of wavelength by implementation of an optical parametric oscillator opens the way to a variety of fundamental and practical applications.

We perform accurate Doppler-limited spectroscopy of the S(0) 1-0 line in molecular hydrogen, achieving accuracy at the level of  $10^{-6}$  cm<sup>-1</sup>. We demonstrated the first optical realization of three SI units in a difficult to access 4 - 20 K temperature regime: temperature (kelvin), amount of substance per unit volume (mole · meter<sup>-3</sup>) and pressure (pascal). We optically measured a part of the H<sub>2</sub> phase diagram covering over three orders of magnitude in pressure. This considerably improved the accuracy of the previous best p(T) curve. We also determined using optical methods the conversion of the ortho-para H<sub>2</sub> spin isomers with high temporal resolution.

---

<sup>1</sup>M. Słowiński, M. Makowski, K. L. Sołtys, K. Stankiewicz, S. Wójtewicz, D. Lisak, M. Piwiński and P. Wcisło, *Rev. Sci. Instrum.* **93**, 115003 (2022)

Abstract number: P7  
 Tuesday 14:00-15:30

## Metastable two-dimensional Coulomb crystals

Mizukami N.<sup>1,2</sup>, Gatta G.<sup>2,3</sup>, Duca L.<sup>1,2</sup>, Sias C.<sup>†1,2</sup>

<sup>1</sup>*Istituto Nazionale di Ricerca Metrologica, INRIM, Torino, Italy*

<sup>2</sup>*European Laboratory for Nonlinear Spectroscopy, LENS, Sesto Fiorentino, Italy*

<sup>3</sup>*University of Florence, Firenze, Italy*

<sup>†</sup>c.sias@inrim.it

Particles with long-range repulsive interactions form, at a sufficient low temperature, spatially ordered crystals, the shape of which depends from the frequencies of the confining potential. Under specific conditions, the system exhibits bistability, i.e. two distinct metastable configurations can coexist<sup>1,2</sup>, and transitions between them may be driven by thermal fluctuations<sup>3</sup>.

In this work, we investigate bistability in two-dimensional Coulomb crystals composed of Ba<sup>+</sup> ions confined in a two-dimensional plane. Using Monte Carlo simulations, we calculate the energies of different configurations and reveal a double-well structure, where the relative depth of each well — each corresponding to a metastable configuration — can be tuned by adjusting the trap aspect ratio.

Experimentally, we realize a crystal of six ions and identify a bistable regime in which the ions arrange either in a hexagonal configuration or in a pentagonal configuration with one ion at the center the trap (see Fig. 1). We observe bistability through photon scattering and find that the probability of occupying the lower-energy configuration increases with the energy imbalance between the two wells.

Furthermore, by quenching the trap aspect ratio, we can populate a highly excited metastable configuration and witness its relaxation dynamics. Through configuration-resolved detection with sub-millisecond time resolution, we observe the exponential decay of the system toward the lowest-energy state.

Our study establishes a new platform to explore phenomena such as second-order phase transitions and quantum superpositions of crystalline configurations, and provides insights into defect formation in two-dimensional Coulomb crystals.

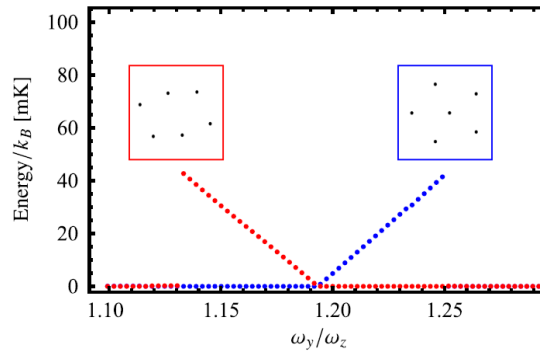


Figure 1: Energies of the metastable crystal configurations of 6 ions as a function of the confining potential aspect ratio. Depending on the trap aspect ratio  $\omega_y/\omega_z$ , a Coulomb crystal can have two different configurations: a pentagon shape (blue dots) and an hexagon configuration (red dots). The energy of the configurations are found by using a Monte Carlo simulation. For each value of  $\omega_y/\omega_z$ , an offset equal to the lowest energy configuration is subtracted to both configurations energies.

<sup>1</sup>H. Oike *et al.*, *Nature Phys.* **12**, 62 (2016).

<sup>2</sup>D. Kiesenhofer *et al.*, *PRX Quantum* **4**, 020317 (2023).

<sup>3</sup>P. Haenggi, P. Talkner, and M. Borkovec, *Rev. Mod. Phys.* **62**, 251 (1990).

Abstract number: P8  
Tuesday 14:00-15:30

## High precision measurement of atom number in a mesoscopic cold atomic ensemble using fluorescence imaging

**Yadav P.<sup>1</sup>, Singh N.<sup>1</sup>, Santra B.<sup>1</sup>**

<sup>1</sup>*Indian Institute of Technology Delhi, New Delhi, India*

<sup>†</sup>Poonam.Yadav@physics.iitd.ac.in, bsantra@physics.iitd.ac.in

The technique of laser cooling and trapping of neutral atoms has emerged as a powerful tool, enabling various research pursuits and applications including precision spectroscopy, quantum information processing, atom interferometry, and quantum computing. To harness the full potential of cold atom systems in evolving technologies, characterizing the losses occurring during accurate atom counting becomes crucial. Here, we investigate the limiting noise sources existing during the detection of an ensemble of cold  $^{133}\text{Cs}$  atoms by measuring the two-sample atom variance, which captures both fluorescence noise and atom number fluctuations arising from atom loss. Upon identifying the photon shot noise and additional noise common to all atoms in the cloud, we have deduced the loss compensated atom number. We then study the influence of atom loss dynamics during fluorescence imaging of an ensemble of cold atoms in free space. We measure the one-body loss rate constant,  $\gamma$ , due to collisions with the background gases, and two-body loss rate constant,  $\beta$ , arising from inelastic collisions due to light assisted collisions. We further study the loss rates at different detunings of the imaging light. These investigations help in counting the accurate atom numbers in free space. Our study paves the way to achieve high-fidelity read out of quantum states for applications in quantum computing and sensing.

Abstract number: P9  
Tuesday 14:00-15:30

## Second-long light-pulse interferometry at pKs

**Rasel E. M.**<sup>†1</sup> for the QUANTUS and MAIUS, q-gyro, CARIOQA-PMP, terra-Q and dq-mat cooperation

<sup>1</sup>*Leibniz Universität Hannover and Excellence Cluster Quantum Frontiers Welfengarten 1, 30167 Hannover, Germany,  
+49 511 19203*

<sup>†</sup>rasel@iqo.uni-hannover.de

In recent years experiments pioneered generation of and light-pulse interferometry with quantum gases in space. The duration of the free fall of atoms in light-pulse interferometers is a strong lever for the achievable precision. We demonstrate interferometers in the drop tower where atoms are coherently split for seconds, which has been so far only reached in large atomic fountains, and investigate the spatial coherence of the ensembles. The interferometers are operated with Bose-Einstein condensates enabling protocols to reach extremely low expansion energies. We exploit our interferometer to analyse the imperfections of our protocols and contrast it with a model of our magnetic lens. The demonstrated methods are of interest for inertial quantum sensors as proposed for satellite gravimetry and investigated by the EU project CARIOQA-PMP. Moreover, the development of those methods is enormously accelerated by new facilities, namely Gravitowers and Einstein Elevators, considerably extending the rate of microgravity experiments. As a first step we compare the performance of our apparatus in the drop tower and Gravitower in Bremen.

Abstract number: P10

Tuesday 14:00-15:30

## Discrete time crystals with bouncing potassium Bose-Einstein condensates

**Zaheer A.<sup>1</sup>, Bouras M.<sup>1</sup>, Gunawardana C.<sup>1</sup>, Singh A.<sup>1</sup>, Giergiel K.<sup>2</sup>, Sacha K.<sup>3</sup>, Sidorov A.<sup>†1</sup>, Hannaford P.<sup>1</sup>**

<sup>1</sup>*Optical Sciences Centre, Swinburne University of Technology, Melbourne, Australia*

<sup>2</sup>*CSIRO Manufacturing, Melbourne, Australia*

<sup>3</sup>*Institute of Theoretical Physics, Jagiellonian University, Krakow, Poland*

<sup>†</sup>asidorov@swin.edu.au

Recently, a great interest has been devoted to proposals and the realizations of time crystals where a periodically driven many-body system spontaneously breaks time-translation symmetry and exhibits an ultra-stable subharmonic motion locked to and synchronized with the periodic drive. These time crystals will be robust against external perturbations and may be useful in quantum technology applications.

Our project aims to experimentally demonstrate that weakly interacting Bose condensed atoms bouncing on a periodically driven atomic mirror can break time-translational symmetry to form a discrete time crystal<sup>1</sup>. The resonantly tuned bouncing ensemble can evolve along long-lived stable orbits with a period multiple times larger than the driving period, thus exhibiting subharmonic oscillations and creating a large number of atomic lattice sites in the time domain. Our approach<sup>2</sup> is based on the use of potassium-39 atoms which have several broad Feshbach resonances to precisely tune attractive atomic interactions in the vicinity of the zero crossing. We employ a two-dimensional (2D) magneto-optical trap (MOT) to load a 3D MOT with about  $10^9$  potassium atoms cooled down to 2.6 mK temperature. The small hyperfine splitting of the excited state prevents laser cooling to reach the Doppler limit; so we consequently employ a hybrid D2/D1 MOT and grey molasses on the D1 line to cool the atoms down to 6  $\mu$ K temperature. Then we load the cold atomic ensemble to a 1064 nm crossed-beam dipole trap and we have recorded four broad Feshbach resonances at 32.6, 59, 163 and 403 G magnetic fields. We use the 32.6 G Feshbach resonance for the evaporative cooling of the potassium-39 atoms and will report our progress towards achieving quantum degeneracy in the optical dipole trap.

In our approach we will explore bouncing of the Bose condensed atomic ensemble dropped from about 150  $\mu$ m onto the atomic mirror made from a 532 nm fibre laser beam and modulated with 2.8 kHz frequency. The mirror modulation synchronized with the atomic bouncing period can form 30 stable wavepackets (the temporal lattice sites) which maintain their shapes bouncing from the driven mirror. If the scattering length is tuned to a small negative value (about  $-1.6a_0$ ) tunneling between neighboring lattice sites is suppressed and a big discrete time crystal ( $s = 30$ ) will be formed. The creation of time crystals occupying a large number of temporal lattice sites will offer great opportunity to perform condensed matter physics phenomena in the time domain including “time-tronics”<sup>3</sup> – a time-based analogue of electronics or atom-tronics.

<sup>1</sup>K. Sacha, *Physical Review A* **98**, 013613 (2015).

<sup>2</sup>K. Giergiel *et al.*, *New Journal of Physics* **22**, 085004 (2020).

<sup>3</sup>K. Giergiel, P. Hannaford and K. Sacha, *arXiv*: 2406.06387 (2024).

Abstract number: P11  
 Tuesday 14:00-15:30

## High resolution spectroscopy of molecules confined in gas cells of sub-wavelength thickness

Mouhanna H.<sup>1,2</sup>, Garcia Arellano G.<sup>1,2</sup>, de Aquino Carvalho J. C.<sup>1,2</sup>, de Melo N.<sup>1,2</sup>, Challali F. C.<sup>3</sup>, du Burck F.<sup>1,2</sup>, Maurin I. C.<sup>1,2</sup>, Darquié B.<sup>1,2</sup>, Laliotis A.<sup>†1,2</sup>

<sup>1</sup>Laboratoire de Physique des Lasers, Université Sorbonne Paris Nord, F-93430, Villetaneuse, France

<sup>2</sup>CNRS, UMR 7538, LPL, 99 Avenue J.-B. Clément, F-93430 Villetaneuse, France

<sup>3</sup>Laboratoire des Sciences des Procédés et des Matériaux, UPR CNRS 3407, Université Sorbonne Paris Nord, France

†laliotis@univ-paris13.fr

Miniaturized atomic vapor cells of nanometric thickness have become promising platforms for fundamental measurements, metrology and quantum technologies. For example, nanometric cells have been used for exploring Dicke-type effects of confinement<sup>1</sup>, measuring Casimir-Polder interactions, fabricating compact atomic clocks and probing collective effects. Extending these experiments to molecular gases is a fascinating prospect for applications in compact frequency referencing and for testing fundamental quantum electrodynamics using increasingly complex quantum objects. Towards this end, experiments have been performed with platforms such as hollow core fibers, tapered nanofibers and integrated waveguides. Moreover, selective reflection experiments with molecules have also been performed<sup>2</sup>.

Here, we present our pioneering experiments probing molecular rovibrations of gases confined in micro-metric cells, whose thickness is comparable to the excitation wavelengths. We work in two distinct regions of the electromagnetic spectrum, probing  $\nu_1 + \nu_3$  resonances of acetylene at  $1.530\ \mu\text{m}$ , within the telecommunications wavelength range, as well as the  $\nu_3$  and  $\nu_2$  resonances of  $\text{SF}_6$  and  $\text{NH}_3$  respectively, in the mid-infrared fingerprint region around  $10.55\ \mu\text{m}$ . Thin-cell confinement allows us to explore and demonstrate Dicke-narrowing effects, probing molecules with linear sub-Doppler transmission spectroscopy. Our first experiment, reported recently in Nature Communications<sup>3</sup> uses a cell with a thickness that varies between  $5.2\text{-}5.5\ \mu\text{m}$ . This corresponds to  $7\lambda/2$  and  $\lambda/2$  thickness for acetylene and  $\text{SF}_6$  or  $\text{NH}_3$  rovibrations respectively. We also report measurements in a second cell of thickness ranging from  $600\text{-}1200\ \text{nm}$  allowing us to explore tighter molecular confinement. The transmission spectra displaying sub-Doppler characteristics due to the coherent Dicke narrowing are analyzed by means of a theoretical model<sup>4</sup> making specific assumptions about the physics and dynamics of confined molecules. In all the above measurements, the model reproduces exceptionally well the experimental data.

We focus our analysis on both the absolute signal amplitude and spectral lineshape. This allows us to confirm, within the limits of our precision, the hypotheses concerning the collisions with the cell-windows, the Maxwell-Boltzmann thermal distribution of velocities and the rotational redistribution (Boltzmann repartition function) of molecules after desorption from the wall. This is an important result, as the equilibrium conditions of confined gases have been put into question<sup>5</sup>. Furthermore, our analysis confirms that our spectroscopic technique can be used to determine molecular transition strengths and therefore enrich molecular databases. We demonstrate this by providing new data on the  $\text{SF}_6$  greenhouse molecule for which databases are notoriously incomplete.

A major perspective resulting from this work is the measurement of Casimir-Polder interactions with molecules. For this purpose, we are currently building a new experiment to probe the strong HF rovibration at  $2.5\ \mu\text{m}$ . This experiment will allow us to probe strongly confined HF gas in a nanocell ( $100\text{nm}$  thickness) and measure the effects of molecular orientation in Casimir-Polder interactions.

<sup>1</sup>G. Dutier *et al.*, *Europhys. Lett. EPL*, **63**, 35–41 (2003).

<sup>2</sup>J. Lukusa Mudiayi *et al.*, *Phys. Rev. Lett.*, **127**, 043201 (2021).

<sup>3</sup>G. Garcia Arellano *et al.*, *Nat. Commun.*, **15**, 1862 (2024).

<sup>4</sup>G. Dutier, S. Saltiel, D. Bloch, M. Ducloy, *J. Opt. Soc. Am. B*, **20**, 793 (2003).

<sup>5</sup>P. Todorov and D. Bloch, *J. Chem. Phys.*, **147**, 194202 (2017).

Abstract number: P12  
Tuesday 14:00-15:30

## Spectroscopic measurements of the Rydberg-surface Casimir-Polder interaction

Butery E.<sup>1,2</sup>, Dutta B.<sup>1,2</sup>, Boldt C.<sup>3</sup>, Santos S.<sup>1,2</sup>, Pedri P.<sup>1,2</sup>, Scheel S.<sup>3</sup>, Laliotis A.<sup>†1,2</sup>

<sup>1</sup>Laboratoire de Physique des Lasers, Université Sorbonne Paris Nord, F-93430, Villetaneuse, France

<sup>2</sup>CNRS, UMR 7538, LPL, 99 Avenue J.-B. Clément, F-93430 Villetaneuse, France

<sup>3</sup>Institut für Physik, Universität Rostock, Albert-Einstein-Straße 23-24, D-18059 Rostock, Germany.

<sup>†</sup>laliotis@univ-paris13.fr

Highly excited (Rydberg) atoms have exaggerated properties making them extremely sensitive to external electromagnetic fields and interacting strongly with their environment. Atomic vapor cells represent an attractive platform for studying Rydberg atoms and fabricating quantum devices. For example, Rydberg atoms in vapor cells have been used as sensitive detectors of electric fields of frequencies ranging from DC up to the THz range but also as single photon sources for quantum technology applications exploiting collective phenomena due to the Rydberg blockade effect <sup>1</sup>.

Rydberg atoms also find applications in fundamental physics, in particular for the measurement of dispersive interactions of the Casimir-Polder type (atom-surface interactions) <sup>2</sup> or of the van der Waals type (atom-atom interactions). One major advantage of Rydberg atoms is that they expose limitations in the traditional perturbative approach of Casimir-Polder (CP) theory <sup>3,4</sup>. Indeed, in the extreme near-field (i.e. when the atomic radius is no longer negligible compared to the atom-surface distance), the dipole approximation breaks down and higher-order terms need to be considered. Our recent theoretical study on Rydberg-surface interactions has provided calculations of the dipole-dipole terms that scale as  $-C_3/z^3$  as well as quadrupole-quadrupole and dipole-octupole terms that scale as  $-C_5/z^5$ , clearly demonstrating that higher order terms could be experimentally relevant in vapor nanocell spectroscopy <sup>4</sup>.

Here, we report on extensive experimental measurements of the Rydberg-surface interaction using spectroscopy in cesium vapor nanocells of a thickness ranging roughly from 200-700nm, as well as selective reflection spectroscopy on a macroscopic cesium all-sapphire cell. Atoms are first excited to the  $Cs(6P_{1/2})$  level with a 894nm pump laser and subsequently a green laser  $\approx 510$ nm probes Rydberg  $nD_{3/2}$  or  $nS_{1/2}$  states, where the principal quantum number  $n$  ranges between 15-17. Our experiments evidence the dipole-dipole term of the Casimir-Polder interaction providing a measurement of the  $C_3$  coefficient for cesium Rydberg states. Furthermore, our experiment clearly evidences an additional interaction that induces shifts and broadens the linewidth of the probed transitions in the vicinity of the dielectric windows of our cells. We believe that this interaction is due to electric fields that are either generated by patch charges (trapped on the surface or induced by the excitation lasers), or by cesium adsorbants. We show that the different polarizability (of opposing sign) between  $S$  and  $D$  Rydberg states can be exploited to extract quantitative measurements of the strength and distance scaling ( $z$ -dependence) of such parasitic electrostatic interactions.

Our experiments suggest that the sensitivity of Rydberg atoms to external electric fields could provide a unique tool for probing electrostatic interactions in the vicinity of surfaces. This could allow systematic error corrections in Casimir-Polder experiments with excited or even ground state atoms that aim at putting bounds on the existence of non-Newtonian gravity <sup>5</sup>. We are currently exploring the possibility of coating the internal window interfaces with conducting 2D material such as graphene to reduce the influence of parasitic charges. This could allow us to probe atoms closer to the surface, at distances around 100nm, where quadrupole interactions ( $C_5$  coefficient) could be experimentally attainable for the first time.

<sup>1</sup>H. Kubler, J. P. Shaffer, T. Baluktsian, R. Loew, T. Pfau, *Nat. Photon.*, **4**, 112–116 (2013).

<sup>2</sup>V. Sandoghdar et al., *Phys. Rev. Lett.* **68**, 3432–3435 (1993).

<sup>3</sup>J. A. Crosse et al., *Phys. Rev. A* **82**, 3010901 (2010).

<sup>4</sup>B. Dutta et al., *Phys. Rev. Res.* **6**, L022035 (2024).

<sup>5</sup>A. Laliotis, B-S. Lu, M. Ducloy, D. Wilkowski, *AVS Quantum Sci.* **3**, 043501 (2021).



Abstract number: P13  
 Tuesday 14:00-15:30

## Developing a quantum gas microscope with programmable lattices

**Rosa-Medina R.**<sup>†1,2</sup>, **Safa I.**<sup>1</sup>, **Waddington S.**<sup>1</sup>, **Schubert T.**<sup>1</sup>, **Léonard J.**<sup>1,2</sup>

<sup>1</sup> *Atominstitut, Technische Universität Wien, Vienna, Austria*

<sup>2</sup> *Institute of Science and Technology Austria (ISTA), Klosterneuburg, Austria*

<sup>†</sup>rodrigo.rosa-medina@tuwien.ac.at

Experiments with ultracold atoms in optical lattices offer a versatile platform for engineering and probing strongly correlated quantum matter. While quantum gas microscopy has significantly advanced the field, enabling unprecedented single-site resolution, current experimental setups are often constrained by rigid lattice configurations and slow cycle times.

Here, we present our ongoing efforts to develop a next-generation quantum gas microscope for fermionic and bosonic lithium atoms. Our approach relies on atom-by-atom assembly of small lattice systems employing auxiliary optical tweezers combined with all-optical cooling techniques to facilitate sub-second experimental cycles, as schematically depicted in Fig. 1. By leveraging holographic projection techniques using a programmable digital micromirror device, we create tailored optical lattices with dynamically reconfigurable geometries. Our approach opens diverse research avenues, ranging from quantum simulation of fractional quantum Hall states to frustrated phases with unconventional geometries

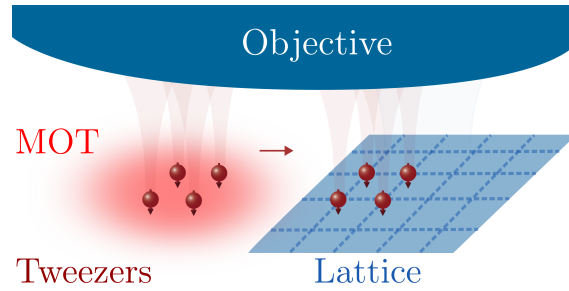


Figure 1: Atom-by-atom assembly of reconfigurable optical lattices.

Abstract number: P14

Tuesday 14:00-15:30

## Heterodyne cavity ring-down spectroscopy exploiting eigenmode frequencies for high-fidelity measurements

Cygan A.<sup>†</sup>, Wójtewicz S., Jóźwiak H., Kowzan G., Stolarczyk N., Bielska K., Wcisło P., Ciuryło R., Lisak D.

*Institute of Physics, Faculty of Physics, Astronomy and Informatics, Nicolaus Copernicus University in Toruń,  
Grudziadzka 5, 87-100 Toruń, Poland*

<sup>†</sup>agata@fizyka.umk.pl

Measuring low light absorption with uncertainty below 1 per mil ( $^{\circ}/_{\text{oo}}$ ) is essential for various applications. While popular cavity ring-down spectroscopy (CRDS) offers ultrahigh precision (below  $0.01^{\circ}/_{\text{oo}}$ ), its accuracy is often limited to  $5^{\circ}/_{\text{oo}}$  due to inaccuracies in light intensity measurements. To overcome this, we leverage the optical frequency information embedded in the ring-down cavity's electromagnetic field. By performing heterodyne detection and Fourier analysis of the ring-downs, we extract precise cavity mode frequencies as well as cavity mode widths and generate a high-fidelity dispersive and absorptive spectra of a gaseous sample. Our heterodyne cavity ring-down spectroscopy (HCRDS) method<sup>1</sup> achieves sub-per-mil accuracy, validated by ab initio CO line intensity results and HD line-shape data, with long-term repeatability of dispersion measurements at the  $10^{-4}$  level. The new method, similarly as recent cavity buildup dispersion spectroscopy<sup>2</sup>, does not require step scanning the laser frequency through the optical cavity modes, so it is much faster than our earlier developed cavity mode-dispersion spectroscopy (CMDs)<sup>3</sup> and cavity mode-width spectroscopy (CMWS)<sup>4</sup>. On the other hand, it enables the flexible selection of the most linear range of a detector transfer function, thus eliminating the major contribution to the measurement error in the conventional CRDS. Strictly speaking, new approach combines the speed of CRDS with accuracy of CMDs and CMWS techniques<sup>5,6</sup>. Moreover, it can be easily implemented for broadband measurements using optical frequency combs<sup>7</sup>. The HCRDS method shows promise for improving the accuracy of many spectroscopy-based research fields, such as fundamental studies of QED in molecular systems, atmospheric remote sensing, isotope ratio metrology, thermometry and establishment of primary gas standards based on quantum properties of molecules.

<sup>1</sup>A. Cygan *et al.*, *Science Advances* **11**, eadp8556 (2025).

<sup>2</sup>A. Cygan *et al.*, *Communications Physics* **4**, 1 (2021).

<sup>3</sup>A. Cygan *et al.*, *Optics Express* **23**, 14472 (2015).

<sup>4</sup>A. Cygan *et al.*, *Optics Express* **21**, 29744 (2013).

<sup>5</sup>K. Bielska *et al.*, *Physical Review Letters* **129**, 1 (2022).

<sup>6</sup>A. Cygan *et al.*, *Optics Express* **27**, 21811 (2019).

<sup>7</sup>D. Lisak *et al.*, *Scientific Reports* **12**, 1 (2022).

Abstract number: P15  
 Tuesday 14:00-15:30

## The quantum offset of velocity imaging-measured electron energies

Blondel C.<sup>†</sup>, Drag C.,

Laboratoire de physique des plasmas, Centre national de la recherche scientifique, Sorbonne université, université Paris-Saclay, Observatoire de Paris, Ecole polytechnique, Institut polytechnique de Paris, route de Saclay, F-91128 Palaiseau, France

<sup>†</sup>christophe.blondel@lpp.polytechnique.fr

Thirty years ago, electron spectrometry made a leap forward due to the advent of electron imaging devices, which made it possible to visualize complete photoelectron distributions, at the only expense of a projection onto the detection plane by a uniform electric field. The principle of slow electron velocity imaging, or SEVI<sup>1</sup>, has been that the maximum intensity circles obtained in the projection directly visualize the set of transverse velocities of the detected electrons. Correspondingly, the squared radii of those circles would directly provide a measure of the electron energies<sup>2</sup>. This point of view, however, has constantly ignored the fact that these maximum intensity circles are no stigmatic images of a pointlike source, but fringes formed near caustic surfaces, or electron rainbows. In such a case, as G.B. Airy observed, “the maximum illumination does not take place at the Geometrical Caustic (...) but (...) on the luminous side of the geometrical position of the rainbow”<sup>3</sup>. As a consequence, the long-lasting confusion made, for electrons, between the radius of the caustic and the radius of the attached brilliant fringe, respectively  $R_C$  and  $R_0$  on figure 1, has resulted in a systematic underestimation of electron energies.

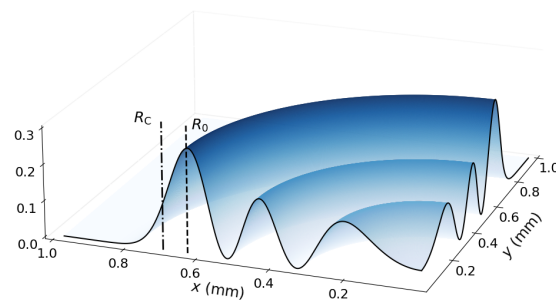


Figure 1: Quadrant of the theoretical 2D-distribution obtained by projection of 100  $\mu\text{eV}$  photoelectrons by a 423 V/m electric field on a plane detector, with  $R_C$  the maximum radius allowed with a positive kinetic energy and  $R_0$  the radius of the brilliant fringe usually observed in slow electron velocity imaging experiments. Taking  $R_0$  for  $R_C$  leads to a systematic underestimation of the electron energy.

The quantity  $\Delta$  by which the energy has been underestimated only depends on the electric field  $F$  (and of fundamental constants)<sup>4</sup>:  $\Delta = 1.01879 \dots \sqrt[3]{(\hbar q F)^2 / 2m}$ . Numerically, this is an 18  $\mu\text{eV}$  bias in a 380 V/m electric field. SEVI-measured electron affinities, which are about one third of the electron affinities of reference nowadays, have probably been overestimated by a similar amount. The electron affinities measured by photodetachment microscopy<sup>5</sup> are not affected.

<sup>1</sup>A. Osterwalder, M.J. Nee, J. Zhou and D.M. Neumark, *J. Chem. Phys.* **121**, 6317 (2004).

<sup>2</sup>C. Bordas, F. Paulig, H. Helm and D.L. Huestis, *Rev. Sci. Instrum.* **67**, 2257 (1996).

<sup>3</sup>G. B. Airy, *Trans. Cambridge Philos. Soc.* **6**, 379 (1838).

<sup>4</sup>C. Blondel and C. Drag, *Phys. Rev. Lett.* **134**, 043001 (2025).

<sup>5</sup>C. Valli, C. Blondel and C. Delsart, *Phys. Rev. A* **59**, 3809 (1999).

Abstract number: P16  
Day

## Experimental Demonstration of Tunable Spin-Phonon Coupling in Trapped Ions via Optical Tweezers

Chen Y.<sup>†1,2,3</sup>, Cui J.-M.<sup>1,2,3,4</sup>, Zhou Y.-F.<sup>1,2,3</sup>, An E.-T.<sup>1,2,3</sup>, Huang Y.-F.<sup>1,2,3,4</sup>, Li C.-F.<sup>1,2,3,4</sup>, Guo G.-C.<sup>1,2,3</sup>

<sup>1</sup> CAS Key Laboratory of Quantum Information, University of Science and Technology of China, Hefei 230026, China

<sup>2</sup> Anhui Province Key Laboratory of Quantum Network, University of Science and Technology of China, Hefei 230026, China

<sup>3</sup> CAS Center For Excellence in Quantum Information and Quantum Physics, University of Science and Technology of China, Hefei 230026, China

<sup>4</sup> Hefei National Laboratory, University of Science and Technology of China, Hefei 230088, China

<sup>†</sup>cy1998@mail.ustc.edu.cn

Trapped ion systems, leveraging their high fidelity and all-to-all connectivity, exhibit significant potential for quantum computing and simulation. However, the complexity of phonon modes in large-scale ion arrays limits high-fidelity operations. Optical tweezer technology, by locally modulating ion phonon modes, provides a novel approach to address this challenge. In this work, we experimentally demonstrate for the first time the ability of optical tweezers to control phonon frequencies and spin-phonon coupling coefficients in an ion chain: In the experiment, a focusing light field of 554 nm was used to generate optical tweezers with a maximum frequency of approximately 250 kHz; we quantitatively characterized the modulation of ion phonon spectra and spin-phonon coupling coefficients through Raman-transition-excited phonon sidebands, achieving a coupling coefficient variation amplitude of 50%. The results reveal that optical tweezers can significantly modify ion-phonon coupling strength, thereby enabling control of phonon-mediated inter-ion interactions. This work establishes an experimental foundation for realizing parallel high-fidelity quantum gates and programmable quantum simulators. Future optimization of tweezer power and array technology is expected to further enhance control capabilities and expand application scenarios.

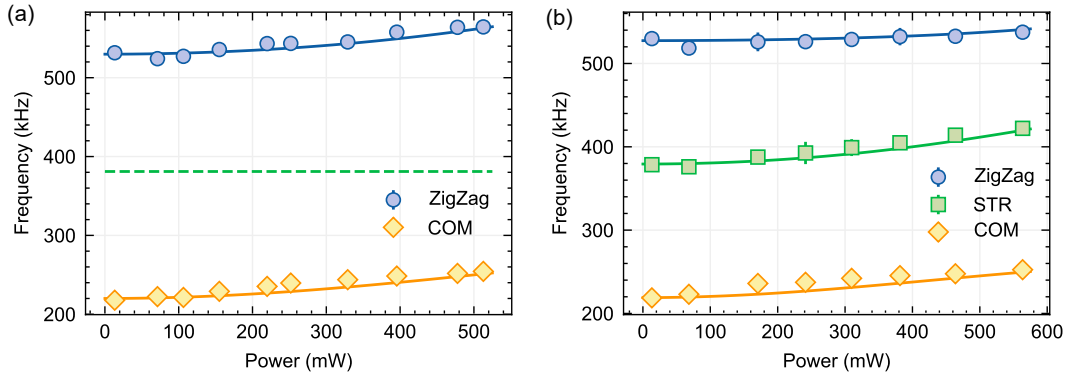


Figure 1: Modification of phonon frequencies in a three-ion chain via optical tweezers. (a) Central ion, (b) End ion.

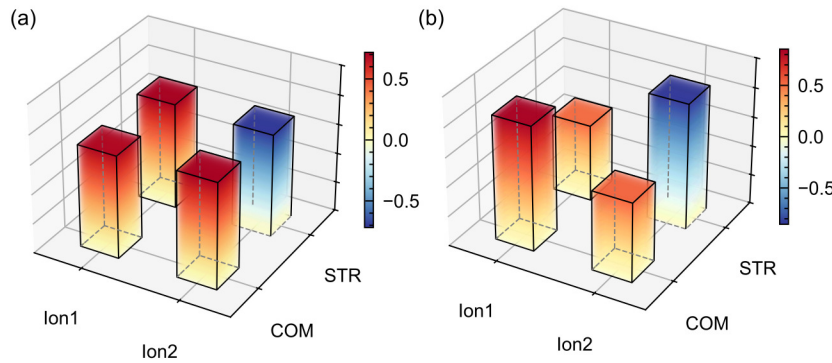


Figure 2: Modification of Spin-Phonon Coupling Coefficients. (a) No tweezers, (b) Tweezers on Ion 2.

Abstract number: P17  
Tuesday 14:00-15:30

## Realization of a doped quantum antiferromagnet with dipolar tunnelings in a Rydberg tweezer array

Qiao M.<sup>†1</sup>, Emperauger G.<sup>1</sup>, Chen C.<sup>1,2</sup>, Homeier L.<sup>3,4</sup>, Hollerith S.<sup>5</sup>, Bornet G.<sup>1</sup>, Martin R.<sup>1</sup>, Gély B.<sup>1</sup>, Klein L.<sup>1</sup>, Barredo D.<sup>1,6</sup>, Geier S.<sup>7</sup>, Chiu N.-C.<sup>5</sup>, Grusdt F.<sup>8,9</sup>, Bohrdt A.<sup>9,10</sup>, Lahaye T.<sup>1</sup>, Browaeys A.<sup>1</sup>  
<sup>1</sup> Université Paris-Saclay, Institut d'Optique Graduate School, CNRS, Laboratoire Charles Fabry, 91127 Palaiseau Cedex, France  
<sup>2</sup> Institute of Physics, Chinese Academy of Sciences, Beijing 100190, China  
<sup>3</sup> JILA and Department of Physics, University of Colorado, Boulder, CO, 80309, USA  
<sup>4</sup> Center for Theory of Quantum Matter, University of Colorado, Boulder, CO, 80309, USA  
<sup>5</sup> Department of Physics, Harvard University, Cambridge, Massachusetts 02138, USA  
<sup>6</sup> Nanomaterials and Nanotechnology Research Center (CINN-CSIC), Universidad de Oviedo (UO), Principado de Asturias, 33940 El Entrego, Spain  
<sup>7</sup> Physikalisches Institut, Universität Heidelberg, Im Neuenheimer Feld 226, 69120 Heidelberg, Germany  
<sup>8</sup> Department of Physics and Arnold Sommerfeld Center for Theoretical Physics (ASC), Ludwig-Maximilians-University at München, Theresienstr. 37, München D-80333, Germany  
<sup>9</sup> Munich Center for Quantum Science and Technology (MCQST), Schellingstr. 4, München D-80799, Germany  
<sup>10</sup> University of Regensburg, Universitätsstr. 31, Regensburg D-93053, Germany  
<sup>†</sup>mu.q.phys@gmail.com

Doping an antiferromagnetic Mott insulator is central to our understanding of a variety of phenomena in strongly-correlated electrons, including high-temperature superconductors. To describe the competition between tunneling  $t$  of hole dopants and antiferromagnetic (AFM) spin interactions  $J$ , theoretical and numerical studies often focus on the paradigmatic  $t$ - $J$  model, and the direct analog quantum simulation of this model in the relevant regime of high-particle density has long been sought. Here, we realize a doped quantum antiferromagnet with next-nearest neighbour (NNN) tunnelings  $t'$  and hardcore bosonic holes using a Rydberg tweezer platform. We utilize coherent dynamics between three Rydberg levels, encoding spins and holes, to implement a tunable bosonic  $t$ - $J$ - $V$  model allowing us to study previously inaccessible parameter regimes. We observe dynamical phase separation between hole and spin domains for  $|t/J| \ll 1$ , and demonstrate the formation of repulsively bound hole pairs in a variety of spin backgrounds. The interference between NNN tunnelings  $t'$  and perturbative pair tunneling gives rise to light and heavy pairs depending on the sign of  $t$ . Using the single-site control allows us to study the dynamics of a single hole in 2D square lattice (anti)ferromagnets. The model we implement extends the toolbox of Rydberg tweezer experiments beyond spin-1/2 models to a larger class of  $t$ - $J$  and spin-1 models.

Our results are fourfold. First, in a 1D chain, using our ability to prepare initial product states and to tune the ratio of tunneling strength  $t$  to magnetic spin interaction  $J$ , we observe a dynamical phase separation between holes and spins and probe the properties of repulsively bound hole pairs. Second, we probe the interplay between NNN tunneling  $t'$  and the perturbative pair tunneling induced by NN tunneling  $t$ . Depending on the sign of the hole tunneling  $t'$ , this leads to constructive or destructive interference, which allows us to control the effective mass of the hole pairs, as well as their mobility. Third, we investigate the influence of the spin background on the pair's mass and binding energy. Last, we perform single-hole experiments in a 2D array both for an FM and AFM spin background. In particular, in the FM case, we observe the influence of the dipolar tail of the interactions.

Abstract number: P18  
Tuesday 14:00-15:30

## Measurement and feedforward correction of the fast phase noise of lasers

Denecker T.<sup>1,2</sup>, Chew Y. T.<sup>1</sup>, Guillemant O.<sup>1</sup>, Watanabe G.<sup>1,2</sup>, Tomita T.<sup>1,2</sup>, Ohmori K.<sup>1,2</sup>,  
de Léséleuc S.<sup>†1,3</sup>

<sup>1</sup>*Institute for Molecular Science, National Institutes of Natural Sciences, Okazaki, Japan*

<sup>2</sup>*SOKENDAI (The Graduate University for Advanced Studies), Okazaki, Japan*

<sup>3</sup>*RIKEN Center for Quantum Computing (RQC), RIKEN, Wako, Japan*

<sup>†</sup>sylvain.deleseleuc@riken.jp

Lasers are the workhorse of quantum engineering in the atomic-molecular-optic community. However, phase noise of the laser, which can be especially large in popular semiconductor-based lasers, can limit gate fidelity. Here, we present a fully-fiberized instrument detecting and correcting the fast, sub-microsecond, phase fluctuations of lasers<sup>1</sup>. We demonstrate a measurement noise floor of less than  $0.1 \text{ Hz}^2/\text{Hz}$ , and a noise suppression of more than 20 dB for Fourier frequencies in the 1 to 10 MHz region (reaching up to 30 dB at 3 MHz), where noise is critical for Rydberg-based quantum gates. Finally, we observe the improvement offered by this fast phase noise eater on a Raman transition driven by two such stabilized lasers. These measurement and correction techniques are important tools for high-fidelity manipulation of the excited electronic states of atoms and molecules.

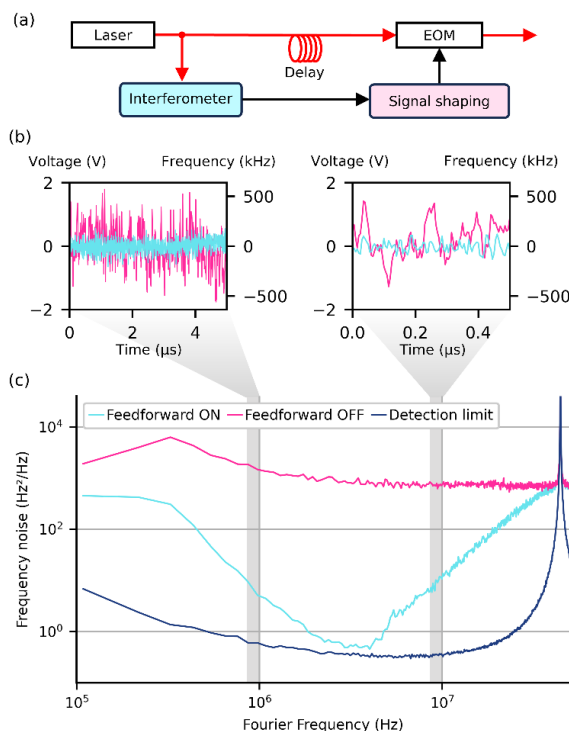


Figure 1: Measurement and correction of fast phase noise. (a) Schematic of the phase noise eater. (b) Time traces of the measured frequency noise with (in blue) and without (in pink) the feedforward correction. (c) Frequency noise PSD with and without the correction. The dark blue curve is the detector noise floor. A cancellation of more than 30 dB is achieved at a Fourier frequency of 3 MHz, where the noise is suppressed down to  $0.5 \text{ Hz}^2/\text{Hz}$ .

<sup>1</sup>T. Denecker et al., arxiv:2411.10021

Abstract number: P19  
Tuesday 14:00-15:30

## Precision spectroscopy of CO for gas metrology

Wang J.<sup>†1</sup>, Li J.-K.<sup>1,2</sup>, Yin R.-H.<sup>3</sup>, Huang Q.<sup>2</sup>, Tan Y.<sup>1,3</sup>, Hu C.-L.<sup>3</sup>, Sun Y. R.<sup>4</sup>, Hu S.-M.<sup>1,2,3,\*</sup>

<sup>1</sup>Hefei National Laboratory, University of Science and Technology of China, Hefei 230088, China

<sup>2</sup>State Key Laboratory of Molecular Reaction Dynamics, Department of Chemical Physics, University of Science and Technology of China, Hefei 230026, China

<sup>3</sup>Hefei National Research Center of Physical Sciences at the Microscale, University of Science and Technology of China, Hefei 230026, China

<sup>4</sup>Institute of Advanced Science Facilities, Shenzhen, 518107, China

<sup>†</sup>jinwang@ustc.edu.cn; \*smhu@ustc.edu.cn

High-precision line intensities are of great value in various applications, such as greenhouse gas metrology, planetary atmospheric analysis, and trace gas detection. Here, we report recent progress in SI-traceable measurements of transition intensities for the CO molecule. Using cavity-enhanced spectroscopy, we conducted Doppler broadened spectroscopy of the second-overtone transitions of CO (1.57  $\mu\text{m}$ ). By simultaneously measuring absorption and dispersion, we achieved cross-validation of the experimental results, determining line intensities with an accuracy of 0.1%<sup>1</sup>. These results show excellent agreement with ab initio calculations<sup>2</sup>. However, intensity ratios for transitions from different rotational levels of CO, measured with uncertainties below 0.01%, reveal a systematic deviation from theoretical predictions. Advances in both experimental techniques and theoretical calculations for molecules like CO will play an important role in advancing primary gas metrology based on optical measurements.

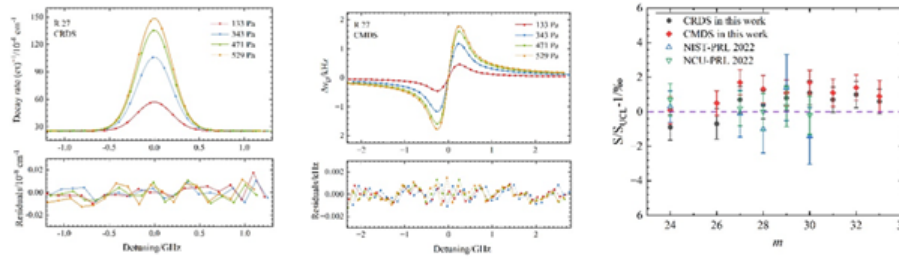


Figure 1: Figure 1: (Left): CRDS spectra of the R(27) line of  $^{12}\text{C}^{16}\text{O}$  (single scan) measured at 299 K, with a pure CO sample gas of different pressures. Speed-dependent Voigt (SDV) profiles were used in the fit. (Middle): CMDS spectra of the R(27) line of  $^{12}\text{C}^{16}\text{O}$  (single scan) measured at 299 K, with a pure CO sample gas of different pressures. Speed-dependent Voigt (SDV) profiles were used in the fit. (Right): comparison of line intensities obtained in this work and literature. The horizontal axis is  $m = J + 1$  for transitions in the R branch. All values were normalized to the calculated values given by the UCL group.

<sup>1</sup>J. Wang, *et al.*, *Metrologia* **61**, 065003 (2024).

<sup>2</sup>K. Bielska *et al.*, *Phys. Rev. Lett.* **129**, 043002 (2022).

Abstract number: P20

Tuesday 14:00-15:30

## Towards a measurement of the electron's electric dipole moment with molecules in a lattice

Athanasakis-Kaklamanakis M., Peng G., Li S., Septien-Gonzalez H., Lim J., Sauer B. E., Tarbutt M. R.<sup>†</sup>  
Imperial College London, United Kingdom

<sup>†</sup>m.tarbutt@imperial.ac.uk

Precision experiments using heavy polar molecules are sensitive to the electric dipole moment of the electron (eEDM), whose measurement would be evidence of CP violation in the fundamental forces, potentially revealing physics beyond the Standard Model. Despite significant improvements in the precision of eEDM searches in the past decade, only upper bounds have been successfully placed so far, with the currently most stringent limit placed at  $|d_e| < 4.1 \times 10^{-30} e \text{ cm}$ .<sup>1,2</sup> At Imperial College London, a new experiment to search for the eEDM is being constructed using ultracold YbF molecules. We aim to prepare the molecules in a magneto-optical trap (MOT), transfer them into an optical lattice, and then probe the eEDM at the level of  $10^{-31}$ - $10^{-32} e \text{ cm}$ .<sup>3</sup>

The electronic structure of YbF makes it amenable to direct laser cooling,<sup>4</sup> although low-lying metastable electronic states make the cooling more complicated<sup>5</sup>. We will present our results on the production of very slow YbF molecules using a 1 K cryogenic buffer gas source followed by radiation-pressure slowing, our efforts to capture these molecules in a MOT, and the design of our ultra-low-magnetic-noise science chamber.

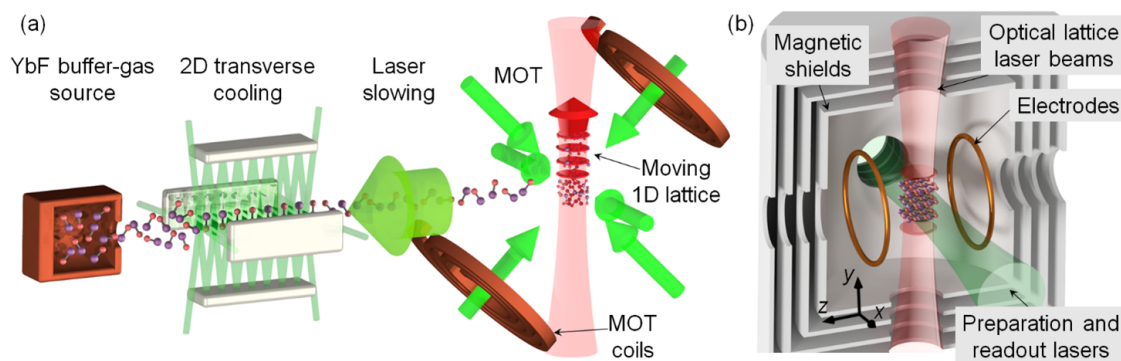


Figure 1: Figure 1: Schematic illustration of the experiment to search for the eEDM with ultracold YbF in a lattice at Imperial College London. (a) Laser cooling, slowing, and trapping of YbF. (b) Conceptual schematic of the science chamber where the eEDM measurement protocol will be carried out.

<sup>1</sup>T. S. Roussy, *et al.*, *Science* **381**, 6653 (2023).

<sup>2</sup>ACME collaboration, *Nature* **562**, 7727 (2018).

<sup>3</sup>N. J. Fitch *et al.*, *Quantum Science and Technology* **6**, 014006 (2021).

<sup>4</sup>N. J. Fitch and M. R. Tarbutt, *Advances in Atomic, Molecular, and Optical physics* **70**, 157-262 (2021).

<sup>5</sup>S. Popa *et al.*, *Phys. Rev. X* **14**, 021035 (2024).



Abstract number: P21  
 Tuesday 14:00-15:30

## Probing Nuclear Spin-Dependent Parity-Violation in $^{133}\text{Cs}$ Using Relativistic Coupled-Cluster Theory

Chakraborty A.<sup>†</sup>, Sahoo B. K.  
*Physical Research Laboratory, Gujarat, India*  
<sup>†</sup>arupc794@gmail.com

The Standard Model (SM) of particle physics is one of the most successful theories in modern physics, providing a comprehensive framework to describe fundamental particles and their interactions. However, despite its remarkable accuracy in explaining a wide range of experimental results, the SM is widely regarded as incomplete. Numerous efforts have been made to probe physics beyond the SM (BSM), particularly through high-energy particle collisions in accelerator-based experiments. However, direct signatures of BSM physics have remained elusive, despite strong indirect evidence suggesting its existence. As a result, alternative approaches have gained significant attention, particularly precision low-energy experiments that can provide indirect but highly sensitive tests of new physics. To extract meaningful results from these experiments, high-precision atomic calculations are essential. One example is atomic parity-violation (PV), which has been precisely measured in  $^{133}\text{Cs}$ <sup>1</sup>. Studying PV is key for testing the SM's predictions and detecting potential deviations that might indicate new physics. Moreover, nuclear spin-dependent (NSD) PV effects are closely linked to the nuclear anapole moment (NAM), a parity-violating moment that arises due to weak interactions within the nucleus. Detecting and understanding NAM is crucial for advancing our knowledge of nuclear structure and fundamental interactions<sup>2</sup>. We have implemented relativistic coupled-cluster theory at the singles and doubles approximation (RCCSD) to calculate the NSD PV electric dipole (E1) transition amplitudes ( $E1_{\text{PV}}^{\text{NSD}}$ ) between different hyperfine levels ( $F_f - F_i$ ) of the  $6s\ ^2S_{1/2} - 7s\ ^2S_{1/2}$  transition in  $^{133}\text{Cs}$ <sup>3</sup>. To validate our results, we have also calculated these amplitudes with the Dirac-Hartree-Fock (DHF) method, coupled-perturbed-Dirac-Hartree-Fock (CPDF), random phase approximation (RPA) and the combined CPDF-RPA method and compared them with previously reported results.

<sup>1</sup>C. S. Wood et al., *Science* **275**, 1759 (1997).

<sup>2</sup>Ya. B. Zeldovich, *Zh. Eksp. Teor. Fiz.* **33**, 1531 (1957) [*Sov. Phys. JETP* 6, 1184 (1957)].

<sup>3</sup>A. Chakraborty and B. K. Sahoo *Phys. Rev. A* **110**, 022812 (2024).

Abstract number: P22  
 Tuesday 14:00-15:30

## Multilevel Electromagnetically Induced Transparency Cooling

**Fouka K.**<sup>†1,2</sup>, **Shankar A.**<sup>3</sup>, **Tan T. R.**<sup>4</sup>, **Safavi-Naini A.**<sup>1,2</sup>

<sup>1</sup>*Institute for Theoretical Physics, Institute of Physics, University of Amsterdam, Science Park 904, 1098 XH Amsterdam, The Netherlands*

<sup>2</sup>*QuSoft, Science Park 123, 1098 XG Amsterdam, The Netherlands*

<sup>3</sup>*Indian Institute Of Technology Madras, 600036 Chennai, India*

<sup>4</sup>*School of Physics, University of Sydney, NSW 2006 Sydney, Australia*

<sup>†</sup>s.k.fouka@uva.nl

Electromagnetically Induced Transparency (EIT) cooling<sup>1 2</sup> is a well-established method for preparing trapped ion systems in their motional ground state. However, isolating a three-level system, as required for EIT cooling, is often challenging or impractical. In this work, we extend the EIT cooling framework to multilevel systems where the number of ground states exceeds the number of excited states, ensuring the presence of at least one dark state<sup>3</sup>. We develop a formalism that allows us to accurately determine the cooling rate in the weak sideband coupling regime<sup>4</sup> and provides an approximate estimate for cooling rates beyond this regime, without the need for explicit simulation of the motional degree of freedom. Our work clarifies the connection between the cooling rate and the absorption spectrum, offering a pathway for efficient near-ground-state cooling of ions with complex electronic structures.

<sup>1</sup>G. Morigi, J. Eschner, and C. H. Keitel, *Physical Review Letters* **85**, 4458 (2000).

<sup>2</sup>G. Morigi, *Physical Review A* **67**, 033402 (2003).

<sup>3</sup>D. Finkelstein-Shapiro, S. Felicetti, T. Hansen, T. Pullerits, and A. Keller, *Physical Review A* **99**, 053829 (2019).

<sup>4</sup>S. Zhang, J.-Q. Zhang, W. Wu, W.-S. Bao, and C. Guo, *New Journal of Physics* **23**, 023018 (2021).

Abstract number: P23  
 Tuesday 14:00-15:30

## Optical tweezer optimisation for trapped-ion quantum simulation

Robalo Pereira C.<sup>†1</sup>, Diepeveen N.A.<sup>1</sup>, Mazzanti M.<sup>3</sup>, Ackerman Z.E.D.<sup>1</sup>, Gallagher L.P.H.<sup>1</sup>,  
 Schüssler R. X.<sup>3</sup>, Safavi-Naini A.<sup>2,4</sup>, Gerritsma R.<sup>1</sup>

<sup>1</sup>Van der Waals-Zeeman Institute, University of Amsterdam, The Netherlands

<sup>2</sup>Institute for Quantum Electronics, ETH Zürich, Switzerland

<sup>3</sup>Institute for Theoretical Physics, University of Amsterdam, The Netherlands

<sup>4</sup>QuSoft, Amsterdam, The Netherlands

<sup>5</sup>GSI Helmholtzzentrum für Schwerionenforschung, Darmstadt, Germany

<sup>†</sup>m.c.robalo Pereira@uva.nl

Trapped ions offer a natural platform for quantum simulation. They provide advantageous conditions such as long coherence times and natural organization into lattice crystalline structures with fully interconnected interactions<sup>12</sup>. With this setup one can perform quantum simulations by engineering spin Hamiltonians whose interactions are mediated by the crystal's phonon modes<sup>34</sup>. Our novel approach adds optical tweezers, i.e. very tightly-focused light, which is used to manipulate the ion crystals' sound-wave spectra by pinning a number of individual ions. This allows extra tunability over the ion interactions, paving the way to the simulation of a wide range of spin-Hamiltonians<sup>567</sup>. We show experimental progress on a trapped-ion tweezer setup, Fig. 1 detailing a tweezer optimization routine, alignment on the ions and beam characterization for a resonant tweezer and for a high-power, off-resonant tweezer, requiring direct and indirect detection methods<sup>8</sup>. This tweezer will provide the required deep trapping potential to modify the crystal's phonon spectrum.

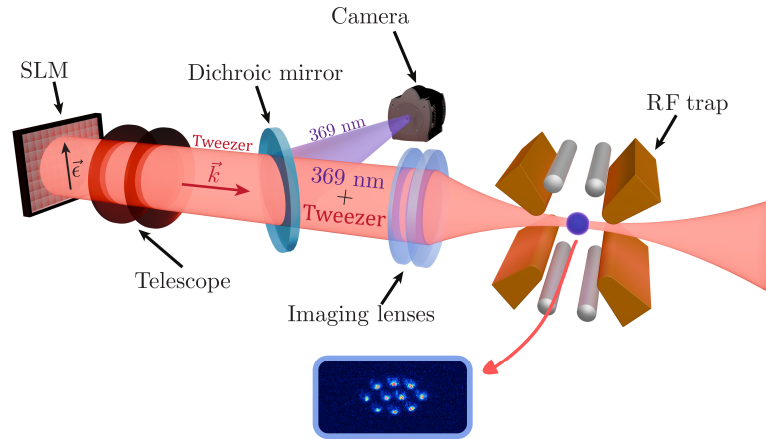


Figure 1: Tweezer alignment on an ion crystal. The tweezer is generated with a spatial light modulator (SLM), pinning individual ions inside the Paul trap. The ion fluorescence used for mapping the tweezer is collected by the camera.

<sup>1</sup>R. Blatt, D. Wineland, *Nature* **453**, 1008-15 (2008).

<sup>2</sup>Wang, P. *et al.*, *Nat Commun* **12**, 233 (2021)

<sup>3</sup>P. Richerme, *Phys. Rev. A* **94**, 032320 (2016).

<sup>4</sup>R. Nath *et al.*, *New J. Phys.* **17**, 065018 (2015).

<sup>5</sup>J.D.Espinoza *et al.*, *Phys. Rev. A* **104**, 013302 (2021)

<sup>6</sup>M. Mazzanti *et al.*, *Phys. Rev. Lett.* **127**, 260502 (2021)

<sup>7</sup>L.Bond *et al.*, *Phys. Rev. A* **106**, 042612 (2022)

<sup>8</sup>M. Mazzanti *et al.*, *Phys. Rev. A* **110**, 043105 (2024)

Abstract number: P24  
Tuesday 14:00-15:30

## Measurement of Ground-State Hyperfine Splitting in Muonic Hydrogen: The FAMU Experiment

**Baruzzo M.**<sup>†1</sup> on behalf the FAMU collaboration  
<sup>1</sup>National Institute of Nuclear Physics, INFN, Trieste, Italy  
<sup>†</sup>marco.baruzzo@ts.infn.it

The FAMU experiment (Fisica degli Atomi Muonici) aims to provide valuable insights into the proton's magnetic structure, delivering new data for high-precision QED calculations and improving our understanding of the muon-proton interaction. Its ultimate goal is to refine the measurement of the proton Zemach radius with a precision of 1%.

The FAMU method is based on muonic hydrogen spectroscopy, to measure the hyperfine splitting of the 1S state. In the experiment, muonic hydrogen atoms are produced by stopping muons, generated at the ISIS Neutron and Muon Facility at Rutherford Appleton Laboratory (RAL), UK, in a high-pressure cryogenic hydrogen target. Once thermalized, the muonic hydrogen is exposed to a laser pulse. If the laser wavelength is tuned precisely to induce a spin flip, expected around 0.183 eV, the subsequent de-excitation releases excess kinetic energy, enhancing the natural muon transfer rate from hydrogen to higher-Z nuclei. To exploit this effect, a small amount of oxygen is introduced into the gas target. The spin-flip transition induced by the mid-IR radiation is then observed as a change in the characteristic muonic oxygen X-ray emission rate, which occurs after the muon transfer<sup>1</sup>.

The experiment requires a pulsed, tunable, high-energy, narrow-linewidth mid-infrared laser, specifically developed for this purpose. The laser system is based on the Difference Frequency Generation (DFG) process, with a 1064 nm pump produced by a Nd:YAG single-mode pulsed laser. The signal is tuned around 1262 nm using a Cr:forsterite laser, which is then boosted through a multi-stage amplifier<sup>2</sup>. The resulting idler, at 6.78  $\mu\text{m}$ , has a linewidth less than 30 pm with an energy exceeding 1 mJ<sup>3</sup>.

During the four data acquisition campaigns conducted so far, the laser has demonstrated tunability with minimum steps of less than 10 pm and a central wavelength stability of about 3 pm. Additionally, the laser system has demonstrated the capability to consistently exceed 1.5 mJ of energy while maintaining the stringent stability and spectral purity required for the experiment. One of its most distinctive features is the ability to operate continuously over extended periods, sustaining optimal performance for weeks without interruption. This high level of reliability is achieved through a meticulous feedback control system, which actively monitors and regulates key parameters to ensure long-term operation stability. As a result, the need for frequent operator intervention is significantly reduced, enhancing both efficiency and ease of use in demanding experimental conditions. Through continuous advancements, including improvements in pump signal quality and optimized beam reshaping, the efficiency of the DFG process within the nonlinear crystal has been significantly enhanced. As a result, the system now delivers an unprecedented energy output of 3 mJ, setting a new benchmark at this wavelength.

So far, the experiment has collected data at 25 wavelengths, covering a total range of 650 pm, as shown in Figure 1 with additional campaigns planned for 2025. The collaboration is also working on the METrology and Nonlinear optics for Precision muonic HYdrogen physicS (MENPHIS) project, which aims to improve the stability of the laser system by replacing the Cr:forsterite oscillator with an OPO. This contribution will present an overview of the FAMU experiment, with a particular focus on the laser system and its performance.

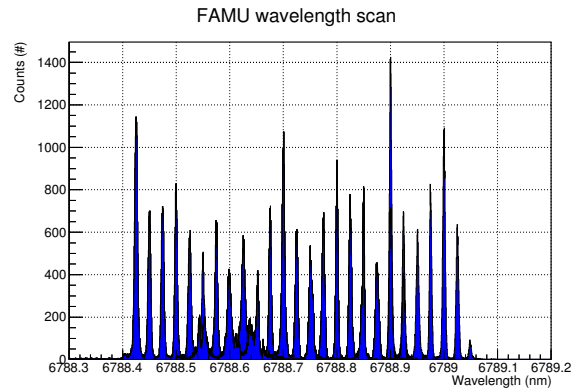


Figure 1: The wavelength covered by FAMU experiment during 2023 and 2024 data campaigns.

<sup>1</sup>C. Pizzolotto *et al.*, *Eur. Phys. J. A* **56**, 185 (2020).

<sup>2</sup>L.I. Stoychev *et al.*, *Rev. Sci. Instrum.* **90**, 9 (2019).

<sup>3</sup>M. Baruzzo *et al.*, *Optics & Laser Technology* **179**, 111375 (2024).

Abstract number: P25  
 Tuesday 14:00-15:30

## Optimal Floquet state engineering for large scale atom interferometers

Calmels L.<sup>1</sup>, Beldjoudi S.<sup>1</sup>, Bigard C.<sup>1</sup>, Rodzinka T.<sup>1</sup>, Béguin A.<sup>1</sup>, Allard B.<sup>1</sup>, Gauguet A.<sup>1</sup>

<sup>1</sup> Laboratoire Collisions Agrégats Réactivité (LCAR/FERMI), Université de Toulouse and CNRS, Toulouse, France

<sup>†</sup>gauguet@irsamc.ups-tlse.fr

We present a novel approach to matter-wave optics based on the stroboscopic stabilization of quantum states within an accelerated optical lattice<sup>1</sup>. This method exploits Floquet engineering to systematically identify quantum states that exhibit optimal transport, integrating a range of atom optics techniques for large momentum transfer. These include adiabatic manipulations, such as Bloch-type acceleration, as well as highly non-adiabatic regimes involving Bragg pulses<sup>2</sup>. By exploiting the Floquet framework, we achieve precise state-to-state control in high-dimensional Hilbert spaces, overcoming the limitations of conventional brute-force numerical methods. Using this approach, we have experimentally demonstrated highly efficient coherent acceleration of cold atoms, with an efficiency greater than 0.9995 per photon recoil ( $\hbar k$ ). Furthermore, we have realized atom interferometers with an unprecedented momentum separation of  $600\hbar k$  between the two arms [\[180\]](#).

I will present the technical and fundamental limitations of our method and explore its potential to support interferometers with momentum separations beyond  $1000\hbar k$ . Such advances could open up new opportunities in precision metrology and quantum technologies. In particular, this development addresses a key challenge in the realization of large-scale atom interferometers, which are critical for future gravitational wave detection and fundamental physics tests.

<sup>1</sup>T. Rodzinka, E. Dionis, L. Calmels, L. *et al.*, *Nat. Commun* **15**, 10281 (2024).

<sup>2</sup>A. Béguin, T. Rodzinka, L. Calmels, B. Allard, and A. Gauguet, *Phys. Rev. Lett.*, **131**, 143401 (2023).

Abstract number: P26  
 Tuesday 14:00-15:30

## Absolute Quantum Gravimetry in the Field

**Richard J.**<sup>†1</sup>, **Antoni-Micollier L.**<sup>1</sup>, **Gautier R.**<sup>1</sup>, **Bertier P.**<sup>1</sup>, **Vermeulen P.**<sup>1</sup>, **Janvier C.**<sup>1</sup>, **Majek C.**<sup>1</sup>,  
**Desruelle B.**<sup>1</sup>, **Ménoret V.**<sup>1</sup>

<sup>1</sup>*Exail Quantum Systems, Gradignan, France*

<sup>†</sup>jeremie.richard@exail.com

Absolute gravity measurements at the level of  $10 \text{ nm.s}^{-2}$  using cold atoms have been demonstrated in the laboratory in 1992<sup>1</sup> and have ever since received an increasing interest from the metrology and geophysics communities. In 2015 Muquans, now Exail Quantum Systems, introduced the Absolute Quantum Gravimeter (AQG)<sup>2</sup>, a pioneering industrial field sensor based on cold atom physics. Cutting-edge technology developments provided the necessary easy-of-use, autonomy, and robustness for field deployment. In 10 years of production, more than 20 units have been produced for various geophysical applications including hydrology, geodesy and volcanology.

Here we present a comparison of the sensitivity of these instruments at our facility before shipment, demonstrating reproducible performance in the range of  $600 - 800 \text{ nm.s}^{-2} \cdot \sqrt{\text{Hz}}$ , with a stability better than  $10 \text{ nm.s}^{-2}$  after an hour of integration. We also present improvements to the systematic effects budget, necessary to evaluate the trueness of the AQG.

In addition, we introduce the novel Differential Quantum Gravimeter (DQG), a double quantum gravimeter capable of simultaneously measuring both the gravity and the vertical gravity gradient. We present the performance of the first DQG in the lab and show how these results translate to field applications, ranging from archaeology to hydrology.

<sup>1</sup>M. Kasevich and S. Chu, *Applied Physics B* **54**, p. 321-332 (1992).

<sup>2</sup>V. Ménoret *et al.*, *Scientific Reports* **8**, pp.12300 (2018).

Abstract number: P27  
 Tuesday 14:00-15:30

## Quantum Gates with Trapped Ions and Optical Tweezers

Ackerman Z. E. D.<sup>†1</sup>, Gallagher L. P. H.<sup>1</sup>, Mazzanti M.<sup>2</sup>, Schüssler R. X.<sup>3</sup>, Diepeveen N.<sup>1</sup>, Robalo Pereira C.<sup>1</sup>, Safavi-Naini A.<sup>4,5</sup>, Spreeuw R. J. C.<sup>1</sup>, Gerritsma R.<sup>1</sup>

<sup>1</sup>*Van der Waals – Zeeman Institute, Institute of Physics, University of Amsterdam, The Netherlands*

<sup>2</sup>*Institut für Quantenelektronik, ETH Zürich, Switzerland*

<sup>3</sup>*GSI Helmholtzzentrum für Schwerionenforschung, Darmstadt, Germany*

<sup>4</sup>*QuSoft, The Netherlands*

<sup>5</sup>*Institute for Theoretical Physics, Institute of Physics, University of Amsterdam, The Netherlands*

<sup>†</sup>z.e.d.ackerman@uva.nl

An ion can experience an off axis, spin-dependent dipole force caused by strong polarization gradients of tightly focused optical tweezers<sup>1</sup>. We present a novel two-qubit quantum gate as an implementation of this effect<sup>2</sup>. This tweezer-driven quantum gate requires only a single beam per ion and promises a fidelity of  $F \geq 0.999989$  without the necessity of ground-state cooling of the ions.

In this poster, I will elaborate on our current experimental setup and our progress in developing a programmable UV hollow-tweezer array, aimed at minimizing photon scattering and AC Stark shift. Our proposed setup integrates an acousto-optical deflector and a spatial light modulator to facilitate precise control over the beam shape while enabling rapid switching between ion pairs for implementing the quantum gates.

<sup>1</sup>R.J.C. Spreeuw, *PRL* **125**, 233201 (2020).

<sup>2</sup>M. Mazzanti, R. Gerritsma, R. J. C. Spreeuw, and A. Safavi-Naini, *PRR* **5**, 033036 (2023).

**Abstract number: P28**  
**Tuesday 14:00-15:30**

## Measuring G with atom interferometry

**Lei J.-Y.<sup>1</sup>, Luo H.-Q.<sup>1</sup>, Xu Y.-Y.<sup>1</sup>, Mao D.-K.<sup>1</sup>, Cao L.-S.<sup>1</sup>, Zhou M.-K.<sup>1</sup>, Duan X.-C.<sup>1</sup>, Hu Z.-K.<sup>†1</sup>**

<sup>1</sup>MOE Key Laboratory of Fundamental Quantities Measurement, Hubei Key Laboratory of Gravitation and Quantum Physics, School of Physics, Huazhong University of Science and Technology, Wuhan, 430074, People's Republic of China

<sup>†</sup>zkhu@hust.edu.cn

Newton's gravitational constant  $G$  is a fundamental physical constant that describes the strength of gravitational force, with a value of approximately  $6.67430 \times 10^{-11} \text{ m}^3 \text{ kg}^{-1} \text{ s}^{-2}$ . Since Henry Cavendish first measured  $G$  using the torsion balance method in 1798, there have been over 300 measurements conducted to date. However, many high-precision experiments yield results that differ more than their respective uncertainties, making  $G$  the least precisely known fundamental physical constant. Achieving a measurement of  $G$  with an uncertainty below 100 ppm (parts per million) is an extremely challenging task. The significant discrepancies between  $G$  values obtained from different experiments may be due to unknown systematic errors. To obtain a reliable value for  $G$ , our laboratory has employed two independent methods: the "torsion balance period method" and the "angular acceleration method." The results from these two methods agree within their respective uncertainties. A third independent method for measuring  $G$  is the "atom interferometry method." The key feature of atom interferometry is that the test mass consists of freely falling microscopic atoms. Unlike macroscopic torsion balances, this method avoids issues related to suspension and macroscopic electric field effects. The current measured value of  $G$  is  $6.6531(67)(40) \times 10^{-11} \text{ m}^3 \text{ kg}^{-1} \text{ s}^{-2}$ , with a relative uncertainty of 1213 ppm.



Abstract number: P29  
Tuesday 14:00-15:30

# Test of the gravitational redshift with single-photon-based atomic clock interferometers

Liu J.<sup>1</sup>, Xu Y.-Y.<sup>†1</sup>, Fang X.-T.<sup>1</sup>, Cao L.-S.<sup>1</sup>, Zhou M.-K.<sup>1</sup>, Duan X.-C.<sup>1</sup>,  
Hu Z.-K.<sup>†1</sup>

<sup>1</sup>MOE Key Laboratory of Fundamental Quantities Measurement, Hubei Key Laboratory of Gravitation and Quantum Physics, School of Physics, Huazhong University of Science and Technology, Wuhan, 430074, People's Republic of China

<sup>†</sup>xuyaoyaoleo@hust.edu.cn; zkhu@hust.edu.cn

The gravitational redshift (GR), as predicted by Einstein's general theory of relativity, posits that two identical clocks situated at different gravitational potentials will tick at different rates. In this study, we explore the impact of the GR on a single-photon-based atom interferometer (ACI) and propose a corresponding testing scheme.

By thinking of atoms in a superposition state as a clock, a single-photon-based atom interferometer will have a clock, which has several hundreds of THz of frequency, such as Sr single-photon-based atomic clock interferometers.

Introducing a GR violation factor  $\alpha$ , the frequency of atomic clock:

$$\omega_{\text{clock}} = \omega_a \cdot (1 + (1 + \alpha) \cdot \frac{gz}{c^2}) \quad (0)$$

where  $g$  is the gravitational acceleration,  $c$  is the speed of light,  $z$  is the height of clock,  $\omega_a$  is the frequency of the energy level difference of an atom.

The GR effect on ACI is equivalence with two coherent atomic clock ticking at different altitudes to accumulation phase difference such as Fig. 1. Therefore, we can test the gravitational redshift effect by means of interference.

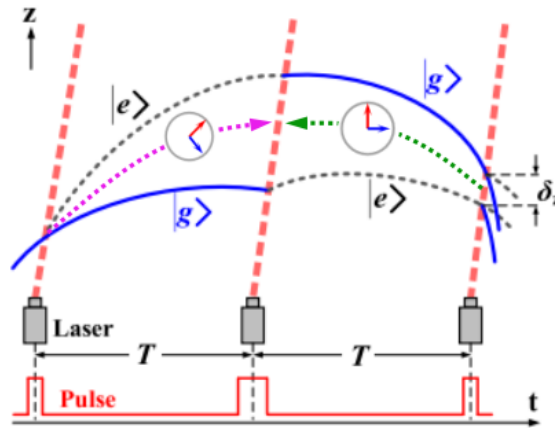


Figure 1: Space-time diagram with the finite speed of light (FSL).

Such as in a 10-meter fountain, the equivalent clock separation height difference caused by free-falling atoms is about 5 meters, and the frequency difference caused by the GR effect will accumulate over time as phase information that will be captured by the interferometer. According to the limits of quantum projection noise, an anticipated GR test ultimate precision can be  $10^{-5}$  level in a 10-meter fountain for our proposed approach.

Abstract number: P30  
Tuesday 14:00-15:30

## Microwave spectroscopy of ultracold sodium least-bound molecular states

**Yao Z.**<sup>1</sup>, **Ballu M.**<sup>1</sup>, **Mirmand B.**<sup>1</sup>, **Papoular D. J.**<sup>2</sup>, **Badr T.**<sup>1</sup>, **Perrin H.**<sup>1</sup>, **Perrin A.**<sup>†1</sup>

<sup>1</sup>Université Sorbonne Paris Nord, Laboratoire de Physique des Lasers,  
CNRS UMR 7538, 99 av. J.-B. Clément, F-93430 Villetaneuse, France

<sup>2</sup>Laboratoire de Physique Théorique et Modélisation,  
CNRS UMR 8089, CY Cergy Paris Université, 95302 Cergy-Pontoise, France

<sup>†</sup>aurelien.perrin@univ-paris13.fr

The scattering length, a key parameter quantifying the strength of atomic interactions, is of fundamental importance in the study of ultracold atomic systems. Precise knowledge of the scattering length is essential for accurately describing the degenerate quantum gases. Within the Born-Oppenheimer approximation, the scattering length is determined by the short-range interaction potential experienced by the atoms. Enhanced understanding of this potential can be achieved through more precise measurements of the energy of molecular bound states. Consequently, improvements in the precision of bound-state energy determinations can refine the evaluation of the scattering length.

In this study, we performed microwave spectroscopy of the least-bound states of sodium using an atom chip<sup>1</sup>, achieving a significant enhancement in the precision of their energy measurements at zero magnetic field. The precision was improved by three orders of magnitude, from the MHz to the kHz range. Our experimental results were compared with numerical calculations based on the latest interpolation of sodium interaction potentials<sup>2</sup>. The comparison reveals good agreement, despite minor discrepancies in the zero-field energy of the molecular states.

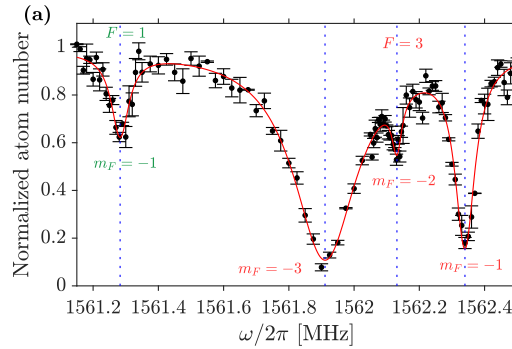


Figure 1: Photoassociation spectroscopy of molecular total angular momentum states ( $F = 1, 3$ ) within the  $\{f_1 = 1, f_2 = 2\}$  manifold, revealing the Zeeman structure. Here,  $f_1$  and  $f_2$  denote the total angular momentum of each constituent atom. Four distinct resonances, corresponding to specific  $F, m_F$  states as indicated in figure, were observed. Each black disk represents the mean remaining atom number, averaged over three experimental measurements, after a 30 ms microwave pulse with a field amplitude of  $|B| = 0.61\text{G}$ . Error bars indicate the standard deviation across these measurements. The red line is a curve fit to a sum of four Lorentzian functions. The static magnetic field amplitude used is  $B_s = 0.89(1)\text{G}$ .

<sup>1</sup>M. Ballu, B. Mirmand, T. Badr, H. Perrin, and A. Perrin, *Phys. Rev. A* **110**, article number (2024).

<sup>2</sup>S. Knoop *et al.*, *Phys. Rev. A* **83**, 042704 (2011).

Abstract number: P31

Tuesday 14:00-15:30

## Calculation of polarizabilities of low-lying states of silver

Filin D.<sup>†1</sup>, Porsev S.G.<sup>1</sup>, Cheung C.<sup>1</sup>, Safronova M.S.<sup>1</sup>

<sup>1</sup>University of Delaware, Newark, Delaware 19716, USA

<sup>†</sup>dfilin@udel.edu

The transition-metal silver atom has recently begun to attract increased attention from theorists and experimentalists. For example, atomic silver can be used in optical lattice clocks using the electric quadrupole  $4d^{10}5s\ ^2S_{1/2} - 4d^95s^2\ ^2D_{5/2}$  transition as a clock transition. One of the other interesting features of silver is its ability to form ultracold, highly polar diatomic molecules containing the silver atom (in its ground state) interacting with a noble gas, an alkali-metal or an alkaline-earth-metal atom.

To support the experimental efforts, we calculated the dc and ac polarizabilities (at the wavelengths 532 nm and 1064 nm convenient for laser trapping) for the lowest-lying even and odd-parity states of Ag. A specific feature of the Ag atom is that along with the states belonging to the configuration  $4d^{10}x$  (where  $x \equiv 5, 6s; 5, 6p, 5d$ , etc.), there are also low-lying states with the unfilled 4d shell  $4d^95s^2\ ^2D_{3/2,5/2}$ .

To calculate the properties of the  $4d^{10}x$  states, we used a single-electron method, such as many-body perturbation theory (MBPT) over the residual Coulomb interaction, or using an all-order, linearized coupled-cluster single-double (LCCSD) method. For calculating the properties of the  $4d^95s^2\ ^2D_{3/2,5/2}$  states, a single electron approach is not applicable. In this case, we consider Ag as an atom with many valence electrons and apply the 11- and 17-electron configuration interaction (CI) method.

Abstract number: P32  
Tuesday 14:00-15:30

## Qubit control based on various transition lines of $^{171}\text{Yb}$ atoms in optical tweezers

**Mun J.**<sup>†1,2</sup>, **Song Y.**<sup>1</sup>, **Kim K.**<sup>1</sup>, **Han J. H.**<sup>1</sup>, **Bae D.**<sup>1</sup>, **Oh S.**<sup>2</sup>, **Bae J.**<sup>2</sup>

<sup>1</sup>*Korea Research Institute of Standards and Science, Daejeon, Republic of Korea*

<sup>2</sup>*Korea Advanced Institute of Science and Technology, Daejeon, Republic of Korea*

<sup>†</sup>jcmun@kriss.re.kr

$^{171}\text{Yb}$  atom array platform provides a versatile system for quantum technology due to its rich internal level structure, which enables unique qubit controls based on various transition lines. First, nuclear spin qubits in the ground( $^1\text{S}_0$ ) and clock states( $^3\text{P}_0$ ) offer high coherence and fast single-qubit gates through a single beam Raman transition. Second, the ground-clock qubit serves as a basic element for frequency metrology such as optical clock. Lastly, the clock-Rydberg qubit leverages strong interactions to simulate complex quantum systems and implement multi-qubit gates, and can be driven via a one-photon transition. Furthermore, combining these qubits allows advanced quantum techniques, such as erasure conversion, mid-circuit operations, and two-qubit encoding, and a bridge between quantum computation and sensing.

In this presentation, we introduce the fundamental principles of these qubits and discuss the key techniques used to enhance coherence and atom control. Nuclear spin qubit is controlled by single-beam Raman transition based on modulated laser pulses. Also, ground-clock qubit control is demonstrated by using a Hz-linewidth clock transition laser, and coherence is improved by additional ground state cooling. Finally, clock-Rydberg qubit control is implemented with a shaped laser beam for one-photon transition.

Abstract number: P33  
Tuesday 14:00-15:30

## Spatially resolved Rydberg Doppler thermometry of a cold gas

Trivedi K.N.<sup>1,2</sup>, Solé Cardona E.<sup>1</sup>, Bégoc B.<sup>1,2</sup>, Carminati M.<sup>2</sup>, Bonaccorsi T.<sup>2</sup>, Donofrio R.<sup>2</sup>, Morsch O.<sup>1,2</sup>

<sup>1</sup>National Institute of Optics, CNR, Firenze, Italy

<sup>2</sup>Department of Physics, University of Pisa, Italy

†oliver.morsch@cnr.it

Rydberg atoms have become popular in recent years as a versatile physical platform for quantum sensing<sup>1</sup>. Typically, sensing applications are related to measuring electromagnetic fields. Here we show that Rydberg excitations can also be used to measure the velocity distribution, and hence temperature, of an atomic gas (rubidium in our case) via the Doppler broadening of a narrow Rydberg excitation line (typically only a few kHz for high-lying Rydberg states with principal quantum number above  $\approx 60$ ). In a two-photon excitation scheme, it is furthermore possible to achieve spatial resolution by intersecting the excitation beams at right angles (Fig. 1(a)). We demonstrated this spatial resolution by measuring the effective reduction of the width of the momentum distribution at the centre of a ballistically expanding cold cloud. As a first application (Fig. 1(b)), we measured the spatially varying temperature in a Rb magneto-optical trap<sup>2</sup>. Our method can in principle be used to measure temperatures as low as a few hundred nK with a spatial resolution of a few microns.

In our experiments, Rydberg excitations are detected using a channeltron, which gives us spatial information on the position of the Rydberg atoms belonging to a certain velocity class via their arrival time at the channeltron and thus allows us to measure position-velocity correlations. We used this feature to characterize the non-thermal velocity distribution resulting from Doppler heating with blue-detuned cooling lasers (Fig. 1(c)).

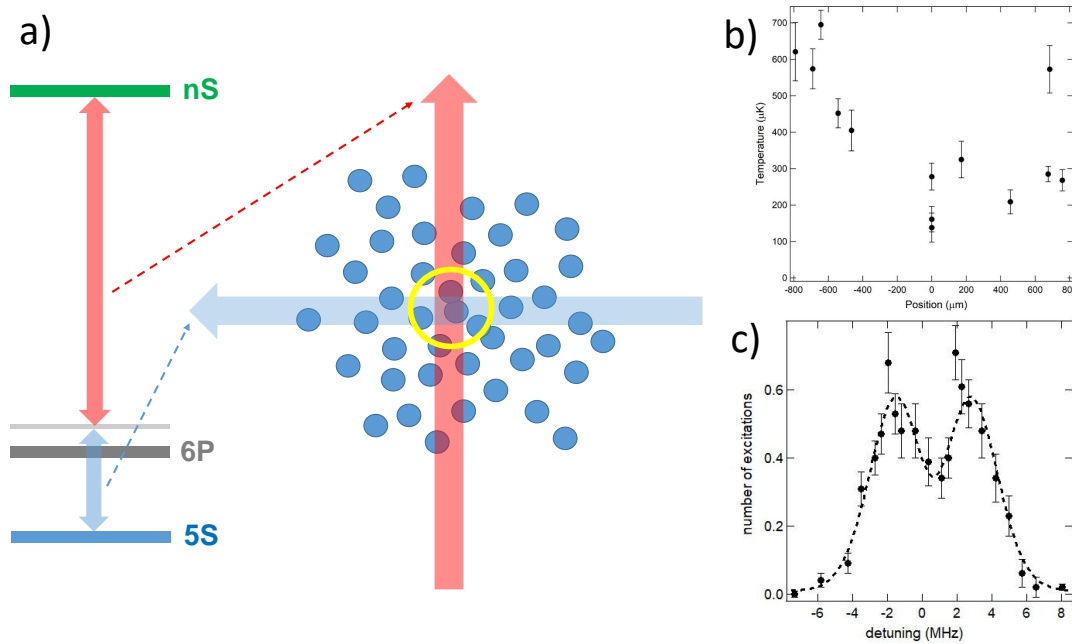


Figure 1: a) Scheme for spatially resolved Rydberg Doppler thermometry using two-photon excitation with laser beams crossing at right angles. b) Measurement of local temperature in a Rb magneto-optical trap. c) Non-thermal velocity distribution (laser detuning on the horizontal axis) in a Doppler-heated cloud.

<sup>1</sup>C.S. Adams, J.D. Pritchard, J.P. Shaffer, *J. Phys. B* **53**, 012002 (2020).

<sup>2</sup>A.S. Arnold, P.J. Manson, *JOSA B* **17**, 497 (2000).

Abstract number: P34  
Tuesday 14:00-15:30

## Multi-species cold-atom interferometry for inertial measurements

Landru M.<sup>†1</sup>, Cadoret M.<sup>2</sup>, Bidel Y.<sup>1</sup>, Bonnin A.<sup>1</sup>, Schwartz S.<sup>1</sup>, Bresson A.<sup>1</sup>, Godard A.<sup>3</sup>, Zahzam N.<sup>1</sup>

<sup>1</sup>ONERA DPHY - SLM, Palaiseau, France

<sup>2</sup>LCM - CNAM, La Plaine Saint-Denis, France

<sup>3</sup>ONERA DSG, Palaiseau, France

<sup>†</sup>mal.landru@onera.fr

Using wave properties of matter, cold atoms can become tiny quantum sensors with high stability and sensitivity to inertial quantities, such as rotation or acceleration. The principle of a cold-atom gravimeter is the following: cold atoms (at a few  $\mu\text{K}$ ) free fall in an ultra-high vacuum chamber, submitted to the Earth gravity  $g$ . While they are falling, one can probe the atoms with lasers in a matter-wave Mach-Zehnder interferometer: carefully-tuned laser pulses will transfer momentum to the atoms which will result in the matter wave being separated, deflected and recombined. At the end of the interferometer, the value of  $g$  can be obtained by measuring the phase of the atoms via fluorescence detection.

Contrary to their classical counterparts, cold-atom accelerometers suffer from dead times between each measurement (corresponding to the laser cooling sequence) and have a limited measurement range. However, they do benefit from an unrivalled stability and allow to perform absolute measurements in dynamic environments. Since classical and atomic sensors have complementary strengths and weaknesses, they are both commonly combined to create hybrid sensors. Unfortunately, hybrid sensors could be limited by the intrinsic noise of the classical sensor. Nonetheless, there could be another way to make the best of the atomic accelerometer: manipulating different atomic species simultaneously inside the same sensor. Indeed, there are insightful configurations using 3 atomic species ( $^{85}\text{Rb}$ ,  $^{87}\text{Rb}$  and  $^{133}\text{Cs}$ ) instead of one<sup>1</sup>. One could decrease dead times by 'juggling'<sup>2</sup> between the 3 species such that while one species is being laser-cooled, the other is free-falling in the matter-wave Mach-Zehnder and the third species is being detected. Another configuration could enable simultaneous 3D acceleration measurements.

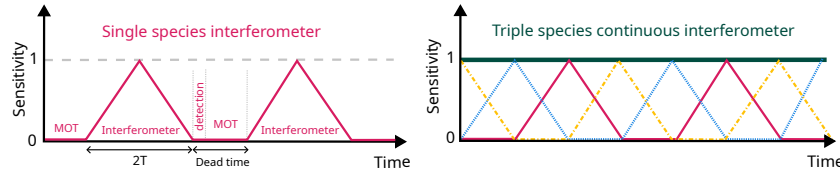


Figure 1: Continuous triple-species configuration. The dead times of one species are filled in by the other species.

The challenge is to imagine and set up ingenious configurations to exploit the full potential of the triple-species gravimeter, dealing with interspecies interactions while keeping the set-up compact and robust for possible applications in dynamic environment. In this regard, we have developed an all-fibered laser system based on telecom laser diodes at  $1.5\ \mu\text{m}$  and at  $1.9\ \mu\text{m}$ . First demonstrations of simultaneous cooling and trapping of the three atomic species have been carried out. The characteristics of the different magneto-optical traps, such as loading time or atom number, now need to be studied, as they provide information, notably on the multi-species collisions. Meanwhile, a numerical simulation is developed to investigate the impact of dead times and explore the advantages of a multi-species sensor in the context of on-board marine measurements.

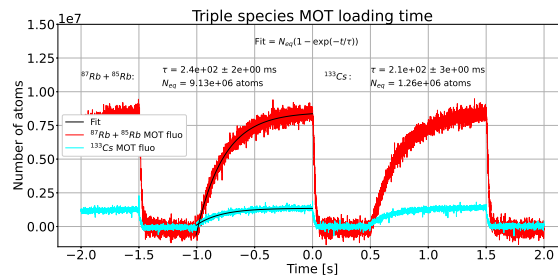


Figure 2: Loading curves of the triple species MOT

<sup>1</sup>A. Bonnin *et al.*, *Applied Physics B* **124**, 181 (2018).

<sup>2</sup>M. Meunier *et al.*, *Physical Review A* **90**, 6 (2014).

Abstract number: P35  
Tuesday 14:00-15:30

## Improvement of Short-Term Stability in a Compact Laser-Cooled Rb Atomic Clock

Park S. E.<sup>†1</sup>, Park S.<sup>1,2</sup>, Seo M.<sup>1</sup>, Park Y.-H.<sup>1</sup>, Hong H.-G.<sup>1</sup>, Lee S.-B.<sup>1</sup>, Lee J. H.<sup>1</sup>, Kang S.<sup>1</sup>, Seo S.<sup>1</sup>, Kwon T. Y.<sup>1</sup>

<sup>1</sup>Korea Research Institute of Standards and Science, Daejeon, South Korea

<sup>2</sup>Chonnam National University, Gwangju, South Korea

<sup>†</sup>parkse@kriss.re.kr

Atomic clocks are essential for modern timekeeping and navigation systems. However, traditional atomic clocks, such as hydrogen masers, are large and power-intensive, limiting their use in portable applications. To overcome these limitations, several laser-cooled atomic clocks are being developed, and some have already been commercialized.<sup>1,2,3,4</sup> In this work, we present a miniaturized laser-cooled atomic clock based on a loop-gap microwave cavity. The loop-gap cavity provides a significant reduction in both size and weight compared to conventional cylindrical cavities.<sup>5</sup>

Figure 1(a) shows an image of the physics package, enclosed by magnetic shields. The cavity features eight symmetrically placed holes around the central axis, which serve as access points for the laser cooling beams, fluorescence observation, and symmetric microwave feeding. This design results in a cavity volume that is eight times smaller than traditional microwave cavities. The measured linewidth of the Ramsey spectrum is 19.6 Hz, which is limited by the free-fall distance of the atomic cloud within the cavity. The frequency stability, as compared to a hydrogen maser, has been improved by reducing local oscillator noise and increasing the number of trapped atoms. The best short-term stability achieved is  $4.5 \times 10^{-13} \tau^{-1/2}$ , as shown in Figure 1(b). The miniaturized design and impressive performance make this technology suitable for various mobile applications, such as navigation satellites, portable ground-based timekeeping instruments, and other high-precision timekeeping devices.

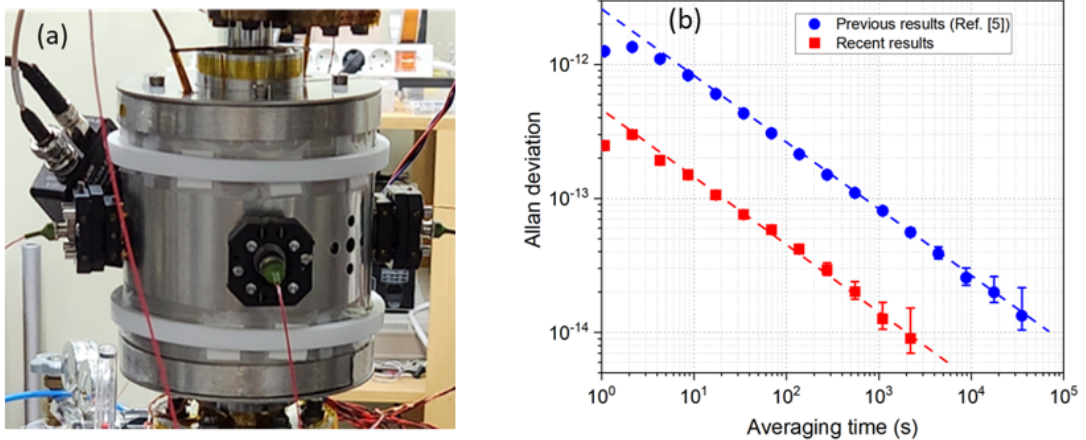


Figure 1: (a) Physics package of the compact cold atom clock. (b) Frequency stability of the compact cold-atom clock, measured relative to a hydrogen maser. The red dashed line represents  $\sigma_y(\tau) = 4.5 \times 10^{-13} \tau^{-1/2}$ .

<sup>1</sup>F. X. Esnault, D. Holleville, N. Rossetto, S. Guerandel, and N. Dimarcq, *Phys. Rev. A*, **82**, 033436 (2010).

<sup>2</sup>P. Liu, Y. L. Meng, J. Y. Wan, X. Wang, Y. Wang, L. Xiao, H. Cheng, and L. Liu, *Phys. Rev. A*, **92**, 062101 (2015).

<sup>3</sup>cRb-Clock, See <https://spectradynamics.com/products/crb-clock/> (last accessed March. 10, 2025).

<sup>4</sup>MuClock, See <https://www.muquans.com/product/muclock/> (last accessed March. 10, 2025).

<sup>5</sup>S. Lee, G. W. Choi, H. G. Hong, T. Y. Kwon, S.-B. Lee, M.-S. Heo, and S. E. Park, *Appl. Phys. Lett.*, **119**, 064002 (2021).

Abstract number: P36

Tuesday 14:00-15:30

## Microscopy of density-wave ordering in strongly interacting Fermi gases

**Fabre A.**<sup>†1,2</sup>, **Bühler T.**<sup>1,2</sup>, **Bolognini G.**<sup>1,2</sup>, **Xue Z.**<sup>1,2</sup>, **Zwettler T.**<sup>1,2</sup>, **Del Pace G.**<sup>1,2</sup>, **Brantut J.-P.**<sup>1,2</sup>

<sup>1</sup>Laboratory for Quantum Gases, EPFL, Lausanne, Switzerland

<sup>2</sup>Quantum Science and Engineering Center, EPFL, Lausanne, Switzerland

<sup>†</sup>aurelien.fabre@epfl.ch

Quantum simulation using experimental platforms based on ultracold atoms provides a powerful approach to studying complex many-body systems that are intractable for a large number of particles using conventional numerical methods. While most studies have focused on short-range interactions, their combination with long-range interactions remain largely unexplored.

Cavity quantum electrodynamics (cavity QED) offers a promising platform to investigate such interactions by mediating long-range coupling between atoms via cavity photons. In the strong coupling regime, atoms undergo a second-order phase transition from a disordered to an ordered phase under an external transverse drive, a phenomenon extensively studied with bosonic quantum gases. We explore this transition in a spin-balanced ensemble of interacting fermionic <sup>6</sup>Li atoms, where both short-range and long-range interactions compete at low temperatures.

I will present our recent experimental results on probing this phase transition using not only the detection of the leakage field but also high-resolution absorption imaging of the *in situ* atomic density. This led to the observation of atomic ordering as the transition is crossed, based on recorded atomic densities featuring a periodic modulation. Importantly, the photonic and atomic signals are observed from the same quantum trajectory of the hybrid system in a single shot. Our measurements reveal the correlation between the intracavity field and the observed spatial ordering of atoms, even in the presence of significant fluctuations stemming from the initial seeding of the instability.

The ability to probe and control atomic gases at the micrometer scale has been crucial in quantum gas experiments in the last decades, particularly with the advent of quantum gas microscopes. We anticipate that the integration of high-resolution imaging with our cavity-QED setup will unlock new opportunities, such as the direct observation of spatial correlations and the precise manipulation of the atomic trapping potential.



**Abstract number: P37**  
**Tuesday 14:00-15:30**

## A $^{171}\text{Yb}$ - $^{173}\text{Yb}$ cold-atom comagnetometer

**Luo W.<sup>1</sup>, Zhang J.<sup>1</sup>, Yang Y.<sup>1,3</sup>, Wang Y.<sup>1</sup>, Xia T.<sup>†2</sup>, Lu Z.<sup>†1,2</sup>**

<sup>1</sup>*Hefei National Research Center for Physical Sciences at the Microscale, School of Physical Sciences, University of Science and Technology of China, Hefei, Anhui, China.*

<sup>2</sup>*Hefei National Laboratory, University of Science and Technology of China, Hefei, 230026, Anhui, China.*

<sup>3</sup>*Present address: JILA, National Institute of Standards and Technology and University of Colorado, Department of Physics, University of Colorado, Boulder, CO, USA.*

<sup>†</sup>txial@ustc.edu.cn <sup>†</sup>ztlu@ustc.edu.cn

This article presents a cold-atom comagnetometer utilizing two isotopes of ytterbium. Spin sensors, renowned for their high sensitivity, are vital in precision measurements. Comagnetometer often employs different spin responders to mitigate magnetic noise. Despite the proven effectiveness of vapour cell systems in various fields, cold atom systems demonstrate notable advantages by eliminating inherent systematic errors found in vapour cell architectures, and are capable of achieving micron-scale precision. Our implementation uses  $^{171}\text{Yb}$  (with nuclear spin 1/2) and  $^{173}\text{Yb}$  (with nuclear spin 5/2) to realize a cold-atom comagnetometer. We detailedly analyzed environmental magnetic field suppression ratios and systematic errors, and investigated the vector and tensor light shift introduced by optical trap, along with other potential systematic errors. Additionally, we observed and analyzed dispersive effects arising from tensor shifts. In experiments involving 10s of phase accumulation, our device achieved a magnetic noise suppression factor greater than  $8 \times 10^4$ . Furthermore, we determined the absolute-value ratio of the nuclear magnetic moments between the two isotopes  $|\text{R}_{\text{NMM}}| = 0.726076(3)$ , improving upon known results by an order of magnitude. Cold-atom comagnetometer opens up new avenues in quantum technology, and aids future explorations in fundamental physics.

Abstract number: P38  
Tuesday 14:00-15:30

## Excited-state magnetic properties of carbon-like calcium $\text{Ca}^{14+}$

Chen S.<sup>†1</sup>, Spieß L. J.<sup>1</sup>, Wilzewski A.<sup>1</sup>, Wehrheim M.<sup>1</sup>, Gilles J.<sup>1,2</sup>, Surzhykov A.<sup>1,2</sup>, Benkler E.<sup>1</sup>, Filzinger M.<sup>1</sup>, Steinel M.<sup>1</sup>, Huntemann N.<sup>1</sup>, Cheung C.<sup>3</sup>, Sergey G. Porsev<sup>3</sup>, Bondarev A. I.<sup>4,5</sup>, Safronova M. S.<sup>3</sup>, Crespo López-Urrutia J. R.<sup>6</sup>, Schmidt P. O.<sup>1,7</sup>

<sup>1</sup>Physikalisch-Technische Bundesanstalt, Braunschweig, Germany

<sup>2</sup>Institut für Mathematische Physik, Technische Universität Braunschweig, Germany

<sup>3</sup>Department of Physics and Astronomy, University of Delaware, USA

<sup>4</sup>Helmholtz-Institut Jena, Germany

<sup>5</sup>GSI Helmholtzzentrum für Schwerionenforschung GmbH Darmstadt, Germany

<sup>6</sup>Max-Planck-Institut für Kernphysik, Heidelberg, Germany

<sup>7</sup>Institut für Quantenoptik, Leibniz Universität Hannover, Germany

<sup>†</sup>shuying.chen@quantummetrology.de

Highly charged ions (HCI) have extreme properties due to the proximity of electrons to the nucleus, including low sensitivity to external field perturbations and high sensitivity to nuclear physics test<sup>2</sup>. The low number of electrons also allows precise theoretical calculations for HCI parameters, which can be compared to experimental measurements. Magnetic field properties of HCI are of interest for both theoretical and experimental research and for fundamental physics tests as well as time and frequency metrology. So far, the ground state g-factor measurements of HCI in Penning traps facilitate the most accurate tests of strong field QED. However, excited-state g-factors are difficult to measure using the same Penning trap techniques, due to the limited lifetime of the excited state. Furthermore, the second-order Zeeman shift coefficient has not been measured for any HCI up to now, which is important for the systematic uncertainty evaluation of HCI-based optical clock development.

In this work, we demonstrate g-factor measurements of the excited state of highly charged  $\text{Ca}^{14+}$  with a relative uncertainty of  $10^{-6}$  by estimating the magnetic field using a co-trapped  $\text{Be}^+$  ion. The experimental result is compared to newly-performed theoretical calculations and finds excellent agreement. The comparison highlights the significance of the frequency-dependent Breit contribution to the atomic structure, and particularly the negative energy states and QED effects on magnetic moments, which have not been considered before in such a system. Furthermore, we measured the second-order Zeeman effect coefficient  $C_2$  and verified the predicted small second-order Zeeman shift in  $\text{HCI}^3$ , which will advance the further development of HCI-based optical clock. The technique presented here can be extended to other HCI with optical transitions.

<sup>1</sup>Spieß *et al.*, *arXiv:2502.18926* (2025).

<sup>2</sup>Kozlov *et al.*, *Rev. Mod. Phys.* **90**, 045005 (2018).

<sup>3</sup>Gilles *et al.*, *Phys. Rev. A* **110**, 052812 (2024).

Abstract number: P39  
Tuesday 14:00-15:30

## Enhancement of Kerr Nonlinearity in Quantum Dot Molecules Via Tunneling Mechanism

Mukherjee R.<sup>†1</sup>, Hazra R.<sup>2</sup>, Borgohain N.<sup>3</sup>

<sup>1</sup>Theoretical Photonics Group, Department of Physics, Sarala Birla University, Ranchi, India-835103

<sup>2</sup>Department of Humanities and Sciences, Malla Reddy Engineering College for Women, Secunderabad, Telangana, India-500100

<sup>3</sup>Department of Physics, University of Science & Technology Meghalaya, India-793101

<sup>†</sup>rohitmukherjee670@gmail.com

In recent years, quantum dot molecules (QDMs) have exhibited intriguing optical properties in infrared regimes through their interaction with electromagnetic fields<sup>1</sup>. These properties hold significant implications for various photonics applications, including optical data storage, quantum communications, computing, and information processing<sup>2</sup>. In this paper, we present a unique approach to enhance Kerr nonlinearity in coupled QDMs via tunneling induced transparency. In such systems, the width of the transparency could be modulated by utilizing tunneling between two quantum dots. The Kerr nonlinearity of the system can be enhanced by an order of  $10^6$  as compared to other quantum dot molecules. We hope the investigation could be useful for the application of optical switching based devices using semiconductor quantum dots.

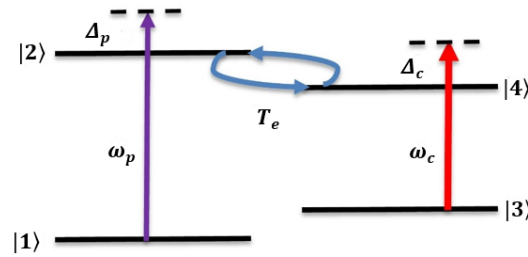


Figure 1: Schematic energy level diagram of quantum dot molecules (QDMs) with interacting probe ( $\omega_p$ ) and control ( $\omega_c$ ) fields.

<sup>1</sup>X. Q. Luo, Z. Z. Li, T. F. Li, W. Xiong and J. Q. You, *Optics Express* **26**, 32585 (2018).

<sup>2</sup>Y. Wang, J. Ding and D. Wang, *European Physical Journal D* **74**, 190 (2020).

Abstract number: P40  
Tuesday 14:00-15:30

## Hong-Ou-Mandel interference of more than 10 indistinguishable atoms

Quensen M.<sup>†1,2</sup>, Hetzel M.<sup>1,2</sup>, Santos L.<sup>1</sup>, Smerzi A.<sup>3,4,5</sup>, Tóth G.<sup>6,7,8,9</sup>, Pezzè L.<sup>3,4,5</sup>, Klempt C.<sup>1,2</sup>

<sup>1</sup>*Institut für Quantenoptik, Leibniz Universität Hannover, Germany*

<sup>2</sup>*Deutsches Zentrum für Luft- und Raumfahrt e.V., DLR-SI, Hannover, Germany*

<sup>3</sup>*National Institute of Optics, CNR, Firenze, Italy*

<sup>4</sup>*European Laboratory for Nonlinear Spectroscopy, LENS, Sesto Fiorentino, Italy*

<sup>5</sup>*Quantum Science and Technology in Arcetri, QSTAR, Firenze, Italy*

<sup>6</sup>*University of the Basque Country, UPV/EHU, Bilbao/Leioa, Spain*

<sup>7</sup>*IKERBASQUE, Basque Foundation for Science, Bilbao, Spain*

<sup>8</sup>*Donostia International Physics Center, DIPIC, San Sebastián, Spain*

<sup>9</sup>*HUN-REN Wigner Research Centre for Physics, Budapest, Hungary*

<sup>†</sup>martin.quensen@dlr.de

When two indistinguishable bosons interfere at a beam splitter, they both exit through the same output port. This foundational quantum-mechanical phenomenon, known as the Hong-Ou-Mandel (HOM) effect, has become a cornerstone in the field of quantum information. It also extends to many indistinguishable particles, resulting in complex interference patterns. However, despite its fundamental and applied interest, the many-particle effect has only been observed in notoriously lossy photonic systems, and a realization with atomic systems has remained elusive until now. Here, we demonstrate HOM interference with up to 12 indistinguishable neutral atoms in a spinor BEC (sketch of measurement idea in Fig. 1a), showing negligible loss. Our single-particle counting clearly reveals parity oscillations and a bunching envelope (Fig. 1b), two defining features of the multi-particle HOM effect. We confirm genuine multi-partite entanglement in the generated Twin-Fock states using a novel criterion based on parity. By extracting the states' Fisher information, we observe that their phase sensitivities increase with the same scaling as those of ideal Twin-Fock states (Fig. 1c). Our technique offers the potential for scaling to much larger particle numbers, presenting promising applications in quantum information with indistinguishable particles and Heisenberg-limited atom interferometry.

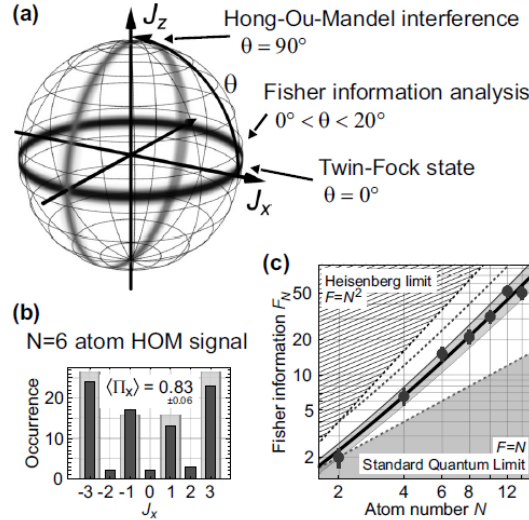


Figure 1: (a) Twin-Fock states  $|\frac{N}{2}\rangle_1 |\frac{N}{2}\rangle_2$  are generated through spin-changing collisions in our spinor Bose-Einstein condensate (BEC). We induce interference via Rabi oscillations, which correspond to rotations of the state's Husimi distribution on the generalized Bloch sphere. A  $90^\circ$  rotation resembles the mode coupling of a 50:50 beamsplitter. Finally, we count the state's mode occupation numbers using a low-noise fluorescence detection, achieving single-atom resolution. (b) Multi-particle Hong-Ou-Mandel interference results in the output state exhibiting only even mode occupation numbers, demonstrated by a recorded parity  $\Pi_x$  close to unity (light gray bars: ideal state). (c) We probe the state's phase sensitivity through small rotation angles and observe that the Fisher information  $F_N$  increases with particle number  $N$  parallel to that of ideal Twin-Fock states (solid line with shaded confidence region: fit of  $F_N = 0.58(7) \left( \frac{N^{1.95(7)}}{2} + N \right)$ ).

Abstract number: P41  
Tuesday 14:00-15:30

# Towards quantum limited milligram scale optomechanics

Valencia G.<sup>1</sup>, Agafonova S.<sup>1</sup>, Hosten O.<sup>†1</sup>

<sup>1</sup>*Institute of Science and Technology Austria (ISTA), 3400 Klosterneuburg, Austria*

<sup>†</sup>Onur.Hosten@ist.ac.at

Precision sensing with mechanical oscillators is a central goal in optomechanics. This is a highly active area of research and has enabled advances in fields ranging from gravitational wave detection<sup>1</sup> to experiments probing the interface of gravity and quantum mechanics<sup>2</sup>. Torsional oscillators are particularly attractive in this context because they are naturally well-isolated from environmental noise. Moreover, systems in the milligram mass range lie in a unique regime where quantum behavior remains accessible while gravitational effects may begin to play a role. Therefore, they are promising candidates for probing possible gravitational effects on quantum systems.

To explore this regime, we propose placing a torsional pendulum inside an optical cavity designed to sense and manipulate angular motion with high sensitivity. The optical mode in the cavity follows a zigzag path that is particularly responsive to yaw rotations (see Fig. 1), enabling the detection of small torsional displacements<sup>3</sup>. The high sensitivity of this configuration arises from the fact that a small angular displacement changes the zigzag mode length, leading to measurable shifts in the cavity resonance.

We are currently making progress in the experimental setup. As part of my contribution, I am working on the characterization of the free-space test cavity prior to integration into the vacuum chamber. This includes measuring its finesse and optical losses using the highly reflective mirrors intended for the final system. These measurements are essential for evaluating the optical performance and stability of the cavity. In the near future, this system could open new opportunities in torque sensing, optical cooling of rotational modes, and studies of quantum behavior in gravity-sensitive regimes.

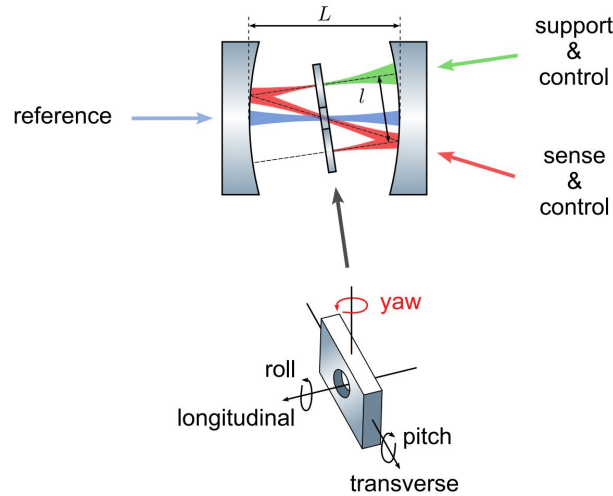


Figure 1: Schematic of the torsion sensing concept. A suspended torsion pendulum with a hole in the center and highly reflective coatings on both sides is inserted into a two-mirror optical cavity.

<sup>1</sup>S. M. Aston *et al.*, *Class. Quantum Grav.* **29**, 235004 (2012).

<sup>2</sup>T. Westphal, H. Hepach, J. Pfaff and M. Aspelmeyer, *Nature* **591**, 225–228 (2021).

<sup>3</sup>S. Agafonova, U. Mishra, F. Diorico and O. Hosten, *Phys. Rev. Res.* **6**, 013141 (2024).

Abstract number: P42  
 Tuesday 14:00-15:30

## Precision spectroscopy of $^{88}\text{Sr}$ with direct readout of the $^3\text{P}_n$ metastable states

**Kristensen S. L.**<sup>†1,2</sup>, **Kumar A.**<sup>1,2,3</sup>, **Blatt S.**<sup>1,2,3</sup>, **Bloch I.**<sup>1,2,3</sup>

<sup>1</sup>*Max-Planck-Institute for Quantum Optics, Garching, Germany*

<sup>2</sup>*Munich Center for Quantum Science and Technology, Munich, Germany*

<sup>3</sup>*Ludwig-Maximilians-Universität, Munich, Germany*

<sup>†</sup>sofus.kristensen@mpq.mpg.de

Optical lattice clocks operating with ultra cold strontium or ytterbium offer unprecedented precision and accuracy in timekeeping. With fractional frequency uncertainties down to the  $10^{-18}$  level, they enable scientific and technical advances from fundamental physics to global positioning systems.

We are developing a next-generation optical atomic clock, where spin squeezing of optically trapped  $^{88}\text{Sr}$  atoms will allow us to surpass the standard quantum limit of the atomic interrogation. To improve the short-term stability of the atomic clock, our experiment aims to demonstrate low-latency optical qubit readout made possible by rapid and direct imaging of the ground and metastable clock states.

Here, I will discuss the progress of the experiment, presenting our latest results of lattice trapping and spectroscopy of the magnetically induced clock transition in  $^{88}\text{Sr}$ , and discuss the next steps towards rapid-readout entanglement-enhanced quantum metrology.

Abstract number: P43  
Tuesday 14:00-15:30

## Laser spectroscopy of the Th229 nuclear clock transition

Masuda T.<sup>†1</sup>, Beeks K.<sup>2</sup>, Col L.<sup>2</sup>, Fukunaga Y.<sup>1</sup>, Guan M.<sup>1</sup>, Hiraki T.<sup>1</sup>, Kazakov G.<sup>2</sup>, Leitner A.<sup>2</sup>, Morawetz I.<sup>2</sup>, Ogake R.<sup>1</sup>, Okai K.<sup>1</sup>, Riebner T.<sup>2</sup>, Sasao N.<sup>1</sup>, Schaden F.<sup>2</sup>, Schneider F.<sup>2</sup>, Schumm T.<sup>2</sup>, Shimizu K.<sup>1</sup>, Sikorsky T.<sup>2</sup>, Takatori S.<sup>1</sup>, Yoshimi A.<sup>1</sup>, Yoshimura K.<sup>1</sup>,

<sup>1</sup>Research Institute for Interdisciplinary Science, Okayama University, Okayama, 700-8530, Japan

<sup>2</sup>Institute for Atomic and Subatomic Physics, Atominstut, TU Wien, Vienna 1020, Austria

<sup>†</sup>masuda@okayama-u.ac.jp

<sup>229</sup>Th has the low nuclear first excited state (<sup>229m</sup>Th) with the excitation energy of 8.356 eV. This allows excitation using vacuum ultraviolet lasers. In addition, the lifetime of the state is expected to be  $\sim 10^3$  second. These unique properties open up the possibility of realizing a clock based on nuclear energy levels, called nuclear clocks. Despite it has long been known that <sup>229</sup>Th has such an interesting state, laser excitation has been difficult to achieve. In 2024, however, the world's first laser excitation of <sup>229</sup>Th was finally realized using <sup>229</sup>Th-doped CaF<sub>2</sub><sup>1</sup>. Following this, two other groups also reported laser excitations, leading to rapid advances in research on <sup>229</sup>Th<sup>2,3</sup>.

Our group has conducted experiments using the high-intensity synchrotron radiation facility, SPring-8, in Japan, to excite <sup>229</sup>Th to <sup>229m</sup>Th via its second excited state<sup>4</sup> and observe the de-excitation light from <sup>229m</sup>Th using <sup>229</sup>Th-doped CaF<sub>2</sub><sup>5</sup>. The detection system<sup>6</sup> efficiently reduces radioluminescence background events and can also be used for laser excitation experiments.

Recently, we have developed a vacuum ultraviolet pulsed laser at Okayama University and have launched a laser spectroscopy project. The laser pulses are generated from two injection-seeded Titanium:Sapphire master oscillators, BBO-crystal-based third harmonic generation system, and four-wave mixing in Xe gas medium. The schematic of the laser system is shown in Figure 1. In this presentation, we will introduce an overview of our laser and detection systems and the status of our laser spectroscopy.

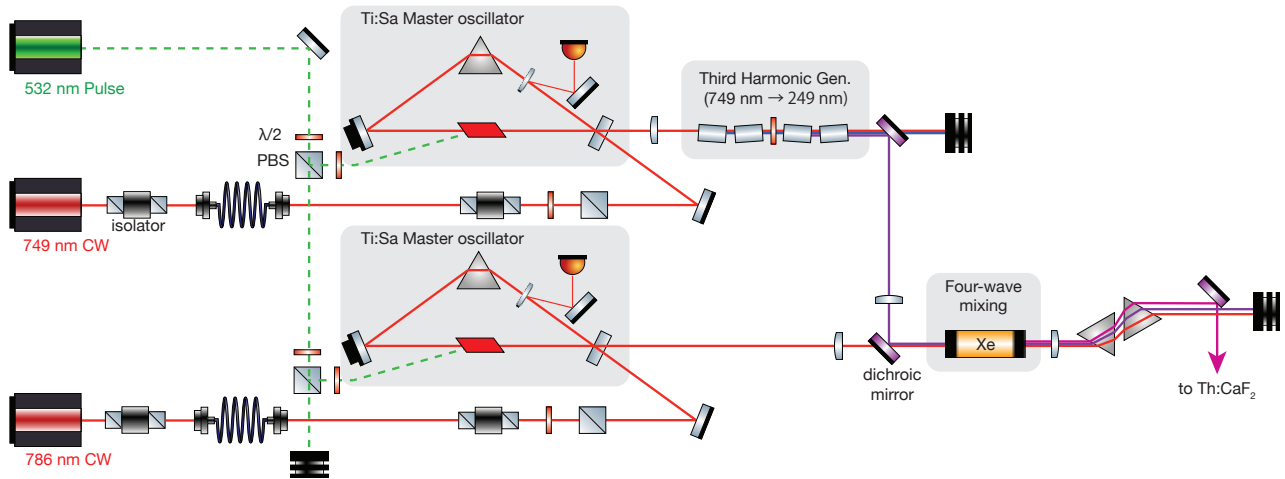


Figure 1: Schematic of the pulsed VUV laser system. Each Ti:Sa master oscillator generates narrow linewidth 749 nm (or 786 nm) pulses. The 749 nm pulses are converted to 249 nm pulses at the third harmonic generation part, which consists of four BBO crystals. The 249 nm and 786 nm pulses are then collinearly injected into the Xe gas. The generated VUV pulses in the Xe cell via four-wave mixing are separated from the fundamentals by the triangle prism pair and shot to the Th:CaF<sub>2</sub> crystal target.

<sup>1</sup>J. Tiedau *et al.*, *Phys. Rev. Lett.* **132**, 182501 (2024).

<sup>2</sup>R. Elwell *et al.*, *Phys. Rev. Lett.* **133**, 013201 (2024).

<sup>3</sup>C. Zhang *et al.*, *Nature* **633**, 63 (2024).

<sup>4</sup>T. Masuda *et al.*, *Nature* **573**, 238 (2019).

<sup>5</sup>T. Hiraki *et al.*, *Nat. Commun.* **15**, 5536 (2024).

<sup>6</sup>T. Hiraki *et al.*, *Interactions* **245**, 14 (2024).

Abstract number: P44  
Tuesday 14:00-15:30

## Measurement of 477 nm magic wavelength for strontium clock transition

Ma X.<sup>1</sup>, Das S.<sup>1,2</sup>, Wilkowski D.<sup>1,2,3</sup>, Kwong C.C.<sup>†1,2</sup>

<sup>1</sup>Centre of Quantum Technologies, National University of Singapore, Singapore

<sup>2</sup>Nanyang Quantum Hub, School of Physical and Mathematical Sciences, Nanyang Technological University, Singapore

<sup>3</sup>Majulab, International Joint Research Unit IRL 3654, CNRS, Université Côté d'Azur, Sorbonne Université, National University of Singapore, Nanyang Technological University, Singapore

†changchikwong@ntu.edu.sg

Atomic states undergo light shifts in the presence of electromagnetic field, which usually leads to shifts in the transition frequencies between two atomic states. However, for a light at the magic wavelength the polarizabilities of the two atomic states are equal, resulting in a transition frequency that is unshifted. Magic wavelength traps have played important roles in optical lattice clocks<sup>1</sup> and neutral atom tweezer arrays<sup>2</sup>.

In this work, we measure a new magic wavelength for the strontium-88  $5s^2\ ^1S_0 \rightarrow 5s5p\ ^3P_0$  clock transition. In particular, we target a magic wavelength that is expected between the wavelengths of the two transitions  $5s5p\ ^3P_0 \rightarrow 5s5d\ ^3D_1$  and  $5s5p\ ^3P_0 \rightarrow 5p^2\ ^3P_1$ . This magic wavelength is expected to have the largest polarizability among all magic wavelengths that are red-detuned from the  $5s^2\ ^1S_0 \rightarrow 5s5p\ ^1P_1$  transition.

To perform our experiment, we transfer around  $10^5$  strontium-88 atoms from a MOT<sup>3</sup> to a three-dimensional optical lattice. We use well-known 813.4 nm magic wavelength laser beams for the optical lattice. We perform a spectroscopy of the clock transition with and without shining an additional laser beam close to 477 nm onto the atoms. The shift of the clock resonance transition is obtained from the measured spectra (see Figure). We perform this measurement as a function of the 477 nm laser frequency and power. The magic wavelength condition occurs when zero shift is observed even in the presence of the 477 nm laser beam, regardless of its optical power. This occurs at 628728.3(1) GHz<sup>4</sup>.

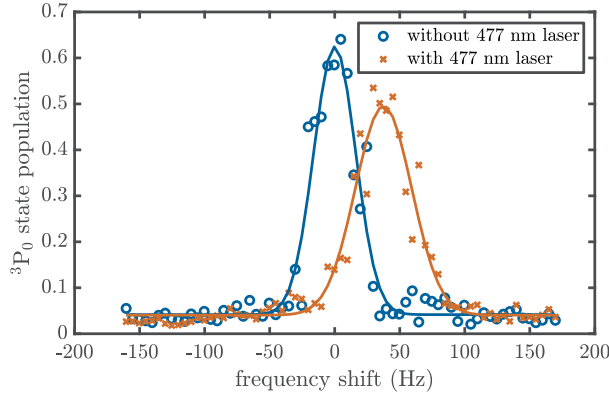


Figure 1: An example of the spectra with and without the presence of 477 nm laser beam, showing the shift of the clock transition resonance. The measurement is done at 477 nm laser frequency of 628720.0 GHz.

This new magic wavelength can be useful to create short lattice spacing optical lattices, which allow for a close packing of atoms for quantum simulation or studies of cooperative effects. Furthermore, this 476.8 nm magic wavelength can play the role of Bragg pulses for application in atomic clock interferometry, where the  $^1S_0$  and  $^3P_0$  states participate simultaneously in the interferometer<sup>5</sup>. Compared to the 813.4 nm magic wavelength, this new wavelength can lead to larger momentum transfer and better atom interferometry sensitivity.

<sup>1</sup>H. Katori, *Nat. Photonics* 5, 203 (2011).

<sup>2</sup>A. Young *et al.*, *Nature* 588, 408 (2020).

<sup>3</sup>J. Li *et al.*, *AVS Quantum Sci.* 4, 046801 (2022)

<sup>4</sup>X. Ma, S. Das, D. Wilkowski, C.C. Kwong, manuscript in preparation.

<sup>5</sup>J. Li *et al.*, manuscript in preparation.



Abstract number: P45  
Tuesday 14:00-15:30

# Optimal control in phase space applied to minimal-time transfer of thermal atoms in optical traps

Gavryusev V.<sup>†1,2,3</sup>, Morandi O.<sup>4</sup>, Nicoletti S.<sup>4</sup>, Giardini V.<sup>2,1</sup>, Guariento L.<sup>1</sup>, Fantini A.<sup>1</sup>, Storm S.<sup>1</sup>, Catani J.<sup>3,2</sup>, Inguscio M.<sup>5</sup>, Cappellini G.<sup>3,2</sup>, Fallani L.<sup>1,2,3</sup>

<sup>1</sup>Department of Physics and Astronomy, University of Florence, Via G. Sansone 1, 50019, Sesto Fiorentino, Italy

<sup>2</sup>European Laboratory for Non-Linear Spectroscopy (LENs), University of Florence, Via N. Carrara 1, 50019, Sesto Fiorentino, Italy

<sup>3</sup>National Institute of Optics (CNR-INO), National Research Council, Via N. Carrara 1, 50019, Sesto Fiorentino, Italy

<sup>4</sup>Department of Mathematics and Informatics 'Ulisse Dini', University of Florence, Viale Morgagni 67/A, 50134, Florence, Italy

<sup>5</sup>University Campus Bio-Medico, Via Álvaro del Portillo 21, 00128, Rome, Italy

<sup>†</sup>vladislav.gavryusev@unifi.it

We present an optimal control procedure for the non-adiabatic transport of ultracold neutral thermal atoms in optical tweezers arranged in a one-dimensional array<sup>1</sup>, with focus on reaching minimal transfer time. The particle dynamics are modeled first using a classical approach through the Liouville equation and second through the quantum Wigner equation to include quantum effects. Both methods account for typical experimental noise described as stochastic effects through Fokker-Planck terms, such as laser phase noise, finite atom temperature, beam-pointing and depth fluctuations of the tweezer trap. The optimal control process is initialized with a trajectory computed for a single classical particle and determines the phase-space path that minimizes transport time and ensures high transport fidelity to the target trap.

We study the optimal control procedure to steer a <sup>88</sup>Sr atom from an 0.1 mK deep initial trap to a target site at a 10  $\mu$ m distance, aiming to reach a fidelity above 99.5%. We identify an absolute minimum with flying time of 7.36  $\mu$ s (see Fig. 1), which is close to the theoretical lower physical boundary, and with a high fidelity of 99.97% in the classical case. The optimum solution derived in the quantum case for a <sup>6</sup>Li atom, leveraging the same trajectory and flying time, provides a fidelity of 98.95%. We test the robustness of the optimal control procedure and we analyze the heating of the atom that occurs during the transport, identifying avenues to achieve a favorable trade-off between the transfer speed and the energy increase.

Furthermore, we are currently testing these predictions on a novel apparatus with <sup>88</sup>Sr atoms trapped in reconfigurable optical tweezers<sup>2</sup>. Preliminary results and progress towards experimental validation of the optimal solutions are presented. This technique provides the fastest and most efficient method for relocating atoms from an initial configuration to a desired target arrangement, minimizing time and energy costs while ensuring high fidelity. Such an approach may be highly valuable to initialize large atom arrays for quantum simulation or computation experiments.

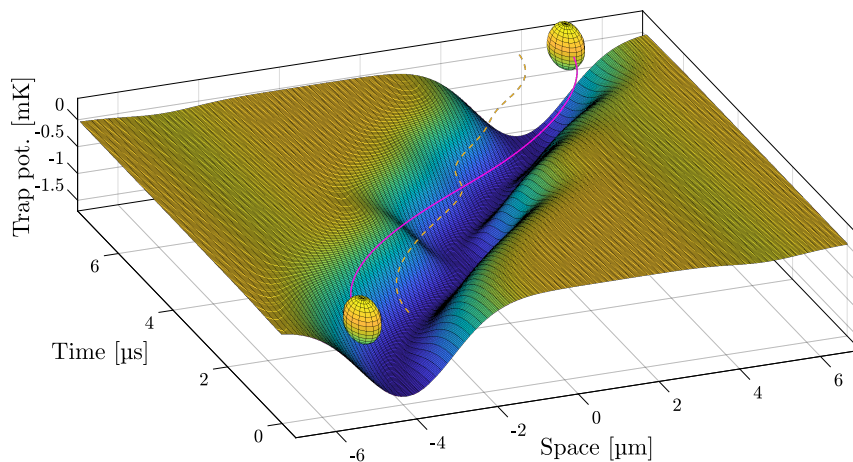


Figure 1: Time evolution of the atom position associated to the optimal time  $t_f = 7.36 \mu$ s. The particle trajectory is depicted in magenta. The 3D plot depicts the time evolution of the tweezers profile and the dashed yellow curve depicts the evolution of the center of the tweezers position. The spheres indicate the initial and final position of the atom.

<sup>1</sup>O. Morandi, S. Nicoletti, V. Gavryusev, L. Fallani, *arXiv e-prints*, arXiv:2501.10494 (2025).

<sup>2</sup>V. Gavryusev *et al.*, *Quantum 2.0 Conference and Exhibition proceedings*, QTh2A.2 (2024).

Abstract number: P46

Tuesday 14:00-15:30

## Collective light scattering in ordered 1D chains of dysprosium atoms

Biagioni G.<sup>†1</sup>, Hofer B.<sup>1</sup>, Bloch D.<sup>1</sup>, Bonvalet N.<sup>1</sup>, Browaeys A.<sup>1</sup>, Ferrier-Barbut I.<sup>1</sup>

<sup>1</sup> Université Paris-Saclay, Institut d'Optique Graduate School, CNRS, Laboratoire Charles Fabry, 91127, Palaiseau, France

<sup>†</sup>giulio.biagioni@institutoptique.fr

Understanding and controlling the light-matter interaction is crucial for many applications ranging from quantum metrology to quantum computing. While the interaction of light with a single quantum emitter is well understood, an ensemble of many emitters coupled by a resonant probe is a complex open quantum system. Programmable arrays of atoms in optical tweezers are particularly appealing for these kinds of problems, since the geometrical ordering offers the possibility to enhance the collective behavior exploiting the constructive and destructive interference between the emitters.

Here, we present a novel experimental apparatus of single dysprosium atoms trapped in one-dimensional tweezer arrays<sup>12</sup>. We employ a magic wavelength for the 626 nm intercombination transition, allowing for high-fidelity imaging. We then build defect-free atomic arrays with variable interparticle distances, reaching spacings of the order of a few transition wavelengths. In this regime, we report recent measurements of collective light scattering, manifesting in frequency shifts of the 626 nm transition<sup>3</sup>. Thanks to the flexibility of the tweezers setup, we measure the shift as a function of the interatomic distance. Relying on the interplay between the narrow intercombination transition and a broader transition at 421 nm, we develop an imaging scheme capable of resolving the internal state of the atoms trap by trap. We measure the propagation of the excitations along the array, highlighting the interference effect between the drive field and the field radiated by the atoms at the origin of the observed frequency shifts. We also perform measurements in the strong excitation regime with Ramsey spectroscopy, and we observe a dependence on the waiting time between the two Ramsey pulses due to the finite lifetime of the excitations. This measurement allows us to draw a connection between the linear optics regime and the strong excitation limit typical of optical atomic clocks.

Finally, we will discuss the implementation of a narrowline cooling scheme in non-magic trap conditions, with which we reach a 75 % occupation of the motional ground state in the radial direction of the tweezers. The increased control on the motional degree of freedom will find application in future light scattering experiments, in which suppressing the thermal disorder is important so as not to hinder many-body interference effects<sup>4</sup>.

<sup>1</sup>D. Bloch, B. Hofer, S. R. Cohen, A. Browaeys and I. Ferrier-Barbut, *Physical Review Letters* **131**, 203401 (2023).

<sup>2</sup>D. Bloch, B. Hofer, S. R. Cohen, M. Lepers, A. Browaeys and I. Ferrier-Barbut, *Physical Review A* **110**, 033103 (2024).

<sup>3</sup>B. Hofer, D. Bloch, G. Biagioni, N. Bonvalet, A. Browaeys and I. Ferrier-Barbut, <https://arxiv.org/abs/2412.02541> (2024)

<sup>4</sup>R.T. Sutherland and F. Robicheaux, *Physical Review A* **94**, 013847 (2016)

Abstract number: P47  
 Tuesday 14:00-15:30

## A highly accurate $^{171}\text{Yb}^+$ ion optical clock at NPL for metrology and tests of fundamental physics

Curtis E. A.<sup>†</sup>, Regan P., Tofful A., Godun R. M.  
 National Physical Laboratory, Teddington, United Kingdom

<sup>†</sup>anne.curtis@npl.co.uk

The accuracy and stability of state-of-the-art optical frequency standards, or optical clocks, can be used to advance technologies that require precision in position, navigation and timing, supporting synchronisation of communication networks, very-long-baseline interferometry, radio telescope arrays, and timestamping for financial markets, as well as navigation and timing provision of global satellite navigation systems. In addition, improvements in clock stability and accuracy enhance their use in tests of General Relativity and for investigating fundamental physics beyond the Standard Model<sup>1</sup>.

Optical clocks are reporting systematic frequency uncertainties at the parts-in- $10^{18}$  level and below, an improvement of two orders of magnitude compared to the current best realisations of the SI second, whose definition is based on a microwave transition in  $^{133}\text{Cs}$ . In light of this progress, the frequency metrology community has produced a roadmap towards the redefinition of the SI second in terms of optical frequency, providing a list of conditions that must be met before the redefinition<sup>2</sup>. Simultaneous optical frequency ratio measurements involving more than one optical clock, either co-located or in different laboratories or countries via interconnected fibre networks can enable direct exploration of clock performance at the part-in- $10^{17}$  level and below, providing a necessary check of the estimated uncertainties of optical clock systems.

At the UK's National Physical Laboratory (NPL) we are addressing these requirements for improved accuracy with the development of an optical frequency standard based on a single trapped  $^{171}\text{Yb}^+$  ion. The electronic structure of the  $^{171}\text{Yb}^+$  ion provides two clock transitions that are used for optical frequency metrology: the ultranarrow  $^2\text{S}_{1/2} \rightarrow ^2\text{F}_{7/2}$  electric octupole transition (E3), and the broader  $^2\text{S}_{1/2} \rightarrow ^2\text{D}_{3/2}$  electric quadrupole transition (E2). The E3 transition is particularly well suited for accurate timekeeping, with a strong, laser-accessible cooling transition, low sensitivity to electric and magnetic fields, and an extraordinarily narrow transition linewidth corresponding to an upper-state lifetime of  $\sim 1.6$  years. Its unique atomic structure provides high sensitivity to variations in time of the fine structure constant that can be exploited for tests of fundamental physics.

We will describe the  $^{171}\text{Yb}^+$  optical clock system at NPL, with an estimated fractional systematic frequency uncertainty of  $2.2 \times 10^{-18}$ , and discuss the system improvements behind its robust, high-uptime operation<sup>3</sup>. We will report on the latest absolute frequency measurements and optical frequency ratio measurements against local and distant clocks, via satellite links and optical fibre networks linking European institutes. The NPL  $^{171}\text{Yb}^+$  E3 clock has submitted frequency data to the International Bureau of Weights and Measures (BIPM), with the aim of contributing to International Atomic Time (TAI) to support the international effort to redefine the SI second. Finally, we will describe how frequency data from our clock is being used to investigate physics beyond the Standard Model, including ultralight scalar dark matter theories<sup>4,5</sup>.

<sup>1</sup>A. D. Ludlow, M. M. Boyd, J. Ye, E. Peik and P. O. Schmidt, *Review of Modern Physics* **87**, 637 (2015).

<sup>2</sup>N. Dimarcq *et al.*, *Metrologia*, **61**, 012001 (2024).

<sup>3</sup>A. Tofful *et al.*, *Metrologia* **61**, 045001 (2024).

<sup>4</sup>B. M. Roberts *et al.*, *New Journal of Physics* **22**, 093010 (2020).

<sup>5</sup>N. Sherrill *et al.*, *New Journal of Physics* **25**, 093012 (2023).

Abstract number: P48  
 Tuesday 14:00-15:30

## Single-beam grating-chip 3D and 1D optical lattices

Bregazzi A.<sup>1</sup>, McGilligan J. P.<sup>1</sup>, Griffin P. F.<sup>1</sup>, Riis E.<sup>1</sup>, Arnold A. S.<sup>1†</sup>

<sup>1</sup>Dept. of Physics, 107 Rottenrow, University of Strathclyde, Glasgow G4 0NG, UK

<sup>†</sup>aidan.arnold@strath.ac.uk

Ultracold atoms are crucial for unlocking truly precise and accurate quantum metrology and provide an essential platform for quantum computing, communication, and memories. One of the largest ongoing challenges is the miniaturization of these quantum devices. Here, we show that the typically macroscopic optical lattice architecture at the heart of many ultraprecise quantum technologies can be realized with a single-input laser beam on the same diffractive chip already used to create the ultracold atoms. Moreover, this inherently ultrastable platform enables access to a plethora of new lattice dimensionalities and geometries, ideally suited for the design of high-accuracy, portable quantum devices<sup>1</sup>.

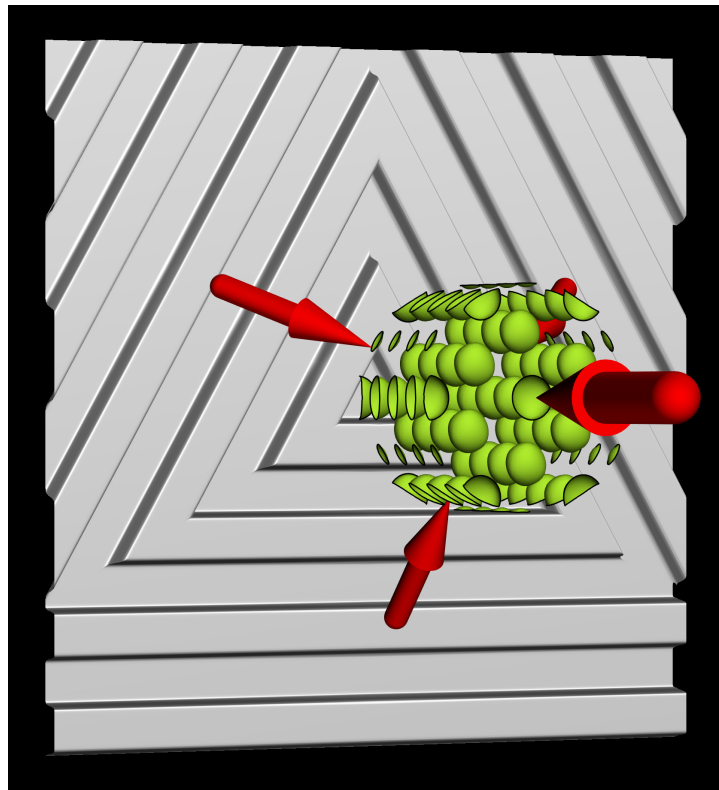


Figure 1: A triangular diffraction grating, when illuminated by a single laser beam (large arrow), creates diffracted orders (thin arrows) with stable phases locked to the grating surface. Here we illustrate the 3D optical lattice generated by the four combined laser beams, but 1D and 2D lattice geometries can be created with the same microfabricated grating chip.

<sup>1</sup>A. Bregazzi, J. P. McGilligan, P. F. Griffin, E. Riis and A. S. Arnold, *Phys. Rev. Lett.* **134**, 013001 (2025).

Abstract number: P49  
 Tuesday 14:00-15:30

## Bose-Einstein Condensation of Photons in Variable Potentials

**Wolf N.**<sup>†1</sup>, **Redmann A.**<sup>1</sup>, **Panico R.**<sup>1</sup>, **Vewinger F.**<sup>1</sup>, **Schmitt J.**<sup>1,2</sup>, **Weitz M.**<sup>1</sup>

<sup>1</sup>*Institute of Applied Physics, University of Bonn, Germany*

<sup>2</sup>*University of Heidelberg, Germany*

<sup>†</sup>n.wolf@iap.uni-bonn.de

While thermalization of radiation through contact with matter is a well-established concept, it has been shown only relatively recently that when applying this concept to low-dimensional photon gases, optical quantum gases with tunable chemical potential can be realized, which allows for the realization of Bose-Einstein condensates of photons<sup>1</sup>. Such experiments have been realized in dye-solution-filled optical microcavities and to date also in semiconductor systems, the latter realizing a system that much resembles a VCSEL-platform<sup>1,2,3</sup>.

We here report the demonstration of thermalization and Bose-Einstein condensation of a two-dimensional photon gas into the ground state of a periodically closed ring lattice<sup>4</sup>. This four-site ring lattice, superimposed by a harmonic trapping potential, is realized by imprinting a corresponding surface structure onto one of the cavity mirrors via controlled mirror surface delamination. The photons thermalize to room temperature by repeated absorption and emission processes on the dye molecules. Above a critical photon number, a macroscopic occupation of photons in the linear combination of site eigenstates with zero phase winding is observed, which constitutes the ground state of the system. Furthermore, the fixed phase relation of photons at different sites of the ring lattice has been verified interferometrically.

For future experiments, we expect that thermalization of photons in lattices in the presence of effective interactions, as feasible when engineering strong effective Kerr-interaction through cascaded second order nonlinearities, offers prospects for the preparation of entangled many-body states in a thermal equilibrium process when they constitute the system ground state.

In related research, we investigate the thermalization of photons in metallic mirror micropotentials in the cavity system. Utilizing laser milling as a structuring technique allows for micrometer-scale radii of curvature, thereby enabling trapping frequencies in the THz regime. The wide angular range of the reflectivity of metallic mirrors is expected to be beneficial in the search for phase-space build up of light by radiative contact to matter. We report on initial experimental observations with this newly developed metallic microcavity platform.

<sup>1</sup>J. Klaers, J. Schmitt, F. Vewinger, and M. Weitz, *Nature* **468**, 545–548 (2010).

<sup>2</sup>R. C. Schofield *et al.*, *Nature Photonics* **18**, 1083-1089 (2024).

<sup>3</sup>M. Pieczarka *et al.*, *Nature Photonics* **18**, 1090-1096 (2024).

<sup>4</sup>A. Redmann, C. Kurtscheid, N. Wolf, F. Vewinger, J. Schmitt, and M. Weitz, *Physical Review Letters* **133**, 093602 (2024).

Abstract number: P50  
Tuesday 14:00-15:30

## Trapped-Ion Electric Noise Spectrum Analyzer Assisted by Optical Tweezers

Cui J.-M.<sup>†1,2,3,4</sup>, Chen Y.<sup>1,2,3</sup>, Zhou Y.-F.<sup>1,2,3</sup>, An E.-T.<sup>1,2,3</sup>, Huang Y.-F.<sup>1,2,3,4</sup>, Li C.-F.<sup>1,2,3,4</sup>, Guo G.-C.<sup>1,2,3</sup>

<sup>1</sup> CAS Key Laboratory of Quantum Information, University of Science and Technology of China, Hefei 230026, China

<sup>2</sup> Anhui Province Key Laboratory of Quantum Network, University of Science and Technology of China, Hefei 230026, China

<sup>3</sup> CAS Center For Excellence in Quantum Information and Quantum Physics, University of Science and Technology of China, Hefei 230026, China

<sup>4</sup> Hefei National Laboratory, University of Science and Technology of China, Hefei 230088, China

<sup>†</sup>jmcui@ustc.edu.cn

Quantum sensors offer unparalleled sensitivity and spatial resolution, serving as essential tools for cutting-edge physics research. Electric field measurements based on trapped ions have achieved remarkable sensitivity, though their measurement range is typically limited to the MHz regime. In this work, we present a method to enhance both the sensitivity and measurement range of a single-ion probe by combining it with an optical tweezer. By leveraging the optical tweezer to generate an equivalent magnetic gradient on the ion, we demonstrate the measurement of electric field noise spectral density using spin-locking techniques. The minimum detectable signal is  $2.2(5) \times 10^{-11} \text{ V}^2 \text{ m}^{-2} \text{ Hz}^{-1}$ , and we show the capability to extend the detection frequency range into the GHz regime by modulating the light intensity. The dynamic magnetic gradient generated by the modulated optical tweezer is both strong and flexible, enabling the measurement of weak electric field spectra in a large range, as demonstrated in this work. Since the effect of the equivalent magnetic gradient on a spin is general, our work opens new possibilities for quantum spin detectors assisted by optical tweezers.

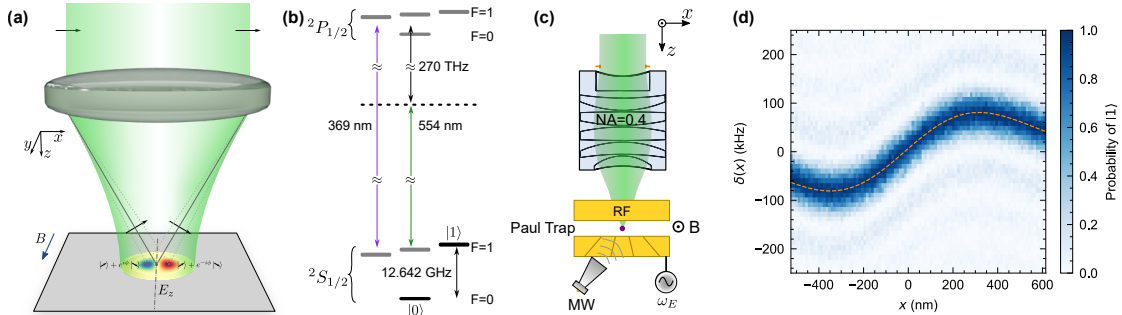


Figure 1: Equivalent magnetic field gradient (EMFG) generated by an optical tweezer interacting with a trapped ion.

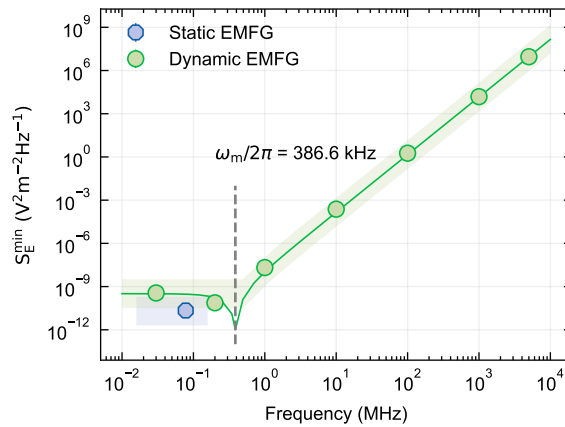


Figure 2: The minimum detectable signal of sensing with dynamic magnetic field gradients in different frequency ranges. The reduction in ion displacement at high frequencies leads to decreased sensitivity of the sensor.

Abstract number: P51  
 Tuesday 14:00-15:30

## High resolution laser spectroscopy towards exotic lanthanide and actinide isotopes for nuclear physics

Ajayakumar A.<sup>1</sup>, Au M.<sup>1</sup>, Bernerd C.<sup>1</sup>, Buker H.<sup>1</sup>, Chrysalidis K.<sup>1</sup>, Elle M.<sup>1,2</sup>, Fedosseev V.<sup>1</sup>, Heinke R.<sup>1,3</sup>, Jaradat A. A. H.<sup>1,3</sup>, Mancheva R.<sup>1,2</sup>, Reilly J.<sup>1</sup>, Rossel R.<sup>1</sup>, Rothe S.<sup>1</sup>, Wessolek J.<sup>1,3</sup>

<sup>1</sup>CERN, CH-1211 Geneva 23, Switzerland

<sup>2</sup>KU Leuven, Instituut voor Kern-en Stralingsfysica, B-3001 Leuven, Belgium

<sup>3</sup>Department of Physics and Astronomy, The University of Manchester, Manchester M13 9PL, United Kingdom

Our understanding of the atomic and nuclear properties of the chemical elements known as the actinides (atomic number  $Z \geq 89$ ) is an essential prerequisite for unraveling the structure of the superheavy elements at the end of Mendeleev's table. These findings are expected to have immediate applications in radio-ecology and nuclear medicine<sup>1</sup>. A European Union funded Marie Curie ITN network, named Laser Ionization and Spectroscopy of Actinides (LISA), was established to specifically target this region of the nuclear chart with different laser spectroscopy techniques. As a part of the LISA research network, significant progress has been taking place in the actinide research<sup>2</sup>.

In heavy nuclei, the long-range Coulomb repulsion between protons becomes increasingly comparable to the short-range strong nuclear force, which poses challenges to nuclear stability. The atomic shells of such heavy elements are strongly influenced by enhanced electron correlation and relativistic effects, which complicates the level scheme of the electronic orbitals and ultimately the chemical behaviour of these elements. The evolution of the established nuclear shell closures and regions of deformation toward the driplines remains difficult to predict based on the properties of nuclei close to stability. New experimental data is therefore necessary to better understand the trends of nuclear properties as functions of proton and neutron numbers and to rigorously test and refine nuclear models. Laser spectroscopy can be used to identify and perform a detailed characterization of electronic levels in such systems with high precision. For a known atomic levels, the subtle differences in the level energies in the members of an isotopic chain, and the arising hyperfine splitting for nuclei with a non-vanishing nuclear spin can be assessed to deduce fundamental nuclear ground-state properties such as nuclear moments and spins and also the changes of their size<sup>3</sup>.

As the atomic number increases, the scarcity of information becomes apparent because experimental investigations become increasingly complex and challenging due to decreasing sample quantities and short lifetime. Hence our experiments are performed, coupling with radioisotope production directly at online facilities. The radioactive species of interests are produced by spallation, fragmentation, fission and fusion-evaporation reactions. The conventional methods used at these facilities are often adapted to the element production process and would usually need to be further developed to achieve higher sensitivity. In order to improve the spectroscopic sensitivity and efficiencies, different techniques such as the gas cell/gasjet technique<sup>4,5</sup> is being employed in facilities such as GANIL (France)<sup>6</sup>, GSI (Germany)<sup>7</sup>. Similarly, the actinide and lanthanide regions are studied at ISOLDE, CERN using the LIST technique<sup>8</sup>. There has been increasing interest in extracting the less known nuclear spin and moments towards the proton emitting nuclei providing insights into how the deformation changes as the proton drip line is crossed and the nucleus starts to emit protons. It thus allows elucidation of shape evolution and deeper understanding of shell effects. The 2025 ISOLDE LIST runs aim to campaign the laser spectroscopy of several exotic isotopes of lanthanides such as Pm, Tm, Ho and Lu.

In this talk, I will summarize the different techniques used for the laser spectroscopic study of lanthanides and actinides and some of the significant results achieved through the LISA ITN research network. The first high-resolution laser spectroscopy results on Er obtained with the in-gas jet technique at the GANIL-SPIRAL2 facility, in preparation for the first experiments with the S<sup>3</sup>-Low Energy Branch<sup>9</sup>, will be presented. The measured isotope-shift and hyperfine structure data will be presented for stable isotopes of Er. The second part of my talk will introduce the in-source spectroscopy at ISOLDE, focusing on the LIST/PI-LIST technique. An outlook on the recent measurements on Pm isotopes ( $N=71-92$ ) and planned measurements for the year will be summarised<sup>10</sup>.

<sup>1</sup>J. Johnson *et al.*, *Sci. Rep.***13**,1347(2023)

<sup>2</sup><https://lisa-itn.web.cern.ch/conferences-publications>

<sup>3</sup>X. F. Yang *et al.*, *Prog. Part. Nucl. Phys.* **129**(2023)

<sup>4</sup>C. Granados *et al.*, *Phys. Rev. C* **96**(2017)

<sup>5</sup>R. Ferrer *et al.*, *Nat. Commun.* **8**,14520(2017)

<sup>6</sup>F. Déchery *et al.*, *Eur. Phys. J. A* **51**(6)(2015)

<sup>7</sup>S. Raeder *et al.*, *Nucl. Instrum. Methods Phys. Res. Sect. B* **463**,272(2020)

<sup>8</sup>S. Heinke *et al.*, *Nucl. Instrum. Methods Phys. Res. Sect. B* **541**(2023)

<sup>9</sup>A. Ajayakumar *et al.*, *Nucl. Instrum. Methods Phys. Res. Sect. B*(2023)

<sup>10</sup>K. Chrysalidis *et al.*, *INTC proposal to ISOLDE*(2023)

Abstract number: P52  
Tuesday 14:00-15:30

## Cavity design simulation to reduce cavity-related errors in atomic fountain clocks

Park Y.-H., Hong H.-G., Lee S.-B., Kwon T. Y., Lee J.H.,  
Kang S., Seo S., Seo M.H., Heo M.-S., Park S.E.<sup>†</sup>

Korea Research Institute of Standards and Science, Daejeon 34113, Republic of Korea

<sup>†</sup>parkse@kriss.re.kr

Relatively large uncertainties are associated with resonators in atomic fountain clocks due to cavity pulling, distributed cavity phase (DCP), and microwave lensing effects. The resonance frequency change with temperature of a microwave cavity is about 100 kHz/K, which is comparable to the resonator linewidth, so temperature stabilization of atomic clocks is important to reduce the frequency change due to cavity pulling effect. F. Zheng *et al.* have introduced dissimilar metals<sup>1</sup> to reduce the temperature sensitivity of the cylindrical cavity, which inevitably has a very long choke structure. If the choke length is around an odd multiple of microwave quarter wavelength, the field inside the choke will resonate and affect the  $m \geq 1$  DCP errors. The following figure shows the  $m = 1$  eigenfrequencies as a function of choke length in a Cs fountain microwave resonator with an inner radius of 26 mm. When the mode frequency approaches the clock transition frequency, it can cause a large  $m = 1$  DCP error, so it is crucial to adjust the choke length to avoid this. In this conference, we will present the effects of the choke structure on the  $m = 0, 1$ , and 2 DCP errors.

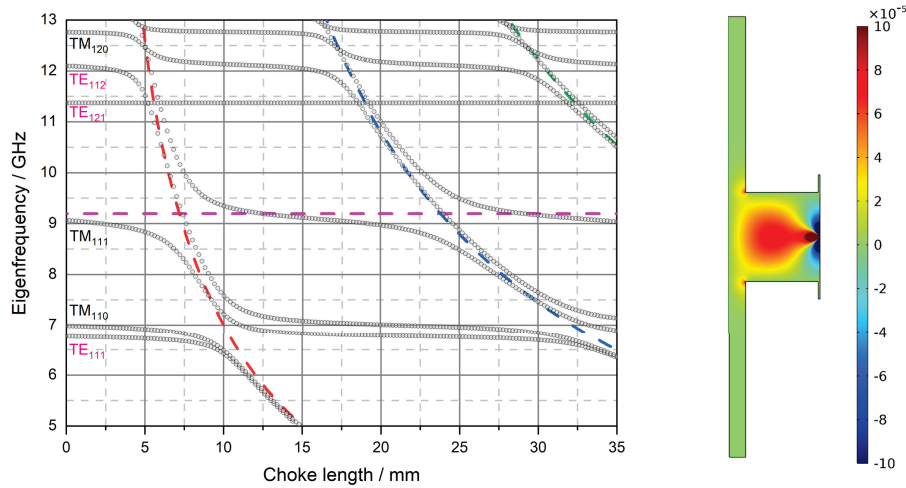


Figure 1: Left graph shows the  $m = 1$  eigenfrequencies (circles) against choke lengths in a cylindrical cavity. The horizontal dashed line represents the Cs clock transition frequency while the dashed slanted lines stand for the choke resonance. The choke and cylinder modes produce avoided mode crossings or simple overlaps depending on whether or not there is coupling between them. Right figure shows an example of the  $m = 1$  imaginary field distribution inducing the  $m = 1$  DCP error.

<sup>1</sup>F. Zheng *et al.*, *IEEE Transactions on Microwave Theory and Techniques* **71**, 4 (2023).



Abstract number: P53  
Tuesday 14:00-15:30

## Long optical cavity storage time and active RAM cancellation towards frequency stabilisation at $1 \times 10^{-18}$

Parke A. L., Schioppo M.<sup>†</sup>

National Physical Laboratory (NPL), Hampton Road, Teddington, United Kingdom

<sup>†</sup>marco.schioppo@npl.co.uk

Here we present our recent work on active cancellation of residual amplitude modulation (RAM) for ultrastable lasers at NPL<sup>1</sup>, using an x-cut annealed-proton-exchanged (APE) lithium niobate waveguide electro-optic phase modulator (EOM)<sup>2</sup>. The impact of RAM on the fractional frequency stability of a cavity-stabilised laser depends on the frequency discriminator of the cavity<sup>3</sup>, which is proportional to its optical storage time. A ringdown measurement of the newly built 68 cm long cavity used in this work is shown in Fig.1(a), corresponding to an optical storage time of  $\sim 300 \mu\text{s}$ . We show that by utilising this cavity and actively cancelling RAM we are able to reduce the RAM-induced fluctuation of the Pound-Drever-Hall (PDH)<sup>4</sup> error signal to a corresponding fractional frequency level below  $10^{-18}$  at averaging times greater than 2 s, as shown in Fig.1(b). This level is more than one order of magnitude below the thermal-noise-limited fractional frequency instability of our cavity, estimated at  $2 \times 10^{-17}$ . We discuss the main technical contributors of noise for our RAM measurement and characterisation set-up. Minimisation of RAM is essential to achieve state-of-the-art laser frequency stability and to enhance cavity-stabilised laser frequency predictability, positively impacting the use of these lasers as optical flywheels in optical time scales. Our set-up can also be used to evaluate RAM performance of the various EOM technologies being developed by industry and academia.

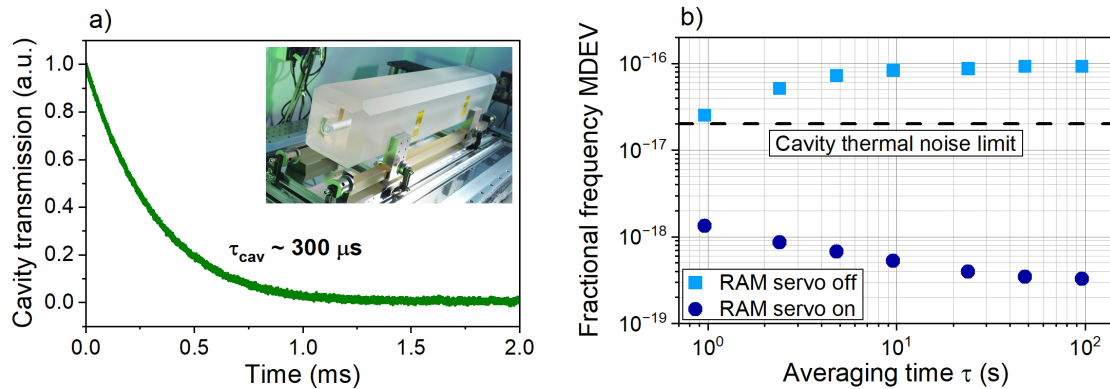


Figure 1: Figure 1: (a) In-vacuum ringdown measurement of the 68 cm long optical reference cavity used in this work, displayed in the inset (without vacuum housing). (b) Modified Allan deviation (MDEV) plot of RAM-induced fluctuation of the PDH error signal expressed in fractional frequency units, with RAM cancellation off (squares) and on (circles). The error bars are within the size of the markers and the linear drift of the cavity has been removed.

<sup>1</sup>M. Schioppo *et al.*, *Nat. Commun.* **13**, 212 (2022).

<sup>2</sup>E.L. Wooten *et al.*, *IEEE J. Sel. Top. Quantum Electron.* **6**, 69-82 (2000).

<sup>3</sup>W. Zhang *et al.*, *Opt. Lett.* **39**, 1980-1983 (2014).

<sup>4</sup>E.D. Black, *Am. J. Phys.* **69**, 79-87 (2001).

Abstract number: P54  
Tuesday 14:00-15:30

## Ultrastable lasers at NPL with fractional frequency instability below $10^{-16}$

Schioppo M.<sup>†</sup>, Parke A. L.

National Physical Laboratory (NPL), Teddington, United Kingdom

<sup>†</sup>marco.schioppo@npl.co.uk

Here we report on the development of cavity-stabilised lasers at NPL with fractional frequency instability below  $10^{-16}$  to enable state-of-the-art stability and continuous operation of optical clocks<sup>1</sup> at NPL, to enhance contribution to the BIPM roadmap towards the redefinition of the SI second based on optical standards<sup>2</sup>. To this end we focused on the development of optical reference cavities operating at room temperature, to achieve at the same time state-of-the-art stability, simplicity of use and continuous operation.

We present the latest achievements of our 48.5 cm long optical cavity<sup>3</sup>, displayed in Fig.1(a), with thermal-noise-limited fractional frequency instability measured at  $6 \times 10^{-17}$ , exhibiting low non-linear drift, measured using optical clocks as reference. This has enabled NPL optical clocks<sup>4,5</sup> to use more advanced spectroscopy schemes, such as Ramsey<sup>6</sup> and autobalanced Ramsey<sup>7</sup>. We discuss our design choices for a newly built 68 cm long cavity, displayed in Fig.1(b), with an estimated thermal-noise-limited fractional frequency instability at  $2 \times 10^{-17}$ . We present our strategies to reduce sensitivity to accelerations and minimise pressure-induced instability. We show preliminary stability and drift measurements using the 48.5 cm long cavity as a reference.

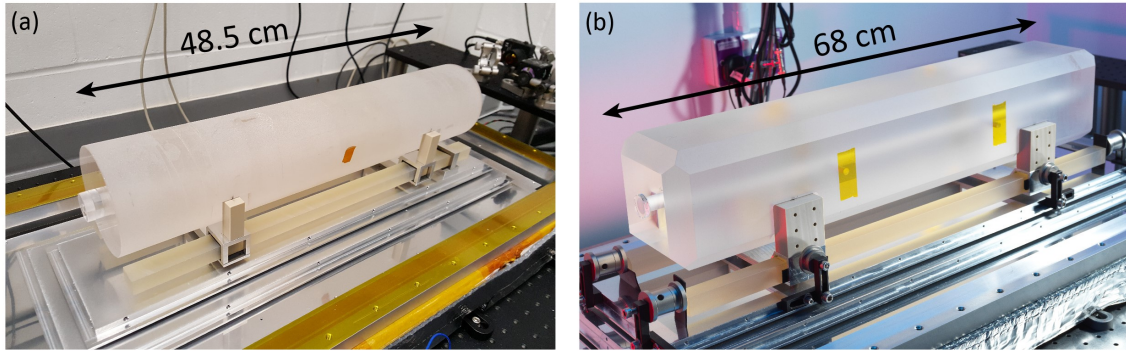


Figure 1: Photographs of the NPL optical reference cavities used in this work. Both systems are operated at room temperature and each hosted inside three layers of radiative thermal shields and in a vacuum chamber (not shown here) with a pressure at the  $10^{-8}$  mbar level.

<sup>1</sup>A. D. Ludlow, M. M. Boyd, J. Ye, E. Peik and P. O. Schmidt, *Rev. Mod. Phys.* **87**, 637 (2015).

<sup>2</sup>N. Dimarcq *et al.*, *Metrologia* **61**, 012001 (2024).

<sup>3</sup>M. Schioppo *et al.*, *Nat. Commun.* **13**, 212 (2022).

<sup>4</sup>A. Tofful *et al.*, *Metrologia* **61**, 045001 (2024).

<sup>5</sup>R. Hobson *et al.*, *Metrologia* **57**, 065026 (2020).

<sup>6</sup>N. F. Ramsey, *Phys. Rev.* **78**, 695 (1950).

<sup>7</sup>C. Sanner, N. Huntemann, R. Lange, C. Tamm and E. Peik, *Phys. Rev. Lett.* **120**, 053602 (2018).

Abstract number: P55  
 Tuesday 14:00-15:30

## A cavity-microscope for micrometer-scale control of atom-photon interactions

**Dubois L.**<sup>†1</sup>, **Orsi F.**<sup>1</sup>, **Bhatt R. P.**<sup>1</sup>,  
**Fedotova E.**<sup>1</sup>, **Eichenberger M. A.**<sup>1</sup>, **Sauerwein N.**<sup>1</sup>, **Brantut J-P.**<sup>1</sup>,

<sup>1</sup> *Institute of Physics and Center for Quantum Science and Engineering, EPFL, Lausanne, Switzerland*

<sup>†</sup>lea.dubois@epfl.ch

Cavity quantum electrodynamics (cQED) studies the strong interaction between matter and the electromagnetic field of an optical cavity: the enhanced interaction is useful both for reading the properties of the atoms with a fast, sensitive and weakly destructive measurement and for quantum simulation where atoms interact at distance by exchanging photons with each other. A core limitation of these systems is that cavity-based measurements inherently result in a loss of spatial information, as they provide only an averaged signal representing the properties of the atoms across the entire cavity field.

I will first describe the development of a device referred to as a cavity-microscope designed to overcome this challenge, integrating both a high-finesse optical cavity and a pair of high numerical-aperture lenses within a single setup. This device enables the coupling of a precisely localized microscopic region of an atomic cloud to the cavity field. As a result, we generate a micrometrically-resolved reconstruction of the spatial density profile of the atomic cloud by scanning the microscope focus<sup>1</sup>.

With this remarkable ability to control and program light-matter interactions, I will report our progress towards the understanding of the physics of superradiant many body systems using cQED. I will also present the development of optical methods — integrated with the cavity microscope — to randomize cavity-mediated interactions. These advancements pave the way for novel analog quantum simulations of programmable, all-to-all interacting systems, which are particularly relevant for exploring exotic states of matter. In particular, this platform opens the doors to investigate holographic quantum matter, including models such as the Sachdev-Ye-Kitaev model<sup>2</sup> which describes a system of  $N$  fermionic modes coupled by random interactions.

<sup>1</sup>F. Orsi, *et al.*, *PRX Quantum* **5**, 040333 (2024).

<sup>2</sup>P. Uhrich, S. Bandyopadhyay, N. Sauerwein, J. Sonner, J.P. Brantut, and P. Hauke, *arXiv*, 2303.11343 (2023).

**Abstract number: P56**  
**Tuesday 14:00-15:30**

## Bell correlations with multicomponent Bose-Einstein condensates

**Kobus A.<sup>1</sup>, Li X.<sup>2</sup>, Gajda M.<sup>†1</sup>, You L.<sup>2,3</sup>, Witkowska E.<sup>1</sup>**

<sup>1</sup>*Institute of Physics, Polish Academy of Sciences, 02-668 Warsaw, Poland*

<sup>2</sup>*State Key Laboratory of Low Dimensional Quantum Physics, Department of Physics, Tsinghua University, Beijing 100084, China*

<sup>3</sup>*Beijing Academy of Quantum Information Sciences, Beijing 100193, China*

<sup>†</sup>gajda@ifpan.edu.pl

Bell correlations are named after physicist John Stewart Bell, who first described them in 1964. They refer to correlations between the outcomes of measurements performed on two or more particles that cannot be explained by any local hidden variable theory. In quantum systems, these correlations are often used to demonstrate the non-classical nature of quantum mechanics and the limitations of classical theories. Today, however, non-trivial Bell correlations play a crucial role in the development of quantum technologies, leveraging the unique properties of quantum systems to perform tasks beyond the capabilities of classical technologies, including quantum teleportation, quantum cryptography, and quantum computing. We theoretically and experimentally explore Bell correlations in spin- $f$  Bose-Einstein condensates using a data-driven approach <sup>1</sup> with a focus on the role of measurement settings. We define protocols for certifying Bell correlations in such systems with squeezed states. These Bell correlations are then verified using recent experimental results for spin-1 BECs <sup>2</sup> Our results reveal the fundamental characteristics of the multisetting Bell scenario in spin- $f$  bosonic systems.

<sup>1</sup>G. Müller-Rigat, A. Aloy, M. Lewenstein, and I. Frérot, *PRX Quantum* **2**, 030329 (2021).

<sup>2</sup>J. Cao, X. Li, T. Mao, W. Xu, and L. You, (2023) *arXiv:2312.10480* (2023).

Abstract number: P57  
 Tuesday 14:00-15:30

## Transportable strontium optical lattice clock for geodesy at the few-cm height level

**Nosske I.**<sup>†1</sup>, **Vishwakarma C.**<sup>1</sup>, **Lücke T.**<sup>1</sup>, **Lisdat C.**<sup>1</sup>

<sup>1</sup>*Physikalisch-Technische Bundesanstalt (PTB), Braunschweig, Germany*

<sup>†</sup>ingo.nosske@ptb.de

Transportable high-performance optical atomic clocks are currently being developed worldwide. Due to the gravitational redshift – a general relativistic effect – they serve as quantum sensors of the local gravity potential. It is anticipated that they will allow to determine the Earth's gravity potential<sup>1</sup> with even greater accuracy than is currently possible by state-of-the-art geodetic methods<sup>2</sup>. They also enable frequency comparisons between institutes, for example between those which are currently not yet connected by an accurate frequency comparison link.

Here we describe the second-generation transportable <sup>87</sup>Sr optical lattice clock of PTB, which is operational since early 2023 and outperforms its predecessor<sup>3</sup> in several ways. The fractional frequency uncertainty of the clock's blackbody radiation shift – often the leading systematic in strontium lattice clocks – is reduced below  $1 \times 10^{-18}$ , as the atoms are interrogated inside a well-characterized thermal shield at  $-50^\circ\text{C}$ <sup>4</sup>. We describe our efforts to ensure a reproducible lattice light shift after transportation to another site, which includes the use of a frequency comb for logging the lattice laser frequency and of a  $\mu$ -metal shield for a stable magnetic field environment. Taking all frequency shifts into account, the total systematic clock uncertainty is evaluated to be below  $5 \times 10^{-18}$ . Using an ultrastable transportable laser<sup>5</sup>, the fractional clock frequency instability is about  $5 \times 10^{-16}/\sqrt{\tau/\text{s}}$  after an averaging time  $\tau$ , which corresponds to a height measurement resolution of  $8\text{ cm}/\sqrt{\tau/\text{hour}}$  utilizing the gravitational redshift.

The atomic clock is installed in an air-conditioned car trailer and operated after several transportations. We briefly review its performance during its recent off-campus measurement campaigns in England<sup>6</sup>, southern Germany and Italy.

<sup>1</sup>J. Grotti *et al.*, *Phys. Rev. Appl.* **21**, L061001 (2024).

<sup>2</sup>H. Denker *et al.*, *J. Geod.* **92**, 487-516 (2018).

<sup>3</sup>S. B. Koller *et al.*, *Phys. Rev. Lett.* **118**, 073601 (2017).

<sup>4</sup>I. Ushijima, M. Takamoto, M. Das, T. Ohkubo and H. Katori, *Nat. Photonics* **9**(3), 185-189 (2015).

<sup>5</sup>S. Herbers, S. Häfner, S. Dörscher, T. Lücke, U. Sterr and C. Lisdat, *Opt. Lett.* **47**(20), 5441-5444 (2022).

<sup>6</sup>International Clock and Oscillator Networking (ICON) Collaboration, arXiv:2410.22973 (2024).

Abstract number: P58  
 Tuesday 14:00-15:30

## Magic Wavelengths for $^{85}\text{Rb}$ and $^{133}\text{Cs}$ atoms based Active Optical Clocks in Visible-Near Infrared Spectrum

Jyoti A.<sup>†1</sup>, Kaur M.<sup>2</sup>, Chen J.<sup>1,3</sup>

<sup>1</sup>*Institute of Quantum Electronics, School of Electronics, Peking University, Beijing-100871, P.R. China*

<sup>2</sup>*Department of Physics, Chandigarh University, Mohali-140413, Punjab, India*

<sup>3</sup>*Hefei National Laboratory, Hefei-230088, P.R. China*

<sup>†</sup>arora.jyoti326@gmail.com

Manipulation of neutral atoms along with the modern laser cooling and trapping techniques have revolutionized the field of atomic physics, especially for the innovation among atomic clocks. In order to realize highly precise and accurate atomic clocks, it is evident to obtain a high S/N ratio, which is actually inversely proportional to Allan deviation. Keeping this in mind, we have calculated magic wavelengths for active clock transitions in  $^{85}\text{Rb}$  and  $^{133}\text{Cs}$  atoms, viz,  $5S_{1/2}-6P_{1/2,3/2}$  and  $6S_{1/2}-7P_{1/2,3/2}$ , respectively, particularly in visible-near-infrared spectrum, owing to the fact that Allan deviation rapidly decreases as we move on to higher wavelengths of electromagnetic spectrum, making them more acceptable for newer navigation systems, quantum computation devices as well as tools for high-precision experiments. Moreover, to ascertain the accuracy of our results, the comparative analysis of the evaluated dynamic dipole polarizabilities of the involved states has been carried out with the available literature values. We believe that these results will serve as a foundation towards solving the hindrances of trapping of Rb and Cs atoms in the evolution of active atomic clocks.

Abstract number: P59  
 Tuesday 14:00-15:30

## Towards a spin-squeezing-enhanced atom interferometer in an optical cavity

Pupic A.<sup>†1</sup>, Fulbright Gheorghita E.<sup>1</sup>, Wald S.<sup>1</sup>, Hosten O.<sup>1</sup>

<sup>1</sup>*Institute of Science and Technology, Klosterneuburg, Austria*

<sup>†</sup>Andrea.Pupic@ist.ac.at

Atom interferometers are state-of-the-art devices that exploit the wave-like nature of matter to measure various physical observables, including (but not limited to) acceleration forces, time, and magnetic fields<sup>1</sup>. The phase resolution of classical interferometers is limited by the standard quantum limit. Many atom interferometer schemes that entangle the internal spin states have demonstrated successful metrological enhancement up to 18.5 dB, and direct phase measurement enhancement (in a Ramsey sequence) up to 11.8dB<sup>2,3</sup>. However, there is room for improvement for atom interferometers which map the entangled atomic states onto momentum space (spatially separated arms). Most recently, a group in Hannover demonstrated an atom interferometric gravimeter with 1.7 dB entanglement enhancement<sup>4</sup>.

We report the progress of our experiment: a spin-squeezed Mach-Zehnder atom interferometer enabled by atom-light interactions. A high-finesse traveling-wave cavity mediates both the far-off-resonant dipole trap and counter-propagating Raman tones. Initial atom-atom correlations are generated through one-axis twisting and quantum non-demolition protocols. State-dependent Raman kicks transfer momentum, mapping internal degrees of freedom and correlations to momentum space. Specifically, we present updates on cavity characteristics, atomic state preparation via optical pumping, squeezing protocols, and AC Stark shift compensation.

<sup>1</sup>S. S. Szigeti, O. Hosten, and S. A. Haine, *Applied Physics Letters* **118**, 140501 (2021).

<sup>2</sup>O. Hosten, N. J. Engelsens, R. Krishnakumar and M. A. Kasevich, *Nature* **529**, 505-508 (2016).

<sup>3</sup>S. Colombo, E. Pedrozo-Peñafiel, A. F. Adiyatullin, Z. Li, E. Mendez, C. Shu and V. Vuletic, *Nature Physics* **18**, 925-930 (2022).

<sup>4</sup>C. Cassens, B. Meyer-Hoppe, E. Rasel and C. Klempt, *Phys. Rev. X* **15**, 011029 (2025).

Abstract number: P60  
 Tuesday 14:00-15:30

## Silicon Nitride microresonators for narrowband entangled photon-pair generation

**Famà F.**<sup>†1</sup>, **Virzì S.**<sup>1</sup>, **Dello Russo S.**<sup>2</sup>, **Clivati C.**<sup>1</sup>, **Gionco C.**<sup>1</sup>, **Siciliani de Cumis M.**<sup>2</sup>, **Donadello S.**<sup>1</sup>, **Meda A.**<sup>1</sup>, **Cerrato E.**<sup>1</sup>, **Gramegna M.**<sup>1,3</sup>, **Genovese M.**<sup>1,3</sup>, **Levi F.**<sup>1</sup>, **Degiovanni I. P.**<sup>1,3</sup>, **Calonico D.**<sup>1</sup>

<sup>†</sup>INRIM, strada delle cacce 91, 10135 Torino, Italy

<sup>2</sup>Agenzia Spaziale Italiana, Centro di Geodesia Spaziale “G. Colombo”, Matera, Italy

<sup>3</sup>INFN, sezione di Torino, via P. Giuria 1, 10125 Torino, Italy

<sup>†</sup>f.fama@inrim.it

Entangled photon-pair generation in nonlinear media holds great promise, not only for advancing fundamental quantum physics but also for enabling secure communications, quantum computing, and next-generation information processing<sup>1,2</sup>. Although traditional platforms like atomic transitions and cavity-enhanced bulk crystals have been utilized, photonic integrated circuits (PICs) have recently emerged as a compelling alternative due to their compactness, low weight, and reduced power requirements<sup>3</sup>. Within this context, microresonators exploiting spontaneous four-wave mixing offer a scalable and efficient on-chip photon-pair source<sup>4</sup>. Notably, their compatibility with standard Complementary Metal-Oxide-Semiconductor (CMOS) processes makes them particularly attractive for integration into existing telecom infrastructure.

In this work, we investigate photon-pair generation in a silicon nitride microresonator through cavity-enhanced spontaneous four-wave mixing. The structure consists of a ring-shaped resonator with an intrinsic quality factor  $Q \sim 5 \times 10^6$ , evanescently coupled to a straight waveguide, resulting in a loaded Q-factor of  $QL \sim 2.5 \times 10^6$  under critical coupling. A resonance mode centered in the telecom C-band (1535–1565 nm), the standard for optical data transmission, is chosen as the pump. We observe the generation of three distinct photon-pair modes symmetrically spaced around the central wavelength, each exhibiting unique frequency detuning.

To assess photon correlations, we focus on the first photon pair and analyze it using the  $g^{(1,1)}$  function, with detection carried out via superconducting nanowire single-photon detectors while tuning system parameters. Furthermore, we explore the statistical properties of individual photons of the pair through measurements of the  $g^{(2)}$  function. These results not only reveal the expected transition from thermal to Poissonian statistics as a function of detection delay, but also offer insight into the spectral bandwidth of the emitted photons—providing a time-resolved approach to characterizing their coherence properties.

This preliminary study underscores the potential of high-Q silicon nitride microresonators as efficient, narrowband sources of entangled photon pairs, with characterization methods that naturally complement spectroscopic analysis.

<sup>1</sup>H-S. Zhong *et al.*, *Science* **370**,1460-1463 (2020).

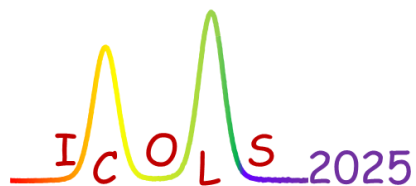
<sup>2</sup>H. Kimble, *Nature* **453**, 1023–1030 (2008).

<sup>3</sup>E. Pelucchi *et al.*, *Rev Phys* **4**, 194–208 (2022).

<sup>4</sup>Y. Wang *et al.*, *Appl. Phys. Rev.* **1**, 011314 (2021).



*Poster session 2*  
*Abstracts*



Abstract number: P61  
 Wednesday 14:00-15:30

## Study on the clock-line sideband cooling of Yb atoms

Jin T. Y.<sup>1</sup>, Zhang T.<sup>1</sup>, Qi Q. C.<sup>1</sup>, Lei S.<sup>1</sup>, Feng S. Z.<sup>1</sup>, Xia Y.<sup>1</sup>, Chang H.<sup>1</sup>, Zhang J. X.<sup>1</sup>, Liu X.<sup>1</sup>, Wang J. Y.<sup>1</sup>, Zhang R.<sup>1</sup>, Tang Z. M.<sup>†1</sup>, Xu X. Y.<sup>‡1,2,3</sup>

<sup>1</sup>State Key Laboratory of Precision Spectroscopy, East China Normal University, Shanghai, China

<sup>2</sup>Shanghai Research Center for Quantum Sciences, Shanghai, China

<sup>3</sup>Shanghai Branch, Hefei National Laboratory, Shanghai, China

<sup>†</sup>zmtang@lps.ecnu.edu.cn, <sup>‡</sup>xyxu@phy.ecnu.edu.cn

Sideband cooling (SBC) is a powerful technique for cooling atoms to their motional ground state, critical in quantum sciences. In Yb atoms, the ultra-narrow spin-forbidden  $6s^2\ ^1S_0 - 6s6p\ ^3P_0$  clock transition serves as one of the most precise optical clocks and provides an ideal pathway for resolved SBC of Yb atoms. However, conventional SBC of Yb atom requires pulsed cooling and repumping cycles to address the long-lived excited states in clock transitions, introducing experimental complexity and limiting efficiency. Here we introduce two novel methods for SBC of Yb and demonstrate the first realization of fully continuous clock-line SBC of Yb atoms in optical lattices.

In our setup, a 578-nm laser is employed for SBC on the  $^1S_0 - ^3P_0$  clock transition, while a 1389-nm laser drives the repumping transition  $3P_0 - 3D_1$ , followed by spontaneous decay back to the internal ground state  $1S_0$  through the intermediate state  $3P_1$ . The atoms are initially cooled in a 399-nm magnetic optical trap (MOT) for primary cooling, followed by a 556-nm MOT for secondary cooling. In the secondary cooling, we used two stages of 556-nm MOT loading. Then the atoms are loaded into the 759-nm optical lattice. Prior to SBC, the atoms exhibit a temperature of 4.4  $\mu$ K.

*In situ optical switching.* -By exploiting the repumping-induced light shift as an in situ optical switch, we achieve quasi-uninterrupted SBC, in which the cooling laser remains continuously active while the repumping laser is rapidly toggled at sub-millisecond timescales by using an internal frequency-shift keying technique. In our platform, this strategy reduces the axial temperature of Yb atoms in optical lattices from 4.4  $\mu$ K to 0.74  $\mu$ K (average vibrational occupation  $\langle n_z \rangle = 0.03$ ), substantially extending trap lifetimes and coherence times while simplifying experimental overhead.

*Magic frequency repumping.* -We identify a hyperfine-mediated magic frequency for the repumping laser that nullifies the light shifts of the clock transition, enabling simultaneous, unmodulated operation of both the cooling and repumping lasers. This innovation achieves fully continuous SBC with zero deadtime and further reduces atomic temperature to 0.66  $\mu$ K ( $\langle n_z \rangle = 0.016$ ), a critical advance for high-duty-cycle quantum metrology.

Our methods not only unlock the full potential of SBC for Yb atoms but are readily adaptable to diverse atomic systems confined in optical lattices and tweezer arrays, and some trapped-ion systems. By elucidating the AC Stark mechanisms underlying prior intermittent SBC schemes, this work resolve fundamental limitations while establishing a streamlined, simplified SBC technique for ultracold preparation of atomic ensembles in trapping potentials, paving the way for scalable quantum technologies with enhanced coherence and precision.

Abstract number: P62  
 Wednesday 14:00-15:30

## ECNU Yb optical lattice clocks with both instability and systematic uncertainty below $5 \times 10^{-18}$

Zhang T.<sup>\*1</sup>, Qi Q.C.<sup>\*1</sup>, Jin T.Y.<sup>\*1</sup>, Lei S.<sup>1</sup>, Xia Y.<sup>1</sup>, Feng S.Z.<sup>1</sup>, Chang H.<sup>1</sup>, Zhang J.X.<sup>1</sup>, Liu X.<sup>1</sup>, Wang J.Y.<sup>1</sup>, Zhang R.<sup>1</sup>, Tang Z.M.<sup>1</sup>, Xu X.Y.<sup>†1,2,3</sup>

<sup>1</sup>State Key Laboratory of Precision Spectroscopy, East China Normal University, Shanghai, China

<sup>2</sup>Shanghai Research Center for Quantum Sciences, Shanghai, China

<sup>3</sup>Shanghai Branch, Hefei National Laboratory, Shanghai, China

\*These authors contributed equally to this work.

†xyxu@phy.ecnu.edu.cn

The pursuit of optical atomic clocks with  $10^{-18}$  to  $10^{-19}$ -level precision is driving breakthroughs in timekeeping and metrology while enabling tests of fundamental physics, searches for dark matter, and measurements of spacetime curvature. Here we report advancements in the stability and accuracy of the Yb optical lattice clock at East China Normal University (ECNU).

In 2024, we developed an ultra-stable laser system with a thermal noise limit exceeding our previous implementations. We performed synchronous comparisons between two clocks (Yb1 and Yb2) using 200-ms clock laser pulses and achieved initial short-term instability of  $5 \times 10^{-16}/\sqrt{\tau}$  and long-term instability of  $5 \times 10^{-18}$  at 32768 s for a single clock. Through optimization, including suppression of technical noise in the ultra-stable laser system (e.g., environmental vibrations and Pound-Drever-Hall servo-loop noise) and rigorous evaluation of systematic frequency shifts (e.g., collisional, BBR, lattice, and Zeeman shifts), we achieved enhanced clock spectra stability using 400-ms interrogation pulses. By decoupling the clock laser frequency noise and the systematic effects, we identified the collisional frequency shift as the primary limitation in long-term instability. Further suppressing atomic number fluctuations in both the Yb1 and Yb2 clocks and extending the clock laser pulse duration to 400 ms, we achieved the enhanced synchronous comparison with each clock to average at a rate of  $3.2 \times 10^{-16}/\sqrt{\tau}$  and a long-term instability of  $2.4 \times 10^{-18}$  at 8000 s.

Evaluation of systematic uncertainty revealed that the dominant contributions arise from the lattice AC Stark, density, and BBR shifts. Specifically, we obtained the uncertainty budget of the Yb2 clock by adjusting the experimental conditions of Yb1. The lattice shift, determined by varying the lattice depth from 162 Er to 362 Er under normal clock operation conditions at  $U = 190(2)$  Er, resulted in a fractional uncertainty of  $3.3 \times 10^{-18}$ . The density shift, characterized through atomic population modulation via Zeeman slower power adjustment, contributed  $2.3 \times 10^{-18}$  uncertainty. The BBR shift, assessed using calibrated platinum resistance sensors and finite-element modeling, yielded  $1.8 \times 10^{-18}$  uncertainty. We also evaluated the secondary contributions, such as the first- and second-order Zeeman, servo errors, background gas collision shifts and the minor terms, and found that their total contribution is around  $1 \times 10^{-18}$ . The combined systematic fractional uncertainty reached  $4.6 \times 10^{-18}$ , with a total frequency shift of -1.17 Hz.

Our work establishes the ECNU Yb clock as an advanced platform in precision metrology, with both instability and systematic uncertainty below  $5 \times 10^{-18}$ , paving the way for future tests of fundamental physics and next-generation time-keeping.

Abstract number: P63  
Wednesday 14:00-15:30

## A dual-species optical tweezer array of Na and Cs Rydberg atoms

Cimmino R. T.<sup>†1,2,3</sup>, Wang Y.<sup>1,2,3</sup>, Wang K.<sup>1,2,3</sup>, Kemeny A. H.<sup>1,2,3</sup>, Ni K-K.<sup>1,2,3</sup>

<sup>1</sup>Department of Physics, Harvard University, Cambridge, Massachusetts 02138, USA

<sup>2</sup>Department of Chemistry and Chemical Biology, Harvard University, Cambridge, Massachusetts 02138, USA

<sup>3</sup>Harvard-MIT Center for Ultracold Atoms, Cambridge, Massachusetts 02138, USA

<sup>†</sup>rcimmino@g.harvard.edu

Optical tweezer arrays of neutral atoms interacting via Rydberg states have proven to be a promising platform for realizing quantum computation and studying the properties of quantum many-body entangled states. In a dual-species array, two different atomic species are trapped in independent colocalized tweezer arrays in which each species can be separately imaged and excited. This offers a natural implementation of crosstalk-free readout of ancilla qubits in quantum error correction schemes, and affords a high degree of flexibility in tuning interactions within and between atomic species. In this work, we present a dual-species array of sodium and cesium atoms. We create arbitrary-geometry 2D arrays of both species in tandem and coherently excite them to Rydberg states. We demonstrate that the interspecies Rydberg interaction can be made either attractive or repulsive by an appropriate choice of Rydberg state on each species. We leverage this to perform non-destructive readout of one species by another, and present our progress towards larger-scale quantum simulations on our dual-species platform.

Abstract number: P64  
Wednesday 14:00-15:30

## Uncertainty evaluation of KRISS-AGRb-1 and development status of new atomic gravimeter toward the accuracy of below $10 \text{ nm/s}^2$

Lee S.-B.<sup>†1</sup>, Lee. S.<sup>1,2</sup>, Kwon. T. Y.<sup>1</sup>, Park. S. E.<sup>1</sup>, Seo. S.<sup>1</sup>, Hong. H. G.<sup>1</sup>, Lee. J. H.<sup>1</sup>, Park. Y. -H.<sup>1</sup>, Kang. S.<sup>1</sup>, Seo. M. H.<sup>1</sup>

<sup>1</sup>1. Korea Research Institute of Standards and Science, Daejeon 34113, Republic of Korea

<sup>2</sup>2. Department of Physics, Chonnam National University, Gwangju, 61186, Republic of Korea

<sup>†</sup>lsbum@kriss.re.kr

An absolute atomic gravimeter based on an atom interferometer has surpassed the sensitivity of its classical counterpart FG5X by about one order of magnitude. However, it is still not the case and comparable in terms of accuracy, which remains in the range of  $20 \text{ nm/s}^2$  to  $50 \text{ nm/s}^2$  for absolute values<sup>1 2 3 4</sup>. The most dominant factor is the wavefront distortion of the Raman laser that manipulates the atomic wavepacket to form the atom interferometer and also imprints its phase onto the phase factor of the atomic wavepacket during manipulating. This effect is related to the ballistic expansion of the atomic source, which is described by its atomic temperature, and does not appear at zero atomic temperature. Therefore, It is advantageous to further lower the temperature of the atomic cloud. it is also beneficial to increase the interrogation time, which causes the phase uncertainty due to the wave front to increase relatively less compared to the increasing total phase difference. Here, we report the uncertainty evaluation of the atomic gravimeter KRISS-AGRb-1 (Fig.1a), based on  $^{87}\text{Rb}$  atoms developed at KRISS, with the total uncertainty of below  $30 \text{ nm/s}^2$ , mainly limited by a wavefront distortion. We also present a method to overcome the uncertainty caused by the wavefront distortion and achieve an accuracy of below  $10 \text{ nm/s}^2$ . This is accomplished by introducing a new physical package based on Cs atoms, which have a relatively smaller recoil velocity because of its larger mass, and by compensating for bias by directly measuring the wavefront distortions induced by all optical elements. We have now constructed a compact physical package (Fig.1b) capable of integration times longer than  $T = 200 \text{ ms}$ , based on Cs atom and fountain configuration, and have cooled the atoms to less than  $1 \text{ } \mu\text{K}$ .

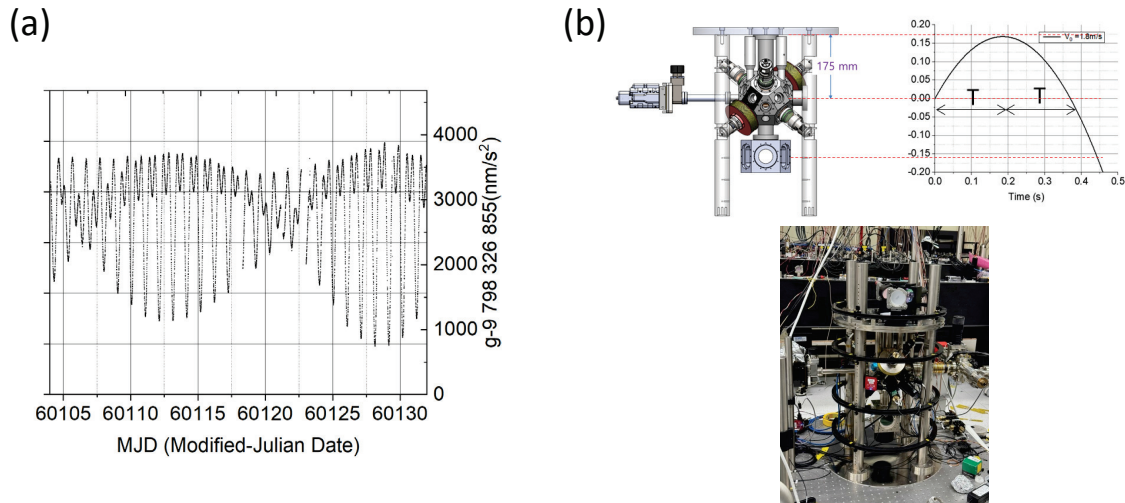


Figure 1: (a)  $g$  measured continuously for about a month using atomic gravimeter KRISS-AGRb-1. (b) Schematic diagram and photo of the physical package of new Cs atomic gravimeter .

<sup>1</sup>S. C. Freier *et al.*, *J. Physics: Conf. Ser* **723**, 012050 (2016).

<sup>2</sup>A. Louchet-Chauvet *et al.*, *New Journal of Physics* **13**, 065025 (2011).

<sup>3</sup>S.-K. Wang *et al.*, *Metrologia* **55**, 360 (2018).

<sup>4</sup>Y.-Y. Xu *et al.*, *Metrologia* **59**, 055001 (2022).

Abstract number: P65  
 Wednesday 14:00-15:30

# Precision Spectroscopy of the Fine-Structure in the $a^3\Sigma_u^+(\nu = 0)$ and $c^3\Sigma_g^+(\nu = 4)$ States of the Helium Dimer

Wirth V.<sup>1</sup>, Holdener M.<sup>1</sup>, Merkt F.<sup>†1,2,3</sup>

<sup>1</sup>*Institute of Molecular Physical Science, ETH Zurich, Zurich, Switzerland*

<sup>2</sup>*Quantum Center, ETH Zurich, Zurich, Switzerland*

<sup>3</sup>*Department of Physics, ETH Zurich, Zurich, Switzerland*

<sup>†</sup>frederic.merk@phys.chem.ethz.ch

The helium dimer ( $\text{He}_2$ ), having only four electrons, no nuclear spin and being the prototypical example of a Rydberg molecule<sup>1</sup>, serves as a benchmark system for testing *ab initio* calculations. In recent years, highly accurate calculations from first principles including relativistic and quantum-electrodynamical effects of molecular three- and four-electron systems have become feasible<sup>2,3,4,5</sup>. Accurate experimental data on the lowest-lying electronic states of  $\text{He}_2$  are needed to validate the current level of theory, but are scarce in the literature. Especially the fine structure in the triplet manifold, arising from the spin-spin and spin-rotation interactions, has only been measured for a few rovibrational levels in the  $a^3\Sigma_u^+$  state<sup>6,7,8,9,10,11,12</sup> and for only three rovibrational levels ( $\nu = 4$ ,  $N \in \{8, 10, 12\}$ ) in the  $c^3\Sigma_g^+$  state<sup>9</sup>.

We report on a high-resolution spectroscopic study of the fine structure of the  $a^3\Sigma_u^+(\nu = 0)$  and  $c^3\Sigma_g^+(\nu = 4)$  states of  $\text{He}_2$  including all rotational levels of the  $c^3\Sigma_g^+(\nu = 4)$  state up to  $N = 10$ . The experiments combined a dense cold supersonic beam of  $\text{He}_2$  in the  $a^3\Sigma_u^+$  metastable state generated by a cryogenic pulsed valve, and single-mode laser radiation in a geometric arrangement optimized to suppress Doppler shifts. Measurements were performed using a two-color resonant two-photon ionization scheme. A narrowband continuous-wave laser was used drive transitions from the fine-structure levels of the  $a^3\Sigma_u^+(\nu = 0)$  to those of the  $c^3\Sigma_g^+(\nu = 4)$  state. The c-state levels were then photoionized with a pulsed dye laser for background-free detection.

The absolute level positions of the  $a^3\Sigma_u^+(\nu = 0)$  and  $c^3\Sigma_g^+(\nu = 4)$  fine-structure levels could be determined to within 1 MHz and better in a linear-least squares fit including the transition frequencies of Ref.<sup>9</sup> and fine-structure intervals of Ref.<sup>12</sup>.

The rotational, spin-spin and spin-rotation constants with their respective centrifugal distortions and the band origin were fitted in a global weighted nonlinear least-squares fit to the measured transition frequencies, again including the measurements of Refs.<sup>9</sup> and <sup>12</sup>. Significant improvements in the precision of the molecular constants were achieved compared to the previous measurements.

The  $c^3\Sigma_g^+$  state is of particular interest also because its potential-energy curve exhibits a local maximum and its high vibrational levels ( $\nu = 3$  and 4) undergo tunneling predissociation. The high spectral resolution enabled the characterization of the rotational-state-dependent tunneling dynamics through the observation of line broadening. The broadening was found to be in good agreement with calculated values, which were obtained by determining the energy dependence of the phase-shift of the scattering wavefunctions.

<sup>1</sup>G. Herzberg, *Annu. Rev. Phys. Chem.* **38**, 27-56 (1987)

<sup>2</sup>W. Cencek, J. Komasa, K. Pachucki, K. Szalewicz, *Phys. Rev. Lett.* **95**, 233004 (2005)

<sup>3</sup>E. Mátyus, *J. Chem. Phys.* **149**, 194112 (2018)

<sup>4</sup>D. Ferenc, V. I. Korobov, E. Mátyus, *Phys. Rev. Lett.* **125**, 213001 (2020)

<sup>5</sup>B. Rácsai, D. Ferenc, Á. Margócsy, E. Mátyus, *J. Chem. Phys.*, **160**, 211102 (2024)

<sup>6</sup>M. L. Ginter, *J. Chem. Phys.* **42**, 561-568 (1965)

<sup>7</sup>W. Lichten, M. V. McCusker, T. L. Vierima, *J. Chem. Phys.* **61**, 2200-2212 (1974)

<sup>8</sup>W. Lichten, T. Wik, *J. Chem. Phys.* **69**, 98-100 (1978).

<sup>9</sup>M. Kristensen, N. Bjerre, *J. Chem. Phys.* **93**, 983-990 (1990).

<sup>10</sup>I. Hazell, A. Norregaard, N. Bjerre, , *J. Mol. Spectrosc.* **172**, 135-152 (1995)

<sup>11</sup>C. Focsa, P. Bernath, R. Colin, *J. Mol. Spectrosc.* **191**, 209-214 (1998)

<sup>12</sup>L. Semeria, P. Jansen, G. Clausen, Josef A. Agner, H. Schmutz, F. Merkt, *Phys. Rev. A* **98**, 062518 (2018)

Abstract number: P66  
 Wednesday 14:00-15:30

## All optical ultracold atoms in microgravity

Metayer C.<sup>1</sup>, Le Mener J.<sup>1</sup>, Jarlaud V.<sup>3</sup>, Pelluet C.<sup>2</sup>, Veyron R.<sup>4</sup>, Gerent J.B.<sup>5</sup>, Huang R.<sup>1</sup>, Beraud E.<sup>6</sup>  
 Garraway B.<sup>1</sup>, Bernon S.<sup>1</sup>, Battelier B.<sup>†1</sup>

<sup>1</sup>LP2N, Laboratoire Photonique Numérique et Nanosciences, Université de Bordeaux, IOGS and CNRS, 1 Rue François Mitterrand, 33400 Talence, France

<sup>2</sup>Centre National d'Etudes Spatiales, 18 avenue Edouard Belin, 31400 Toulouse, France

<sup>3</sup>Exail, 1 rue François Mitterrand, 33400 Talence, France

<sup>4</sup> ICFO - Institut de Ciències Fòniques, The Barcelona Institute of Science and Technology, 08860 Castelldefels, Barcelona, Spain

<sup>5</sup> Department of Physics and Astronomy, Bates College, Lewiston, Maine 04240, US

<sup>6</sup> Department of Physics and Astronomy, University of Sussex, Falmer, Brighton, BN1 9QH, UK

<sup>†</sup>baptiste.battelier@institutoptique.fr

Most cold atoms experiment in microgravity platforms and in Space are achieved using atom chips, leading to strong constraints in terms of optical access and inhomogeneities of the magnetic fields<sup>1,2,3</sup>. Alternatively, dipole traps doesn't have these drawbacks but challenge difficulties to produce atomic samples at ultra low temperature and large atom numbers in absence of gravity. Here, we report on the all-optical production of ultracold atoms in microgravity using a combination of grey molasses cooling, light-shift engineering and optical trapping in a painted potential. The time-averaged potential allows to increase the initial phase space density and collision rate which favors the evaporative process. This efficient cooling leads to the production of an ultra cold gas of  $2 \times 10^4$  Rubidium atoms at a temperature below 100 nK in weightlessness in less than 4 seconds. This experiment is performed onboard the 0g plane during 20 second long parabolic flights. Alternatively, similar experiments was performed in a lab-based 3-m high Einstein elevator<sup>4</sup> resulting in  $4 \times 10^4$  condensed atoms every 13.5 s, with a temperature as low as 35 nK. In this system, the atomic cloud can expand in weightlessness for up to 500 ms.

This latter platform is particularly suitable for atom interferometry. Recent advances in this field have led to the development of quantum inertial sensors with outstanding performance in terms of sensitivity, accuracy, and long-term stability. For ground-based implementations, these sensors are ultimately limited by the free-fall height of atomic fountains required to interrogate the atoms over extended timescales. This limitation can be overcome in Space and in unique "microgravity" facilities such as drop towers or free-falling aircraft. These facilities require large investments, long development times, and place stringent constraints on instruments that further limit their widespread use. The available "up time" for experiments is also quite low, making extended studies challenging. Our experiment is mounted to a moving platform that mimics the vertical free-fall trajectory every 13.5 seconds. With a total interrogation time of  $2T=200$  ms, we demonstrate an acceleration sensitivity of  $6 \times 10^{-7}$  m.s<sup>-2</sup> per shot, limited primarily by the temperature of our atomic samples. We further demonstrate the capability to perform long-term statistical studies by operating the Einstein Elevator over several days with high reproducibility. These represent state-of-the-art results achieved in microgravity and further demonstrates the potential of quantum inertial sensors in Space. Our microgravity platform is both an alternative to large atomic fountains and a versatile facility to prepare future Space missions.

Atom interferometry using ultracold atoms will allow to surpass the current limitations due to residual rotations. Our platform is suitable to study and characterize the double diffraction regime to prepare future Space missions for accelerometry (CARIOQA), Earth observation and fundamental physics such as the test of the Weak Equivalence Principle<sup>5</sup>.

Our work also paves the way for studies of ultracold matter physics at low energies on ground or in Space. As an example, we present an all optical method to produce shell shaped traps for ultracold atoms in microgravity. Our scheme exploits optical double dressing of the ground state to create a short range strongly repulsive central potential barrier. Combined with a long range attractive central potential, this barrier forms the shell trap. We show that a pure spherical bubble, reaching the quasi 2D regime for standard atom numbers, could be formed from two crossed beams with a parabolic profile. An analytical study shows that the relevant characteristics of the trap depends on the ratio of the ground and excited state polarisabilities and the lifetime of the excited state. As a benchmark, we provide quantitative analysis for a realistic configuration for Rubidium ensembles, leading to a 370 Hz transverse confinement with 35  $\mu$ m radius bubble with trap residual scattering of less than 10 s<sup>-1</sup>.

<sup>1</sup>T. Von Zoest *et al.*, *Science* **328**, 1540-1543 (2010).

<sup>2</sup>D. Becker *et al.*, *Nature* **562**, 391-395 (2018).

<sup>3</sup>D. Aveline *et al.*, *Nature* **582**, 193-197 (2020).

<sup>4</sup>G. Condon *et al.*, *Phys.Rev.Lett.* **123**, 240402 (2019).

<sup>5</sup>C. Struckmann *et al.*, *Phys. Rev. D* **109**, 064010 (2024).

Abstract number: P67  
Wednesday 14:00-15:30

## A High-Data-Rate Fermionic Quantum Simulator in Optical Lattices

Qiu L.<sup>†1,2</sup>, von Haaren A.<sup>1,2</sup>, Groth R.<sup>1,2</sup>, Qesja J.<sup>1,2</sup>, Muscarella L.<sup>1,2</sup>, Franz T.<sup>1,2</sup>, Hilker T.<sup>3,1</sup>, Bloch I.<sup>1,2,4</sup>,  
Preiss P.<sup>1,2</sup>

<sup>1</sup>Max Planck Institute of Quantum Optics, Garching, Germany

<sup>2</sup>Munich Center for Quantum Science and Technology, Munich, Germany

<sup>3</sup>University of Strathclyde, Glasgow, UK

<sup>4</sup>Ludwig Maximilian University of Munich, Munich

<sup>†</sup>liyang.qiu@mpq.mpg.de

The study of strongly correlated fermionic systems lies at the core of some of the most interesting problems in material science, quantum chemistry, and particle physics; however, simulating many fermions presents an outstanding computational challenge — even with qubit-based quantum computers of near-term architectures. Fermionic quantum simulators, where fermionic statistics are built-in on a hardware level, offer a promising alternative. Here, we present recent results from our new quantum gas microscope of fermionic lithium in optical lattices. Leveraging a compact chamber design, deep optical trap loading, and rapid cooling, we accelerate state preparation to achieve high data rates. Our system features robust single-site, spin-resolved detection, which enables the extraction of a wealth of information for the analog simulation of the Fermi-Hubbard model. Additionally, with the development of single-fermion gates via addressed Raman rotations and two-fermion gates through controlled collisions in optical superlattices, we aim to pave the way toward fermionic quantum information processing.



Abstract number: P68  
 Wednesday 14:00-15:30

## Measuring External Electric Fields Using Stark and Zeeman Effects in Rydberg-EIT Vapor Cells

Fang S.-C.<sup>†1</sup>, Chen Y.-C.<sup>1</sup>, Su H.-J.<sup>1</sup>, Chen Y.-H.<sup>\*1</sup>

<sup>1</sup>Department of Physics, National Sun Yat-Sen University, Kaohsiung 80424, Taiwan

<sup>†</sup>scottfang860422@gmail.com; <sup>\*</sup>yihsin.chen@mail.nsysu.edu.tw

Rydberg atoms have proven valuable in numerous studies due to their high polarizability and strong dipole-dipole interactions, making them highly sensitive to external magnetic and electric fields<sup>1</sup>. In our experiments, we utilize the Stark and Zeeman effects to measure electric fields. By employing two counter-propagating laser beams, we achieve Rydberg electromagnetically induced transparency (EIT), exciting atoms to the 53D Rydberg state. A reference cell and a science cell are used in our setup, with the reference signal serving as a baseline for determining the electric field-induced frequency shift. However, the presence of alkali-metal atoms absorbed on the inner surface of the vapor cell leads to non-zero conductivity in the glass due to several layers of coating<sup>2</sup>. These absorbed alkali-metal atoms induce an electric-field-screening effect through laser-induced photo desorption at the cell's surface<sup>3</sup>, making it difficult to measure the DC Stark shift. We observed that switching the electric field can transiently disrupt the shielding effect, allowing the energy shift to become observable within a short time by alternating the applied electric field. The shielding effect has been studied systematically. Additionally, a magnetic field was applied to the reference cell to induce the Zeeman effect, while an electric field was applied to the science cell to observe the Stark shift<sup>4</sup>. By determining the Stark shift from the Zeeman shift and the electric field strength, we can calculate the frequency shift induced by the external electric field. This approach opens the potential for precise measurement of external electric fields, paving the way for significant advancements in future electric field experiments.

<sup>1</sup>T. Vogt, M. Viteau, J. Zhao, A. Chotia, D. Comparat, and P. Pillet, Dipole Blockade at Förster Resonances in High Resolution Laser Excitation of Rydberg States of Cesium Atoms, *Phys. Rev. Lett.* **97**, 083003 (2006).

<sup>2</sup>Y.-C. Chen, S.-C. Fang, H.-H. Lin, J.-W. Dong, and Y.-H. Chen, Investigation of alkali vapor diffusion characteristics through microchannels, *Phys. Fluids* **34**, 072004 (2022).

<sup>3</sup>K. Mohapatra, T. R. Jackson, and C. S. Adams, Coherent Optical Detection of Highly Excited Rydberg States Using Electromagnetically Induced Transparency, *Phys. Rev. Lett.* **98**, 113003 (2007).

<sup>4</sup>H.-J. Su, J.-Y. Liou, I.-C. Lin, and Y.-H. Chen, Optimizing the Rydberg EIT spectrum in a thermal vapor, *Opt. Express* **30**, 1499 (2022).

Abstract number: P69  
Wednesday 14:00-15:30

## Precision spectroscopy and frequency determination of the hyperfine components of the P(63) 4-4 transition of molecular iodine near 652 nm

**Manzoor S.**<sup>1,2</sup>, **Chiarotti M.**<sup>1,2</sup>, **Meek S. A.**<sup>5</sup>, **Santambrogio G.**<sup>2,3,4</sup>, **Poli N.**<sup>†1,2</sup>

<sup>1</sup>Dipartimento di Fisica e Astronomia, Università degli Studi di Firenze, Via G. Sansone 1, 50019 - Sesto Fiorentino, Italy

<sup>2</sup>Laboratorio Europeo di Spettroscopia Non-Lineare, LENS Via N. Carrara 1, I-50019 Sesto Fiorentino, Italy

<sup>3</sup>Istituto Nazionale di Ricerca Metrologica, INRIM, Via Nello Carrara, 1 50019 Sesto Fiorentino, Italy

<sup>4</sup>CNR-INO, Istituto Nazionale di Ottica, Via N. Carrara 1, I-50019 Sesto Fiorentino, Italy

<sup>5</sup>Homer L. Dodge Department of Physics and Astronomy, Center for Quantum Research and Technology, University of Oklahoma, 440 W. Brooks St., Norman, OK 73019, USA

<sup>†</sup>nicola.poli@unifi.it

We report the observation of the hyperfine spectrum of the weak P(63) 4-4 line of the B–X electronic transition of molecular iodine  $^{127}\text{I}_2$  near 652.4 nm, using frequency-modulated saturated absorption spectroscopy<sup>1</sup>. In particular, we identified an interesting overlap between the hyperfine transitions of this iodine line and the ultraviolet  $^1\text{S}_0 - ^3\text{P}_1$  narrow intercombination transition of cadmium atoms at 326.2 nm. This overlap occurs at the second harmonic of the master laser source, making it a relevant reference for precision spectroscopy of atomic cadmium<sup>2</sup>. Figure 1 illustrates the simulated rovibrational spectrum of iodine near 652.4 nm, highlighting the overlap with cadmium transitions.

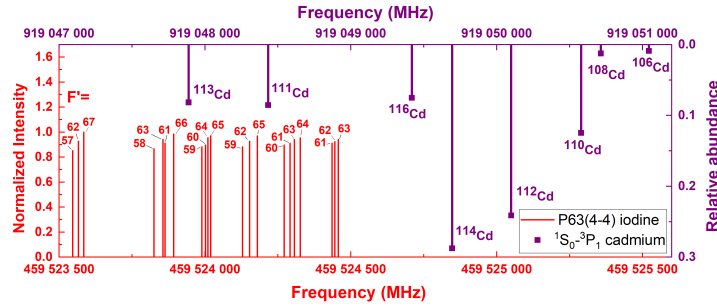


Figure 1: Calculated absolute frequencies of the hyperfine components of the P(63) 4-4 transition of  $\text{I}_2$  around 652.397 nm (approximately 459 524 600 MHz), identifying all 21 expected components. The hyperfine parameters were set to the existing literature values -  $\Delta eQq = 1957.67$  MHz and  $\Delta C = 0.0214$  MHz and temperature  $T_{\text{rot}} = 293$  K. The plot also shows the overlap with the second harmonic of the Cd intercombination transition at 326.2 nm. The top x-axis shows the transition frequencies ( $2\nu$ ) of the eight stable isotopes of Cd.

Using an optical frequency comb, we improved the precision of the frequency of the hyperfine transitions by a factor of 250 compared to previous studies. We used these data to determine the electric quadrupole ( $\Delta eQq$ ) and magnetic spin-rotation ( $\Delta C$ ) constants, along with the center of gravity of the P(63) 4-4 transition. The hyperfine parameters obtained from our measurements are summarized in Table 1, showing agreement with the existing literature values<sup>3 4</sup>.

Table 1: Hyperfine structure parameters. The dagger (†) indicates the recommended final parameters.

Parameters	Fit Results (This work)	Literature values
$\Delta eQq$ (MHz)	1 957.67 (71)	1 957.672 (25) <sup>†</sup>
$\Delta C$ (kHz)	20.37 (60) <sup>†</sup>	21.4 (10)
$f_{(\text{C.G.})}$ (MHz)	459 524 036.90 (12) <sup>†</sup>	459 524 056 (30)
Origin ( $v' = 4$ ) (MHz)	486 021 343.15 (12)	486 021 362 (30)

This work contributes to refining the iodine atlas, improving the accuracy of empirical formulae, and providing a valuable frequency reference for precision spectroscopy of the cadmium intercombination transition. This work has been supported by the MIUR "NextGenerationEU" European program, under the project PRIN2022-ISOTOP (Prot. 2022Z8LX9L).

<sup>1</sup>S. Manzoor *et al.*, *Optics Express* **32**, 44683-44693(2024).

<sup>2</sup>S. Manzoor *et al.*, *Optics Letters* **47**(10), 2582-2585(2022).

<sup>3</sup>Gerstenkom, S. and Luc, P., *J. Phys. France* **46**, 867-881 (1985).

<sup>4</sup>B. Bodermann *et al.*, " *The Eur. Phys. J. D* **19**, 31-44 (2002).

Abstract number: P70  
 Wednesday 14:00-15:30

## Collisions in a quantum gas of bosonic $^{23}\text{Na}^{39}\text{K}$ molecules

Meyer zum Alten Borgloh M.<sup>1</sup>, Heier J.<sup>†1</sup>, von Gierke F.<sup>1</sup>, Gersema P.<sup>1</sup>, Voges K. K.<sup>2</sup>, Karam C.<sup>3</sup>,  
 Karpa L.<sup>1</sup>, Dulieu O.<sup>3</sup>, Ospelkaus S.<sup>1</sup>

<sup>1</sup>Leibniz Universität Hannover, Institut für Quantenoptik, Germany

<sup>2</sup>Centre for Cold Matter, Blackett Laboratory, Imperial College London, United Kingdom

<sup>3</sup>Université Paris-Saclay, CNRS, Laboratoire Aimé Cotton, France

<sup>†</sup>heier@iqo.uni-hannover.de

We present our experiments with quantum gases of polar  $^{23}\text{Na}^{39}\text{K}$  molecules, discussing both atom-molecule and molecule-molecule collisions, as well as methods to obtain collisional control.

First, we study collisions between NaK and K in different hyperfine states<sup>1</sup> and share our observations of magnetically tunable resonances in these ensembles. Secondly, we focus on molecule-molecule collisions. Although  $^{23}\text{Na}^{39}\text{K}$  is chemically stable against the exchange reaction  $2\text{NaK} \rightarrow \text{Na}_2 + \text{K}_2$ , the ensemble undergoes universal two-body loss. We investigate the origin of this molecular loss<sup>2</sup> and outline an alternative method for its suppression, namely two-photon optical shielding<sup>3</sup>, which could replace previously demonstrated methods such as microwave shielding. The concept utilizes a coherent two-photon transition to create a potential barrier, which prevents the colliding molecules from reaching short range where interactions of the two molecules can lead to loss. Working at the point of the two-photon resonance  $\delta = 0$  should simultaneously prevent additional scattering loss by the shielding light in the long range. Lastly, we discuss the experimental implementation of this method.

<sup>1</sup>K. K. Voges, P. Gersema, T. Hartmann, S. Ospelkaus, and A. Zenesini, *Phys. Rev. Research* **4**, 023184 (2022).

<sup>2</sup>P. Gersema, K. K. Voges, J. Lin, J. He *et al.*, *Phys. Rev. Lett.* **127**, (2021).

<sup>3</sup>C. Karam *et al.*, *Phys. Rev. Research* **5**, 033074 (2023).

Abstract number: P71  
Wednesday 14:00-15:30

## Single Strontium Atoms in Optical Tweezer Arrays for Quantum Simulation

**Giardini V.**<sup>†1,2,3</sup>, **Guariento L.**<sup>1,3,4</sup>, **Fantini A.**<sup>1,3</sup>, **Shawn S.**<sup>1,3</sup>, **Catani J.**<sup>3,2</sup>, **Inguscio M.**<sup>5,2,3</sup>, **Cappellini G.**<sup>3,2</sup>, **Gavryusev V.**<sup>1,2,3</sup>, **Fallani L.**<sup>1,2,3</sup>

<sup>1</sup>Department of Physics and Astronomy, University of Florence, Via G. Sansone 1, 50019, Sesto Fiorentino, Italy

<sup>2</sup>European Laboratory for Non-Linear Spectroscopy (LENs), University of Florence, Via N. Carrara 1, 50019, Sesto Fiorentino, Italy

<sup>3</sup>National Institute of Optics (CNR-INO), National Research Council, Via N. Carrara 1, 50019, Sesto Fiorentino, Italy

<sup>4</sup>Department of Physics Ettore Pancini, University of Napoli Federico II, Via Cinthia 21, 80126, Napoli, Italy

<sup>5</sup>University Campus Bio-Medico, Via Alvaro del Portillo 21, 00128, Rome, Italy

†giardiniv@lens.unifi.it

Arrays of single neutral atoms trapped in optical tweezers have emerged as a powerful platform for quantum simulation, quantum computation, and precision metrology<sup>12</sup>. In particular, alkaline-earth(-like) atoms such as strontium (Sr) offer unique advantages because of their narrow optical transitions, which are particularly useful for laser cooling and precision spectroscopy, and long-lived metastable states enabling high-fidelity quantum operations. Excitation towards the Rydberg state can be achieved via both single- and two-photon excitation processes. These highly excited states exhibit strong interactions that can be precisely engineered to simulate various spin models, control energy transport dynamics, and implement entangling quantum gates<sup>3</sup>.

We built an ultra-high vacuum apparatus for trapping single <sup>88</sup>Sr atoms in a programmable optical tweezer array. The atomic source (a commercial solution provided by AOSense) integrates a Zeeman slower and a 2D magneto-optical trap, delivering a continuous flux of pre-cooled atoms into a rectangular fused silica cell manufactured by Japan Cell, where the main experiment is conducted. The vacuum system is maintained at a stable pressure of  $1 \times 10^{-11}$  Torr by a SAES D500 Starcell vacuum pump. To achieve ultra-cold temperatures, we use a two-stage MOT that first exploits the  $^1S_0 \rightarrow ^1P_1$  transition at 461 nm to cool the atoms down to 7 mK and then the  $^1S_0 \rightarrow ^3P_1$  intercombination transition at 689 nm to further reduce their temperature to 6  $\mu$ K [Figure 1(a)]. From the second-stage MOT, the atoms are loaded directly into an optical tweezer array (see Figure 1(b)), which is generated by focusing a 813 nm beam on the atoms through a high numerical aperture (NA= 0.55) objective from Special Optics. The tweezer arrays, featuring arbitrary geometries, are created by imprinting a phase mask on the trapping beam via a spatial light modulator (SLM), while two crossed acousto-optic deflectors (AODs) enable dynamic reordering<sup>4</sup>. The atoms trapped in the tweezers are cooled to the motional ground state through Sisyphus cooling, and a light-assisted collisions process induces two-body losses that result in an occupancy probability of approximately 50 % [Figure 1(c)]. Imaging is performed by collecting fluorescence from the trapped atoms using the same high-NA objective as that that generates the tweezers. The collected light is then directed to an Orca Quest qCMOS camera, which enables high-resolution single-atom detection and a fidelity > 99.5%.

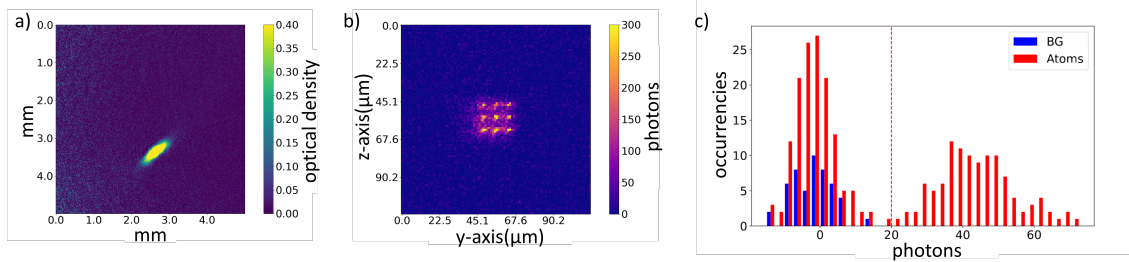


Figure 1: a) Absorption imaging of the second stage MOT, with a temperature  $T = 5.4 \mu\text{K}$  and a density  $n = 4 \times 10^{10} \text{ cm}^{-3}$ . b) Fluorescence imaging of atoms trapped in a  $3 \times 3$  array of tweezers. c) Histogram of the photon counts of the atoms, with two distinct peaks for 0 or 1 atom, with a loading efficiency of about 50 % and an imaging fidelity > 99.5%

<sup>1</sup>A. Browaeys and T. Lahaye, *Nature Physics* **16**, 132 (2020).

<sup>2</sup>M. Endres et al., *Science* **354**, 1024 (2016)

<sup>3</sup>M. Saffman, T.G. Walker, K. Mølmer, *Rev. Mod. Phys.* **82**, 2313 (2010)

<sup>4</sup>D. Barredo, de Léséleuc S., Lienhard V., T. Lahaye and A. Browaeys *Science* **354**, 6315 (2016).

Abstract number: P72  
 Wednesday 14:00-15:30

## Towards scalable trapped-ion quantum computing

**Cline J. R. K.**<sup>†1</sup>, Quantinuum Commercial Operations Team<sup>1</sup>, Quantinuum Test and Development Team<sup>1</sup>,  
 and Quantinuum Theory Team<sup>1</sup>

<sup>1</sup>Quantinuum, 303 South Technology Court, Broomfield, Colorado 80021, USA

<sup>†</sup>julia.cline@quantinuum.com

One of the main challenges facing large-scale quantum computing is scaling systems to more qubits while maintaining high fidelity operations. In this poster, we describe our efforts at Quantinuum in scaling trapped-ion quantum computers based on the quantum charge-coupled device architecture. We describe the set of benchmarking experiments we performed to characterize a commercially available quantum computer,<sup>1,2</sup> as well as present a selection of recent results of quantum circuits that have been run on the system<sup>3,4</sup>.

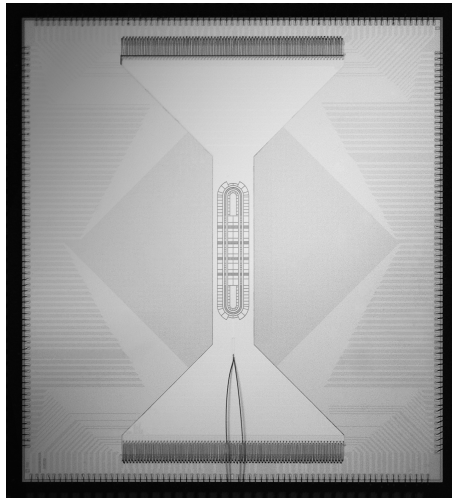


Figure 1: The trap of Quantinuum's H2 commercial quantum computer.

Incorporated into Quantinuum's H2 commercial quantum computer are several scalable features such as electrode broadcasting, multi-layer RF routing, and MOT loading. In addition, transport of ions through multiple junctions have been demonstrated on multiple Quantinuum traps<sup>5</sup>. In this talk, I will discuss these key technology demonstrations on our roadmap to scaling, as well as recent progress in integrated photonics and other enabling technologies.

<sup>1</sup>S. A. Moses *et al.*, *Phys. Rev. X* **13**, 041052 (2023).

<sup>2</sup>M. DeCross *et al.*, *arXiv*, 2406.02501 (2024).

<sup>3</sup>Y. Hong, E. Durso-Sabina, D. Hayes, and A. Lucas, *Phys. Rev. Lett.* **133**, 180601 (2024).

<sup>4</sup>A. Paetznick *et al.*, *arXiv*, 2404.02280 (2024).

<sup>5</sup>R. D. Delaney *et al.*, *Phys. Rev. X* **14**, 041028 (2024).

**Abstract number: P73**  
**Wednesday 14:00-15:30**

## Development of a Compact Cold Atom Interferometric Rotation Sensor

**Abraham J. J.<sup>1</sup>, Freearde T.<sup>1</sup>,**

<sup>1</sup>*School of Physics and Astronomy, University of Southampton, England, United Kingdom*

<sup>†</sup>ja7g17@soton.ac.uk

Atom interferometry involves splitting, redirecting, and recombining of the atomic wavefunction to produce interference, where inertial effects contribute to the phase shifts of the interference fringes. In Point Source Atom Interferometry (PSI), the correlation between position and velocity of cold atoms in an expanding ball is used to produce a spatial interference pattern across the atomic cloud, where phase shifts due to rotations and accelerations can be distinguished in a single-shot measurement. PSI is therefore a promising technique for performing gyroscopic measurements in inertial navigation applications. As a step towards this goal, we are developing a cold atom rotation sensor, featuring a compact, fibre-based Raman laser system, which will be mounted on a transportable rack. We describe the design, latest progress, and future plans for our interferometer.

Abstract number: P74  
 Wednesday 14:00-15:30

## Implementation of Delta-Kick squeezing in an atom interferometer

**Piest B.**<sup>†1</sup>, **Mhammedi N.**<sup>1</sup>, **Beaufils Q.**<sup>1</sup>, **Corgier R.**<sup>1</sup>, **Pereira Dos Santos F.**<sup>1</sup>

<sup>1</sup>*Laboratoire Temps Espace (LTE), Observatoire de Paris, Université PSL, Paris, France*

<sup>†</sup>baptist.piest@obspm.fr

Atom interferometers are versatile devices to detect accelerations or rotations with high sensitivity and accuracy with important applications in geodesy, navigation and fundamental physics. The phase readout of light-pulse atom interferometers with classical input states is naturally limited by the quantum projection noise leading to the standard quantum limit. In this case, the sensitivity to accelerations is given by  $\Delta a = 1/(kT^2\sqrt{N})$  per shot with the scale factor  $kT^2$  and the atom number  $N$ . Increasing the sensitivity of atom interferometers is one of the main challenges in the field. Conducting experiments in long baseline facilities or microgravity can considerably increase the sensitivity by maximizing the free evolution times  $T$ . A different approach to further improve the performance of atom interferometers is given by circumventing the standard quantum limit using entangled states. This has successfully been demonstrated in recent experiments by the groups of J. Thomson<sup>1</sup> and C. Klempt<sup>2</sup>. These experiments made use of strong cavity-atom coupling in a high-finesse cavity and spin-collisions in a dipole trap, respectively.

In our experiment we strive to implement and analyze the recently proposed technique of Delta-Kick squeezing<sup>3</sup> and demonstrate an entanglement-enhanced gravimeter operating below shot noise. The entanglement is generated by the non-linear interatomic interactions of a focused Bose-Einstein condensate (BEC) of Rb-87 atoms which leads to momentum squeezing. The experiment is operated at LTE and has previously been used to investigate Casimir-Polder forces between Rb-87 atoms and a polished surface<sup>4</sup>. Since then, it is being prepared for the implementation of Delta-Kick squeezing. In this contribution, I will discuss the experimental setup, the planned implementation of the entanglement-enhanced interferometer and show our recent progress.

<sup>1</sup>G. Greve et al. Nature **610**, 472-477 (2022)

<sup>2</sup>C. Cassens et al. Phys. Rev. X **15**, 011029 (2025)

<sup>3</sup>R. Corgier et al. Phys. Rev. Lett. **127**, 183401 (2021)

<sup>4</sup>Y. Balland et al. Phys. Rev. Lett. **133**, 113403 (2024)

Abstract number: P75  
Wednesday 14:00-15:30

## Performance Comparison of Dual Comb Spectrometers with MHz and GHz Repetition Rate

Pal M.<sup>1</sup>, Eber A.<sup>1</sup>, Fürst L.<sup>1</sup>, Hruska E.<sup>1</sup>, Ossiander M.<sup>1,2</sup>, Bernhardt B.<sup>†1</sup>

<sup>1</sup>Institute of Experimental Physics, Graz University of Technology, Petersgasse 16, 8010 Graz, Austria

<sup>2</sup>Harvard John A. Paulson School of Engineering and Applied Sciences, 9 Oxford Street, Cambridge, MA 02138, USA

<sup>†</sup>mithun.pal@tugraz.at

Dual comb spectroscopy (DCS) is a powerful technique that enables high-resolution, high-speed spectroscopic measurements across various applications<sup>1</sup>. To fully exploit the potential of DCS, it is essential to adapt two key parameters dependent on the diverse applications: the repetition rate, the permitted detuning frequency, and the phase stability between the two frequency combs. This work demonstrates and compares the performance of the fundamental (near-infrared / NIR) and frequency doubled (visible / VIS) radiation of two Yb-doped fiber laser-based DCS systems with 80 MHz and 1 GHz repetition rates. Yb-doped fiber lasers have already proven their efficacy in DCS across higher optical frequency regimes<sup>2,3,4</sup>. The 80 MHz system utilizes two mode-locked frequency combs for the DCS experiment, and a phase-locked feed-forward stabilization scheme<sup>5</sup> is utilized for coherent averaging. Meanwhile, a 1 GHz-DCS system comprises a free-running single-cavity dual comb source and operates at two wavelength regions (NIR and VIS) simultaneously with several kHz detuning frequency, resulting in a high-temporal-resolution. A post-processing algorithm<sup>6</sup> is used for coherent averaging of dual comb traces for several seconds to get excellent SNR.

The characterization of both systems is evaluated by monitoring the absorption spectra of ammonia (NH<sub>3</sub>) in the NIR and iodine (I<sub>2</sub>) in the VIS. The spectral overlap between both DCS systems (80 MHz and 1GHz) enables a direct comparison of absorption features, emphasizing the unique advantages of each system.

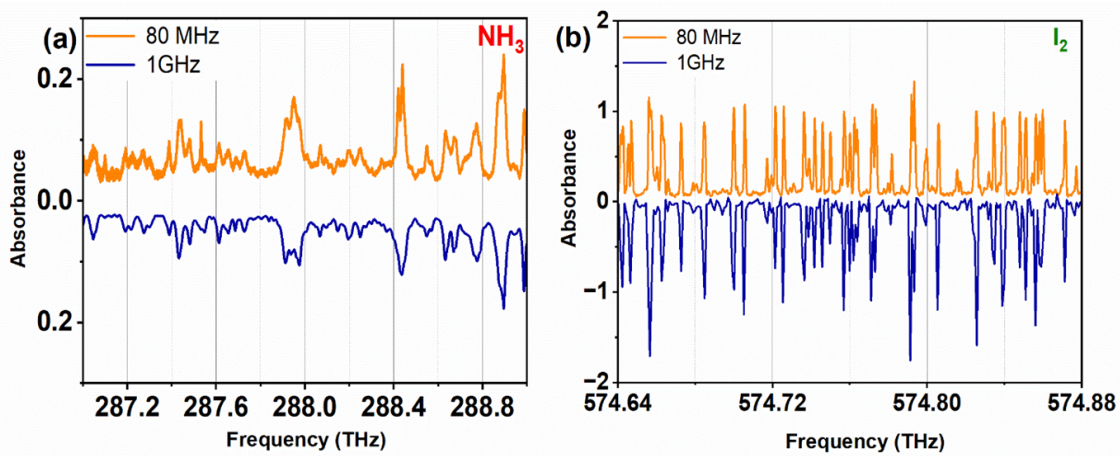


Figure 1: Measured (a) NH<sub>3</sub> absorption spectra in NIR and (b) I<sub>2</sub> absorption spectra in VIS with 80 MHz and 1 GHz DCS systems.

<sup>1</sup>I. Coddington, N. Newbury, and W. Swann, *Optica* **3**, 414–426 (2016).

<sup>2</sup>L. Fürst *et al.*, *Optica* **11**, 471–477 (2024).

<sup>3</sup>B. Bernhardt *et al.*, *Nature Photonics* **4**, 55–57 (2010).

<sup>4</sup>A. Eber *et al.*, *Optics Express* **32**, 6575–6586 (2024).

<sup>5</sup>M. Pal *et al.*, arXiv:2412.05972 (2024). <https://arxiv.org/abs/2412.05972>

<sup>6</sup>“selfCorrectIGMs- File Exchange - MATLAB Central,” MathWorks File Exchange (2018). <https://de.mathworks.com/matlabcentral/fileexchange/69759-selfcorrectigms>

<https://de.mathworks.com/matlabcentral/fileexchange/69759-selfcorrectigms>



Abstract number: P76  
Wednesday 14:00-15:30

# Confinement induced resonances in alkali – alkaline earth atom mixtures

Oghittu L.<sup>†1,2</sup>, Thekkepatt P.<sup>3</sup>, van Druten N. J.<sup>3</sup>, Schreck F.<sup>3</sup>, Mehta N. P.<sup>1,4,6</sup>, Rittenhouse S. T.<sup>1,4,6</sup>, Safavi-Naini A.<sup>1,2</sup>

<sup>1</sup>*Institute for Theoretical Physics, Institute of Physics, University of Amsterdam, Science Park 904, 1098 XH Amsterdam, the Netherlands*

<sup>2</sup>*QuSoft, Science Park 123, 1098 XG Amsterdam, the Netherlands*

<sup>3</sup>*Van der Waals-Zeeman Institute, Institute of Physics, University of Amsterdam, 1098 XH Amsterdam, the Netherlands*

<sup>4</sup>*Department of Physics and Astronomy, Trinity University, San Antonio Texas 78212, USA*

<sup>5</sup>*Department of Physics, the United States Naval Academy, Annapolis, MD, 21402, USA*

<sup>6</sup>*ITAMP, Center for Astrophysics — Harvard & Smithsonian, 60 Garden St., Cambridge, Massachusetts 02138, USA*

<sup>†</sup>l.oghittu@uva.nl

Alkali-alkaline earth atom dimers are a promising platform for quantum simulation<sup>1</sup>, precision measurements and quantum chemistry<sup>2</sup> thanks to their sizable electric and magnetic dipole moments. However, unlike bialkali dimers, their creation via magneto-association is challenging due to the non-magnetic ground state of alkaline earth atoms, which is responsible for very narrow Feshbach resonances. In this study, we present an alternative approach for the formation of weakly bound molecules of alkali-alkaline earth atoms, which relies on confinement-induced resonances (CIRs) in strongly interacting lower-dimensional systems.

In our work, we investigate the scattering properties of an ultracold mixture of two atomic species confined by quasi-1D harmonic potentials. In this regime, the two-body interspecies interaction is modeled by an effective 1D zero-range pseudopotential, whose coupling strength is derived as a function of the 3D scattering length<sup>3</sup>. We characterize the emergence of CIRs and study how they are affected by the mismatched trapping frequency of the two atomic species (see Figure 1).

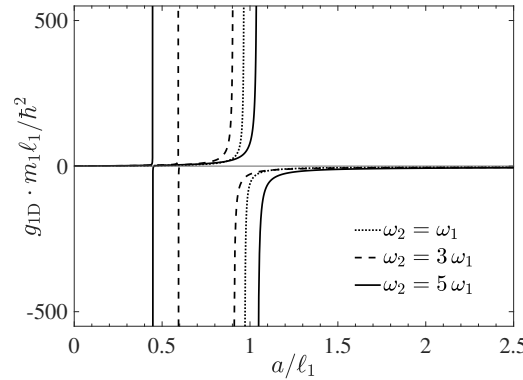


Figure 1: Effective interaction strength  $g_{1D}$  as a function of 3D scattering length  $a$  for different ratios between the trap frequencies of the two species. Lengths are in units of the oscillator length  $\ell_1 = \sqrt{\hbar/(m_1\omega_1)}$  of species 1. When  $\omega_2 = \omega_1$  (dotted), one single resonance is present<sup>4</sup>. When  $\omega_2 \neq \omega_1$  (dashed and solid), the broad resonance is shifted and a narrow additional resonance appears.

These results are applied to the case of a Bose-Fermi mixture of <sup>87</sup>Rb and <sup>87</sup>Sr, where the eigenenergy spectrum reveals the presence of CIRs due to the coupling between center-of-mass excited bound states and lower-lying trapped states. For this specific mixture, we calculate the positions of CIRs and find values of the experimentally accessible parameters for which they can be exploited to create weakly bound dimers.

<sup>1</sup>A. Micheli *et al.*, A toolbox for lattice-spin models with polar molecules, *Nat. Phys.* **2** 341 (2006)

<sup>2</sup>J. L. Bohn *et al.*, Cold molecules: progress in quantum engineering of chemistry and quantum matter, *Science* **357**, 1002 (2017)

<sup>3</sup>V. Peano *et al.*, Confinement-induced resonances for a two-component ultracold atom gas in arbitrary quasi-one-dimensional traps, *New J. Phys.* **7**, 192 (2005)

<sup>4</sup>M. Olshanii, Atomic scattering in the presence of an external confinement and a gas of impenetrable bosons, *Phys. Rev. Lett.* **81**, 938 (1998)

Abstract number: P77

Wednesday 14:00-15:30

## Laser-pulse induced helium trimer dynamics

**Blume D.**<sup>1</sup>, **Guan Q.**<sup>2</sup>, **Kruse J.**<sup>3</sup>, **Kunitski M.**<sup>3</sup>, **Dörner R.**<sup>3</sup>

<sup>1</sup>Homer L. Dodge Department of Physics and Astronomy & Center for Quantum Research and Technology, The University of Oklahoma, 440 W. Brooks Street, Norman, Oklahoma 73019, USA

<sup>2</sup>Department of Physics and Astronomy, Washington State University, Pullman, Washington 99164-2814, USA

<sup>3</sup>Institut für Kernphysik, Goethe-Universität, 60438 Frankfurt am Main, Germany

†doerte.blume-1@ou.edu

Motivated by ongoing pump-probe spectroscopy experiments<sup>1</sup>, this work develops a theoretical framework for describing the rovibrational wave packet dynamics that ensues when a single weakly-bound van der Waals trimer is exposed to a short, sub-picosecond linearly polarized pump laser pulse<sup>2</sup>. The intensity  $I$  of the pump laser is chosen such that excitation and ionization of the electronic degrees of freedom are negligible while excitation of the wavepacket in the nuclear degrees of freedom is non-negligible. The numerical treatment, which takes advantage of the fact that the laser pulse is very short compared to typical molecular time scales, is based on a wave packet decomposition that utilizes hyperspherical coordinates. The framework is applied to the extremely floppy bosonic helium trimer. A convergence analysis of the partial wave decomposition is conducted. The kinetic energy release and orientation dynamics are presented. While the dynamics of more strongly-bound van der Waals trimers such as, e.g., the argon trimer display negligible coupling between vibrational and rotational degrees of freedom, rendering a description within a rigid-body picture appropriate, those of weakly-bound trimers display non-negligible coupling between vibrational and rotational degrees of freedom, rendering a description within a rigid-body picture inappropriate. It is shown that a model that constructs the helium trimer dynamics from the dynamics of the helium dimer captures a number of key characteristics of the alignment signal, including the interference between different angular momentum wave packet components.

<sup>1</sup>J. Kruse *et al.*, manuscript in preparation.

<sup>2</sup>Q. Guan, J. Kruse, M. Kunitski, R. Dörner, and D. Blume, Modeling the laser-pulse-induced helium trimer dynamics, *Physical Review A* **111**, 023108 (2025).

Abstract number: P78  
 Wednesday 14:00-15:30

## Production and stabilization of a spin mixture of ultracold dipolar Bose gases

Lecomte M.<sup>1</sup>, Journeaux A.<sup>1</sup>, Veschambre J.<sup>1</sup>, Dalibard J.<sup>1</sup>, Lopes R.<sup>†1</sup>

<sup>1</sup>Laboratoire Kastler Brossel, Collège de France, CNRS, ENS-Université PSL, Sorbonne Université, Paris, France

<sup>†</sup>raphael.lopes@lkb.ens.fr

Mixtures of ultracold gases with long-range interactions are expected to open new avenues in the study of quantum matter. Natural candidates for this research are spin mixtures of atomic species with large magnetic moments. However, the lifetime of such assemblies can be strongly affected by the dipolar relaxation that occurs in spin-flip collisions. Here we present experimental results for a mixture composed of the two lowest Zeeman states of <sup>162</sup>Dy atoms, that act as dark states with respect to a light-induced quadratic Zeeman effect. We show that, due to an interference phenomenon, the rate for such inelastic processes is dramatically reduced with respect to the Wigner threshold law. Additionally, we determine the scattering lengths characterizing the s-wave interaction between these states, providing all necessary data to predict the miscibility range of the mixture, depending on its dimensionality<sup>1</sup>.

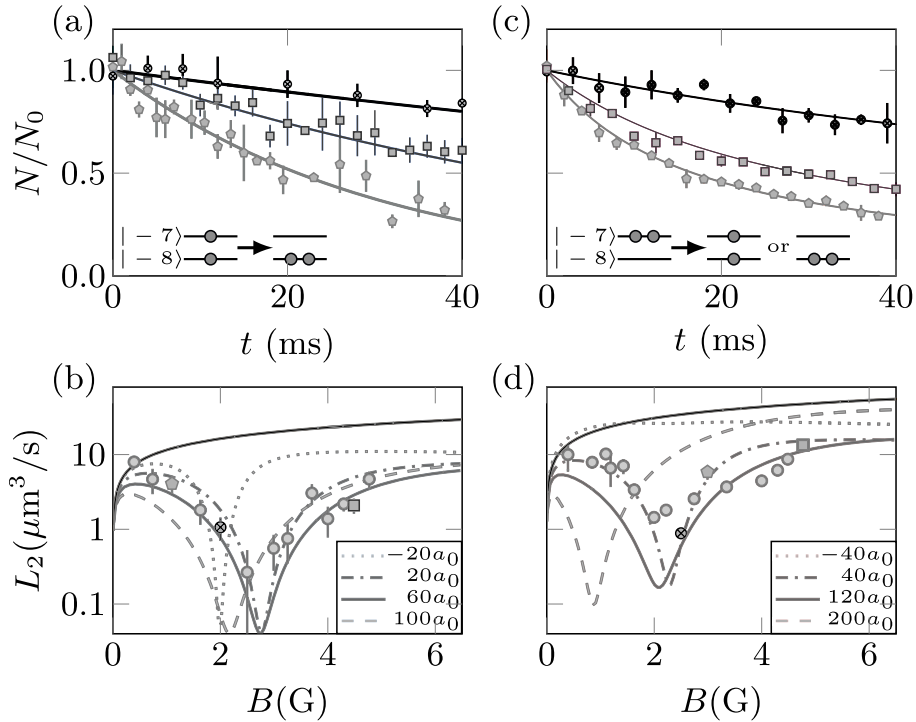


Figure 1: Dipolar relaxation. Time evolution of the atom number in state  $|-7\rangle$  for (a) minority component in  $|-7\rangle$  ( $< 5\%$  immersed in the majority component  $|-8\rangle$  (pentagon  $B = 1.1$  G, crossed circle  $B = 2.0$  G, and square  $B = 4.5$  G) and for (c) pure sample in  $|-7\rangle$  (crossed circle  $B = 2.5$  G, pentagon  $B = 3$  G and square  $B = 4.77$  G). (b) Two-body loss rate as a function of  $B$  for the case of a minority component in  $|-7\rangle$ . The lines correspond to theoretical predictions for scattering length:  $a_{78} = -20a_0$  (dotted line),  $a_{78} = 20a_0$  (dash dot line),  $a_{78} = 60a_0$  (full line) and  $a_{78} = 100a_0$  (dashed line). (d) Two-body loss rate as a function of  $B$  for the case of a pure sample in  $|-7\rangle$ . The lines correspond to theoretical predictions for scattering length:  $a_{77} = -40a_0$  (dotted line),  $a_{77} = 40a_0$  (dash dot line),  $a_{77} = 120a_0$  (full line), and  $a_{77} = 200a_0$  (dashed line). The upper dark lines correspond to the Wigner law  $\propto \sqrt{B}$ .

<sup>1</sup>M. Lecomte, A. Journeaux, J. Veschambre, J. Dalibard, R. Lopes, *Phys. Rev. Lett.* **134**, 013402 (2025).

Abstract number: P79  
Wednesday 14:00-15:30

## A portable, cost-efficient microwave spectrometer and its application to Matrix isolation spectroscopy for searching physics beyond the standard model

**Dinesan H.**<sup>†1</sup>, **Lahs S.**<sup>1</sup>, **Manceau M.**<sup>2</sup>, **Cournol A.**<sup>2</sup>, **Lecordier L.**<sup>2</sup>, **Battard T.**<sup>1</sup>, **Darquie B.**<sup>2</sup>, **Comparat D.**<sup>1</sup>

<sup>1</sup>Université Paris-Saclay, CNRS, Laboratoire Aimé Cotton, 91405, Orsay, France

<sup>2</sup>Laboratoire de Physique des Lasers CNRS UMR 7538 / Université Sorbonne Paris Nord, Villetaneuse, France

<sup>†</sup>hemanth.dinesan@universite-paris-saclay.fr

We present our compact, cost-efficient, microwave spectrometer based on Free Induction Decay (FID) detection<sup>1</sup> with an incredibly high SNR  $> 107$  (demonstrated by measuring the  $J=0 \rightarrow J=1$  transition of OCS molecule at 12.163 GHz at the room temperature). This instrument is referenced to the metrologically reference grade clock signal from SYRTE and with such high levels of SNR, our instrument opens perspectives for a range of applications: from (i) the determination of increasingly accurate molecular parameters and the refinement of line shape models to improve existing atmospheric and astrophysics databases to (ii) tests of fundamental physics, such as the search for new physics by providing constraints in the time variation of fundamental constants by accurately measuring microwave transition frequencies repeatedly over time. We are currently integrating our apparatus with the cryogenic experiment performing Matrix isolation spectroscopy, to study in detail, the ESR spectrum of Alkali atoms doped in inert gas matrices. The goal of this project is to measure electron Electric Dipole Moment (eEDM) by isolating Cs atoms in the inert gas matrix (Ar, Ne, Kr and Xe), aiming for a target sensitivity of  $10^{-36}$  e.cm<sup>2</sup>. Matrix isolation spectroscopy has huge potential and its more advantageous compared to the other conventional techniques based on gas phase because it provides high dopant density ( $1 \times 10^{18}$  atoms/cm<sup>3</sup>), long coherence time ( $\sim 0.1$  s) and good optical pumping capacity<sup>3</sup>. The SNR of our microwave spectrometer can be further enhanced by an order of magnitude, if we go down to cryogenic temperatures. Some of our recent results are reported here.

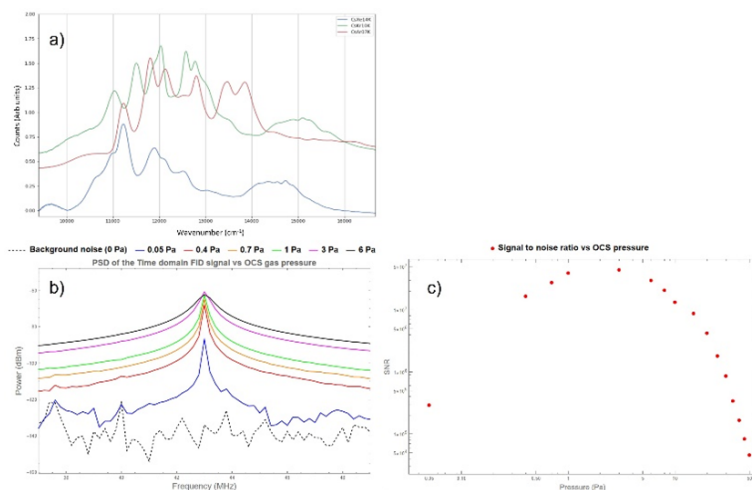


Figure 1: Figure 1: a) Transmission spectra of Cs doped in inert gas matrices (Xe, Kr and Ar) at cryogenic temperatures. Two triplet structures show two trapping sites, b) PSD of the Time domain FID signal corresponding to the OCS transition at 12.163 GHz measured with the microwave spectrometer and c) Signal-to-Noise Ratio (SNR) of the instrument as a function of gas pressure.

<sup>1</sup>J. Ekkers and W.H. Flygare, *Review of Scientific instruments* **47**, 448 (1976).

<sup>2</sup>M. Arndt, S.I. Kanorsky, A. Weis and T.W. Haensch, *Physical Lett A* **6**, 174 (4) (1993).

<sup>3</sup>S. Upadhyay *et al.*, *PRA* **100**, 063419 (2019).

Abstract number: P80  
 Wednesday 14:00-15:30

## A High-Resolution Ion Microscope to Spatially Observe Ion-Rydberg Interactions

Krauter J.<sup>1</sup>, Herrera-Sancho O. A.<sup>1,2</sup>, Berngruber M.<sup>1</sup>, Meinert F.<sup>1</sup>, Löw R.<sup>1</sup>, Pfau T.<sup>†1</sup>

<sup>1</sup>Physikalisches Institut, Universität Stuttgart, Pfaffenwaldring 57, 70569 Stuttgart, Germany

<sup>2</sup>Escuela de Física, Universidad de Costa Rica, 2060 San Pedro, San José, Costa Rica

<sup>†</sup>t.pfau@physik.uni-stuttgart.de

Here, we present the findings of our recent studies on ion-Rydberg atom interactions conducted in the ultracold regime using a high-resolution ion microscope. This experimental apparatus offers temporal and spatial imaging of charged particles with a resolution of at least 200 nm<sup>1</sup>. While neutral ultralong-range Rydberg molecules have been studied extensively in the past, our group has recently observed for the first time charged molecular dimers, consisting of an ion bound to a Rydberg state via a novel flipping-dipole binding mechanism<sup>2</sup>. This discovery enabled *in-situ* imaging of triggered vibrational dynamics<sup>3</sup> in these dimer systems and opened a new domain of ultracold Rydberg chemistry.

Systems combining ions and Rydberg atoms offer various interesting phenomena for research. Already simple pair states consisting of one ion and one Rydberg atom allow for the observation of complex collisional dynamics on steep attractive potential energy curves featuring multiple avoided crossings with adjacent states. Those can lead to a drastic speed-up of the collision process<sup>4</sup>. Avoided crossings can also give rise to molecular bound states by forming potential wells. These bound states between an ion and a Rydberg atom feature huge bond lengths of several micrometers, enabling the direct observation of vibrational dynamics. Further, this binding mechanism is not limited to diatomic molecules but can be extended to polyatomic molecules, for which we expect interactions that are even more intricate. Molecules consisting of three atoms are by nature much richer in their physics compared to dimers, which makes them more interesting, yet also more complicated to study. In particular, for a bound state between two Rydberg atoms and one ion, we therefore predict a rich interaction potential that comprises the interaction between induced dipoles, ion-Rydberg atom interactions, and the Rydberg blockade effect.

<sup>1</sup>C. Veit, N. Zuber, O. A. Herrera-Sancho, V. S. V. Anasuri, T. Schmidt, F. Meinert, R. Löw, and T. Pfau, *Phys. Rev. X* **11**, 011036 (2021).

<sup>2</sup>N. Zuber, V. S. Anasuri, M. Berngruber, Y. Q. Zou, F. Meinert, R. Löw, and T. Pfau, *Nature* **605**, 7910 (2022).

<sup>3</sup>Y. Q. Zou, M. Berngruber, V. S. Anasuri, N. Zuber, F. Meinert, R. Löw, and T. Pfau, *Phys. Rev. Lett.* **130**, 023002 (2023).

<sup>4</sup>M. Berngruber, D. J. Bosworth, O. A. Herrera-Sancho, V. S. Anasuri, N. Zuber, F. Hummel, J. Krauter, F. Meinert, R. Löw, and T. Pfau, *Phys. Rev. Lett.* **133**, 083001 (2024).

Abstract number: P81  
Wednesday 14:00-15:30

## Progress on cold-atoms based quantum atomic clocks at Leonardo Innovation Hub

**Milani G.**<sup>†1</sup>, **Menchetti M.**<sup>1</sup>, **Carpenella V.**<sup>1</sup>, **Proietti M.**<sup>1</sup>, **Dispenza M.**<sup>1</sup>

<sup>1</sup>Leonardo Innovation Hub - Quantum Technologies, Roma, Italy

<sup>†</sup>gianmaria.milani@leonardo.com

We present a novel atomic clock design utilizing cold  $^{87}\text{Rb}$  atoms trapped in a magneto-optical trap (MOT) and interrogated via coherent population trapping (CPT) currently being developed at Leonardo Innovation Hub. Cold atoms provide high stability and precision by minimizing collisional interactions and environmental perturbations. The system implements solutions aimed at the miniaturization of the device, such as the use of grating optics to produce cold atoms from a single incident beam, thus reducing the system's volume and complexity, and the optical interrogation of the microwave (MW) clock transition (Coherent Population Trapping), avoiding the use of a bulky MW cavity. Currently, a compact 6-beams MOT was implemented, routinely trapping more than  $10^7$  atoms at a temperature of  $30\mu\text{K}$  (see Figure 1). The next development will incorporate the measurement of the CPT transition as well as the miniaturization of the optical components by means of photonic integrated circuits (PIC).

This compact atomic clock design enhances precision timekeeping and quantum sensing in application outside the laboratory while, when integrated with a quantum accelerometer and gyroscope, it forms the foundation of a quantum inertial navigation system, offering unparalleled accuracy in environments without GNSS access.

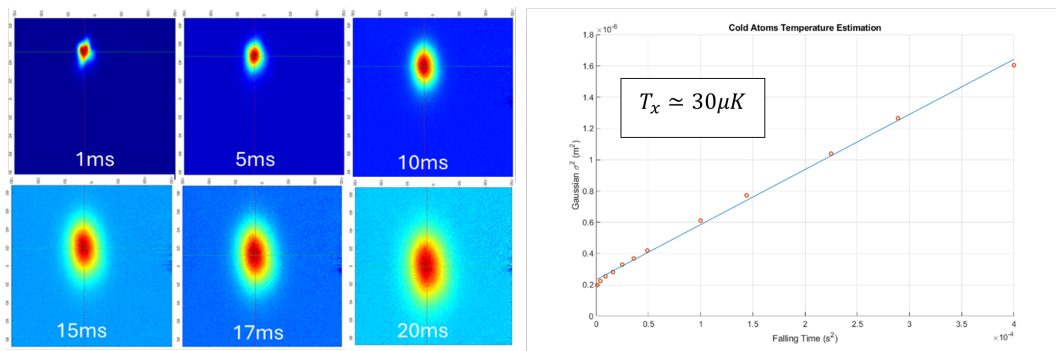


Figure 1: left, Time of Flight (ToF) imaging of the trapped atoms. Right, estimation of the temperature of the cloud from its dimension vs. time of flight.

Abstract number: P82

Wednesday 14:00-15:30

## Measuring the Electron's Electric Dipole Moment Using Ultracold YbF Molecules

**Jenkins R.<sup>†</sup>, Collings F., Wursten E., Ziemba M., Zheng S., Castellini F., Lim J., Sauer B. E, Tarbutt M. R.**  
*Imperial College London, Centre for Cold Matter, Blackett Laboratory, South Kensington Campus, London, SW7 2AZ, UK*

<sup>†</sup>rhys.jenkins@imperial.ac.uk

The standard model predicts a value for the electron's electric dipole moment (eEDM,  $d_e$ ),  $d_e \sim 10^{-35}$  e cm<sup>1</sup>, far smaller than what is predicted by theories beyond the standard model, typically  $d_e \approx 10^{-31}$  -  $10^{-24}$  e cm. To date, the current experimental upper limit is set at  $d_e < 4.1 \times 10^{-30}$  e cm<sup>2</sup>. Further improvements in experimental precision are likely to discover new physics or rule out much of the parameter space of popular theories. The eEDM can be measured through the precession of the electron spin in an applied electric field. The precision is enhanced enormously when the electron is bound into a heavy polar molecule. The statistical precision depends on the spin precession time so a slow, ultracold beam of molecules has the potential to measure the eEDM to greater precision than the current limit.

We use a beam of collimated ultracold YbF molecules produced by a cryogenic buffer gas source and then laser cooled to 100  $\mu$ K in the two transverse axes<sup>3</sup>. Such cooling increases beam brightness and spin-precession time, leading to a projected statistical uncertainty below  $10^{-30}$  e cm<sup>4</sup>. However, magnetic field noise can severely limit the precision of our phase sensitive measurement of  $d_e$ . To overcome this source of noise, we have developed and characterised a novel spin precession region<sup>5</sup>, including ceramic electric field plates, a glass vacuum chamber, magnetometry, and a four-layer magnetic shield with a shielding factor  $> 10^5$ . We prepare the eEDM-sensitive state using stimulated Raman adiabatic passage and detect the molecules with near unit efficiency. We are currently working to reach the shot noise limit of statistical sensitivity.

<sup>1</sup>Y. Ema *et al.*, *Phys. Rev. Lett.* **129**, 231801 (2022).

<sup>2</sup>T. Roussy *et al.*, *Science* **381**, 46-50 (2023).

<sup>3</sup>X. Alauze *et al.*, *Quantum Sci. Technol.* **6**, 044005 (2021).

<sup>4</sup>N.J. Fitch *et al.*, *Quantum Sci. Technol.* **6**, 014006 (2021).

<sup>5</sup>F. Collings *et al.*, *arXiv:2503.21725v1*, (2025).

**Abstract number: P83**  
**Wednesday 14:00-15:30**

## A Momentum State Quantum Computer

**Roe T. H.<sup>†1</sup>, Freegarde T.<sup>1</sup>**

<sup>1</sup>*School of Physics & Astronomy, University of Southampton, Highfield, Southampton SO17 1BJ, U.K.*

<sup>†</sup>T.Roe@soton.ac.uk

Coherent interactions with programmed sequences of resonant laser pulses allow 2-level atoms to be manipulated along a 1-D ladder of momentum states whose binary labelling provides the qubits of a momentum state quantum computer<sup>1</sup>. Combinations of the beamsplitter and mirror pulses used in atom interferometry along with momentum-dependent free evolution<sup>2</sup> permit the creation of logical operations to act upon the qubits, while the associated transfer between internal electronic states provides a mechanism for initialization and read-out.

In our experimental design for a momentum state quantum computer we shall trap and cool neutral Rubidium atoms in a magneto-optical trap (MOT) and manipulate them with pulses from laser beam pairs resonant with the Raman transition between the ground hyperfine states. By constructing a system where the directions of the beams can be exchanged, the recoil momentum of the two-photon transition can be transferred to the atoms in either direction, establishing a ladder of discrete momentum states.

One of the main difficulties in manipulating atomic states with laser pulses is maintaining a high fidelity of state transfer in the presence of intensity inhomogeneities and varying atomic velocities. We have previously shown that optimal control techniques such as Gradient Ascent Pulse Engineering (GRAPE)<sup>3</sup>, developed for spin systems in the field of magnetic resonance, can also be applied to 2-level atoms by varying the phase and amplitude of the laser beams that drive the Raman transition<sup>4</sup>. Optimal control has generally been applied only to individual beamsplitter and mirror pulses, and therefore we aim to use our momentum state quantum computer as a testbed for the optimisation of extended pulse sequences to allow logical gate operations to be performed with high fidelity.

A momentum state quantum computer is principally of interest as a mechanism for the mechanical control of atoms, such as the algorithmic cooling achieved by performing a divide-by-two operation on the momentum state qubits, and may be regarded as an expansion upon the technique of interferometric cooling<sup>5,6</sup>.

<sup>1</sup>T. Freegarde and D Segal, *Phys. Rev. Lett.* **91** (3), 037904 (2003)

<sup>2</sup>M. Carey, J. Saywell, M. Belal and T. Freegarde, *Phys. Rev. A* **99**, 023631 (2019)

<sup>3</sup>N. Khaneja, T. Reiss, C. Kehlet, T. Schulte-Herbrüggen and S. J. Glaser, *J. Magn. Reson.* **172**, 2 (2005)

<sup>4</sup>J. Saywell, M. Carey, M. Belal, I. Kuprov and T. Freegarde, *J. Phys. B* **53**, 085006 (2020)

<sup>5</sup>M. Weitz and T. W. Hänsch, *Europhys. Lett.* **49**, 302 (2000)

<sup>6</sup>A. Dunning, R. Gregory, J. Bateman, M. Himsworth and T. Freegarde, *Phys. Rev. Lett.* **115**, 073004 (2015)



Abstract number: P84

Wednesday 14:00-15:30

# Comb-locked cavity ring-down spectroscopy: combining high precision with ultra-high detection sensitivity in molecular interrogation

Castrillo A.<sup>1</sup>, Fasci E.<sup>1</sup>, Gravina S.<sup>1</sup>, Khan M. A.<sup>1</sup>, D'Agostino V.<sup>1</sup>, Gianfrani L.<sup>†</sup><sup>1</sup>Dipartimento di Matematica e Fisica, Università della Campania "Luigi Vanvitelli", Caserta, Italy<sup>†</sup>livio.gianfrani@unicampania.it

In the last decade, the technology of optical frequency combs (OFCs) has been successfully integrated with cavity-enhanced spectroscopic techniques in a variety of different ways, leading to interesting developments in the field of molecular spectroscopy.<sup>1</sup> More specifically, it has been possible to achieve high detection sensitivity in conjunction with high precision and accuracy in optical frequency measurements. Consequently, metrological-grade qualities have been added to molecular spectra, with relevant implications in various fields of fundamental and applied research.

Here, we report on a few examples of comb-locked cavity ring-down spectroscopy (CL-CRDS) performed in the spectral regions around 1.4 and 2  $\mu\text{m}$ . A first example deals with residual water concentration measurements in ultra-high-purity gases that are needed in manufacturing processes of the semiconductor industry to meet the quality requirements.<sup>2</sup> The CL-CRDS system was based on a hemispherical optical resonator with a finesse as high as 507000, which gave an empty-cavity ring-down time of about 285  $\mu\text{s}$ . Taking advantage of the frequency stability guaranteed by the optical frequency comb, it was possible to implement the strategy of long-term spectra averaging to remove efficiently the effect of mechanical, acoustic, and thermal noises. As a result, we could achieve a minimum detectable absorption coefficient as low as  $3.7 \times 10^{-13} \text{ cm}^{-1}$ , which corresponds to a limit of detection for  $\text{H}_2\text{O}$  in  $\text{N}_2$  of nine parts per trillion and a  $\text{H}_2\text{O}$  partial pressure of  $2 \times 10^{-8} \text{ Pa}$  (or  $2 \times 10^{-10} \text{ mbar}$ ), numbers which set a benchmark for CRDS-based trace water detection.<sup>3</sup> The potential of our approach was further demonstrated by recording the absorption features of rare water isotopologues, such as  $\text{HD}^{16}\text{O}$  and  $\text{HD}^{18}\text{O}$ , in ambient air.

A similar setup was developed for Lamb-dip spectroscopy of several P, Q, and R components of weak vibrational bands of  $\text{C}_2\text{H}_2$ .<sup>4</sup> Selection of the lines was based on the theory of spectroscopic networks (SN), in order to ensure that a large number of transitions, measured previously by precision-spectroscopy investigations, could be connected to the *para* and *ortho* principal components. The analysis of sub-Doppler profiles and the extrapolation of absolute frequencies to zero pressure in each case produced a combined average uncertainty of the measured line-center positions of about 7 kHz with a  $1\text{-}\sigma$  confidence level.<sup>5</sup>

Finally, we report on preliminary results obtained by means of a new CL-CRDS spectrometer, expressly developed to perform accurate tests of quantum chemistry calculations for  $\text{N}_2\text{O}$  and  $\text{CO}_2$  in the spectral region of 2  $\mu\text{m}$ .<sup>6</sup> An example spectrum is shown in Figure 1, together with the results of line-fitting of a vibro-rotational  $\text{CO}_2$  transition at  $4980 \text{ cm}^{-1}$  in a sample of ambient air.

This work has been partially founded by the European Partnership on Metrology project "22IEM03 PriSpecTemp".

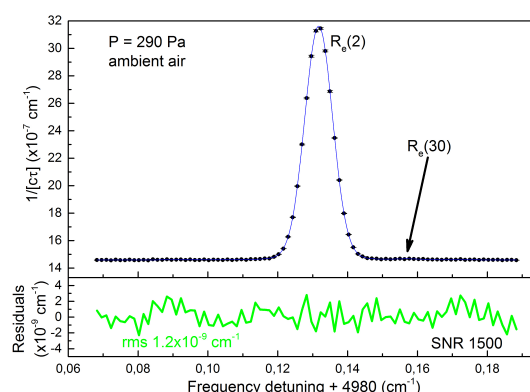


Figure 1:  $\text{CO}_2$  spectrum, as recorded by means of the 2- $\mu\text{m}$  comb-locked CRDS spectrometer.

<sup>1</sup>L. Gianfrani, S.M. Hu, W. Ubachs, *Riv. Nuovo Cimento* **47**, 229 (2024).

<sup>2</sup>E. Fasci *et al.*, *Sens. Actuator A-Phys.* **362**, 114632 (2023).

<sup>3</sup>A. Castrillo *et al.*, *Optica* **11**, 1277 (2024).

<sup>4</sup>E. Fasci *et al.*, *New J. Phys.* **23**, 123023 (2021).

<sup>5</sup>A. Castrillo *et al.*, *Phys. Chem. Chem. Phys.* **25**, 23614 (2023).

<sup>6</sup>V. D'Agostino *et al.*, *Opt. Lett.* **submitted** (2025).

Abstract number: P85  
Wednesday 14:00-15:30

## Ultra-Cold Atoms Interferometry for Space Applications

**Marchesini M.**<sup>†1</sup>, Calviac R.<sup>1</sup>, Metayer C.<sup>1</sup>, Le Mener J.<sup>1</sup>, Battelier B.<sup>1</sup>

<sup>1</sup>LP2N, Laboratoire Photonique, Numérique et Nanosciences; Université Bordeaux, IOGS, CNRS; 1 rue François Mitterrand, 33400 Talence, France

<sup>†</sup>matteo.marchesini@institutoptique.fr

In space, the microgravity environment allows atom interferometer to have much longer time of flights than Earth-based ones. This is expected to result in unprecedented high-precision measurements of inertial forces. However, the miniaturisation efforts needed to have functioning devices in orbit are still huge, with state-of-the-art experiments currently being deployed only inside space stations<sup>1,2</sup>. But future missions, aiming to map the terrestrial gravitational field for applications in geophysics and climate studies, are already being proposed and developed<sup>3</sup>. To pave the way for these missions, ground-based demonstrators are necessary to show the feasibility of such devices, in addition to determining the experimental constraints to which they should be subject.

The *ICE* experiment (Interférométrie atomique à sources Cohérentes pour l'Espace, i.e. atom interferometry for space using coherent sources) aims to be a proof of concept for a transportable dual-species matter-wave interferometer (using laser-cooled Rb and K atoms), to test the *Weak Equivalence Principle* (WEP) in microgravity<sup>4</sup>. The whole experiment is compact and suited for operation on board of airborne vessels (in particular the *Novaspace Zero G aircraft*, which can perform parabolic trajectories granting 20 s of microgravity) for dedicated flight campaigns. Alternatively, the lightweight sensor head ( $\approx 200$  kg) is placed on a *microgravity simulator* installed in our lab, which allows up to 500 ms of microgravity with a high repetition rate<sup>5</sup>.

Using the simulator, our dual interferometer can be used to test the *Universality of Free Fall* (UFF) by measuring the Eötvös parameter  $\eta$ , as well as functioning as a single-axis accelerometer. With a total interrogation time of  $2T = 200$  ms, we demonstrated an acceleration sensitivity of  $6 \times 10^{-7}$  m/s<sup>2</sup> on the vertical axis while in microgravity<sup>6</sup>. Concerning the UFF, at the moment only measurements in 1 g gravity were done, where  $\eta = 0.9 \times 10^{-6}$  was obtained<sup>7</sup>; we predict this value will be improved to  $\sim 10^{-10}$  while running the experiment on the simulator. Even with the present-day results, and using quantum objects as probes rather than classical ones, no WEP violation is however shown.

The above mentioned measurements were performed using atomic clouds cooled down to  $\approx 7$   $\mu$ K. We expect these performances to improve with the use of ultra-cold atoms ( $\approx 30$  nK) while in microgravity. This is because the lower temperature allows higher contrast in the interferometer measurements; moreover the absence of gravity-induced Doppler-shift of the targeted transitions, coupled with the smaller range of velocities of the atoms, makes it possible to enter the *double diffraction regime*<sup>8</sup>, which is the one which *free-falling* experiments in space are subject to.

Currently, we are using the ICE apparatus to test the experimental concepts of the *CARIOQA* space mission (Cold Atom Rubidium Interferometer in Orbit for Quantum Accelerometry)<sup>9</sup>, which aims to develop an orbital quantum accelerometer within the next decade. Its goal will be to perform satellite-based Earth observations, to monitor ice caps evolution in time and support the development of mitigation and adaption measures to climate change. Our contribution consists in analysing the metrological constraints of the experiment to pilot measurement realisation, interpretation and validation, with the aim to improve sensitivity of the apparatus. In particular, we focus on optimising the imaging system of the science package, to achieve quantum projection noise limit while measuring the interferometer outputs.

<sup>1</sup>J. R. Williams *et al.*, *arXiv:2402.14685* (2024)

<sup>2</sup>J. Li *et al.*, *arXiv:2405.20659* (2024)

<sup>3</sup>I. Alonso *et al.*, *EPJ Quantum Technol.* **9**, 30 (2022)

<sup>4</sup>R. A. Nyman *et al.*, *Appl. Phys. B* **84**, 673-681 (2006)

<sup>5</sup>B. Barrett *et al.*, *Nat. Commun.* **7**, 13786 (2016)

<sup>6</sup>C. Pelluet *et al.*, *arXiv:2407.07183* (2024)

<sup>7</sup>B. Barrett *et al.*, *AVS Quantum Sci.* **4**, 014401 (2022)

<sup>8</sup>T. Lévêque, A. Gauguier, F. Michaud, F. Pereira Dos Santos, and A. Landragin, *Phys. rev. Lett.* **103**, 080405 (2009)

<sup>9</sup>T. Lévêque *et al.*, *Proc. SPIE* **12777**, 127773L (2023)

Abstract number: P86  
 Wednesday 14:00-15:30

## Ultracold caesium radioisotopes and isomers for nuclear magnetic octupole moment studies

**Rattanasakuldilok W.<sup>1</sup>, Moore I. D.<sup>1</sup>, Renzoni F.<sup>2</sup>**

<sup>1</sup>University of Jyväskylä, Finland

<sup>2</sup>University College London, United Kingdom

†wrattana@jyu.fi

Constructing a comprehensive nuclear theory by an indirect means of probing the coupling effect between an atomic nucleus and its electrons has been pursued to overcome the extremely complicated nucleon-nucleon interactions. Fundamental nuclear characteristics such as nuclear spin, charge distribution and shape deformation have been extracted across the nuclear chart based on the two lowest order terms in the nuclear electromagnetic multipole expansion<sup>1 2</sup>. However, exploring baffling phenomena and higher-order observables demands exceedingly high-precision measurement, impossibly difficult for a traditional experimental standard. Recently, the focus has been shifted to the next nuclear electromagnetic moment, the magnetic octupole  $\Omega$  moment, which has been deduced in only 21 stable isotopes<sup>3</sup>. Amongst these, the  $\Omega$  measurement of <sup>133</sup>Cs indicated a great deviation from the nuclear shell model prediction<sup>4</sup>. Resolving the magnetic octupole moment  $\Omega$  of Cs therefore presents a promising route towards solving the puzzling nuclear structure, testing the nuclear shell model, as well as setting the benchmark for the long-sought nuclear theory.

To achieve this goal, we put forward the high-precision spectroscopy of ultracold isotopes and isomers of Cs from stable <sup>133</sup>Cs towards neutron-rich <sup>140</sup>Cs to measure their nuclear octupole  $\Omega$  moments systematically. A plethora of atomic-nuclear interplay obtained from a collection of Cs species allows investigating magnetisation effect of the last neutron, the evolution of nuclear shape deformation and nuclear size, and the effect of neutron shell closure which can then be compared to the nuclear shell model calculation. Removal of systematic shifts and uncertainties becomes possible as the measurement is carried out across the radioactive chain, and the  $\Omega$  moments of radioactive isotopes and isomers can be deduced for the first time. In order to access the radioactive and isomeric nuclear species, a dedicated atomic cooling and trapping facility, *Cold Atom Caesium Trap for Atomic Spectroscopy (CACTAS)*, has been developed at the Ion-Guide Isotope Separator On-Line (IGISOL) at the University of Jyväskylä<sup>5 6</sup>. The Cs isotopes and isomers are produced via proton-induced fission of a natural uranium target in a helium buffer gas filled ion guide, extracted from the ion guide via gas flow, accelerated electrostatically to 30 keV, mass-separated, and finally delivered to an implantation chamber. Alternatively, a hot cavity ion source<sup>7</sup> can be installed in the reaction chamber which can operate with both online-mode fission and offline-mode neutron-irradiated Cs solution, the latter of which yields <sup>134</sup>Cs and <sup>135</sup>Cs isotopes. Installed inside the implantation chamber is a thin yttrium foil where implanted Cs ions are neutralised. The yttrium foil is secured on a movable copper mount which can be rotated and linearly driven from the implantation position to the release position inside a cold-atom chamber, situated just above the implantation chamber. Via the same copper mount, Cs atoms diffuse out of the yttrium foil as resistive heating is applied. A special organic coating applied on the inner surface of the cold-atom chamber then allows thermalisation of hot Cs atoms, thereby facilitating a magneto-optical trap (MOT), the initial stage of a cooling and trapping scheme. Further optical cooling methods including optical molasses and degenerate Raman sideband cooling (DRSC) can be applied to obtain temperatures suitable for probing the magnetic octupole  $\Omega$  moments of Cs radioisotopes and isomers.

<sup>1</sup>P. Campbell, I.D. Moore and M.R. Pearson, *Progress in Particle and Nuclear Physics* **86**, (2016).

<sup>2</sup>R.P. de Groote *et al.*, *Physics Letters B* **827**, 136930 (2022).

<sup>3</sup>S. Bofos and T.J. Mertzimekis, *Atomic Data and Nuclear Data Tables* **159**, 101672 (2024).

<sup>4</sup>V. Gerginov, A. Derevianko and C. E. Tanner, *Physical Review Letters* **91**, 7 (2003).

<sup>5</sup>H. Penttilä *et al.*, *EPJ Web of Conferences* **239**, 17002 (2020).

<sup>6</sup>A. Giatzoglou *et al.*, *Nuclear Instruments and Methods in Physics Research Section A: Accelerators, Spectrometers, Detectors and Associated Equipment* **908**, (2018).

<sup>7</sup>M. Reponen *et al.*, *Review of Scientific Instruments* **86**, 123501 (2015).

**Abstract number: P87**  
**Wednesday 14:00-15:30**

# First observation of Muonium 1S-2S F=0 $\rightarrow$ F'=0 transition at J-PARC

S. Yamamoto<sup>1†</sup>, T. Adachi<sup>2</sup>, R. Endo<sup>1</sup>, H. Hara<sup>1</sup>, T. Hiraki<sup>1</sup>, Y. Ikedo<sup>3</sup>, Y. Imai<sup>1</sup>, K. Ishida<sup>3</sup>, S. Kamal<sup>4</sup>,  
S.Kamioka<sup>3</sup>, N. Kawamura<sup>3</sup>, M. Kimura<sup>3</sup>, A. Koda<sup>3</sup>, T. Masuda<sup>1</sup>, T. Mibe<sup>3</sup>, Y. Miyamoto<sup>1</sup>, K.  
Shimomura<sup>3</sup>, P. Strasser<sup>3</sup>, K. Suzuki<sup>5</sup>, S. Uetake<sup>1</sup>, T. Yamazaki<sup>3</sup>, M. Yoshida<sup>3</sup>, K. Yoshimura<sup>1</sup>, C. Zhang<sup>6</sup>

<sup>1</sup>Okayama University, Japan

<sup>2</sup>*Institute of Physical and Chemical Research,RIKEN, Japan*

<sup>3</sup>High Energy Accelerator Research Organization, Japan

<sup>4</sup>*University of British Columbia, Canada*

<sup>5</sup>*Nagoya University, Japan*

<sup>6</sup>*Peking University, China*

<sup>†</sup>s-yama@s.okayama-u.ac.jp

To explore physics beyond the Standard Model of particle physics (BSM) is quite important because the SM is incomplete. One of the most intriguing approach for search of the BSM is precision measurement of energy interval in Muonium. Muonium is an exotic hydrogen-like atom consists of a positive muon  $\mu^+$  and an electron  $e^-$ . This purely leptonic system enables a precise calculation of the energy interval based on the SM, without ambiguity of the charge radius of the nucleus, unlike hydrogen atoms. Thus comparing theoretical prediction and precise measurements of the energy interval provides a precision test of the SM. However, the present uncertainty in the theoretical prediction of the energy interval is limited by muon mass uncertainty. The muon mass is precisely determined from the 1S-2S energy interval of Muonium. Therefore, We focused on measuring the 1S-2S transition frequency of Muonium by Doppler-free two-photon laser spectroscopy.

In this poster, we report the first observation of the 1S-2S ( $F=0 \rightarrow F'=0$ ) transition in Muonium at J-PARC. Since the signal rate of this transition is one third of  $F=1 \rightarrow F'=1$  transition, it was difficult to observe. By continuous improvement of measuring apparatus, the signal rate of 1S-2S ( $F=1 \rightarrow F'=1$ ) transition is  $\simeq 300$  times higher than the previous experiment<sup>1</sup>. Such high signal rate enables us to observe the transition between singlet states and gives a prospect to improve the muon mass uncertainty.

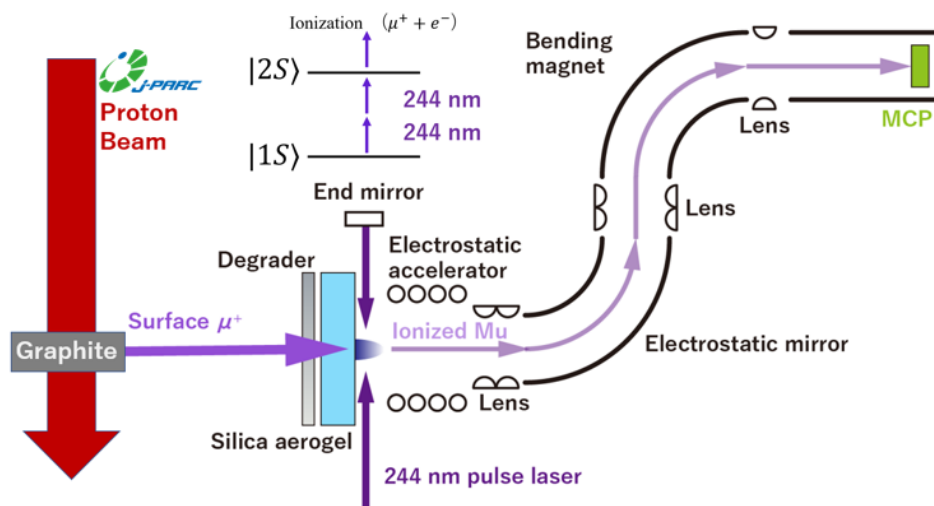


Figure 1: Experimental setup of Muonium 1S-2S laser spectroscopy.

---

<sup>1</sup>Meyer V. *et al.*, *Phys. Rev. Lett.* **84** 1136 (2000)

Abstract number: P88  
 Wednesday 14:00-15:30

## How to Generate XUV Frequency Combs Without Enhancement Resonators?

Muhammad Thariq<sup>†1,2</sup>, Johannes Weitenberg<sup>1,3</sup>, Theodor W. Hänsch<sup>1,2</sup>, Thomas Udem<sup>1,2</sup>, Akira Ozawa<sup>1,4</sup>

<sup>1</sup>Max-Planck-Institut für Quantenoptik, 85748 Garching, Germany

<sup>2</sup>Fakultät für Physik, Ludwig-Maximilians-Universität München, 80799 Munich, Germany

<sup>3</sup>Fraunhofer-Institut für Lasertechnik ILT, 52074 Aachen, Germany

<sup>4</sup>Institute for Multidisciplinary Sciences, Yokohama National University, Yokohama City, 240-8501 Kanagawa, Japan

<sup>†</sup>muhammad.thariq@mpq.mpg.de

The extreme ultraviolet (XUV) frequency comb is indispensable for extending optical frequency metrology into the unexplored wavelength range below 200 nm. With XUV frequency combs, precision spectroscopy for fundamental physics, optical clocks, and laser cooling can be extended into the XUV regime. This includes the spectroscopy of highly charged ions, the recently measured nuclear excitation of  $^{229\text{m}}\text{Th}$ , and our planned experiment on the spectroscopy of the  $\text{He}^+ 1\text{S}-2\text{S}$  transition for testing quantum electrodynamics<sup>1</sup>.

Historically, the generation of XUV lasers has been a daunting task, requiring either particle accelerators or high harmonic generation (HHG) techniques with peak intensities on the order of  $10^{13} - 10^{15} \text{ W/cm}^2$ . In particular, generating XUV frequency combs at a repetition rate exceeding 10 MHz involves cavity-enhanced high harmonic generation (CE-HHG). Our current implementation involves amplifying the average power to 400 W before feeding the laser to an enhancement resonator, where an average circulating power approaching 10 kW is used to generate gas-based HHG<sup>2</sup>. Considering this is a frequency comb, the comb structure must be maintained at high average powers, ensuring low phase noise to prevent carrier collapse during HHG. The use of enhancement resonators (and high-power lasers in general) requires additional complexity and special measures to protect the optical components from the rigors of high-power lasers.

We have generated high harmonics with solid-state HHG using an average power of less than 10 W without an enhancement resonator, significantly simplifying the laser system. This is achieved by reducing the repetition rate by three orders of magnitude to 40 kHz while maintaining sufficient peak power for HHG<sup>3</sup>. The technique relies on pulse picking using an acousto-optic modulator (AOM) that selects pulses at specific intervals, effectively reducing the repetition rate. In the frequency domain, pulse picking can generate additional sidebands from the original comb modes such that the distance between the comb modes is reduced. Due to energy conservation, the action of pulse picking would mean that the newly generated comb modes (and the original comb modes) have a weaker comb mode power that inversely scales to  $m^2$  where  $m$  represents the pulse picking factor (after how many pulses does the AOM pick the pulse). Further low-noise amplification is therefore needed to recover the average power that is “lost” from pulse picking and to increase the peak power for HHG to be feasible. Additional stabilization stages and path length stabilization are crucial to prevent the comb modes from being washed by the technical noise floor.

The laser system uses a Kerr-lens mode-locked Yb:KYW oscillator (1030 nm, 40 MHz). After pulse picking with an AOM, which reduces the repetition rate to 40 kHz, the pulses are amplified by diode-pumped Yb:LuAG amplifiers to 10  $\mu\text{J}$ . The pulses are further compressed to 35 fs using two stages of Multi-Pass Cell Spectral Broadening<sup>4</sup>. The frequency comb structure is maintained by stabilizing one comb mode to an ultra-stable CW laser at 1033 nm. Solid-state HHG is achieved using MgO, generating odd harmonics from the amplified infrared frequency comb. Further XUV comb characterization, such as beam profiling and beat note measurements in the extreme ultraviolet, is currently underway.

The dense comb structure resulting from the low repetition rate is not an issue when addressing ultra-narrow spectroscopic transitions. For a repetition rate of 40 kHz, the spectroscopic target should have an expected linewidth far below 40 kHz to do comb-resolved spectroscopy with this frequency comb, which is often the case for optical clock applications. A dual-comb spectroscopy scheme could be used to measure targets with higher linewidths. A dual-comb allows identifying the comb mode number, even with such a dense frequency comb structure.

This work offers a tantalizing prospect: XUV frequency combs with significantly reduced complexity and average power, making it more accessible and fostering exciting opportunities for exploration across disciplines.

<sup>1</sup>J. Moreno *et al.*, *Eur. Phys. J. D* **77**, 67 (2023).

<sup>2</sup>F. Schmid *et al.*, *APL Photonics* **9**, 026105 (2024).

<sup>3</sup>F. Canella *et al.*, *Optica* **11**, 1 (2024).

<sup>4</sup>J. Schulte *et al.*, *Opt. Lett.* **41**, 4511 (2016).

Abstract number: P89  
Wednesday 14:00-15:30

## Highly Stable Compact Optical Frequency Standard based on Modulation Transfer Spectroscopy on the $^{87}\text{Rb}$ D<sub>2</sub> Line

Sanglok Lee<sup>1,2</sup>, Jeongju Choi<sup>1</sup>, Seji Kang<sup>1</sup>, Sangwon Seo<sup>1</sup>, Hyun-Gue Hong<sup>1</sup>, Jae Hoon Lee<sup>1</sup>, Young-Ho Park<sup>1</sup>, Meung Ho Seo<sup>1</sup>, Sang Eon Park<sup>1</sup>, Taeg Young Kwon<sup>1</sup>, Sang-Bum Lee<sup>†1</sup>  
<sup>1</sup>Korea Research Institute of Standards and Science, Daejeon, 34113, Republic of Korea  
<sup>2</sup>Department of Physics, Chonnam National University, Gwangju, 61186, Republic of Korea

<sup>†</sup>lsbum@kriss.re.kr

Laser frequency stabilization utilizing the D<sub>2</sub> line transition of alkali atoms is essential for implementing high-performance cold atom experiments. In this study, we present a high-performance laser frequency stabilization method employing modulation transfer spectroscopy (MTS) on the rubidium-87 D<sub>2</sub> line transition. Short-term stability improvements are achieved by optimizing the probe and pump beam sizes and intensities, respectively. For the long-term stability, efforts are focused on eliminating stray light throughout the overall optical setup to suppress the residual amplitude modulation (RAM), which is highly sensitive to temperature-induced drift. In our prior publications, we have shown that these methods achieve frequency instability at the  $10^{-14}$  level, methods for analyzing and enhancing frequency stability are now well established.<sup>1,2</sup>

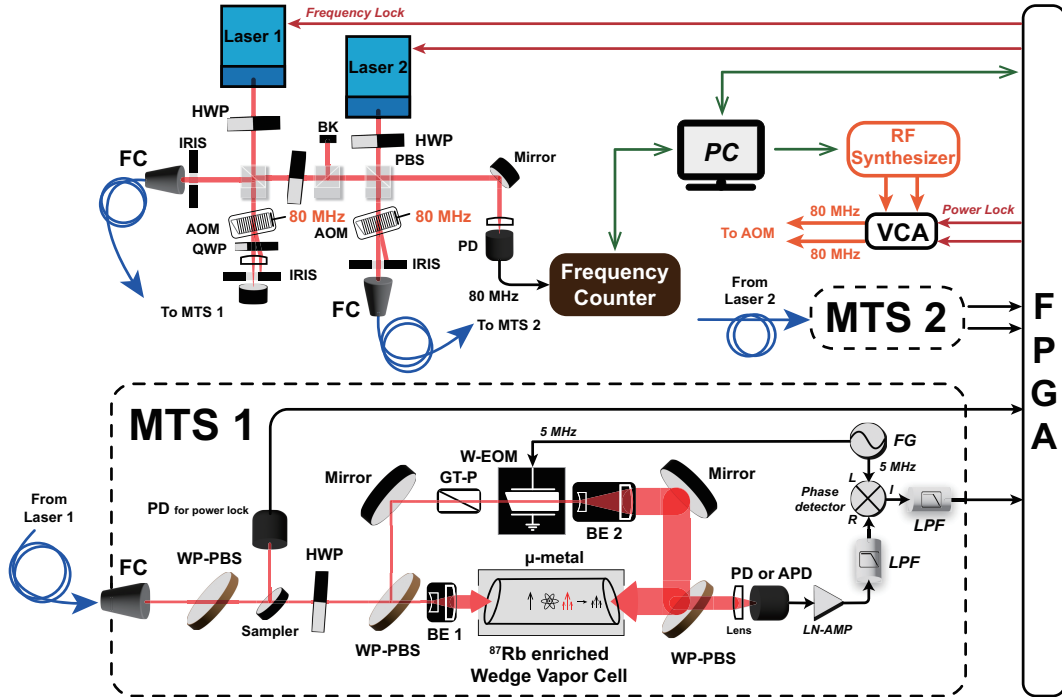


Figure 1: (a) The MTS setup, where wedge optics are primarily used to suppress etalon effects. The components are as follows: FPGA; field-programmable gate array, FC; fiber collimator, HWP; half-wave plate, PBS; polarizing beamsplitter, WP-PBS; wedged plate PBS, GT-P; Glan-Thompson polarizer, W-EOM; wedged crystal electro-optic modulator, AOM; acousto-optic modulator, PD; photodiode, APD; avalanche photodiode, LN-AMP; low-noise amplifier, LPF; low-pass filter, FG; function generator, BE 1&2; beam expander (custom-made). VCA; voltage-controlled attenuator.

As shown in Fig. 1, the frequency instability is measured by beat frequency between two external cavity diode lasers (ECDL). Furthermore, we evaluate the frequency shifts of the  $^{87}\text{Rb}$  D<sub>2</sub> line transition using two independent MTS setups. Firstly, to reduce light shift, an avalanche photodiode (APD) is employed to acquire signals with a sufficient signal-to-noise ratio, and enabling successful frequency locking at very low probe power levels (below 100  $\mu\text{W}$ ). Secondly, the magnitude of the frequency shift induced by the probe-pump beam intersection angle is determined. Finally, the frequency shift resulting from interchanging the vapor cells between the two MTS setups is measured. These experiments demonstrate the potential of this setup as a compact optical frequency standard.

<sup>1</sup>S. Lee et al, *Opt. Lasers Eng.* **146**, 106698 (2021).

<sup>2</sup>S. Lee et al, *Opt. Lett.* **48**, 1020-1023 (2023).

Abstract number: P90  
 Wednesday 14:00-15:30

## Exploiting high-sensitivity and resolution in cavity-enhanced photoacoustic sensors

**Pelini J.<sup>1</sup>, Dello Russo S.<sup>2</sup>, Wang Z.<sup>3</sup>, Galli I.<sup>1</sup>, Cancio Pastor P.<sup>1</sup>, Canino M.<sup>4</sup>, Roncaglia A.<sup>4</sup>, Ren W.<sup>3</sup>, De Natale P.<sup>1</sup>, Siciliani de Cumis M.<sup>2</sup>, Borri S.<sup>†1</sup>**

<sup>1</sup>CNR-INO - Istituto Nazionale di Ottica, and LENS, Via Carrara 1, 50019 Sesto Fiorentino FI, Italy

<sup>2</sup>ASI Agenzia Spaziale Italiana - Centro di Geodesia Spaziale, Località Terlecchia, 75100 Matera, Italy

<sup>3</sup>The Chinese University of Hong Kong, New Territories, Hong Kong SAR, China

<sup>4</sup>CNR-IMM - Istituto per la Microelettronica e Microsistemi, Via P. Gobetti 101, 40129 Bologna, Italy

<sup>†</sup>simone.borri@ino.cnr.it

Among trace-gas optical sensing techniques, photoacoustic sensors stand for their unique combination of sensitivity and flexibility. Thanks to the high number of degrees of freedom offered by this technique, ultra-high detection sensitivities at the part-per-trillion (ppt) levels or below<sup>1,2,3</sup> have been demonstrated by optimizing individually and simultaneously all the key components of the sensing system, such as exploiting mid-infrared semiconductor lasers as the excitation sources and enhancing the available interacting radiant power via high-finesse optical cavities.

In recent years, we started investigating advanced configurations of a cantilever-based sensor, combining the advantages of the photoacoustic technique with the sensitivity enhancement provided by acoustic and optical resonators. In our setup, a 4.5- $\mu\text{m}$  CW quantum cascade laser is used to address fundamental ro-vibrational transitions of  $\text{N}_2\text{O}$ , selected as target molecule to test the sensor performance. We designed and tested several silicon MEMS cantilevers as acoustic transducers, including standard rectangular cantilevers and structures with unconventional shapes. The different cantilever performances have been compared<sup>4</sup> and the most promising structures have been used to study the ultimate detection sensitivity of the sensor in different conditions of operation, also in combination with custom-made dual-tube acoustic resonators<sup>5</sup>.

Particularly interesting scenarios open up when these systems are combined with high-finesse optical cavities. Here, the photoacoustic signal enhancement due to high intracavity optical powers can be explored. Moreover, the generally higher photoacoustic signal guaranteed by this advanced configuration allows to explore unconventional regimes of operation, e.g., low sample pressures, which in standard photoacoustic sensors are out of range.

In the standard “high-pressure” regime, generally meant as pressures around the atmospheric value, optimal for in-field environmental monitoring and air-quality analysis, our setup achieves detection sensitivities down to tens of ppt<sup>6</sup>. Thanks to the cavity power build-up factor and the strong mid-IR molecular transitions, the sensor can be operated also at extremely low power levels (tens of  $\mu\text{W}$ ) still maintaining detection sensitivity at the ppb level. Finally, low sample pressure regimes can be explored, allowing to record sub-Doppler absorption profiles and opening exciting new perspectives for photoacoustic sensors towards an unprecedented combination of high sensitivity and high resolution molecular sensing for this class of devices.

<sup>1</sup>S. Borri, P. Patimisco, I. Galli, D. Mazzotti, G. Giusfredi, N. Akikusa, M. Yamanishi, G. Scamarcio, P. De Natale, and V. Spagnolo, *Appl. Phys. Lett.* **104**, 091114 (2014)

<sup>2</sup>T. Tomberg, T. Hieta, M. Vainio, and L. Halonen, *Analyst* **144**, 2291 (2019)

<sup>3</sup>Z. Wang, Q. Wang, H. Zhang, S. Borri, I. Galli, A. Sampaolo, P. Patimisco, V.L. Spagnolo, P. De Natale, and W. Ren, *Photoacoustics* **27**, 100387 (2022)

<sup>4</sup>J. Pelini, S. Dello Russo, I. Lopez Garcia, M. Canino, A. Roncaglia, P. Cancio Pastor, I. Galli, W. Ren, P. De Natale, S. Borri, and M. Siciliani de Cumis, *Photoacoustics* **38**, 100619 (2024)

<sup>5</sup>S. Dello Russo, J. Pelini, I. Lopez Garcia, M. Canino, A. Roncaglia, P. Cancio Pastor, I. Galli, P. De Natale, S. Borri, and M. Siciliani de Cumis, *Photoacoustics* **40**, 100644 (2024)

<sup>6</sup>J. Pelini, S. Dello Russo, Z. Wang, I. Galli, P. Cancio Pastor, I. Lopez Garcia, M. Concetta Canino, A. Roncaglia, N. Akikusa, W. Ren, P. De Natale, M. Siciliani de Cumis, and S. Borri, *Sens. Actuators B Chem.* **430**, 137313 (2025)

Abstract number: P91  
Wednesday 14:00-15:30

## Towards entanglement generation in a cavity coupled atomic array

Roschinski S.<sup>†1</sup>, Schabbauer J.<sup>1</sup>, von Silva-Tarouca F.<sup>1</sup>, Léonard J.<sup>1,2</sup>

<sup>1</sup>*TU Wien, Atominstitut, Vienna, Austria*

<sup>2</sup>*Institute of Science and Technology Austria, Klosterneuburg, Austria*

<sup>†</sup>stephan.roschinski@tuwien.ac.at

The efficient and deterministic generation of entanglement in a many-body system poses a challenge for analog and digital quantum simulators. While atomic platforms provide great scalability, they mostly rely on local couplings, for instance, collisional or Rydberg interactions. We report on the current status of a new experimental apparatus to strongly couple an atomic tweezer array to a fiber-based Fabry-Pérot cavity. The cavity geometry with short length, small mirror diameter, and large curvature, places us in a unique regime with simultaneously high single-atom cooperativity ( $C = 80$ ) and single-atom addressing and readout. Our setup is optimized for fast repetition rates, owing to loading the tweezer array from a magneto-optical trap which is placed within millimeters from the cavity. We then use an optical dipole trap to transport the atoms into the cavity and load atomic tweezers. In future, harnessing this new control will enable us to engineer entanglement through photon-mediated interactions. Further advantages of this platform include partial nondestructive readout and efficient multi-qubit entanglement operations. In the long term, the proposed platform provides a scalable path to studying many-body systems with programmable connectivity, as well as an efficient atom-photon interface for quantum communication applications.



Abstract number: P92  
Wednesday 14:00-15:30

## Ultrafast high-fidelity state readout of single neutral atom

Huang D.-Y.<sup>†1,2,3,4</sup>, Wang J.<sup>1,2,3</sup>, Li C.-F.<sup>1,2,3,4</sup>, Guo G.-C.<sup>1,2,3,4</sup>

<sup>1</sup>CAS Key Laboratory of Quantum Information, University of Science and Technology of China, Hefei 230026, China

<sup>2</sup>Anhui Province Key Laboratory of Quantum Network, University of Science and Technology of China, Hefei 230026, China

<sup>3</sup>CAS Center For Excellence in Quantum Information and Quantum Physics, University of Science and Technology of China, Hefei 230026, China

<sup>4</sup>Hefei National Laboratory, University of Science and Technology of China, Hefei 230088, China

<sup>†</sup>huangdy1217@mail.ustc.edu.cn

The capability to measure the state of a neutral atom is vital to an atom-based quantum network, for applications including distributed quantum computing and long-distance quantum communication. However, single neutral atoms suffer from low achievable photon scattering rate and shallow trapping potential, which limits the fidelity and speed of state readout process. In our work, by coupling a single neutral atom with a high-finesse fiber-based Fabry-Pérot microcavity (FFPC) in Purcell regime, we realize strong enhancement of the atomic photoemission rate and high overall system efficiency, which enables ultrafast and high-fidelity discrimination of bright and dark hyperfine states of the atom. The readout fidelity can reach 99.1(2)% within 200 ns and 99.985(8)% within 9  $\mu$ s. Furthermore, we demonstrate that state preparation via optical pumping can be efficiently accelerated by a real-time decision protocol based on ultrafast state readout. This work demonstrates the potential to serve as a high-performance atom-photon interface and paves the way to the implementation of a practical atom-based quantum network.

Abstract number: P93  
Wednesday 14:00-15:30

## Towards a quantum gas with multiple long-range interactions

Valtolina G.<sup>†1</sup>, Seifert, J.<sup>1</sup>, Duerbeck, M.<sup>1</sup>, Marulanda J.P.<sup>1</sup>, Choudari B.<sup>1</sup>, Reihls L.<sup>1</sup>, Robledo D.<sup>1</sup>, Wright S.<sup>1</sup>, Sartakov B.<sup>1</sup>, Meijer G.<sup>1</sup>

<sup>1</sup>*Fritz-Haber-Institut der Max-Planck-Gesellschaft, Berlin 14195, Germany.*

<sup>†</sup>valtolina@fhi-berlin.mpg.de

Quantum gases with long-range interactions enable the investigation of new many-body phases, such as supersolidity or self-organization. Long-range interactions are typically studied by using photon-mediated interactions between atoms inside optical cavities <sup>1</sup>, or exploiting dipolar interactions in atoms <sup>2</sup> and molecules <sup>3</sup>. We plan to combine these platforms by creating a quantum gas of dysprosium atoms strongly coupled to an optical cavity, which will enable the investigation of new regimes of long-range ordering. In addition, dysprosium possesses a doublet of metastable states that can be mixed by electric fields <sup>4</sup>. As a result, dysprosium atoms can acquire an additional electric dipolar interaction that can compete with the others. We present preliminary spectroscopic results regarding the behavior of the electric doublet states in large electric field and how we plan to use them in the ultracold regime.

---

<sup>1</sup>H. Ritsch *et al.*, *Rev. Mod. Phys.* **85**, 553 (2013).

<sup>2</sup>L. Chomaz *et al.*, *Rep. Prog. Phys.* **86**, 026401 (2022).

<sup>3</sup>T. Langen *et al.*, *Nat. Phys.* **20**, 05 (2024).

<sup>4</sup>M. Lepers *et al.*, *Phys. Rev. Lett.* **121**, 063201 (2018).

Abstract number: P94

Wednesday 14:00-15:30

## Zeeman-Sisyphus Deceleration of CaF Molecules

Humphreys B.<sup>†1</sup>, Hedley R. J.<sup>1</sup>, Baldock A.<sup>1</sup>, Matthies A. M.<sup>1</sup>, Williams H. J.<sup>1</sup><sup>1</sup>University of Durham, United Kingdom<sup>†</sup>mcwt12@durham.ac.uk

Since the first demonstration of direct laser cooling of molecules, an ever-expanding set of molecular species are being investigated. These include heavier and polyatomic species, with a range of applications from quantum simulation to explorations of cold chemistry. While making fast beams of complex and interesting molecules is becoming routine, slowing them to rest such that they can be trapped remains a significant challenge.

As a step in producing molecules in the ultracold regime, direct laser slowing has proved to be a hugely successful technique, decelerating fast molecular beams to below the capture velocity of a magneto-optical trap ( $\sim 20$  m/s). However, the  $10^4$  photons required to bring a molecular beam to rest makes it impractical for many species, including those with unfavourable branching ratios, long wavelength transitions or large masses.

Zeeman-Sisyphus deceleration presents a novel way to address these concerns. Within the decelerator, molecules propagate through a spatially varying magnetic field. Optical pumping is employed to ensure that the molecules continually climb up the generated potential hills and thus lose kinetic energy in the process. This process requires at least two orders of magnitude fewer photons to be scattered compared to direct laser slowing and as such, Zeeman-Sisyphus deceleration promises to be a highly versatile slowing technique, applicable to a large variety of molecular species.

This technique has previously been demonstrated for  $\text{CaOH}$ <sup>1</sup> and  $\text{YbOH}$ <sup>2</sup>, in a two-stage decelerator made up of cryogenic superconducting solenoids. Here, we present our progress in building upon this work to experimentally realise a Zeeman-Sisyphus decelerator for CaF molecules. Our implementation follows that outlined in the 2016 proposal of this technique<sup>3</sup>, using 80 stages of permanent magnets at ambient temperatures.

<sup>1</sup>B.L. Augenbraun, et al, Phys. Rev. Lett. 127, 263002 (2021)<sup>2</sup>H. Sawaoka, et al, Phys. Rev. A 107, 022810 (2023)<sup>3</sup>N.J. Fitch, and M. R. Tarbutt, ChemPhysChem 17, 22 (2016)

**Abstract number: P95**  
**Wednesday 14:00-15:30**

## Improving optical lattice clock stability with Dick-noise-free architectures

**Favier M.**<sup>†1</sup>, **Easton T.**<sup>1</sup>, **Siadat R.**<sup>1</sup>, **Allen B.**<sup>1</sup>, **Langford B.**<sup>1</sup>, **Scott C.**<sup>1</sup>, **Hill I. R.**<sup>1</sup>  
<sup>1</sup>*National Physical Laboratory, Teddington, United-Kingdom*

<sup>†</sup>maxime.favier@npl.co.uk

Optical atomic clocks are amongst the most advanced metrological tools ever built. The extraordinary stability and accuracy to which they can measure frequency plays a key role in the proposed redefinition of the SI second. In particular, optical lattice clocks (OLCs) offer unprecedented stability, a key figure of merit in the quest for probing new physics such as potential variations of the fine structure constant, or dark matter detection.

However, optical lattice clocks don't perform at their ultimate stability limits, and, in most cases, not even at the limit sets by the quantum projection noise. The main technical limit to the stability of OLCs is the Dick effect. This noise process stems from noise on the local oscillator being aliased due to the clock's pulsed mode of operation. At NPL, we are developing OLCs based on ytterbium with the aim of overcoming the Dick effect. In each of these new clocks, we aim for fractional frequency uncertainties at the  $10^{-18}$  level and instability below  $10^{-16} \tau^{-1}$ .

The first architecture which we are developing is a zero dead-time setup using interleaved pulsed clocks. We are focusing on robust engineering, targeting high-up-time operation in view of the redefinition of the SI second. This will also allow for its use as a frequency reference for a new quantum test and evaluation facility based at NPL. I will present the current status of this build, including results of measurements on ultracold atoms trapped in a two-stage magneto-optical trap.

In a second line of investigation, we are building a zero-dead-time clock using atoms loaded into a conveyor-belt lattice trap and transported to an interrogation region where the clock laser frequency is probed continuously. I will present our recent work on the development of a compact continuous cold atoms source geared toward transportable systems and discuss continuous probing schemes.

Abstract number: P96  
 Wednesday 14:00-15:30

## Mid infrared semiconductor lasers between classical and quantum operation regime

Gabbrielli T.<sup>1</sup>, Pelini J.<sup>1</sup>, La Penna I.<sup>1</sup>, Consolino L.<sup>1</sup>, Mazzotti D.<sup>1</sup>, Cappelli F.<sup>1</sup>, Borri S.<sup>1</sup>, De Natale P.<sup>†1</sup>

<sup>1</sup>CNR-INO - Istituto Nazionale di Ottica and LENS, Via N. Carrara, 1 - 50019 Sesto Fiorentino FI, Italy

<sup>†</sup>paolo.denatale@ino.cnr.it

The growing interest in secure communications as well as in increasingly high performance sensors is making the mid-infrared (MIR) spectral region particularly attractive, thanks to the possibility of implementing long-range free-space communication and molecular sensing with the highest sensitivity levels. For those applications, the development of non-classical light sources in this spectral region is a crucial requirement, enabling the development of quantum sensing and, more generally, MIR quantum technologies.

In this framework, in the last few years we have started investigating the possibility of non-classical light emission from MIR semiconductor lasers, in particular Quantum Cascade Lasers (QCLs) and Interband Cascade Lasers (ICLs). First, we have designed and validated a balanced detection system with 100-MHz bandwidth able to detect MIR light intensity noise down to the quantum level with a clearance up to 9 dB<sup>1</sup>. With this setup, we could exploit, for the first time, the presence of correlations between the modes in an harmonic comb emission from a QCL, generated via Four-Wave Mixing<sup>2</sup>. The measured levels of intensity noise have been lately well reproduced by a semi-classical dynamical model simulating harmonic combs in THz QCLs<sup>3</sup>.

More recently, in our group we could test and unveil the shot-noise-limited operation of both QCLs and ICLs operating CW and at room temperature in the 3-5  $\mu\text{m}$  spectral window<sup>4,5</sup>. These results show the availability of MIR shot-noise-limited radiation from ICLs and, under certain conditions, from QCLs, too. Such progress can significantly improve the overall measurement sensitivity, whenever the intensity noise of the source represents the limiting factor, such as in a number of molecular spectroscopy applications, where the noise coming from the excitation source often plays a role in the final detection sensitivity and precision. In this sense, relying on shot-noise-limited radiation could determine a potential breakthrough, paving the way for unprecedented sensitivity levels.

More generally, our experimental results can provide useful insights for the development of new-generation MIR emitters capable of achieving low-noise performance, so far undisclosed. To achieve this goal, a deeper understanding of the internal processes leading to the generation of spurious technical noise in such sources is fundamental for the modelling and development of novel devices. To this purpose, we are recently testing the electron-to-photon noise transfer function in cascade lasers, in view of a better control of their emissions, hopefully beyond the classical limit.

<sup>1</sup>T. Gabbrielli, F. Cappelli, N. Bruno, N. Corrias, S. Borri, P. De Natale, and A. Zavatta, *Opt. Express* **29**, 14536 (2021)

<sup>2</sup>T. Gabbrielli, N. Bruno, N. Corrias, S. Borri, L. Consolino, M. Bertrand, M. Shahmohammadi, M. Franckie, M. Beck, J. Faist, A. Zavatta, F. Cappelli, and P. De Natale, *Adv. Photon. Res.* **3**, 2200162 (2022)

<sup>3</sup>J. Popp, J. Stowasser, M. A. Schreiber, L. Seitner, F. Hitzelhammer, M. Haider, G. Slavcheva, and C. Jirauschek, *APL Quantum* **1**, 016109 (2024)

<sup>4</sup>G. Marschick, J. Pelini, T. Gabbrielli, F. Cappelli, R. Weih, H. Knötig, J. Koeth, S. Höfling, P. De Natale, G. Strasser, S. Borri, and B. Hinkov, *ACS Photon.* **11**, 395–403 (2024)

<sup>5</sup>T. Gabbrielli, J. Pelini, G. Marschick, L. Consolino, I. La Penna, J. Faist, M. Bertrand, F. Kapsalidis, R. Weih, R., S. Höfling, N. Akikusa, B. Hinkov, P. De Natale, F. Cappelli, and S. Borri, *Opt. Express* (2025, in press)

Abstract number: P97  
Wednesday 14:00-15:30

## Exploiting the light-shift for laser stabilization in atomic clocks

**Gozzelino M.<sup>†1</sup>, Micalizio S.<sup>1</sup>, Levi F.<sup>1</sup>, Calosso C.E.<sup>1</sup>**

<sup>1</sup>*Istituto Nazionale di Ricerca Metrologica, INRIM, Turin, Italy*

<sup>†</sup>m.gozzelino@inrim.it

We introduce the LSL technique, a novel method to stabilize the laser frequency in optically pumped atomic clocks. The method is based on the light shift induced on the clock transition<sup>1</sup> as a frequency discriminator. The same atomic sample used in the clock operation is then exploited, eliminating the need for an external reference. The light-shift is thus turned from a source of perturbation on the clock frequency to a tool for laser stabilization.

We tested the technique using a laser-pumped Rb vapor-cell clock, working in a pulsed regime (the pulsed-optically-pumped Rb clock<sup>2</sup>). LSL alternates two clock sequences having a differential sensitivity to the laser frequency. Real-time digital processing of the two clock signals is performed with an FPGA, recovering information on both the laser frequency and the clock frequency. In Figure 1, we show the typical error signal that is obtained with the LSL technique on the clock vapor cell (containing Rb and a buffer gas) on the D<sub>2</sub> line.

We found that the LSL operates robustly, having a capture range of gigahertz, without significantly compromising clock stability. Indeed, at one-day averaging time, we obtained a laser frequency stability of 3 kHz, comparable to what we typically obtained with a much narrower discriminator provided by a saturated-absorption spectroscopy setup. In our tests, the clock exhibited a white frequency noise of  $3.2 \times 10^{-13} \tau^{-1/2}$  for averaging time up to 4000 s, reaching a floor below  $1 \times 10^{-14}$  up to 100 000 s (drift removed)<sup>3</sup>. These performance levels meet the requirements of next-generation Global Navigation Satellite Systems on-board clocks, and offer the added benefit of a reduced number of laser-system components, as well as increased reliability and robustness. The method is rather general and can be applied to different clocks and atomic species.

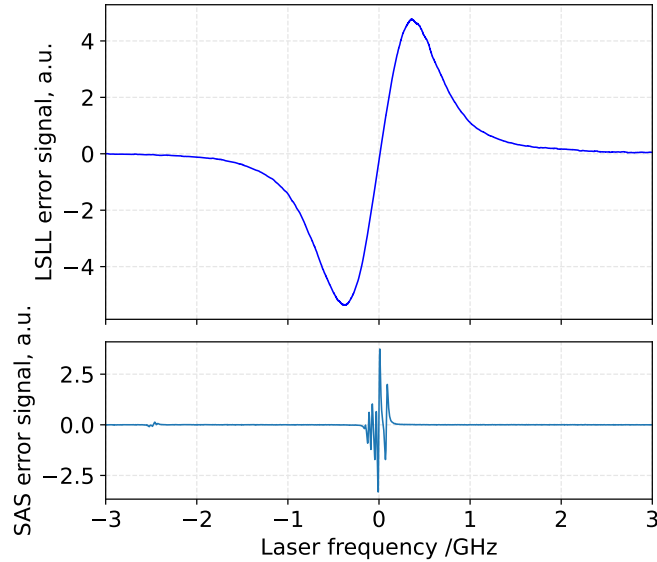


Figure 1: Top: typical error signal obtained with the Ligh-Shift Laser Lock (LSLL) on a cell filled with Rb and 25 Torr of an Ar-N<sub>2</sub> mixture as buffer gas. Bottom: as a comparison, a typical error signal obtained with saturated-absorption setup (SAS) on a reference cell without buffer gas.

<sup>1</sup>B.S. Mathur, H. Tang, and W. Happer., *Physical Review* **vol. 171**, p. 11 (1968)

<sup>2</sup>M. Gozzelino *et al.*, *Scientific Reports*, **vol. 13**, p. 12974 (2023)

<sup>3</sup>C.E. Calosso *et al.*, *Physical Review Applied*, **vol. 22**, pp.034033 (2024)

Abstract number: P98  
Wednesday 14:00-15:30

# High-precision optical frequency measurements: supporting UK industry and academia at NPL

Sun X.<sup>†</sup>, Schioppo M., Parke A. L., Tunesi J.  
National Physical Laboratory (NPL), Teddington, United Kingdom  
<sup>†</sup>xiangnan.sun@npl.co.uk

High-precision optical frequency measurements have emerged as a critical capability across various fields, including fundamental physics research, telecommunications, navigation, and precision metrology. Within the National Physical Laboratory (NPL), a new capability has been developed at the Advanced Quantum Metrology Laboratory (AQML) specializing in optical frequency measurements, particularly targeting areas such as absolute frequency evaluations of optical atomic clocks, and in the verification of optical frequency comb performance. Our work directly supports UK industry and academia by providing access to state-of-the-art optical frequency metrology facilities and expertise, enabling innovation in high-tech sectors and fostering collaborations across both commercial and academic communities.

Figure 1 illustrates simplified schematics of the setup for (a) absolute optical frequency measurement, and (b) evaluation of the instability performance of the “device-under-test” frequency comb (DUT-Comb)<sup>1</sup>. Absolute optical frequency measurements involve the precise determination of three key frequencies, all derived from the same optical frequency comb: the repetition rate ( $f_{\text{rep}} \sim 250$  MHz), the carrier-envelope-offset frequency ( $f_{\text{ceo}}$ ), and the beat frequency ( $f_{\text{beat}}$ ) between the comb and the laser to be measured. To minimize errors and enhance the frequency counter’s resolution, the 32nd harmonic of the repetition rate from the comb is mixed with an 8 GHz signal generated by a frequency synthesizer. All synthesizers and counters are referenced to a 10 MHz time-base signal which is traceable to the UK time scale and the Cs primary frequency standard, thereby ensuring system accuracy. The comb’s instability and inaccuracy contribution to this absolute optical frequency evaluation can then be obtained via simultaneous measurements of the same optical frequency<sup>2</sup> using a second reference comb. By computing the difference between the optical frequencies measured by each comb, any common laser or 10 MHz instability is common-mode-cancelled, leaving only the combined comb contribution.

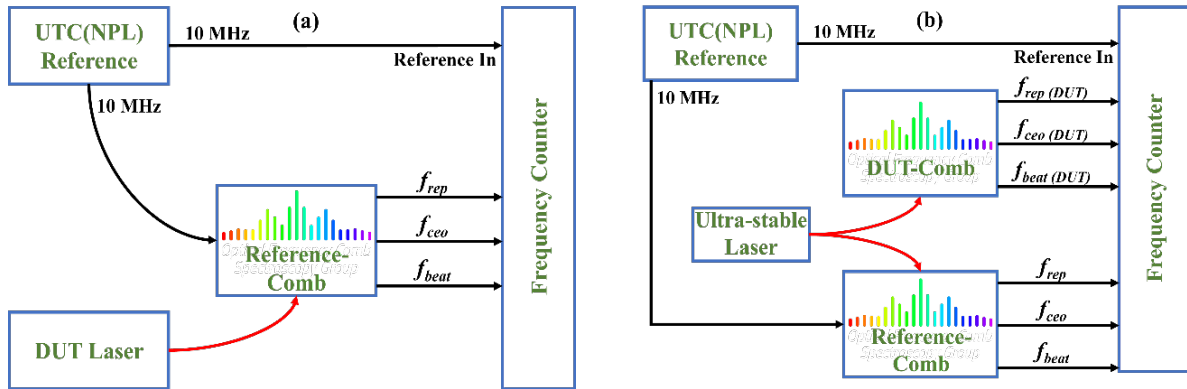


Figure 1: (a) Absolute optical frequency measurement setup. (b) Instability performance comb to comb comparison setup.

We will present our measurement capability and a brief history of our collaborations to demonstrate how the AQML setup can be used to deliver accurate and reliable optical frequency measurements using the systems described above, supporting the UK’s academic and industrial communities.

<sup>1</sup>L.A.M. Johnson *et al.*, *Metrologia* **52**, 62 (2015).

<sup>2</sup>M. Schioppo *et al.*, *Nat. Commun.* **13**, 212 (2022).

Abstract number: P99  
 Wednesday 14:00-15:30

## Bandstructure of a coupled BEC-cavity system: effects of dissipation and geometry

**Baur D.<sup>1</sup>, Hertlein S.<sup>1</sup>, Baumgärtner A.<sup>1</sup>, Stefaniak J.<sup>1</sup>, Esslinger T.<sup>1</sup>, Natale G.<sup>†1</sup>, Donner T.<sup>1</sup>**

<sup>1</sup>*Institute for Quantum Electronics, Eidgenössische Technische Hochschule Zürich, Otto-Stern-Weg 1, CH-8093 Zurich, Switzerland*

<sup>†</sup>gnatale@phys.ethz.ch

Collective excitations provide deep insights into many-body systems, offering a powerful tool to study phase transitions. In our experiment, we load a BEC of  $^{87}\text{Rb}$  into a high-finesse optical cavity, where cavity-mediated interactions, give rise to two distinct roton-like excitation modes. When fully softened, these modes correspond to the two superradiant phases previously observed and studied in Ref.<sup>1</sup>. Due to intrinsic dissipation, the two excited modes couple when their energies approach each other, leading to an exceptional point, mode coalescence and the appearance of a PT-symmetry broken phase<sup>2</sup>.

Using Bragg-spectroscopy, we simultaneously measure these two low-lying excitations, revealing the individual softening of the two modes as the system approaches their respective phase transition, accompanied by diverging susceptibility. By leveraging the full tuneability of our system, we can explore a parameter regime, where the two modes coalesce, observing an exceptional point and the associated dynamical instability. To confirm the experimental findings, we develop a mean-field model based on band theory. This model allows for a detailed analysis of the nature of the two modes and the resulting coalescing mode. The general formulation of this theoretical framework further allows us to uncover the role of the angle between the cavity mode and transverse pump. In particular, it allows us to explain the microscopic mechanisms, responsible for the intricate physics observed when this angle deviates from  $90^\circ$ .

<sup>1</sup>L. Xiangliang et al., *Phys. Rev. Res.* **3**, L012024 (2021)

<sup>2</sup>D. Dreon et al., *Nature* **608**, 494–498 (2022)



Abstract number: P100  
Wednesday 14:00-15:30

## Laser frequency reference with a micro-fabricated Rubidium vapor cell for Doppler-free saturated absorption spectroscopy

Kang S.<sup>†1</sup>, Kwon T. Y.<sup>1</sup>, Park S. E.<sup>1</sup>, Lee S.-B.<sup>1</sup>, Lee J. H.<sup>1</sup>, Seo S.<sup>1</sup>, Park Y.-H.<sup>1</sup>, Seo M. H.<sup>1</sup>, Baek J.<sup>1,2</sup>,  
Hong H.-G.<sup>1</sup>

<sup>1</sup>*Korea Research Institute of Standards and Science, Daejeon, 34113, Republic of Korea*

<sup>2</sup>*Chonnam National University, Gwangju, 61186, Republic of Korea*

<sup>†</sup>seji.kang@kriss.re.kr

Miniaturization of atomic devices, such as atomic clocks and magnetometers, requires compact and reliable frequency-stabilized laser systems. We demonstrate a compact laser system that employs a micro-fabricated Rubidium (Rb) vapor cell designed for frequency-locking based on Doppler-free saturated absorption spectroscopy. Two lithographically patterned chambers in the Rb vapor cell serve to measure the Doppler-broadened background and the saturated absorption spectrum, respectively. The spectroscopy chambers interface with an Rb source, and vacuum conditions are preserved by non-evaporable getters. This configuration enables the observation of saturated absorption lines on a flat background by utilizing the beam traversing through the chambers. We evaluate the stability of the frequency reference, observing its dependence on critical system parameters, such as cell temperature.

Abstract number: P101

Wednesday 14:00-15:30

## Exploring spin-motion models with a quantum gas of polar molecules

**Miller C.<sup>†1</sup>, Lin J.<sup>1</sup>, Carroll A.<sup>1</sup>, Martin P.<sup>1</sup>, de Jongh T.<sup>1</sup>, Ye J.<sup>1</sup>**

<sup>1</sup>*JILA, NIST & the Department of Physics, University of Colorado Boulder, Boulder, CO, USA*

<sup>†</sup>calder.miller@colorado.edu

Optically trapped ultracold polar molecules offer a rapidly maturing platform for quantum science. Due to their strong, long-range, and tunable dipolar interactions, these systems are particularly suitable for realizing spin-motion models with rich many-body physics<sup>1</sup>. Using a spin encoded in rotational states of fermionic <sup>40</sup>K<sup>87</sup>Rb molecules, we demonstrated tuning of Heisenberg XXZ models with electric fields<sup>2</sup> and Floquet engineering of XYZ models with microwave pulse sequences<sup>3</sup>. By additionally regulating motion with optical lattices, we realized highly tunable generalized t-J models<sup>4</sup>. We used Ramsey spectroscopy to explore the out-of-equilibrium dynamics of these systems, observing one-axis and two-axis twisting at short times, and dephasing due to dipolar interactions and their coupling to motion at longer times. We also present progress towards generating metrologically-relevant spin-squeezed states.

In addition to controlling interactions, observing new dynamics and phases predicted for these models requires preparing low-entropy initial states. Building on our previous work on selection of molecules in individual layers of an optical lattice<sup>5</sup> and electric field-assisted evaporative cooling<sup>6</sup>, we report recent progress towards producing a deeply degenerate Fermi gas in an isolated 2D layer, enabling control of the anisotropy of the dipolar interactions. Using a tunable-spacing optical lattice, we compress a K-Rb mixture into a quasi-2D geometry. In this trap, we are able to produce 20,000 ground state molecules at temperatures below the Fermi temperature. Through additional evaporative cooling of the atoms and molecules, we aim to cool the system into deep degeneracy.

<sup>1</sup>S. Cornish, M. Tarbutt and K. Hazzard, *Nature Physics* **20**, 730-740 (2024).

<sup>2</sup>J. Li *et al.*, *Nature* **614**, 70-74 (2023).

<sup>3</sup>C. Miller *et al.*, *Nature* **633**, 332-337 (2024).

<sup>4</sup>A. Carroll *et al.*, *Science* (2025; in press).

<sup>5</sup>W. Tobias *et al.*, *Science* **375**, 1299-1303 (2022).

<sup>6</sup>G. Valtolina, K. Matsuda, W. Tobias, J. Li, L. De Marco and J. Ye, *Nature* **588**, 239-243 (2020).

Abstract number: P102  
Wednesday 14:00-15:30

## Sub-nanosecond 780 nm pulse generation from a continuous wave laser for ultrafast hyperfine-resolved Rydberg excitation

Kocik R. R.<sup>†1,2</sup>, Chew Y. T.<sup>3</sup>, Lienhard V.<sup>4</sup>, Mahesh T. P.<sup>1</sup>, Matsubara T.<sup>1</sup>, Tomita T.<sup>1,2</sup>, Ohmori K.<sup>1,2</sup>, de Léséleuc S.<sup>1,5</sup>

<sup>1</sup>Institute for molecular Science, National Institute of Natural Sciences, Okazaki, Aichi, Japan

<sup>2</sup>SOKENDAI (The Graduate University for Advanced Studies), Hayama, Kanagawa, Japan

<sup>3</sup>Laboratoire Charles Fabry, Institut d'Optique Graduate School, Université Paris-Saclay, Palaiseau, Essonne, France.

<sup>4</sup>Nanomaterials and Nanotechnology Research Center: L'Entregu/El Entregu, Asturias, Spain

<sup>5</sup>Cold-Atom Quantum System Research Team, RIKEN Center for Quantum Computing, Wako, Saitama, Japan

<sup>†</sup>robin@ims.ac.jp

Rydberg atoms are remarkable candidates for realizing quantum operations with ultracold neutral atoms, due to their huge electronic orbitals offering dipolar interaction over micrometer-order distance. While the standard approach to produce such states uses continuous-wave (C-W) laser performing excitation on the sub-microsecond timescale, our group aims at producing Rydberg state in sub-nanosecond timescale, which enables us to exploit strong interaction reaching the GHz range at micrometer range distance ( $C_3 \sim \text{GHz} \cdot \mu\text{m}^3$ ).

In previous work, we have demonstrated the excitation of a single Rydberg level with  $\sim 10$  ps pulse duration, limited by  $\sim 100$  GHz energy separation, using pulsed laser technology<sup>1</sup>. To use a two-level system within the hyperfine structure of  $^{87}\text{Rb}$  (6.8 GHz) as a qubit, excitation timescales of the intermediary state (for the 2 photon Rydberg excitation) must be  $> 100$  ps, allowing for resolution of the hyperfine states.

In this study, we developed a system to generate a 780 nm pulse to excite  $^{87}\text{Rb}$  atoms to the  $5P_{3/2}$  state, with peak power reaching 100 watts with adjustable pulse duration ranging from 100 ps to 1 ns. This system resolves the hyperfine structure while remaining much faster than the intermediate state lifetime ( $\sim 25$  ns).

Our apparatus takes full advantage of pulse shaping at a telecom wavelength, enabling the use of well-established light amplification techniques. The amplified signal is then efficiently converted to the visible spectrum using second harmonic generation (SHG) with a periodically poled lithium niobate (PPLN) crystal. This technique had already proven to be efficient for fast pulse production with decent peak power<sup>2</sup>. We further refined the technique by including an high-speed electronic pulse generator (EPG), driving pulses as short as 100 ps; a method that had already been demonstrated while working directly at 780 nm<sup>3</sup>. We demonstrate an improvement of the pulse duration and peak power by a factor 10 from previous work using SHG, and achieve three orders of magnitude higher peak power for similar duration when working directly at 780 nm.

This system combined with a 480 nm picosecond pulsed laser enables hyperfine state-resolved Rydberg excitation. Furthermore, it opens new avenues for studying collective light-matter interaction, such as superradiance as it allow population inversion on a time-scale two orders of magnitude shorter than the lifetime of the excited state.

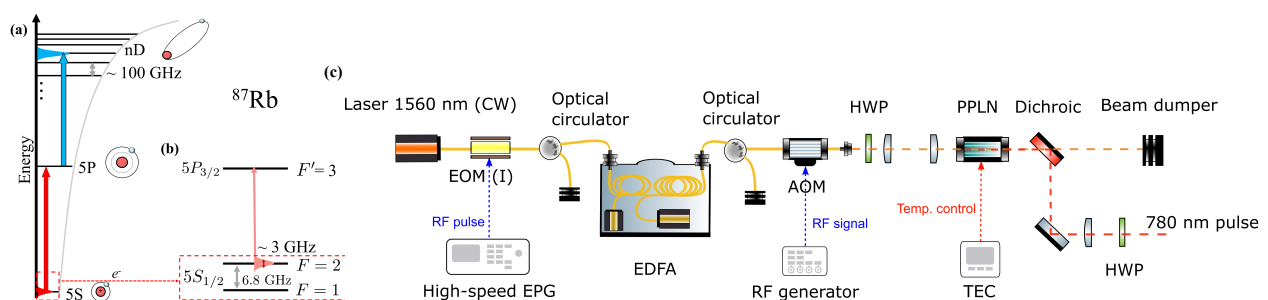


Figure 1: (a) Electronic structure of a Rubidium atom, showing the valence electron in the 5S ground-state, the first excited 5P level and the giant Rydberg  $nD$  orbits. The schematics are not to scale, as the Rydberg states are 1000 times larger than the 5S orbit. (b) Hyperfine structure of the ground-state of  $^{87}\text{Rb}$ . (c) Schematic of the pulsed laser. A 1560 nm C-W laser is shaped into pulses using a fiber Electro-Optical Modulator (EOM), driven by an Electrical Pulse Generator (EPG). Pulses are amplified with an Erbium-Doped Fiber Amplifier (EDFA). A fiber Acousto-Optical Modulator (AOM) is used to control pulse repetition. The conversion to 780 nm is achieved in free space using a PPLN. The remaining 1560 nm light is separated from the converted 780 nm light with a dichroic mirror.

<sup>1</sup>Y. Chew, T. Tomita, T.P. Mahesh, S. Sugawa, S. de Léséleuc, and K. Ohmori, *Nat. Photonics*, **16**, 724 (2022).

<sup>2</sup>J. Dingjan, *et al.*, *Appl. Phys B*, **82**, 47-51 (2006).

<sup>3</sup>C.E. Rogers and P.L. Gould, *Opt. Express*, **24**, 2596-2606 (2016).

Abstract number: P103  
Wednesday 14:00-15:30

## Realizing a spatially correlated lattice interferometer

Liang Y.<sup>1</sup>, Shui H.<sup>1</sup>, Song B.<sup>\*2</sup>, Zhou X.<sup>†1</sup>

<sup>1</sup>School of Electronics, Peking University, China

<sup>2</sup>School of Physics, Peking University, China

\*bsong@pku.edu.cn

†xjzhou@pku.edu.cn

Atom interferometers provide a powerful tool for measuring physical constants and testifying fundamental physics with unprecedented precision<sup>1,2</sup>. However, atom interferometry typically focuses on the phase difference between two paths and utilizes matter waves with fixed coherence. Here, we report on realizing a Ramsey-Bordé interferometer of coherent matter waves dressed by a moving optical lattice in a gravitational field, and explore the resulting interference along multiple paths with tunable coherence<sup>3</sup>. We investigated spatial correlations of atoms both within the lattice and between two arms by interferometry, and observed the emerging multiple interference peaks of the Bose-Einstein condensate with sublattice site resolution (see Fig.1). We further study the time evolution of a novel open atom interferometer where arms are mismatched in space. Our findings agree well with simulations, paving the way for high-precision interferometry with ultracold atoms.

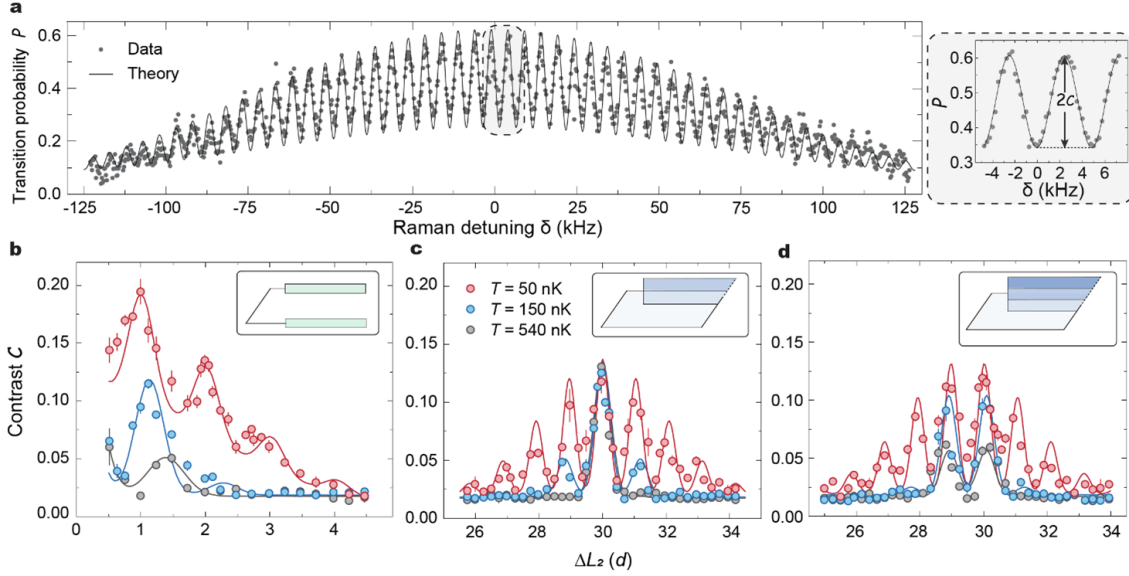


Figure 1: **Interference fringes and contrast.** (a) Representative Ramsey-Bordé fringes with atoms dressed by a moving optical lattice. The transition probability  $P$  oscillates with the Raman detuning  $\delta$ , from which the contrast  $C$  is extracted. (b-d) Contrast of interference fringes as a function of  $\Delta L_2$  for a fixed  $\Delta L_1 = 30d$  ( $T_{R1} = 993\mu s$ ). Data points are the average over three repetitions, and solid lines are simulations. Noticeable peak shifts away from integer lattice spacings are governed by the coherence length and the momentum distribution of atoms. Coherence lengths used in the simulation are  $1.0d$ ,  $1.7d$  and  $3.8d$  for  $T = 50$  nK,  $150$  nK and  $540$  nK respectively.

<sup>1</sup>V. Xu, M. Jaffe, C. D. Panda, S. L. Kristensen, L. W. Clark, and H. Müller, *Science* **366**, 745 (2019).

<sup>2</sup>C. D. Panda, M. J. Tao, M. Ceja, J. Khoury, G. M. Tino, and H. Müller, *Nature* **631**, 515–520 (2024).

<sup>3</sup>Peng Peng et al., arXiv:2406.16847 (2024).

Abstract number: P104  
Wednesday 14:00-15:30

## Parallel rearrangement of single atoms with an SLM for quantum simulation<sup>1</sup>

Spreeuw R. J. C.<sup>†,1,2</sup>, Knottnerus I. H. A.<sup>1,2,3</sup>, Tseng Y.C. (曾于誌)<sup>1,2</sup>, Urech A.<sup>1,2</sup>, Schreck F.<sup>1,2</sup>

<sup>1</sup>Van der Waals-Zeeman Institute, Institute of Physics, University of Amsterdam, Science Park 904, 1098XH Amsterdam, The Netherlands

<sup>2</sup>QuSoft, Science Park 123, 1098XG Amsterdam, The Netherlands

<sup>3</sup>Eindhoven University of Technology, P.O. Box 513, 5600MB Eindhoven, The Netherlands

<sup>†</sup>r.j.c.spreeuw@uva.nl

Large arrays of neutral atoms are emerging as a quintessential tool for quantum simulation and computation. Arrays of up to thousands of single atoms have been demonstrated. To harness the full potential of many interacting single atoms, rearrangement of atoms is needed to create defect-free geometries, and to shuttle atoms in between storage, interaction and imaging zones. Most often, static patterns are made using a spatial light modulator (SLM), with rearrangement of atoms done by acousto-optic deflectors (AODs). This method is limited in the types of moves for parallel sorting of multiple atoms, and becomes prohibitively slow for large arrays.

We present fast parallel rearrangement of atoms in optical tweezers into arbitrary geometries by updating holograms displayed by an ultra-fast SLM<sup>2,3</sup>. In previous work, a modified weighted Gerchberg-Saxton (WGS) algorithm was implemented to update holograms on a high-speed SLM<sup>4</sup>. However, lack of computational strength resulted in slow rearrangement cycles. We demonstrate a linear phase interpolation (LPI) method, controlling not only the position, but also the optical phase of tweezers in successive holograms. Control of the optical phase reduces intensity flicker of tweezers during moves and thus enhances the probability that an atom survives these moves, see Fig. 1. Our method greatly reduces computational complexity and allows us to reach computation and display cycles of 2.76(2)ms on commercial hardware. To show the versatility of our method, we sort the same atomic sample into multiple geometries with success probabilities exceeding 99% per imaging and rearrangement cycle, see Fig. 2. We present results on using our rearrangement method for quantum simulation experiments.

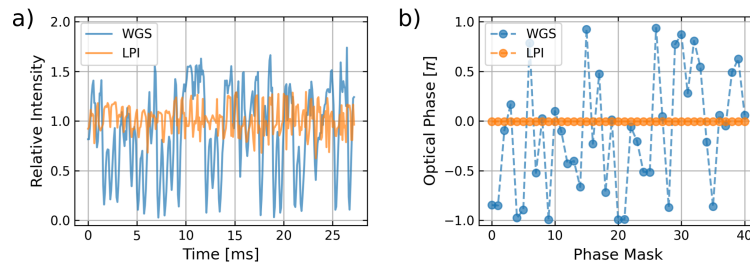


Figure 1: (a) Measured relative intensity of a moving spot made by holograms generated with the WGS algorithm (blue trace) and made with LPI for the special case of identical initial and final tweezer phase (orange trace). While the WGS-generated spot has multiple dips to near zero intensity, the LPI-generated spot stays above 70 % throughout the moves. (b) The calculated optical phase at the location of the moving spots for each hologram displayed during the movement.

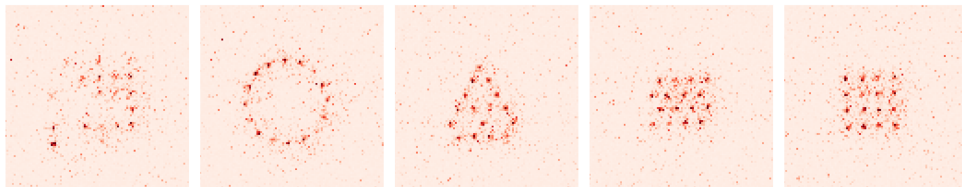


Figure 2: Experimental realization of the same atoms being sequentially rearranged to various geometries. From left to right: image of the initially loaded  $6 \times 6$  array, a circular geometry, a kagome lattice, a triangular lattice and a  $4 \times 4$  array.

<sup>1</sup>This work is part of the Neutral Atom Kat-1 Collaboration of Quantum Delta NL.

<sup>2</sup>Knottnerus *et al.*, arXiv:2501.01391 (2025).

<sup>3</sup>Lin *et al.*, arXiv:2412.14647.

<sup>4</sup>Kim *et al.*, Nat. Comm. **7**, 13317 (2016); Kim *et al.*, Opt. Express **27**(3), 2184 (2019)

Abstract number: P105  
 Wednesday 14:00-15:30

## A compact quantum inertial sensor using atom interferometry

**Preston A.<sup>1</sup>, Freegarde T.<sup>1</sup>, Harvey D.<sup>2</sup>, Dragomir A.<sup>3</sup>, Himsworth M. H.<sup>3</sup>**

<sup>1</sup>*School of Physics & Astronomy, University of Southampton, Highfield, Southampton SO17 1BJ, U.K.*

<sup>2</sup>*Thales Research, Technology & Solution Innovation, Reading, U.K.*

<sup>3</sup>*Aquark Technologies Ltd., Hathaway Close, Eastleigh SO50 4SR, U.K.*

<sup>†</sup>ap3g20@soton.ac.uk

Inertial sensors based upon atom interferometry promise advantages over their classical counterparts in sensitivity and bias and scale factor stability, but have so far required large vacuum systems and long interferometer paths, rendering them bulky and unsuitable for rapid manoeuvring situations.

We are exploring the miniaturization of rotation sensors based upon point-source interferometry<sup>1</sup>, using <sup>85</sup>Rb atoms from a magneto-optical trap that are manipulated using counter-propagating laser beam pairs to drive Raman transitions between ground hyperfine states. Advanced chamber designs, including the use of additive manufacture, allow substantial reductions in size, and will in due course be replaced by truly miniature self-contained systems, produced using planar fabrication techniques, that combine the atom source, vacuum maintenance and optical routing<sup>23</sup>. Novel geometries offer simpler optical access<sup>4</sup>; and optimal control design of interferometer pulses<sup>56</sup> enables fidelity improvements that improve interferometer contrast and bias and scale factor stability and allow sensitivity amplification through large momentum transfer (LMT)<sup>7</sup>.

<sup>1</sup>S. M. Dickerson, J. M. Hogan, A. Sugarbaker, D. M. S. Johnson and M. A. Kasevich, *Physical Review Letters* **111**, 083001 (2013).

<sup>2</sup>J. A. Rushton, M. Aldous and M. D. Himsworth, *Review of Scientific Instruments* **85** (12), 121501 (2014).

<sup>3</sup>J. P. McGilligan, K. Gallacher, P. F. Griffin, D. J. Paul, A. S. Arnold and E. Riis, *Review of Scientific Instruments* **93** (9), 091101 (2022).

<sup>4</sup>R. Roy, J. Rushton, A. Dragomir, M. Aldous and M. Himsworth, *Scientific Reports* **8**, 10095 (2018).

<sup>5</sup>J. Saywell, M. Carey, M. Belal, I. Kuprov and T. Freegarde, *Journal of Physics B: Atomic, Molecular and Optical Physics* **53** (8), 085006 (2020).

<sup>6</sup>N. Dedes, J. Saywell, M. Carey, I. Kuprov and T. Freegarde, *Physical Review A* **108**, 053319 (2023).

<sup>7</sup>J. M. McGuirk, M. J. Snadden and M. A. Kasevich, *Physical Review Letters* **85**, 4498 (2000).

**Abstract number: P106**  
**Wednesday 14:00-15:30**

## Ultrafast imaging of ytterbium tweezer arrays

Muzi Falconi A.<sup>1</sup>, Abdel Karim O.<sup>3,4</sup>, Panza R.<sup>1,3</sup>, Liu W.<sup>3</sup>, Forti R.<sup>1</sup>, Sbernardori S.<sup>1,3</sup>, Marinelli M.<sup>\*1,2</sup>,  
 Scazza F.<sup>†1,3</sup>

<sup>1</sup>*Department of Physics, University of Trieste, Via Valerio 2, 34127 Trieste, Italy*

<sup>2</sup>*CNR-IOM, Area Science park, 34139 Trieste, Italy*

<sup>3</sup>*CNR-INO, Largo Enrico Fermi 6, 50125 Firenze, Italy*

<sup>4</sup>*Department of Physics, University of Napoli, Via Cinthia 21, 80126 Napoli, Italy*

\*matteo.marinelli@units.it

†Francesco.scazza@units.it

Detecting and manipulating individual atoms with high fidelity is essential for quantum simulation, metrology and, with even more stringent requirements, for quantum computing. I will present our recent results on ultrafast single-atom imaging, based on alternated pulses of highly saturated light addressing the broad 1S0-1P1 transition in ytterbium. With this scheme, we achieve in-trap single-atom detection fidelity and survival probability exceeding 99.8% within just few microseconds.

Beyond single-atom detection, we extend this ultrafast imaging scheme to the detection of multiple atoms in free space with single-particle resolution. By preparing and releasing multiply filled traps, we demonstrate single-atom-resolved detection without parity projection. This capability will enable new explorations of correlations and many-body dynamics in tweezer-trapped atomic ensembles.

Finally, will also mention the newest tweezer-based quantum platform under construction at the University of Trieste. This system integrates three key components: a quantum computing unit for executing arbitrary operations, a tweezer-cavity interface for cavity quantum electrodynamics and quantum networking experiments, and an atom reservoir to enable fast experimental cycle times and uninterrupted operations. This architecture will serve as a versatile testbed for advancing neutral atom quantum technologies.

Abstract number: P107  
Wednesday 14:00-15:30

## Robust, rapid laser autolocking with compact radio frequency generators for laser pulse sequencing in field-deployable atom interferometers

Jiang M.<sup>1</sup>, Lu S.-B.<sup>1</sup>, Yao Z.-W.<sup>1,2</sup>, Li R.-B.<sup>\*1,2,3</sup>, Wang J.<sup>1,2,3</sup>, Zhan M.-S.<sup>†1,2,3</sup>

<sup>1</sup>State Key Laboratory of Magnetic Resonance and Atomic and Molecular Physics, Innovation Academy for Precision Measurement Science and Technology, Chinese Academy of Sciences, Wuhan 430071, China

<sup>2</sup>Hefei National Laboratory, Hefei 230088, China

<sup>3</sup>Wuhan Institute of Quantum Technology, Wuhan 430206, China

\*rbli@wipm.ac.cn

†mszhan@apm.ac.cn

High-precision cold atom interferometers have matured as powerful tools for fundamental physics research and are now transitioning to field applications. However, their practical deployment outside laboratory environments faces critical challenges, including robustly, rapidly autolocking the laser frequency and rapidly generating laser pulse sequences for atomic manipulation with compact multi-channel radio frequency (RF) generator. To address these challenges, a discrete biorthogonal wavelet transform-based method is developed for precise localization of atomic transition signals. By calculating the frequency differences and comparing the relative magnitude of these signals which are determined by atomic energy level structures and transition efficiencies, the desired spectral line can be robustly and accurately identified, achieving 99.8% identification rate with merely 0.2% performance degradation under even 50% laser intensity fluctuations, as demonstrated in Fig.1 (a). In addition, a Bayesian optimization framework is implemented to strategically leverage historical search data to accelerate the desired spectral line search, achieving an 87.7% improvement in search efficiency relative to conventional gradual scanning methods, as evidenced by Fig.1 (b). Finally, a highly compact multi-channel RF generator is designed, with one field-programmable gate array (FPGA) controlling eight direct digital synthesizers (DDSs) within a 15 cm × 15 cm footprint. The implemented generator employs an advanced pulse sequence parameter pre-loading technique that completely eliminates FPGA-DDS data transmission during RF pulse sequence operation, thereby achieving an ultra-low frequency switching delay of mere 100 ns while maintaining precise laser pulse generation capabilities, as respectively shown in Fig.1 (c) and (d). This robust, rapid laser frequency autolocking technology and compact multi-channel RF pulse-sequence generator will be beneficial for applications in field-deployable cold atom interferometers.<sup>1</sup>

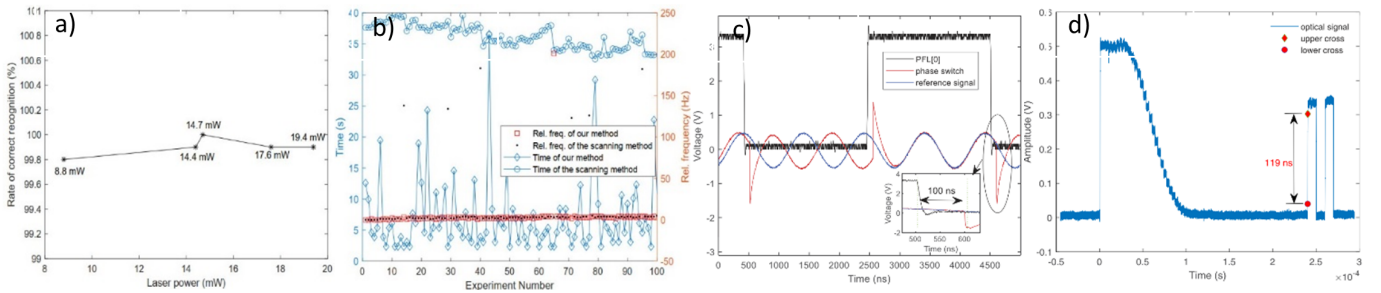


Figure 1: Laser pulse sequence generation for cold atom interferometers. (a) Robustness of spectral line identification of our method against variations of laser intensity. (b) Rapid spectral line search compared to gradual scanning methods. (c) Frequency/amplitude/phase switching delay of an RF signal. (d) Laser pulse sequence for 3D cooling in a cold atom interferometer captured by a photodiode.

<sup>1</sup>M. Jiang et al., *Review of Scientific Instruments* **94**, 093204 (2023).



Abstract number: P108  
Wednesday 14:00-15:30

## Mitigating Residual Electric Field Noise to Enhance the Coherence of Rydberg Atoms

Bahtiyar Mamat<sup>1,2</sup>, Cheng Sheng<sup>3</sup>, Yi-Qing Zhang<sup>1,2</sup>, Xiao-Dong He<sup>†1,4</sup>, Ming-Sheng Zhan<sup>†1,4,5</sup>

<sup>1</sup>State Key Laboratory of Magnetic Resonance and Atomic and Molecular Physics, Wuhan Institute of Physics and Mathematics, Innovation Academy for Precision Measurement Science and Technology, Chinese Academy of Sciences, Wuhan 430071, China

<sup>2</sup>School of Physical Sciences, University of Chinese Academy of Sciences, Beijing 100049, China

<sup>3</sup>Department of Physics, Huazhong Normal University, Wuhan 430079, China

<sup>4</sup>Wuhan Institute of Quantum Technology, Wuhan 430206, China

<sup>5</sup>Hefei National Laboratory, Hefei 230088, China

<sup>†</sup>hexd@apm.ac.cn; mszhan@apm.ac.cn

Rydberg atoms with principal quantum numbers ( $n \gg 1$ ) exhibit extraordinarily large transition dipole moments, resulting in several unique and pronounced atomic properties. These properties include long-range, strong dipole-dipole interactions and enhanced polarizability. Such characteristics render Rydberg atoms fundamentally significant across diverse research frontiers, including quantum computation, quantum simulation, microwave and terahertz field sensing and imaging, as well as hybrid quantum system engineering. Notably, Rydberg excitation can be achieved through either two-photon or single-photon schemes.

We demonstrate single-photon coherent Rydberg excitation in a homonuclear atom array using short-wavelength laser light at 297-nm. However, the use of short-wavelength lasers significantly increases the likelihood of photoelectric effects, which can result in uncontrollable electric fields. By leveraging the high sensitivity of Rydberg atoms to electric fields, we develop a comprehensive understanding of these undesired fields induced by adsorbates and electrons in our single-photon Rydberg excitation experiments, and we conduct systematic investigations.

As shown in Figure 1, we observed significant fluctuations of the background electric field within our experimental vacuum cell. By utilizing the high polarizability of trapped single-atom Rydberg states as sensors, we measured the background electric fields within the cell. In the absence of desorption light (365-nm or 660-nm), we noted broadening of the Rydberg state transition profiles and a frequency shift of  $5.8 \pm 0.2$  MHz. Our results indicate that the primary source of electric field noise is electrons. For the first time, we identified these electrons as originating from the 297-nm laser used for single-photon Rydberg excitation. We confirmed that shining the surfaces of the vacuum cell with 365-nm or 660-nm light effectively reduces electron-induced field noise by promoting photodesorption processes, thereby enhancing the coherence of transitions from the ground state to Rydberg states. We achieved collective excitations of two and four atoms within the Rydberg blockade regime. Finally, we initiated discussions on the Ising model in one-dimensional and two-dimensional atomic arrays<sup>1</sup>.

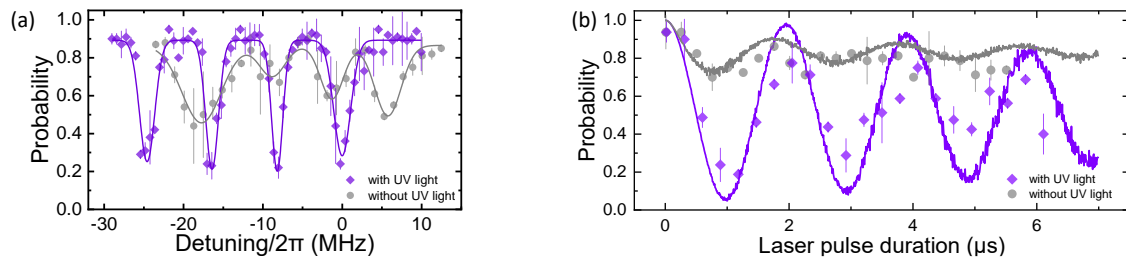


Figure 1: Coherent Rydberg excitation. For simplicity, we choose the center of the peak of  $|53P_{3/2}, m_J = 3/2\rangle$  in the transition spectrum with the UV light as 0 MHz. (a) Ground-Rydberg transition spectra of single atoms under 4.37 Gauss bias magnetic field. The diamond (circle) points are the experimental data with (without) the continuous UV light and solid curves are Gaussian distribution fits to the data. The four peaks in Rydberg spectra represent the ground state to  $53P_{3/2}, m_J = -3/2, -1/2, 1/2, 3/2$  state transition. The optical power of the 297-nm light  $P_{297} = 5.8$  mW, the pulse duration  $t_{297} = 0.2$  ms. (b) Resonant Rabi oscillation between the ground-Rydberg state. The diamond (circle) points are the results with (without) the UV light. The solid curves are the numerical calculation results without parameter fitting. We note that, for all the measurements shown here, each data point is accumulated over 50 experimental shots, and averaged over for two repetitions. The accompanying error bars denote statistical errors.

<sup>1</sup>B. Mamat, et al.C. Sheng, Y.Q. Zhang, J.Y. Hou, P. Xu, K.P. Wang, J. Zhuang, M.R. Wei, M. Liu, J. Wang, X.D. He, and M.S. Zhan, *Phys. Rev. Appl.* **22**, 064021(2024).

Abstract number: P109  
 Wednesday 14:00-15:30

## Mode synchronization in a quantum gas with cavity-mediated interactions

Natale G.<sup>1</sup>, Baumgärtner A.<sup>1</sup>, Stefaniak J.<sup>1</sup>, Baur D.<sup>1</sup>, Hertlein S.<sup>1</sup>, Rivero D.<sup>1</sup>,  
 Esslinger T.<sup>1</sup>, Donner T.<sup>†1</sup>

<sup>1</sup>*Institute for Quantum Electronics, Eidgenössische Technische Hochschule Zürich, Otto-Stern-Weg 1, CH-8093 Zurich, Switzerland*

<sup>†</sup>donner@phys.ethz.ch

Driven open quantum systems exhibit various non-equilibrium phenomena, including phase transitions from stationary to dynamical phases<sup>1</sup>. The emergence of collective dynamics in these transitions is often revealed through the excitation spectrum, which reflects the physical mechanism responsible for the transition. In this work, we explore this mechanism using a Bose-Einstein condensate of <sup>87</sup>Rb atoms interacting with a high-finesse optical cavity and illuminated by a transverse pump laser. This setup inherently supports long-range interactions mediated by the cavity field and incorporates dissipation through photon loss<sup>2</sup>. By implementing Bragg spectroscopy<sup>3</sup>, we probe the system's excitation spectrum and uncover a dissipation-induced regime of synchronization, marked by the coalesce of two roton-like modes. These results demonstrate that synchronization can originate at the quasiparticle level and precede the emergence of a dynamical phase<sup>4</sup>. Our study highlights how dissipation can lead to synchronized behaviors and contributes to a broader understanding of non-equilibrium criticality, paving the way for future investigations into unconventional dynamical quantum phases.

<sup>1</sup>L. M. Sieberer et al., *Phys. Rev. Lett.* **110**, 195301 (2013)

<sup>2</sup>L. Xiangliang et al., *Phys. Rev. Res.* **3**, L012024 (2021)

<sup>3</sup>R. Mottl et al., *Science* **336**, 6088 (2012)

<sup>4</sup>D. Dreon et al., *Nature* **608**, 494–498 (2022)

Abstract number: P110  
Wednesday 14:00-15:30

## Generation of motional squeezed states for neutral atoms in optical tweezers

Lienhard V.<sup>†1,2</sup>, Martin R.<sup>1,3</sup>, Chew Y.<sup>1,3</sup>, Tomita T.<sup>1,4</sup>, Ohmori K.<sup>1,4</sup>, de Léséleuc S.<sup>1,5</sup>

<sup>1</sup>Institute for Molecular Science, National Institutes of Natural Sciences, Okazaki, Japan

<sup>2</sup>Nanomaterials and Nanotechnology Research Center (CINN-CSIC), Universidad de Oviedo, El Entrego, Spain

<sup>3</sup>Université Paris-Saclay, Institut d'Optique Graduate School, CNRS, Laboratoire Charles Fabry, Palaiseau, France

<sup>4</sup>SOKENDAI (the Graduate University for Advanced Studies), Okazaki, Japan

<sup>5</sup>RIKEN Center for Quantum Computing (RQC), Wako, Japan

<sup>†</sup>vincent.lienhard@cinn.es

Optical tweezers are a widely-used tool on several quantum platforms, as they allow for the precise motion control of small objects, including single neutral atoms. The optimal level of control is ultimately set by the quantum fluctuations, which is reached once the atoms have been cool down to the motional ground state via Raman sideband cooling<sup>1</sup>. Here, we go further the standard quantum limit by generating motional squeezed states.

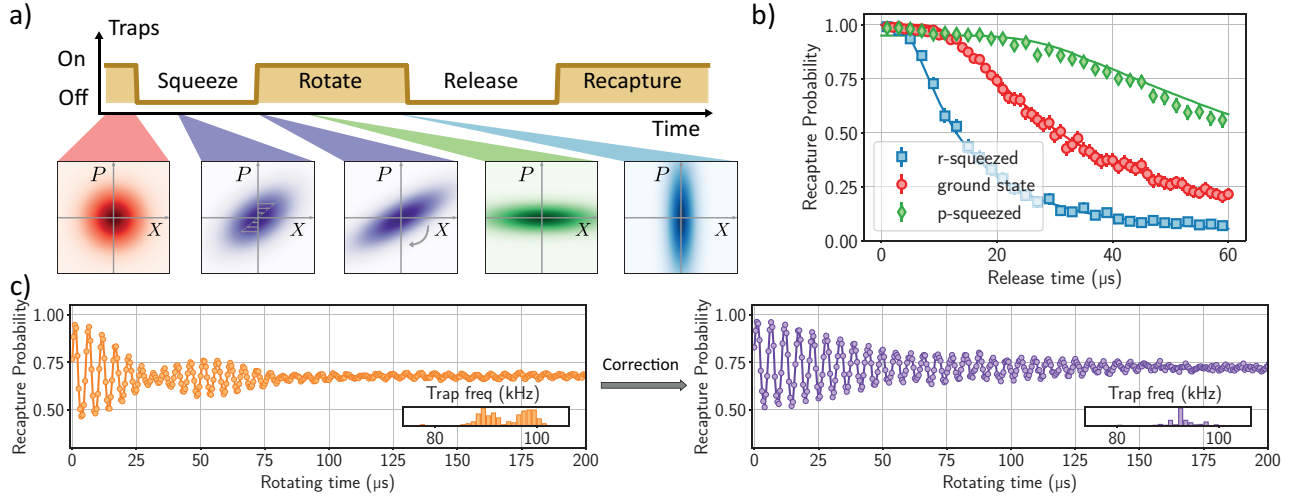


Figure 1: Generation, probing, and collective oscillations of squeezed states. a) Experimental sequence, with sketches of the probability density in the X-P plane through time. b) Measured recapture probabilities for different motional states. c) Recapture probabilities as a function of the rotating time, before and after compensation of the trap shape anisotropy and inhomogeneities. The insets show the histogram of the individual trapping frequencies.

Our protocol, which was originally demonstrated on an optical lattice platform<sup>2</sup>, for the squeezed state preparation and measurement, is displayed in Figure 1a. It relies on the free expansion of the atoms from the trap, shearing the probability distribution in the X-P plane. Then, switching on the trap again, the elongated probability distribution rotates, oscillating between momentum- and position-squeezed states. We end the sequence by a release and recapture experiment to probe the momentum distribution spreading (Figure 1b), hence measuring the squeezing factor.

We demonstrate the generation of 6 dB-squeezed states. The anisotropy of the trap shape, and its inhomogeneities within an array of optical tweezers, affect the squeezing performance. We show how our recently developed holography techniques<sup>3</sup> allow to compensate for it and give enhanced collective squeezed state oscillations (see Figure 1c). We also analyze the inherent limit induced by the optical tweezer anharmonicity. Our work opens perspectives for the exploration of short distance Rydberg-Rydberg interaction<sup>4</sup>, where the effect of position noise would be detrimental. It also paves the way for a further study of spin-motion coupling in Rydberg ensembles<sup>5</sup>.

<sup>1</sup>A. M. Kaufman, B. J. Lester, and C. A. Regal, *Phys. Rev. X* **2**, 041014 (2012).

<sup>2</sup>M. Morinaga, I. Bouchoule, J.-C. Karam, and C. Salomon, *Phys. Rev. Lett.* **83**, 4037 (1999).

<sup>3</sup>Y. T. Chew *et al.*, *Phys. Rev. A* **110**, 053518 (2024).

<sup>4</sup>Y. Chew, T. Tomita, T. P. Mahesh, S. Sugawa, S. de Léséleuc, and K. Ohmori, *Nature Photonics* **16**, 724-729 (2022).

<sup>5</sup>V. Bharti *et al.*, *Phys. Rev. Lett.* **133**, 093405 (2024).

Abstract number: P111  
Wednesday 14:00-15:30

## Robust Bragg diffraction for atom interferometers using optimal control theory

**Martinez-Lahuerta V. J.<sup>1†</sup>, Kirsten-Siemß J.<sup>1</sup>, Li R.<sup>1,2</sup>, Hammerer K.<sup>2</sup>, Gaaloul N.<sup>1</sup>**

<sup>1</sup>Leibniz University Hannover, Institute of Quantum Optics, Hannover, Germany

<sup>2</sup>Leibniz University Hannover, Institute of Theoretical Physics, Hannover, Germany

<sup>†</sup>martinez@iqo.uni-hannover.de

Bragg diffraction is a fundamental technique used to enhance the sensitivity of atom interferometers via large momentum transfer, making these devices among the most precise quantum sensors available today. To further improve their accuracy, it is necessary to achieve control over multiple paths and increase robustness against velocity spread. Recent advancements in sensitivity and robustness under realistic conditions, such as vibrations, accelerations, and other experimental challenges, have been made through the application of optimal control theory<sup>12</sup>.

In this work, we employ this tool to improve single and double Bragg diffractions. For the single Bragg pulses we focus on improving the accuracy of the interferometer by minimizing the diffraction phase. We consider the finite temperature of the incoming wavepacket and the multi-path nature of high-order Bragg diffraction showcased in a Mach-Zender geometry<sup>3</sup>. Our approach leads to diffraction phases on the order of microradians or even below, see Fig. 1. For double Bragg pulses we optimize individual operations via a smooth time-dependent detuning and make them robust against polarization imperfections of the coupling light fields, showing a great improvement of the pulses efficiency<sup>4</sup>.

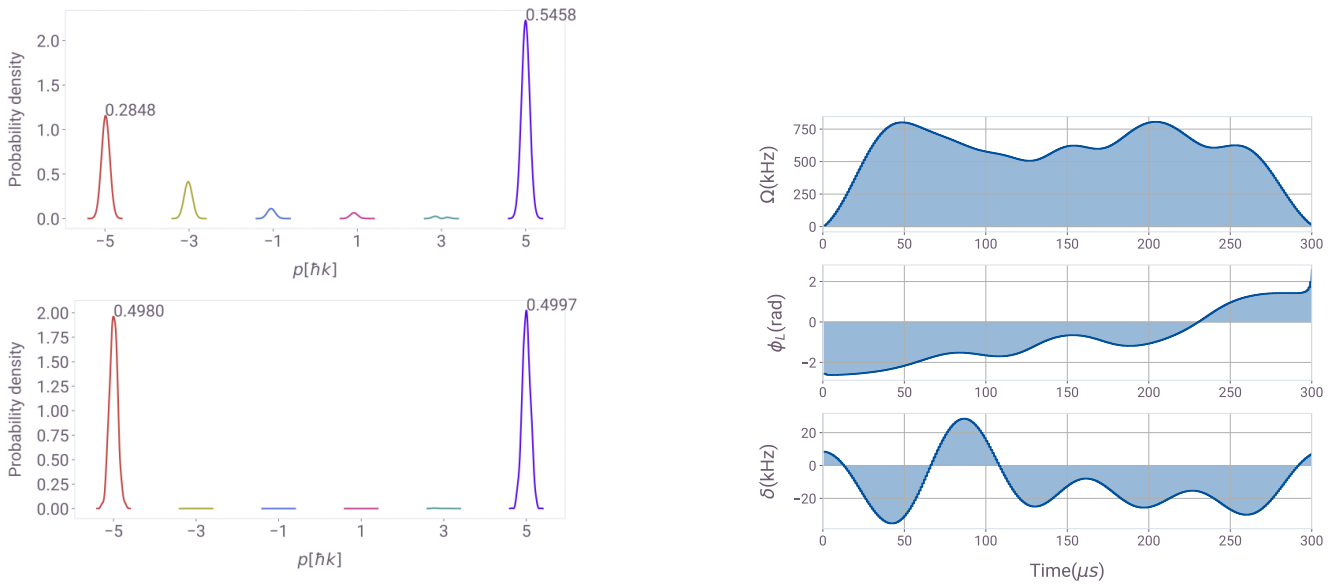


Figure 1: Study of an optimized beam splitter for an incoming wave packet with momentum width  $\sigma_p = 0.1\hbar k$  and Bragg order  $n = 5$ . Top-left: Populations after the interaction with an optimal Gaussian pulse with a peak Rabi frequency of  $\Omega_0 = 34\omega_r$  and a pulse width of  $\tau = 0.145\omega_r^{-1}$ . Bottom-left: Populations after the interaction with an optimal control theory (OCT) pulse, showing an almost perfect beam splitter with smooth Gaussian distributions of the populations in  $|\pm 5\hbar k\rangle$  after the interaction. Right: OCT pulse parameters where a cutoff frequency of 95 kHz has been used for the optimization.

<sup>1</sup>G. Louie, Z. Chen, T. Deshpande and T. Kovachy, *New Journal of Physics* **25**, 083017 (2023).

<sup>2</sup>J. C. Saywell, et al., *Nature Communications* **14**, 10.1038 (2023).

<sup>3</sup>J.-N. Kirsten-Siemß, F. Fitzek, C. Schubert, E. M. Rasel, N. Gaaloul, and K. Hammerer, *Physical Review Letter* **131**, 033602 (2023).

<sup>4</sup>R. Li, V.J. Martinez-Lahuerta, S. Seckmeyer, K. Hammerer and N. Gaaloul, *Physical Review Research* **6**, 043236 (2024).

Abstract number: P112  
 Wednesday 14:00-15:30

## Progress towards atom interferometry using large momentum transfer UV transitions in ultra-cold cadmium

Chiarotti M.<sup>1</sup>, Manzoor S.<sup>1</sup>, Robert P. J.<sup>1</sup>, Poli N.<sup>†,1</sup>

<sup>1</sup> Dipartimento di Fisica e Astronomia & LENS, Università degli Studi di Firenze, Via G. Sansone 1, 50019 - Sesto Fiorentino, Italy

<sup>†</sup> nicola.poli@unifi.it

Today, matter-wave interferometers such as clocks and gravimeters allow precision measurements of time and gravity at unprecedented levels. In all these sensors, the exquisite control of both internal (electronic) and external (center of mass motion) degrees of freedom of ultra-cold atomic samples, enable us to study interactions at their most basic, quantum level, paving the way for new tests of fundamental physics.

In this work, we present the prospects for developing a new atom interferometer based on large-momentum-transfer (LMT) UV/DUV transitions of cadmium atoms. We discuss potential sensitivity improvements using high-power, frequency-stabilized lasers for cadmium  $^1S_0$ – $^3P_0$  clock transition at 332 nm<sup>1</sup> and compare it with the clock transition in strontium. We also describe the production of ultra-cold cadmium samples in an optimized setup<sup>2</sup>, along with the development of novel UV/DUV laser systems specifically designed for this experiment<sup>3</sup>. Prospects for testing physics beyond the Standard Model are also discussed<sup>4</sup>. This work has been supported by the European Research Council, Grant No. 772126 (TICTOCRAV).

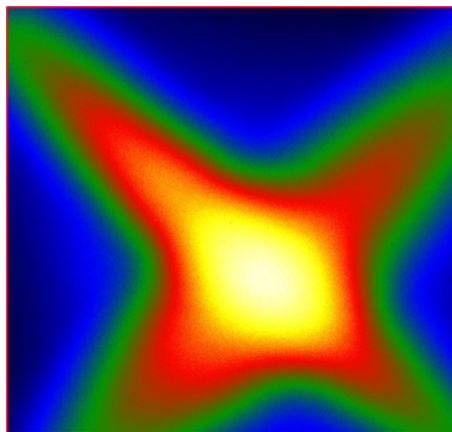


Figure 1: Fluorescence collected by a 2D-MOT of cadmium atoms at 229 nm.

<sup>1</sup>M. Chiarotti et al., *Phys. Rev. X Quantum* **3**, 030348 (2022).

<sup>2</sup>S. Bandarupally, et al., *J. Phys. B: At. Mol. Opt. Phys.* **56**, 185301 (2023).

<sup>3</sup>S. Manzoor et al., *Optics Letters* **47**(10), 2582-2585 (2022). J. N. Tinsley et al. *Optics Express* **29**(16), 25462-25476 (2021).

<sup>4</sup>S. Manzoor et al., *Optics Letters* **47**(10), 2582-2585 (2022). J. N. Tinsley et al. *AVS Quantum Sci.* **6**, 014411 (2024).

Abstract number: P113

Wednesday 14:00-15:30

## Entropy transport between strongly interacting superfluids

Huang M.-Z.<sup>†1</sup>, Fabritius P.<sup>1</sup>, Mohan J.<sup>1</sup>, Talebi M.<sup>1</sup>, Wili S.<sup>1</sup>, Esslinger T.<sup>1</sup>

<sup>1</sup>*Institute for Quantum Electronics and Quantum Center, ETH Zurich, 8093 Zurich, Switzerland*

<sup>†</sup>mhuang@phys.ethz.ch

Superfluids are fascinating quantum many-body ground states that appear in various physical systems. When two superfluid reservoirs are weakly connected, entropy-free supercurrent leads to Josephson oscillations. However, when superfluid reservoirs are strongly connected, for example by a ballistic channel, things can get more complicated. Particles flow with nonlinear, superfluid characteristics, yet they can carry large amount of entropy, significantly beyond the associated entropy production. Here we present experimental observations of such peculiar entropy transport between superfluids of resonantly interacting Fermi gases<sup>1</sup>. Defect-free transport geometry and precise thermometry provide an ideal playground for studying entropy transport in superfluids, so far inaccessible to condensed matter systems. The observed entropy transported per particle is in addition insensitive to the details of the ballistic channel that connects the superfluid reservoirs. This robustness of the entropy per particle even extends to reservoirs above the superfluid transition and away from the unitarity limit (BEC-BCS crossover), pointing to certain universal behavior of the far-from-equilibrium system. We also present new directions of manipulating the transport with either engineered dissipation<sup>2</sup> or coherent Lambda-type driving<sup>3</sup>.

<sup>1</sup>P. Fabritius *et al.*, *Nat. Phys.* **20**, 1091–1096 (2024).

<sup>2</sup>M.-Z. Huang, P. Fabritius, J. Mohan, M. Talebi, S. Wili and T. Esslinger, arXiv:2412.08525.

<sup>3</sup>M. Talebi, S. Wili, J. Mohan, P. Fabritius, M.-Z. Huang and T. Esslinger, *Phys. Rev. Lett.* **133**, 223403 (2024).

Abstract number: P114  
Wednesday 14:00-15:30

## High-resolution spectroscopy of $^{173}\text{Yb}^+$ ions

Jiang J.<sup>†1</sup>, Viatkina A.<sup>2</sup>, JK S.<sup>1</sup>, Filzinger M.<sup>1</sup>, Steinel M.<sup>1</sup>, Lipphardt B.<sup>1</sup>, Peik E.<sup>1</sup>, Surzhykov A.<sup>1,2</sup>,  
Huntemann N.<sup>†1</sup>

<sup>1</sup>Physikalisch-Technische Bundesanstalt, Braunschweig, Germany

<sup>2</sup>TU Braunschweig, Braunschweig, Germany

<sup>†</sup>jian.jiang@ptb.de

<sup>†</sup>nils.huntemann@ptb.de

Trapped  $\text{Yb}^+$  ions of different isotopes have been employed in various fields of AMO physics, including atomic clocks<sup>1</sup>, quantum simulation and quantum information processing<sup>2</sup>, and new physics searches<sup>3</sup>. Compared with other isotopes,  $^{173}\text{Yb}^+$  is a particularly promising candidate for expanding and improving existing research due to its large nuclear spin of  $I = 5/2$ , which gives rise to hyperfine mixing, quantum states with high multiplicity, and high-order nuclear moments.

Optical clocks based on the  $^2\text{S}_{1/2} \rightarrow ^2\text{F}_{7/2}$  transition in  $^{171}\text{Yb}^+$  ( $I = 1/2$ ) are among the most accurate clocks today. However, the excited state of this transition has a lifetime of years due to its weak coupling to the ground state via electric octupole radiation<sup>4</sup>. Such a weak coupling complicates the control of the light shift from the probe laser<sup>5</sup> because the shift is much larger than the resolved linewidth. In  $^{173}\text{Yb}^+$ , this complexity might naturally be simplified because the mixture between the states  $^2\text{P}_{3/2}$  and  $^2\text{F}_{7/2}$  caused by the hyperfine interaction could shorten the lifetime of the latter by up to two orders of magnitude<sup>6</sup>.

Even though promising, high-precision spectroscopy of  $^{173}\text{Yb}^+$  has been impeded so far by its complex atomic structure. In this presentation, we will first discuss our approaches to overcome challenges in laser cooling and state preparation of a single  $^{173}\text{Yb}^+$  ion confined in a Paul trap. We will then present the preliminary results of our current measurements of  $^{173}\text{Yb}^+$ , including the hyperfine structures of the  $^2\text{S}_{1/2}$ ,  $^2\text{D}_{3/2}$  and  $^2\text{F}_{7/2}$  states, and the frequencies and strengths of the  $^2\text{S}_{1/2} \rightarrow ^2\text{D}_{3/2}$  transition and the  $^2\text{S}_{1/2} \rightarrow ^2\text{F}_{7/2}$  transition. Finally, we will conclude by discussing the ongoing comparison of our results with theoretical predictions.

Except for the expected improved performance of clocks based on  $^{173}\text{Yb}^+$ , our results of high-resolution measurements of hyperfine structures also provide stringent tests for calculations of atomic and nuclear structure<sup>7</sup>, which plays a crucial role in the interpretation of various experiments of searching for new physics<sup>8</sup>, and provide the possibility of using these rich structures for implementing the many-state qudit<sup>9</sup> and robust qubit encoding<sup>10</sup>.

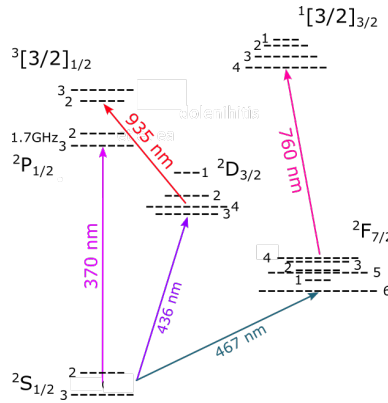


Figure 1: Simplified level scheme of  $^{173}\text{Yb}^+$ .

<sup>1</sup>N. Huntemann *et al.*, *Phys. Rev. Lett.* **116**, 063001 (2016). A. Tofful *et al.*, *Metrologia* **61**, 045001 (2024).

<sup>2</sup>V. So *et al.*, *Sci. Adv.* **10**, eads8011 (2024). S. A. Guo *et al.*, *Nature* **630**, 613 (2024).

<sup>3</sup>C. Sanner *et al.*, *Nature* **567**, 204 (2019). M. Filzinger *et al.*, *Phys. Rev. Lett.* **130**, 253001 (2023).

J. Hur *et al.*, *Phys. Rev. Lett.* **128**, 163201 (2022).

<sup>4</sup>R. Lange *et al.*, *Phys. Rev. Lett.* **127**, 213001 (2021).

<sup>5</sup>N. Huntemann *et al.*, *Phys. Rev. Lett.* **109**, 213002 (2012). C. Sanner *et al.*, *Phys. Rev. Lett.* **120**, 053602 (2018).

<sup>6</sup>V. A. Dzuba *et al.*, *Phys. Rev. A* **93**, 052517 (2016).

<sup>7</sup>D. Xiao *et al.*, *Phys. Rev. A* **102**, 022810 (2020).

<sup>8</sup>N. Fortson, *Phys. Rev. Lett.* **70**, 2383 (1993). J. C. Berengut, *arXiv:2409.01530* (2024).

V. V. Flambaum, *Phys. Rev. Lett.* **131**, 113004 (2023).

<sup>9</sup>Y. Wang *et al.*, *Front. Phys.* **8**, 589504 (2020).

<sup>10</sup>S. P. Jain *et al.*, *Phys. Rev. Lett.* **133**, 260601 (2024).



Abstract number: P115  
Wednesday 14:00-15:30

## Precision Spectroscopy and Nuclear Structure Parameters in ${}^7\text{Li}^+$ ion

Guan Hua<sup>1</sup>, Shaolong Chen<sup>1</sup>, Xurui Chang<sup>1</sup>, Xiaoqiu Qi<sup>2</sup>, Tingyun Shi<sup>†1</sup>, Kelin Gao<sup>†1</sup>

<sup>1</sup>State Key Laboratory of Magnetic Resonance and Atomic and Molecular Physics, Wuhan Institute of Physics and Mathematics, Innovation Academy for Precision Measurement Science and Technology, Chinese Academy of Sciences, Wuhan, China

<sup>2</sup>Department of Physics, Zhejiang Sci-Tech University, Hangzhou, China

<sup>†</sup>tyshi@wipm.ac.cn, klgao@wipm.ac.cn

The helium-like  $\text{Li}^+$  ion is considered a fundamental atomic system due to its spectroscopic properties, encompassing fine and hyperfine structure (HFS), which can be experimentally measured and theoretically calculated with high precision. This system serves as a platform for testing bound-state quantum electrodynamics (QED), determining nuclear properties, and exploring potential physics beyond the standard model. Lithium has two stable isotopes,  ${}^6\text{Li}$  and  ${}^7\text{Li}$ , each with nonzero nuclear spins exceeding  $1/2$ . This makes it an ideal subject for investigating nuclear structure, including the determination of the Zemach radius and nuclear quadrupole moment through Ramsey spectroscopy<sup>1</sup>.

Hyperfine structure refers to the additional splitting of atomic energy levels caused by nuclear spin. The hyperfine level splitting can be expressed as:

$$E_{\text{HFS}} = E_p + E_{\text{ZM}} + E_{\text{Qd}} \quad (0)$$

where  $E_p$  represents the energy of HFS obtained for the case of a point nucleus, and  $E_{\text{ZM}}$  and  $E_{\text{Qd}}$  are contributions generated by the nuclear Zemach radius<sup>2</sup> and the quadrupole moment, respectively. Since the nuclear quadrupole moment does not contribute to the  $2\text{ }^3\text{S}_1$  state, we can extract the Zemach radius by experimentally measuring the HFS of the  $2\text{ }^3\text{S}_1$  state. Subsequently, the obtained Zemach radius and corresponding experimental measurements of the  $2\text{ }^3\text{P}_J$  state are utilized to determine the nuclear quadrupole moment.

The present HFS measurements rely on the optical Ramsey technique employing separated laser fields<sup>3</sup>. The experimental setup is depicted in Fig. 1(a). The HFS is determined by measuring two neighboring transition frequencies which are determined by the fitted central value of the Ramsey spectrum in Fig. 1(b) with a common upper or lower energy level using the time sequence in Fig. 1(c).

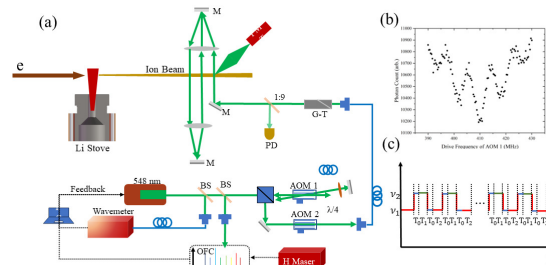


Figure 1: (a)The experimental setup. (b)The Ramsey spectroscopy. (c)The time sequence for the measurement of the hyperfine structure splitting.

By employing an optical Ramsey interference scheme, the accuracy of the HFS measurements of  ${}^7\text{Li}^+$  was experimentally further improved by about half an order of magnitude, with an accuracy of 10 kHz level. Together with bound-state quantum electrodynamics theory, the Zemach radius and the quadrupole moment of the  ${}^7\text{Li}$  nucleus are determined to be  $3.35(1)\text{ fm}^2$  and  $-3.86(5)\text{ fm}^2$ , respectively, with the quadrupole moment deviating from the recommended value<sup>4</sup> of  $-4.00(3)\text{ fm}^2$  by  $1.75\sigma$ . Furthermore, we determined the quadrupole moment ratio of  ${}^6\text{Li}$  to  ${}^7\text{Li}$  as  $0.101(13)$ , exhibiting a  $6\sigma$  deviation from the previous measured value of  $0.020161(13)$  by LiF molecular spectroscopy<sup>5</sup>. The results taken together provide a sensitive test of nuclear structure models, while these discrepancies are perplexing, and we call for additional experimental measurements in atomic and molecular spectroscopy, electron scattering, and related theoretical calculations pertaining to lithium.

<sup>1</sup>H. Guan, X. Q. Qi, *et al.*, *arXiv*: 2403.06384

<sup>2</sup>A. C. Zemach, *Phys. Rev.* **104**, 1771 (1956).

<sup>3</sup>W. Sun, P. P. Zhang, *et al.*, *Phys. Rev. Lett.* **131**, 103002 (2023).

<sup>4</sup>N. Stone, *At. Data Nucl. Data Tables* **111-112**, 1 (2016).

<sup>5</sup>J. Cederberg, D. Olson, *et al.*, *Phys. Rev. A* **57**, 2539 (1998).



Abstract number: P116  
 Wednesday 14:00-15:30

## Universal gate set for optical lattice based atom interferometry

LeDesma C.<sup>1</sup>, Mehling K.<sup>1</sup>, **Wilson J. D.**<sup>†1</sup>, Nicotra M.<sup>2</sup>, Holland M. J.<sup>1</sup>

<sup>1</sup>*JILA & Department of Physics, University of Colorado Boulder, CO 80309-0440, USA*

<sup>2</sup>*College of Engineering and Applied Science, University of Colorado Boulder, Boulder, Colorado 80309, USA*

<sup>†</sup>John.Wilson-6@colorado.edu

We propose a new paradigm for atom interferometry and demonstrate that there exists a universal set of atom optic components for inertial sensing<sup>1</sup>. These components constitute gates with which we carry out quantum operations and represent input-output matterwave transformations between lattice eigenstates. Each gate is associated with a modulation pattern of the position of the optical lattice according to machine-designed protocols. In this methodology, a sensor can be reprogrammed to respond to an evolving set of design priorities without modifying the hardware. We assert that such a gate set is metrologically universal, in analogy to universal gate sets for quantum computing. Experimental confirmation of the designed operation is demonstrated via in situ imaging of the spatial evolution of a Bose-Einstein condensate in an optical lattice, and by measurement of the momentum probabilities following time-of-flight expansion. The representation of several basic quantum sensing circuits is presented for the measurement of inertial forces, rotating reference frames, and gravity gradients.

---

<sup>1</sup>C. Ledesma, K. Mehling, J.D. Wilson, M. Nicotra, M.J. Holland *Phys. Rev. Res.* **7**, 013246 (2025).

Abstract number: P117

Wednesday 14:00-15:30

## Current Advances in the Strontium Optical Lattice Clock and Development of a Cavity-Enhanced System at INRiM

**Salvatierra J. P.<sup>†1</sup>, Barbiero M.<sup>2</sup>, Calonico D.<sup>2</sup>, Levi F.<sup>2</sup>, Tarallo M. G.<sup>†2</sup>**

<sup>1</sup>*Politecnico di Torino, Turin, Italy*

<sup>2</sup>*Istituto Nazionale di Ricerca Metrologica, Turin, Italy*

<sup>†</sup>juan.salvatierra@polito.it

We present the current status and recent developments of the strontium optical lattice clock at the Italian National Metrology Institute (INRiM). In our ongoing work to refine the accuracy budget of the  $^{88}\text{Sr}$  clock, we have concentrated our recent effort on the study of the collisional effects in  $^{88}\text{Sr}$ , which historically have been one of the primary limiting factors in the performance of the bosonic strontium clock<sup>1</sup>. The problem here is tackled with measurements of both the density-dependent frequency shift and spectroscopic investigations of collisional features, carried out in both one-dimensional and two-dimensional optical lattice configurations.

The clock apparatus incorporates an efficient 2D-MOT-based atomic source<sup>2</sup>, which enables complete optical control of the atomic loading rate, and results in a dramatic suppression of oven blackbody radiation and background-gas collisions shifts. The latter is demonstrated by observed lattice lifetimes higher than 20 s. All the cooling and trapping optical radiations are frequency stabilized to a single multiwavelength optical cavity<sup>3</sup>. For the clock laser, which requires more stringent frequency noise properties, we use the same cavity as a pre-stabilization step. To further reduce the noise, we have developed an all-fiber solution that employs a serrodyne phase modulation as an actuator to perform frequency comb assisted spectral purity transfer from a reference optical oscillator with short-term flicker instability of  $10^{-15}$  at 0.1 s of averaging time<sup>4</sup>.

In parallel, we are developing a cavity-enhanced optical lattice clock system. The setup integrates a high-finesse Fabry-Pérot cavity and a bow-tie cavity to enable lattice confinement at the magic wavelength<sup>5</sup>. This system will represent a versatile platform to study atom-light interactions in the quantum regime, including the investigation of the metrological advantages of spin-squeezing generation protocols in passive optical clocks<sup>6</sup>, as well as the exploration of collective radiative phenomena such as superradiance on both the kHz-wide intercombination transition at 689 nm and the mHz-wide clock transition at 698 nm.

<sup>1</sup>C. Lisdat, J. S. R. Vellore Winfred, T. Middelmann, F. Riehle, and U. Sterr, *Phys. Rev. Lett.* **103**, 090801 (2009).

<sup>2</sup>M. Barbiero, M. G. Tarallo, D. Calonico, F. Levi, G. Lamporesi, and G. Ferrari, *Phys. Rev. Appl.* **13**, 014013 (2020).

<sup>3</sup>M. Barbiero, D. Calonico, F. Levi and M. G. Tarallo, *IEEE Trans. Instrum. Meas.*, **71**, 1501509 (2022).

<sup>4</sup>M. Barbiero et al., *Opt. Lett.* **48**, 1958–1961 (2023).

<sup>5</sup>M. G. Tarallo, *EPJ Web Conf.* **230**, 00011 (2020).

<sup>6</sup>A. Caprotti, M. Barbiero, M. G. Tarallo, M. G. Genoni, and G. Bertaina, *Quantum Sci. Technol.* **9**, 015007 (2024).

Abstract number: P118  
 Wednesday 14:00-15:30

## Optically dressed three-level coherence in neutral bosonic alkaline-earth-like species

**P. Robert<sup>†1</sup>**, M. Chiarotti<sup>1</sup>, S. Manzoor<sup>1</sup>, N. Poli<sup>1</sup>, D. O. Sabulsky<sup>2</sup>

<sup>1</sup>*Dipartimento di Fisica e Astronomia LENS, Università degli Studi di Firenze, Via G. Sansone 1, 50019 - Sesto Fiorentino, Italy*

<sup>2</sup>*ARTEMIS, Observatoire de la côte d'Azur, Université Côte d'Azur, CNRS, 96 Boulevard de l'Observatoire, F-06304 Nice CEDEX 4, France*

<sup>†</sup>probert@unifi.it

Addressing the optical clock transition of alkaline-earth-like atoms has attracted growing interest for a potential redefinition of the Système International second <sup>1</sup> and for fundamental physics applications based on inertial sensors <sup>2,3</sup>

In bosonic alkaline-earth-like atoms such as strontium and cadmium, accessing this transition requires external coupling.

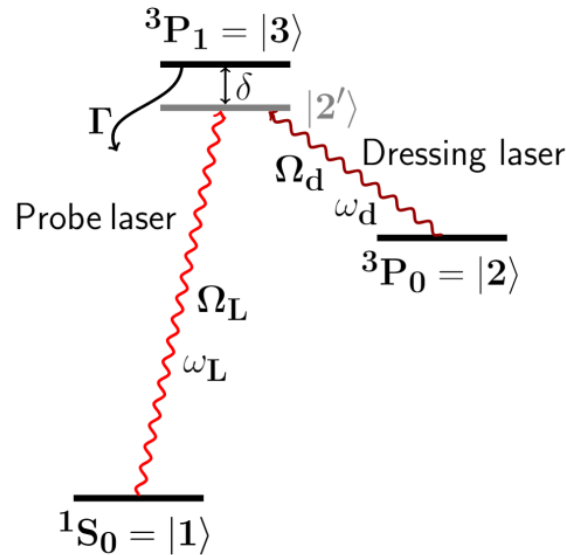


Figure 1: Relevant level structure in neutral alkaline-earth-like. An interaction between  $^1S_0$  and  $^3P_0$  can be observed via application of a coherent electromagnetic field, referred to here as the dressing laser, which facilitates coupling via the intermediate  $^3P_1$  state.

Here, we propose a scheme applied to cadmium, utilizing near-infrared optical dressing to drive a three-level coherence that effectively couples to and addresses the optical clock transition <sup>4</sup>.

P. R. acknowledges the support of the Horizon Europe Grant ID 101080164 (UVQuanT).

<sup>1</sup>A. D. Ludlow et al. *Rev. Mod. Phys.* **87**, 637 (2015).

<sup>2</sup>P. W. Graham et al. *Phys. Rev. Lett.* **110**, 171102 (2013).

<sup>3</sup>L. Hu et al. *Phys. Rev. Lett.* **119**, 263601 (2017).

<sup>4</sup>P. Robert et al. *Phys. Rev. Research* **6**, 043268 (2024).

Abstract number: P119  
Wednesday 14:00-15:30

## Probing the local dispersion of k-vectors in situ with a Bose-Einstein Condensate

Gaudout S., Debavelaere C., Si-Ahmed R., Door M., Cladé P. and Guellati-Khelifa S.

*Laboratoire Kastler Brossel, Sorbonne Université, CNRS, ENS-Université PSL, Collège de France, 75005 Paris, France*

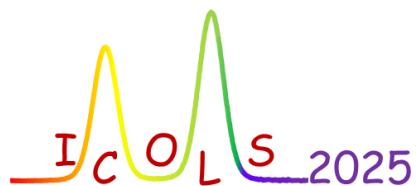
The most stringent test of the Standard Model of particle physics involves comparing values of the fine-structure constant,  $\alpha$ , obtained through different experimental approaches. One such method uses atom interferometry to measure the recoil velocity of an atom after it absorbs or emits a photon. Currently, a significant discrepancy persists between the  $\alpha$  values reported by the only two atom interferometry experiments worldwide<sup>1</sup>. The accuracy of the measurement of the recoil velocity is primarily limited by our knowledge of the laser wave vectors as experienced by the atoms.

To solve this puzzle and to improve the accuracy of the recoil measurement we are currently investigating methods allowing to measure dispersion of wave-vectors due to the distortion of the lasers wavefronts. We demonstrated a novel in-situ technique to map this dispersion across the spatial profile of a laser beam. This method is performed by moving a Bose-Einstein condensate (BEC) coupled with an atom interferometer sensitive to recoil velocities. By adjusting the initial transverse velocity of the BEC, we achieve spatial sensitivity to the laser intensity profile, enabling the construction of a two-dimensional map of the beam's intensity variations and k-vector dispersion. This approach highlights the potential for detecting local defects in the intensity profile, providing insights into the intricate interactions between atoms and laser light.

---

<sup>1</sup>L. Morel, Z. Yao, P. Cladé, S. Guellati-Khelifa, *Nature* **588**, 61 (2020) and R. H. Parker, C. Yu, W. Zhong, B. Estey, and H. Müller, *Science* 360, 191-195 (2018).

*Poster session 3*  
*Abstracts*



Abstract number: P120  
Friday 14:00-15:30

## Fast, robust and laser-free universal entangling gates for trapped-ion quantum computing

Nünnerich M.<sup>1</sup>, Cohen D.<sup>2</sup>, Barthel P.<sup>1</sup>, Huber P. H.<sup>1</sup>, Niroomand D.<sup>1</sup>, Retzker A.<sup>2,3</sup>, Wunderlich Ch.<sup>†1</sup>

<sup>1</sup>Department of Physics, School of Science and Technology, University of Siegen, 57068 Siegen, Germany

<sup>2</sup>Racah Institute of Physics, Hebrew University of Jerusalem, 91904 Jerusalem, Israel

<sup>3</sup>AWS Center for Quantum Computing, Pasadena, CA 91125, USA

<sup>†</sup>christof.wunderlich@uni-siegen.de

Trapped atomic ions are well suited to investigate fundamental questions of quantum physics that require access to and detailed control of individual quantum systems. In addition, this physical platform has set standards for quantum information processing for decades. Here, a novel two-qubit entangling gate for radio frequency (RF)-controlled trapped-ion quantum processors is proposed theoretically and demonstrated experimentally<sup>1</sup>. The speed of this gate is an order of magnitude higher than that of previously demonstrated two-qubit entangling gates using magnetic gradient induced coupling (MAGIC) in a static gradient field. At the same time, the phase-modulated field driving the gate dynamically decouples the hyperfine qubits in  $^{171}\text{Yb}^+$  ions from amplitude and frequency noise, increasing the qubits' coherence time by three orders of magnitude. The gate requires only a single continuous RF field per qubit, making it well suited for scaling a quantum processor to large numbers of qubits. Implementing this entangling gate, we generate Bell states in  $\leq 313 \mu\text{s}$  with fidelities up to  $98_{-3}^{+2}\%$  in a static magnetic gradient of only 19.09 T/m. At higher magnetic field gradients, the entangling gate speed can be further improved to match that of laser-based counterparts. In addition, we report on the design and experimental characterization of a novel planar micro-structured Paul trap-chip for fast entangling quantum gates via MAGIC.

<sup>1</sup>M. Nünnerich, D. Cohen, P. Barthel, P. H. Huber, D. Niroomand, A. Retzker, Ch. Wunderlich, arXiv:2403.04730, accepted for publication in *Physical Review X*.

Abstract number: P121  
Friday 14:00-15:30

# Investigation of isotope shifts and Stark shifts in the strontium Rydberg state via $5s^2\ ^1S_0 \rightarrow 5s5p\ ^1P_1^0 \rightarrow 5p_{1/2}5p_{1/2} \rightarrow 4d_{3/2}nl_j (n^* = 39.4)$

Zhang C.<sup>†1</sup>, Terabayshi R.<sup>1</sup>, Hasegawa S.<sup>1</sup> <sup>1</sup>The University of Tokyo, Japan

<sup>†</sup>zhangchao@sh.t.u-tokyo.ac.jp

Resonance Ionization Spectrometry (RIS) is a highly sensitive analytical method that exploits differences in atomic structure to achieve isotope selectivity. However, applying RIS to the analysis of strontium isotopes ( $^{84}\text{Sr}$ ,  $^{86}\text{Sr}$ ,  $^{87}\text{Sr}$ ,  $^{88}\text{Sr}$ ,  $^{89}\text{Sr}$ , and  $^{90}\text{Sr}$ ) presents challenges due to the small isotope shifts inherent to strontium isotopes and the potential overlap of isotope shifts for  $^{89}\text{Sr}$  and  $^{90}\text{Sr}$  with those of  $^{86}\text{Sr}$  and  $^{87}\text{Sr}$ , stemming from the magic-number nuclear structure of  $^{88}\text{Sr}$ .

This study introduces a three-step resonance ionization scheme ( $5s^2\ ^1S_0 \rightarrow 5s5p\ ^1P_1^0 \rightarrow 5p_{1/2}5p_{1/2} \rightarrow 4d_{3/2}nl_j (n^* = 39.4)$ ) designed to excite strontium atoms from the ground state to the Rydberg state, aiming to enhance the isotope selectivity and the ionization efficiency. Isotope shifts among natural strontium isotopes were investigated in the transitions  $5s^2\ ^1S_0 \rightarrow 5s5p\ ^1P_1^0 \rightarrow 5p_{1/2}5p_{1/2}$ . And Stark shifts of  $^{88}\text{Sr}$  atoms in the Rydberg state  $4d_{3/2}nl_j (n^* = 39.4)$  were systematically studied under varying external static electric fields.

Based on measured isotope shifts of natural strontium isotopes, the isotope shift for  $^{90}\text{Sr}$  against  $^{88}\text{Sr}$  was predicted in the transitions  $5s^2\ ^1S_0 \rightarrow 5s5p\ ^1P_1^0 \rightarrow 5p_{1/2}5p_{1/2}$ . Comparisons with previous studies explained the reason for the spectral overlap between  $^{90}\text{Sr}$  and  $^{86}\text{Sr}$  in strontium transition spectra in the transition  $5s^2\ ^1S_0 \rightarrow 5s5p\ ^1P_1^0$ .

Frequency spectra under this three-step resonance ionization revealed energy level shifts in opposite directions and a transition from quadratic to linear Stark shift when field strength increased, as depicted in Figure 1<sup>1</sup>.

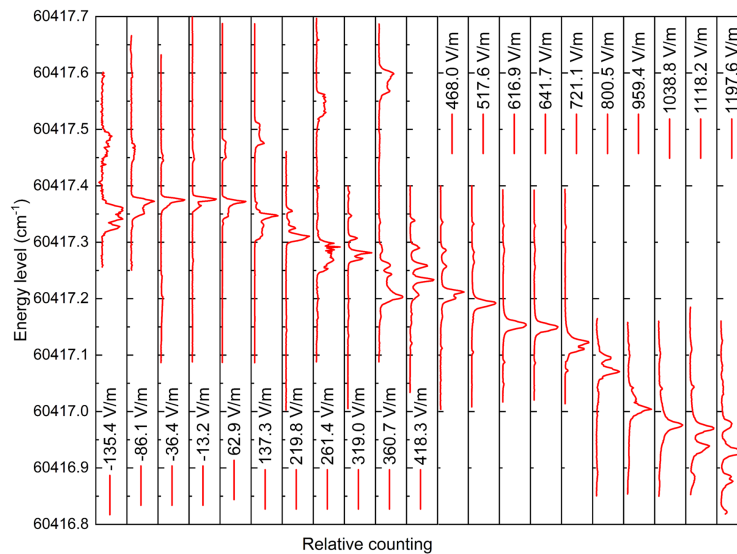


Figure 1: The Stark map for  $^{88}\text{Sr}$  near the energy level with an effective quantum number of 39.4.

This research provides crucial insights for the feasibility of developing multi-step resonance ionization mass spectrometry for strontium isotopes. Future experiments will focus on integrating this resonance ionization approach with laser cooling-ion trap technologies to explore more sensitive isotope detection techniques<sup>2</sup>.

<sup>1</sup>Chao Zhang, Ryohei Terabayashi and Shuichi Hasegawa, *Spectrochimica Acta Part B: Atomic Spectroscopy* **Volume 225**, 107118 (2025).

<sup>2</sup>Kyunghun Jung et al., *Physical Review A* **volume 96**, 043424 (2017).

Abstract number: P122

Friday 14:00-15:30

## High phasespace density of YO molecules

Hillberry L. E.<sup>†1</sup>, Mehling K.<sup>1</sup>, Bureau J. J.<sup>1</sup>, Scheidegger S.<sup>1</sup>, Chen M.<sup>1</sup>, Aggarwal P.<sup>1</sup>, Ye J.<sup>1</sup>

<sup>1</sup>JILA, National Institute of Standards and Technology and the University of Colorado, Boulder, Colorado 80309-0440  
Department of Physics, University of Colorado, Boulder, Colorado 80309-0390, USA

<sup>†</sup>logan.hillberry@jila.colorado.edu

Direct laser cooling of molecules has progressed steadily over the past decade. Now, the combination of single quantum-state control and a large molecular-frame dipole moment in the ground state elevates laser-cooled molecules as a platform for the future of quantum science. Specifically, large dipole moments mediate long range interactions that are of interest for many-body quantum physics and quantum simulation.

I will discuss ongoing work to create a high phasespace density of yttrium monoxide (YO) molecules. Key areas of this discussion include slowing from a buffer-gas-cooled laser ablation source, dual-frequency and convener-belt blue-detuned magneto-optical trapping, gray molasses cooling, and transfer to a crossed-beam optical dipole trap. Beyond these well-established methods, I will present our recent results on two-body collisional loss<sup>1</sup>, the first narrowline laser cooling of a molecule<sup>2</sup>, and progress towards microwave-based collisional shielding. In the near future, shielded collisions will enable rapid thermalization and evaporative cooling. Taken together, our work propels YO as a leading contender for Bose condensation of a directly laser cooled molecule.

<sup>1</sup>J.J. Bureau, K. Mehling, M.D. Frye, M. Chen, P. Aggarwal, J.M. Hutson, J. Ye, *Phys. Rev. A* **110**, L041306 (2024)

<sup>2</sup>K. Mehlin, et.al., arXiv:2503.13838 (2025)



Abstract number: P123  
 Friday 14:00-15:30

## A new machine for many-body physics investigation with dipolar quantum gases

**Lombardi P.**<sup>†1,2</sup>, **Sekhar P.P.**<sup>2</sup>, **Tanzi L.**<sup>1,3</sup>, **Feroli G.**<sup>3,2</sup>, **Modugno G.**<sup>3,2,1</sup>

<sup>1</sup>*National Institute of Optics, CNR, Sesto F.no, Italy*

<sup>2</sup>*LENS, Sesto F.no, Italy*

<sup>3</sup>*University of Firenze, Italy*

<sup>†</sup>lombardi@lens.unifi.it

We present a new setup for the realization of dipolar quantum gas samples of bosonic Dysprosium. Thanks to its large magnetic dipole moment and rich ground-state spin manifold, this system, along with other lanthanides, has emerged as a powerful platform for studying few- and many-body quantum phases of matter<sup>1</sup>. Notable directions for further investigation include supersolid phases<sup>2</sup> in arbitrary potentials (including optical lattices), exotic spinor phases and long-range-interaction spin-lattice models (also introducing synthetic gauge field via Raman coupling), as well as studies of thermodynamics and out-of-equilibrium non-thermal states in reduced dimensions.

The apparatus has been designed with the aim of incorporating some of the most innovative technical approaches developed in recent years and is currently under construction. The atom flux emerging from the oven is directly manipulated using a permanent magnet-based 2D magneto-optical trap, which can capture a large fraction of the atoms (over 10%) and reduce their mean velocity by two orders of magnitude. This stage is oriented such that the pre-cooled sample is free to move toward the science chamber for subsequent cooling stages. Numerical simulations and references in literature suggest that a  $10^5$ -atom dipolar Bose-Einstein condensate can be created with a cycle time of few seconds, enabling non-trivial statistical investigations.

<sup>1</sup>L. Chomaz et al., *Rep. Prog. Phys.* **86**, 026401 (2023).

<sup>2</sup>L. Tanzi et al., *Science* **371**, 6534 (2021).

Abstract number: P124  
Friday 14:00-15:30

## Quantum logic spectroscopy of the hydrogen molecular ion

Fabian Schmid<sup>†1</sup>, David Holzapfel<sup>1</sup>, Ho June Kim<sup>1</sup>, Qianlong He<sup>1</sup>, Nick Schwegler<sup>1</sup>, Oliver Stadler<sup>1</sup>, Martin Stadler<sup>1</sup>, Alexander Ferk<sup>1</sup>, Jonathan P. Home<sup>1</sup>, Daniel Kienzler<sup>1</sup>

<sup>1</sup>Department of Physics, ETH Zürich, Zurich, Switzerland

<sup>†</sup>schmidfab@phys.ethz.ch

I will present our latest results,<sup>1</sup> implementing pure quantum state preparation, coherent manipulation, and non-destructive state readout of the hydrogen molecular ion  $\text{H}_2^+$ .

$\text{H}_2^+$  is the simplest stable molecule, and its structure can be calculated *ab initio* with high precision using quantum electrodynamics. By comparing the calculations with experimental data, fundamental constants can be determined, and the validity of the theory itself can be tested. However, challenging properties such as high reactivity, low mass, and the absence of rovibrational dipole transitions have thus far strongly limited spectroscopic studies of  $\text{H}_2^+$ .

We trap a single  $\text{H}_2^+$  molecule together with a single beryllium ion using a cryogenic Paul trap apparatus, achieving trapping lifetimes of 11 h and ground-state cooling of the shared axial motion.<sup>2</sup> With this platform we have recently implemented *Quantum Logic Spectroscopy* of  $\text{H}_2^+$ . The  $\text{H}_2^+$  molecule is produced in a chosen rovibrational state using resonance-enhanced multiphoton ionization. We use quantum-logic operations between the molecule and the beryllium ion for the preparation of single hyperfine states and non-destructive state readout. In the lowest rovibrational state of ortho- $\text{H}_2^+$  (rotation  $L = 1$ , vibration  $\nu = 0$ ), we achieve a combined state-preparation and readout fidelity of 66.5(8)%. We demonstrate Rabi flopping on several hyperfine transitions using stimulated Raman transitions and microwaves. Utilizing a magnetic field insensitive hyperfine transition driven with a microwave, we perform a proof-of-principle spectroscopy and achieve a statistical uncertainty of 2 Hz in half an hour of measurement time (see Fig. [1](#)).

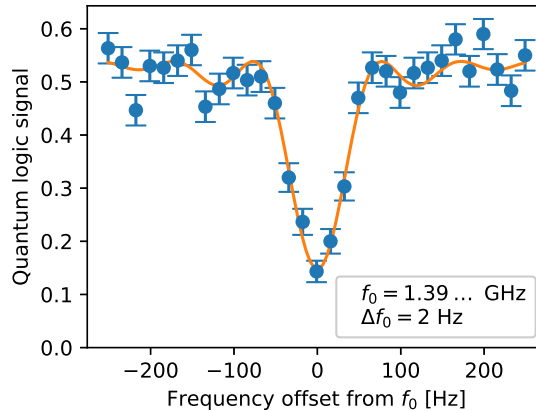


Figure 1: Hyperfine transition in the ( $L = 1$ ,  $\nu = 0$ ) ground state of ortho- $\text{H}_2^+$  measured using quantum logic spectroscopy.<sup>[481](#)</sup> The total measurement time is half an hour, and the statistical uncertainty of the fit is 2 Hz.

We are now performing a systematic measurement of the hyperfine structure which will provide a stringent test of state-of-the-art molecular theory and might enable putting an improved bound on a possible tensor force between the two constituent protons of the  $\text{H}_2^+$  molecule.<sup>3</sup>

Our results pave the way for high-precision rovibrational spectroscopy of single  $\text{H}_2^+$  molecules, which would enable tests of quantum electrodynamics, metrology of fundamental constants such as the proton-electron mass ratio, and the implementation of an optical molecular clock based on the simplest molecule in nature.

<sup>1</sup>D. Holzapfel *et al.*, arXiv:2409.06495 (2024).

<sup>2</sup>N. Schwegler *et al.*, *Phys. Rev. Lett.* **131**, 133003 (2023).

<sup>3</sup>N. F. Ramsey, *Physica* **96A**, 285 (1979).

Abstract number: P125  
Friday 14:00-15:30

## Continuous-wave superradiant laser based on a continuous cold atomic beam

Pargoire Y.<sup>†1</sup>, Laburthe-Tolra B.<sup>1</sup>, Pasquiou B.<sup>1</sup>, Huckans J.<sup>2</sup>, Robert-de Saint-Vincent M.<sup>1</sup>

<sup>1</sup> Université Sorbonne Paris Nord, LPL, France

<sup>2</sup> Commonwealth University of Pennsylvania

<sup>†</sup>yannis.pargoire@univ-paris13.fr

We are building a continuous superradiant laser on the narrow (7.5kHz) intercombination line of <sup>88</sup>Sr using a cold, fast (10-100m/s) atomic beam passing through the mode of a “bad” optical cavity. One of our goals is to study correlations that should arise between atoms, especially near the superradiant threshold.

Superradiant laser is an emerging technology, which is studied theoretically and experimentally to observe the first continuous superradiant emission. This light source can be used as frequency reference. Fundamental quantum fluctuations of the collective atomic dipole set the ultimate laser linewidth, allowing it to be lower than the natural width of the transition and it's frequency to be only slightly dependent on fluctuations in the positions of the cavity mirrors. Continuous superradiant laser can therefore overcome some current limitations of atomic clocks.

In the case of a pulsed superradiant laser, the linewidth is defined as in (1, left). In opposition, the linewidth of a continuous-wave superradiant laser is defined as in (1, right). With our setup, designed to be proof of principle of the continuous-wave superradiant laser in bad-cavity regime, we expect to reach a linewidth of 700Hz on the 7.5kHz natural width. For this purpose, we choose a low (C<1) single-atom cooperativity defined as  $C=g^2/(\kappa\gamma)$ , (C = 0.211 in our setup, with  $g = 2\pi \times 31.54\text{kHz}$  the coupling term between one atom and the cavity light,  $\gamma = 2\pi \times 7.5\text{kHz}$  the natural linewidth of the <sup>1</sup>S<sub>0</sub> – <sup>3</sup>P<sub>1</sub> transition,  $\kappa = 2\pi \times 630\text{kHz}$  the cavity losses) and need a high collective cooperativity (NC»1) with N the atom number inside the cavity.

$$\Delta w_{\text{Pulsed\_SR}} = \frac{Ng^2}{\kappa} \quad \Delta w_{\text{Continuous\_Wave\_SR}} = \frac{4g^2}{\kappa} \quad (0)$$

The dynamics of superradiance is described by the quantity  $N\frac{g^2}{\kappa}$ . For superradiance to occur one needs a superradiance dynamics quicker than the spontaneous emission dynamics, leading to  $N\frac{g^2}{\kappa} \gg \gamma$ . The continuous-wave regime requires a superradiance dynamics quicker than the refreshing rate  $\Gamma_R$  of the cavity, leading to  $N\frac{g^2}{\kappa} \gg \Gamma_R$ .

These conditions fix the minimum atom number to reach the superradiant emission threshold. For an atomic beam with a velocity of  $100\text{m.s}^{-1}$ , this threshold is 80 atoms, a criterion we already fulfilled in our setup.

To achieve, control and characterize superradiance, we use Zeeman slower to tune the atoms velocity, thereby controlling the flux and the refreshing rate. Out of the Zeeman slower, we need to deflect the atoms toward the cavity. For this purpose, we use a moving molasses and started characterizing its efficiency depending on the atom's forward velocity. Then, we use SWAP (Sawtooth Wave Adiabatic Passage) Cooling<sup>2</sup> on the <sup>1</sup>S<sub>0</sub> – <sup>3</sup>P<sub>1</sub> transition to reach  $\mu\text{K}$  temperature along the cavity axis. Finally, we have devised an adiabatic excitation scheme to be implemented just before the atoms reach the cavity, which we are currently testing.

Once our laser is emitting, we will characterize it with a beat note measurement and make photonic quantum correlation measurements. We will use the flexibility of our architecture to test different regimes such as having a distribution of velocity in the cavity axis that could lead to different collective dipoles interesting to study<sup>3</sup> and we will exchange the cavity to decrease the mirror reflectivity and try to reach a lower laser width.

<sup>1</sup>Bruno Laburthe-Tolra, Ziyad Amodjee, Benjamin Pasquiou and Martin Robert-de-Saint-Vincent, *SciPost Phys* **Core** **6**, 015 (2023).

<sup>2</sup>John P. Bartolotta, Matthew A. Norcia, Julia R. K. Cline, James K. Thompson and Murray J. Holland, *Phys. Rev. A* **98**, 023404 (2018).

<sup>3</sup>Simon B. Jäger, Haonan Liu, Athreya Shankar, John Cooper, Murray J. Holland, *Phys. Rev. A* **103**, 013720 (2021).

Abstract number: P126  
Friday 14:00-15:30

## Probing the interaction energy of two $^{85}\text{Rb}$ atoms in an optical tweezer via spin-motion coupling

Jun Zhuang<sup>1</sup>, Peng-Xiang Wang<sup>1,2</sup>, Kun-Peng Wang<sup>1</sup>, Xiao-Dong He<sup>†1,3</sup>, Ming-Sheng Zhan<sup>†1,3,4</sup>

<sup>1</sup>State Key Laboratory of Magnetic Resonance and Atomic and Molecular Physics, Wuhan Institute of Physics and Mathematics, Innovation Academy for Precision Measurement Science and Technology, Chinese Academy of Sciences, Wuhan 430071, China

<sup>2</sup>School of Physical Sciences, University of Chinese Academy of Sciences, Beijing 100049, China

<sup>3</sup>Wuhan Institute of Quantum Technology, Wuhan 430206, China

<sup>4</sup>Hefei National Laboratory, Hefei 230088, China

<sup>†</sup>hexd@apm.ac.cn; mszhan@apm.ac.cn

The inherent polarization gradients in tight optical tweezers can be used to couple the atomic spins to the two-body motion under the action of a microwave spin-flip transition<sup>1</sup>, so that such a spin-motion coupling (SMC) offers an important control knob on the motional states of optically trapped two colliding atoms. We have reported an alternative route to coherently bind two atoms into a weakly bound molecule via the spin-motion coupling<sup>2</sup>.

Here, after preparing two elastically scattering  $^{85}\text{Rb}$  atoms in the three-dimensional ground-state in the optical tweezer, we employed this control in order to probe the colliding energies of elastic and inelastic channels. As shown in Figure 1 the combination of microwave spectra and corresponding s-wave pseudopotential model allows us to infer the effect of the state-dependent trapping potentials on the elastic colliding energies, as well as to reveal how the presence of inelastic interactions affects elastic part of the relative potential<sup>3</sup>. Our work shows that the spin-motion coupling in a tight optical tweezer expand the experimental toolbox for fundamental studies of ultracold collisions in the two body systems with reactive collisions, and potentially for that of more complex interactions, such as optically trapped atom-molecule and molecule-molecule interactions.

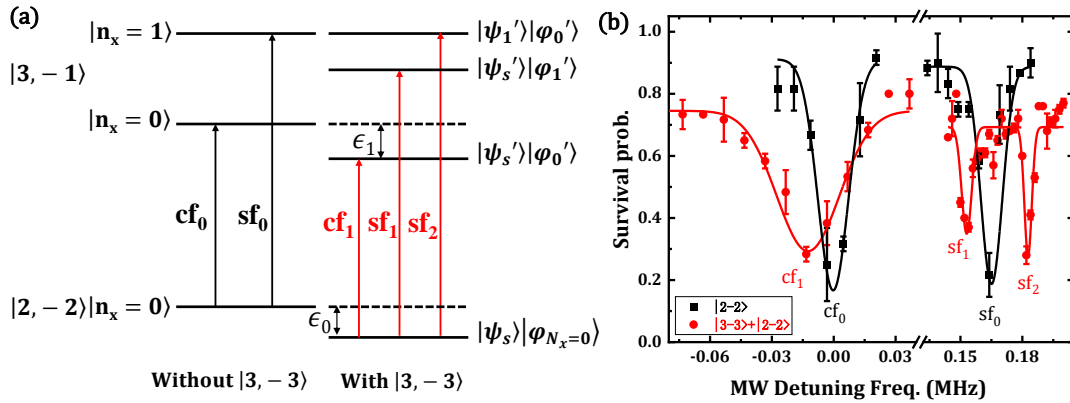


Figure 1: Schematic diagram of the transition and the MW spectra via SMC. (a) Schematic diagram of the vibrational transition of  $^{85}\text{Rb}$  atom. (b) MW spectra for spin flipping of  $|3, -3\rangle|2, -2\rangle \rightarrow |3, -3\rangle|3, -1\rangle$  (red filled circles) and  $|2, -2\rangle \rightarrow |3, -1\rangle$  (black filled squares). The spectra set the single atom transition carrier frequency (3028.0050(8) MHz) as the reference, and the solid curves are Gaussian fits of the data. The detuning frequency of the single-atom carrier peak is  $cf_0 = 0.0(8)$  kHz, while the detuning frequency of the diatomic carrier peak is  $cf_1 = -10.0(9)$  kHz. Furthermore, the detuning frequency of the single-atom sideband peak is measured to be  $sf_0 = 163.2(5)$  kHz. For two-atom system, around the  $sf_0$  two distinct peaks show up:  $sf_1 = 153.0(5)$  kHz and  $sf_2 = 182.8(3)$  kHz.

<sup>1</sup>K. P. Wang, J. Zhuang, X. D. He, R. J. Guo, C. Sheng, P. Xu, M. Liu, J. Wang, and M. S. Zhan, *Chin. Phys. Lett.* **37**, 044209(2020).  
<sup>2</sup>X. D. He, K. P. Wang, J. Zhuang, P. Xu, X. Gao, R. J. Guo, C. Sheng, M. Liu, J. Wang, J. M. Li, G. V. Shlyapnikov, and M. S. Zhan, *Science* **370**, 331(2020).  
<sup>3</sup>J. Zhuang, K. P. Wang, P. X. Wang, M. R. Wei, B. Mamat, C. Sheng, P. Xu, M. Liu, J. Wang, X. D. He, and M. S. Zhan, *Phys. Rev. A* **109**, 043320(2024).

Abstract number: P127  
Friday 14:00-15:30

# Squeezing-enhanced accurate differential sensing under large phase noise

**Robin Corgier<sup>†1</sup>**, **Marco Malitesta<sup>2,3</sup>**, **Leonid A. Sidorenkov<sup>1</sup>**, **Franck Pereira Dos Santos<sup>2,3</sup>**, **Gabriele Rosi<sup>3,4</sup>**, **Guglielmo M. Tino<sup>2, 3, 4, 5</sup>**, **Augusto Smerzi<sup>2,5,6</sup>**, **Leonardo Salvi<sup>3,4,5</sup>**, **Luca Pezzè<sup>2,5,6</sup>**,

<sup>1</sup>*LTE, Observatoire de Paris, Université PSL, Sorbonne Université, Université Lille, LNE, CNRS, 61 avenue de l'Observatoire, 75014 Paris, France*

<sup>2</sup>*Istituto Nazionale di Ottica, Consiglio Nazionale delle Ricerche (INO-CNR), Largo Enrico Fermi 6, 50125 Firenze, Italy.*

<sup>3</sup>*Department of Physics and Astronomy, Università di Firenze, Via Sansone 1 50019 Sesto Fiorentino, Italy*

<sup>4</sup>*Istituto Nazionale di Fisica Nucleare (INFN), Via Sansone 1, 50019 Sesto Fiorentino, Italy*

<sup>5</sup>*Istituto Nazionale di Ottica, Consiglio Nazionale delle Ricerche (INO-CNR), Largo Enrico Fermi 6, 50125 Firenze, Italy.*

<sup>6</sup>*European Laboratory for Nonlinear Spectroscopy (LENS), Via Nello Carrara 1, 50019 Sesto Fiorentino, Italy QSTAR, Largo Enrico Fermi 2, 50125 Firenze, Italy.*

<sup>†</sup>robin.corgier@obspm.fr

The use of entangled quantum states is widely recognized as a key factor in advancing quantum technologies beyond classical limits. While entanglement has enabled higher sensitivities in proof-of-principle experiments under highly controlled conditions, its applicability to real-world measurements remains an open debate. Differential measurement schemes, which effectively reject common-mode noise, are essential in high-precision atom interferometry—spanning from practical applications like underground gravity mapping to fundamental research in dark matter detection and tests of the equivalence principle. Differential atom interferometers are now reaching quantum noise-limited precision<sup>1</sup>. It is therefore crucial to determine whether entangled states can enhance the sensitivity of differential interferometer configurations. In the context of quantum-enhanced metrology, the main challenges consist to integrate compatible entanglement protocols in quantum sensors to enhance precision<sup>2</sup> while ensuring robustness against noise<sup>3</sup> and systematics effects<sup>4</sup>.

Here<sup>4</sup>, we investigate a differential phase measurements between two atom interferometers interrogated by the same laser and benefiting of spin-squeezing dynamics in the limit where the common-mode phase noise spans the full  $2\pi$  range. The differential signal is estimated using model-free ellipse fitting, a robust method requiring no device calibration and resilient to additional noise sources. Our results show that spin-squeezing not only improve the sensitivity of differential measurements but also allow to reduce the inherent measurement bias in ellipse fitting methods, further enhancing accuracy. We benchmark our protocol against the Cramer-Rao bound and compare it with hybrid methods that incorporate auxiliary classical sensors. Our findings provide a pathway to robust and high-precision atom interferometry, in realistic noisy environments and using readily available states and estimation methods.

<sup>1</sup>C. Janvier *et al.*, *Compact differential gravimeter at the quantum projection-noise limit*, *Phys. Rev. A* **105**, 022801 (2022)

<sup>2</sup>R. Corgier *et al.*, *Delta-kick Squeezing* *Phys. Rev. L* **127**, 183401 (2021)

<sup>3</sup>R. Corgier *et al.*, *Quantum-enhanced differential atom interferometers and clocks with spin-squeezing swapping*, *Quantum* **7**, 965 (2023)

<sup>4</sup>R. Corgier *et al.*, *Squeezing-enhanced accurate differential sensing under large phase noise*, arxiv 2501.18256 (2025)

Abstract number: P128

Friday 14:00-15:30

# The Spectroscopic Investigation of Carbon Clusters in a Thermal Source

**Robinson-Tait J.<sup>†</sup>, Kjaer J. K., Eriksen A. S., Gomez-Fernandez L., Thomsen J. W.**

*NNF Quantum Computer Programme, Niels Bohr Institute, University of Copenhagen, Denmark*

<sup>†</sup>julian.robinson-tait@nbi.ku.dk

We investigate the formation of carbon clusters ( $C_n$ ) in a 1500 K carbon source, with the aim of manipulating and controlling these molecules via laser cooling techniques.

The direct laser probing and cooling of neutral carbon (C) has eluded optics labs due to the challenging wavelengths around 150 nm required to do so. At these wavelengths, most materials are lossy. An alternative approach to producing ultra-cold carbon could be found by looking towards carbon containing molecules.

Molecules are typically considered challenging to laser cool due to the many transitions that must be driven to cycle enough photons for a significant cooling force. However, these transitions are often comfortable wavelengths to generate at high power. Pioneering work<sup>1</sup> has identified a series of ten optical transitions in the visible and near-visible regions to laser cool the carbon dimer ( $C_2$ ). We are currently developing laser sources, frequency-stabilized using an optical frequency comb, in preparation for the high-resolution spectroscopic measurements of these transitions. The transitions of the first three rotational bands from the  $a(^3\Pi_u)$  to the  $d(^3\Pi_g)$ ,  $J = 0$  band are shown in figure 1. The data is taken from the ExoMol database<sup>2</sup>.

Carbon dimers are transient species that can form under specific conditions from various carbon sources. Common production methods include electric arc discharges, laser ablation, and chemical synthesis using alkynyl- $\lambda^3$ -iodane compounds. In a thermal source, roughly 10% of the flux is  $C_2$ , with diminishing fractions consisting of larger clusters  $C_n$ . This source will make a suitable starting point for initial spectroscopic tests while more complicated sources are investigated.

An alternative route to radiation pressure manipulation could be ionization of  $C_2$ . Using pulsed lasers, two photons can be used to ionize the molecule<sup>3</sup>.

At the conference, we present our initial results on the formation of carbon dimers and the measured ratios of atomic carbon to carbon clusters at various source temperatures.

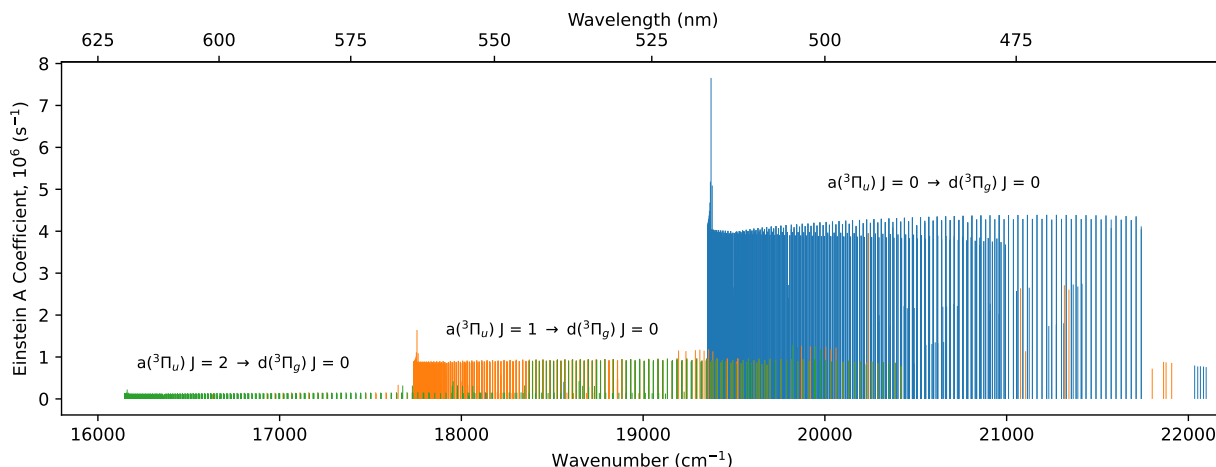


Figure 1: **Swan Band.** The line transitions for the lowest three rotational bands in the  $a(^3\Pi_u)$  to the  $d(^3\Pi_g)$ ,  $J = 0$  for  $C_2$ , taken from the ExoMol database. The three bands are labeled accordingly, but note there is overlap between the lines.

<sup>1</sup>N. Bigagli, D. W. Savin, S. Will, Laser cooling scheme for the carbon dimer ( $^{12}C_2$ ), Phys. Rev. A., 105 (5): L051301

<sup>2</sup>S. N. Yurchenko, I. Szabó, E. Pyatenko, J. Tennyson, ExoMol line lists XXXI: spectroscopy of lowest eight electronic states of  $C_2$ , Monthly Notices of the Royal Astronomical Society, 480 (3): 3397–3411

<sup>3</sup>O. Krechkivska, G. B. Bacskay, B. A. Welsh, K. Nauta, S. H. Kable, J. F. Stanton, T. W. Schmidt; The ionization energy of  $C_2$ . J. Chem. Phys. 144 (14): 144305.

Abstract number: P129  
Friday 14:00-15:30

# Optical Cooling and Trapping of Germanium

Eriksen A. S.<sup>†1</sup>, Robinson-Tait J.<sup>1</sup>, Gómez-Fernández L.<sup>1</sup>, Kjær J.K.<sup>1</sup>, Thomsen J.W.<sup>1</sup>

<sup>1</sup> NNF Quantum Computer Programme, Niels Bohr Institute, University of Copenhagen, Denmark

<sup>†</sup>andrea.eriksen@nbi.ku.dk

We look into the properties of germanium atoms with the purpose of investigating laser cooling and trapping of these atoms by addressing its principal optical transitions, as shown in Figure 1. Understanding the details of the highlighted cooling and repumping transitions will be crucial for achieving efficient population cycling.

Pioneering research has measured hyperfine structure coefficients for some germanium transitions<sup>12</sup>, but the optical properties of germanium remain largely unexplored. The prospect of this work is to do spectroscopic measurements on germanium to map out the hyperfine structure of the <sup>73</sup>Ge (I=9/2) isotope, and the isotope shifts between the stable isotopes which, to our knowledge, has not previously been measured.

The main challenge of laser cooling germanium atoms is that most transitions have wavelengths in the UV-C, resulting in large saturation intensities. Part of this work is to identify an efficient way to generate light at the 209 nm at high enough powers for cooling and trapping to be possible.

In contrast to other laser cooled elements, germanium has a notably low vapour pressure requiring oven temperatures around 1500 K in order to generate a sufficient atomic flux. This necessitates careful considerations in regard to the design of the oven and the vacuum chamber.

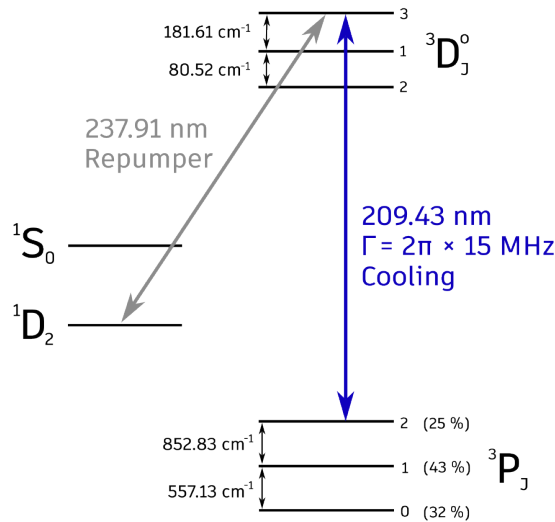


Figure 1: Ge transitions of interest.

<sup>1</sup>W. J. Childs, L. S. Goodman, *Physical Review* **141**, 15 (1966).

<sup>2</sup>A. Kanellakopoulos *et al.*, *Physical Review C* **102**, 054331 (2020).

Abstract number: P130

Friday 14:00-15:30

## Quantum Sensing in Space for Fundamental Physics and Earth Observation

**Gaaloul N.**<sup>†1</sup> for the MAIUS, CUAS, STE-QUEST and CARIOQA consortia

<sup>1</sup>*Leibniz University of Hanover, Institute of Quantum Optics, Hanover, Germany*

<sup>†</sup>gaaloul@iqo.uni-hannover.de

Space-borne quantum technologies and more particularly atom-interferometry-based devices are announcing a new era of strategic, intense space exploitation. Indeed, space offers a unique environment characterized by low-noise and low-gravity necessary for a wide spectrum of applications ranging from time and frequency transfer to Earth observation and the exploration of fundamental laws of physics.

Efforts to operate atom physics experiments in these ideal conditions are however challenged by a number of technical limitations as the extreme miniaturization or power consumption requirements for example. In this contribution, we report about recent advances of pioneering successful space implementations of atom optics experiments<sup>1,2,3,4</sup> as well as about recent mission concepts based on the use of quantum-gas sensors. Of particular interest for Fundamental Physics, is the satellite mission Space-Time Explorer and QUantum Equivalence Principle Space Test (STE-QUEST)<sup>5,6</sup> featuring a dual-species atom interferometer operating over tens of seconds, which will address some of the most fundamental and puzzling questions of physics by testing the universality of free fall with an accuracy better than one part in  $10^{-17}$ , searching for different types of Ultra-Light Dark Matter (ULDM) and testing the foundations of quantum mechanics.

Moreover, atomic sensors could also map temporal variations in Earth's gravity field opening the era of Space Quantum Gravimetry. We will report on the CARIOQA satellite mission pathfinder<sup>7</sup>, recently endorsed by the European Commission. It is set to lay the groundwork for a space Geodesy mission, utilizing atom accelerometers.

<sup>1</sup>D. Becker, et al., Space-borne Bose–Einstein condensation for precision interferometry, *Nature*, **562**, 391 (2018).

<sup>2</sup>M. D. Lachmann, et al., Ultracold atom interferometry in space, *Nature Comm.* **12**, Article number: 1317 (2021).

<sup>3</sup>D. Aveline, et al., Observation of Bose–Einstein condensates in an Earth-orbiting research lab, *Nature*, **582**, 11 (2020).

<sup>4</sup>N. Gaaloul, et al., A space-based quantum gas laboratory at picokelvin energy scales, *Nature Communications*, **13**:7889 (2022).

<sup>5</sup>H. Ahlers, et al., “STE-QUEST: Space Time Explorer and QUantum Equivalence principle Space Test”, arXiv:2211.15412 (2022).

<sup>6</sup>C. Struckmann, et al., Platform and environment requirements of a satellite quantum test of the Weak Equivalence Principle at the  $10^{-17}$  level, *Phys. Rev. D* **109**, 064010 (2024).

<sup>7</sup>T. Lévêque, C. Fallet, J. Lefebvre, et al., Proc. SPIE — ICSO 12777, (2023).



Abstract number: P131  
Friday 14:00-15:30

## Programmable Arrays of Rydberg Ytterbium Atoms for Quantum Computing

**Beller T.**<sup>†1</sup>, **Joshi K.**<sup>4</sup>, **Vanni A.**<sup>1</sup>, **Wolswijk L.**<sup>2</sup>, **Trenkwalder A.**<sup>2,3</sup>, **Catani J.**<sup>2,3</sup>, **Cataliotti F. S.**<sup>1,2,3</sup>, **Roati G.**<sup>2,3</sup>, **Fallani L.**<sup>1,2,3</sup>, **Tanzi L.**<sup>2,3</sup>

<sup>1</sup>*Department of Physics, University of Florence, 50019 Sesto Fiorentino, Italy*

<sup>2</sup>*Istituto Nazionale di Ottica del Consiglio Nazionale delle Ricerche (CNR-INO), Sezione di Sesto Fiorentino, 50019 Sesto Fiorentino, Italy*

<sup>3</sup>*European Laboratory for Non-Linear Spectroscopy (LENS), 50019 Sesto Fiorentino, Italy*

<sup>4</sup>*Department of Physics, University of Naples Federico II, 80126 Naples, Italy*

<sup>†</sup>thomas.beller@unifi.it

We report on the ongoing efforts in developing, as well as initial implementation stages, of an experimental setup for the realization of a quantum computational platform based on neutral fermionic  $^{171}\text{Yb}$  atoms trapped in optical tweezers with reconfigurable geometries.

Leveraging on a richer electronic structure compared to alkali atoms, Ytterbium, amongst alkaline-earth(-like) atoms, enables a variety of different qubit encoding schemes drawing upon the so-called *omg* (optical-metastable-ground) architecture<sup>1</sup>. Indeed, having  $^{171}\text{Yb}$  a nuclear spin  $I = 1/2$ , it is extremely well suited to be used as a purely nuclear-spin qubit, offering a naturally more environmentally isolated system than what achievable with encodings on hyperfine Zeeman states usually employed in alkalis. Moreover, besides a  $J = 0$  ground state, the excited  $6s6p\ ^3P_0$  metastable state, offers an additional purely nuclear-spin manifold, which can be pivotal for the implementation of quantum error correction schemes relying on ancilla and data qubits. The chosen approach for our setup will allow the possibility of coherent control of the ground and metastable nuclear-spin qubits, as well as the optical clock  $^1S_0 \rightarrow ^3P_0$  transition, so as to fully exploit Ytterbium's structure. Multi-qubit gates will instead be implemented exploiting state-selective coupling to Rydberg states.

<sup>1</sup>J. W. Lis, A. Senoo, W. F. McGrew, F. Rönchen, A. Jenkins, and A. M. Kaufman, *Phys. Rev. X* **13**, 041035 (2023).

Abstract number: P132  
Friday 14:00-15:30

## Zero-contrast clock interferometry

**Sanner C.<sup>†1</sup>, Lide M.<sup>1</sup>**

<sup>1</sup>*Colorado State University, Department of Physics, Colorado, USA*

<sup>†</sup>sanner@colostate.edu

Unlike in traditional atom interferometers, where internal degrees of freedom of the split matter waves are not manipulated, one performs in clock interferometers simultaneous spectroscopic interrogation of the interfering particles. Following up on recent work<sup>1</sup> by Z. Zhou et al., we systematically analyze the signal-to-noise ratios (SNRs) for a variety of clock interferometry configurations. We identify the zero-visibility point of the interferometer, where the internal states of the atoms are orthogonal, as a preferred working point in terms of attainable SNR for internal state readout and common-mode external path length noise suppression. This opens new avenues for the design of clock interferometers probing general relativistic proper time.

---

<sup>1</sup>Zhifan Zhou, Sebastian C. Carrasco, Christian Sanner, Vladimir S. Malinovsky and Ron Folman, Geometric phase amplification in a clock interferometer for enhanced metrology, *Science Advances*, in press (2025).

Abstract number: P133  
Friday 14:00-15:30

# Operation of Yb optical lattice clock at sub- $\mu$ K atomic temperature and international clock comparisons

**Goti I.<sup>†1</sup>, Petrucciani T.<sup>1</sup>, Condio S.<sup>1</sup>, Clivati C.<sup>1</sup>, Donadello S.<sup>1</sup>, Levi F.<sup>1</sup>, Calonico D.<sup>1</sup>, Pizzocaro M.<sup>1</sup>**  
<sup>1</sup>*Istituto Nazionale di Ricerca Metrologica (INRIM), 10135 Torino, Italy*

<sup>†</sup>i.goti@inrim.it

In this poster, I will present recent results from IT-Yb1, the Yb lattice clock developed at INRIM (Italy)<sup>1</sup>. These results include the implementation of clock-mediated Sisyphus cooling<sup>2</sup> in the atomic loading sequence and participation in international optical clock comparisons via fiber link.

By introducing Sisyphus cooling for  $T_{\text{cool}} = 300$  ms in the lattice loading sequence of IT-Yb1, we have successfully reduced both the longitudinal ( $T_z$ ) and radial ( $T_r$ ) atomic temperatures below the  $\mu$ K level. As shown in Fig. 1, two sideband spectra were recorded, from which the atomic temperatures and the lattice depth are derived. The purple dots correspond to data where both  $T_z$  and  $T_r$  are about 500 nK. Moreover, we integrated Sisyphus cooling in the entire clock cycle for  $T_{\text{cool}}=50$  ms, allowing us to reduce the usual working condition from a lattice depth of 100 to 50 Er, where Er is the recoil energy. The choice of reducing the Sisyphus time  $T_{\text{cool}}$  represents a compromise between cooling efficiency and minimizing the dead time in the clock cycle, which would otherwise degrade its stability. In our experiment, the dead time is 230 ms, over a total clock cycle time of 350 ms.

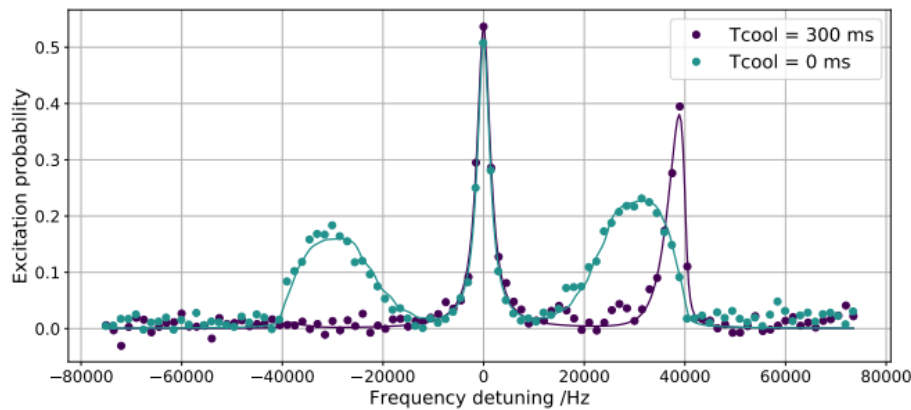


Figure 1: Sideband spectroscopy results obtained without Sisyphus cooling (light blue dots), and with a Sisyphus stage of  $T_{\text{cool}}=300$  ms (purple dots). By adding the Sisyphus cooling procedure, the longitudinal temperature  $T_z$  is reduced from about 4  $\mu$ K to 500 nK and the radial temperature  $T_r$  from 1.5  $\mu$ K to 600 nK. Both spectra are obtained for a lattice depth of 110 Er.

The precise control over the atomic state enabled by Sisyphus cooling significantly benefits the reduction of systematic shifts. Additionally, by exploring a wide range of temperatures and lattice depths, we highlight the importance of accurate atomic temperature measurements for light shift characterization, aiming to establish a reliable and consistent method to evaluate the lattice shift at the  $10^{-18}$  level. These are crucial steps towards the validation of optical standards in view of the upcoming redefinition of the second.

However, it is essential to make direct comparisons to validate the systematic uncertainty of optical frequency standards and investigate the level of agreement between different clocks. To this end, three international clock comparison campaigns were carried out in 2022 (ROCIT campaign), 2023 (ICON campaign) and 2025 (TOCK campaign), where IT-Yb1 was compared for the first time with optical clocks at PTB (Germany), NPL (UK), and SYRTE (France). Frequency ratios were determined through a European fiber link network, which introduces negligible uncertainty<sup>3</sup>. These comparisons enable the measurement of several new frequency ratios. Moreover, the involvement of a large number of optical clocks in different countries facilitates the identification of inconsistencies and allows for the detection of experiments that may not be operating correctly.

<sup>1</sup>I. Goti *et al.*, *Metrologia* **60** (3)

<sup>2</sup>C.-C. Chen *et al.*, *Phys. Rev. Lett.* **133**, 053401 (2024).

<sup>3</sup>C. Clivati *et al.*, *Physical Review Applied* **18** (5), 054009 (2022).

Abstract number: P134  
Friday 14:00-15:30

## Status of the Laser System for Cold Atom Experiments in BECCAL onboard the ISS

**Beck H.<sup>1</sup>, Thaivalappil Sunilkumar H.<sup>1</sup>, Kitzmann M.<sup>1</sup>, Schoch M.<sup>1</sup>, Weise C.<sup>1</sup>, Leykauf B.<sup>1</sup>, Kovalchuk E.<sup>1</sup>,  
Pohl J.<sup>1</sup>, Peters A.<sup>1</sup>, the BECCAL Collaboration<sup>1,2,3,4,5,6,7,8,9,10</sup>**

<sup>1</sup>*Humboldt University Berlin, Germany*

<sup>2</sup>*FBH Berlin, Germany*

<sup>3</sup>*JGU, Mainz, Germany*

<sup>4</sup>*LUH, Hanover, Germany*

<sup>5</sup>*DLR-SI, Hanover, Germany*

<sup>6</sup>*DLR-QT, Hanover, Germany*

<sup>7</sup>*UULM, Ulm, Germany*

<sup>8</sup>*ZARM, Bremen, Germany*

<sup>9</sup>*DLR, Bremen, Germany*

<sup>10</sup>*DLR-SC, Braunschweig, Germany*

<sup>†</sup>hamish@physik.hu-berlin.de

The Bose-Einstein Condensate and Cold Atom Laboratory (BECCAL) has been designed for operation onboard the International Space Station (ISS). This multi-user facility will enable experiments with K and Rb ultra-cold atoms and BECs in microgravity. Fundamental physics will be explored at longer time- and lower energy-scales compared to those achievable on earth.

The BECCAL laser system is comprised of micro-integrated diode lasers, miniaturized free-space optics on Zerodur boards, and a system of fibred components to bring light to the physics package. The design is subject to strict Size, Weight, and Power (SWaP) constraints, and the operation of the system is supported by extensive ground-based systems.

An update on the progress of the laser system is presented, showing the flight model design and the status of ground-based systems built from commercial components.

This work is supported by the DLR with funds provided by the BMWK under grant number 50WP2102.

Abstract number: P135  
Friday 14:00-15:30

## Three-component few-fermion mixtures in one-dimensional geometry

Teske M.<sup>1</sup>, Sowiński T.<sup>†1</sup>

<sup>1</sup>*Institute of Physics, Polish Academy of Sciences, Warsaw, Poland*

<sup>†</sup>tomasz.sowinski@ifpan.edu.pl

This presentation will discuss the many-body ground-state properties of an ultra-cold three-component mixture of a few fermions confined in the one-dimensional harmonic trap and interacting with zero-range forces. The system is described with the Hamiltonian:

$$\hat{H} = \sum_{\sigma} \int dx \hat{\Psi}_{\sigma}^{\dagger}(x) \left[ -\frac{1}{2} \frac{d^2}{dx^2} + \frac{1}{2} x^2 \right] \hat{\Psi}_{\sigma}(x) + \sum_{\sigma \neq \sigma'} g_{\sigma\sigma'} \int dx \hat{\Psi}_{\sigma}^{\dagger}(x) \hat{\Psi}_{\sigma'}^{\dagger}(x) \hat{\Psi}_{\sigma'}(x) \hat{\Psi}_{\sigma}(x), \quad (1)$$

where  $\Psi_{\sigma}(x)$  is the fermionic field operator annihilating particle from the component  $\sigma \in \{A, B, C\}$  at position  $x$ . Starting with a simple system of a two-component mixture of four repulsively interacting particles belonging to components A and B, we explore the impact of interactions with an additional particle from the third component. We find that for any two-component repulsion  $g_{AB}$ , along with increasing interaction with third component  $g = g_{AC} = g_{BC}$ , the system undergoes a structural transition in the spatial ordering of the components. This transition is clearly visible in the single-particle density profiles

$$n_{\sigma}(x) = \langle G | \hat{\Psi}_{\sigma}^{\dagger}(x) \hat{\Psi}_{\sigma}(x) | G \rangle \quad (1)$$

as well as in the inter-component two-particle correlations

$$\mathcal{G}_{AB}(x, x') = \langle G | \hat{n}_A(x) \hat{n}_B(x') | G \rangle - \langle G | \hat{n}_A(x) | G \rangle \langle G | \hat{n}_B(x') | G \rangle. \quad (1)$$

An example of a particular choice of  $g_0 = 0.4$  is presented in Fig. 1. We show that with appropriately adapted scaling techniques this specific transition can be well-understood.

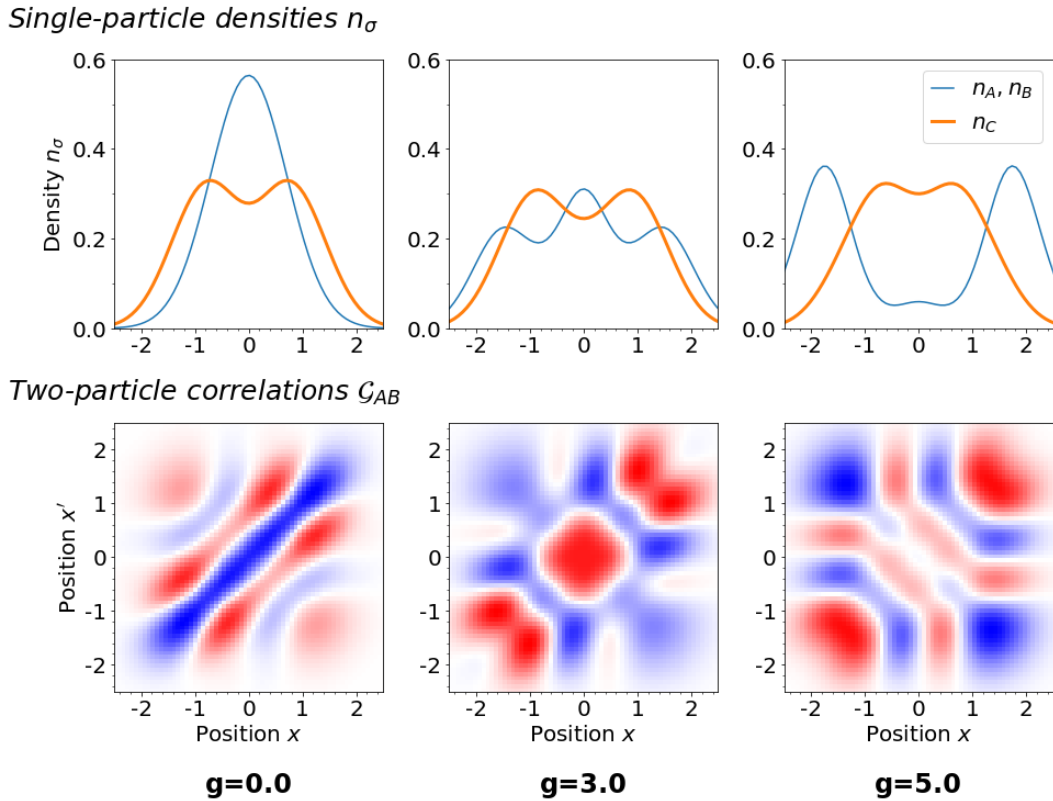


Figure 1: Single-particle density profiles and two-particle correlations for a three-component mixture of fermions obtained for different inter-component interactions. Along with increasing interactions with the third component, the system undergoes structural transition, which we carefully study in the framework of the scaling methods.

Abstract number: P136

Friday 14:00-15:30

## Fano-shaped Feshbach resonances in ultracold dipolar spin mixtures

**Houwman J. J. A.**<sup>†1</sup>, **Lafforgue L.**<sup>1</sup>, **Embacher S.**<sup>2</sup>, **Mark M. J.**<sup>1,2</sup>, **Ferlaino F.**<sup>1,2</sup>

<sup>1</sup>*Universität Innsbruck, Institut für Experimentalphysik, 6020 Innsbruck, Austria*

<sup>2</sup>*Institut für Quantenoptik und Quanteninformation, Österreichische Akademie der Wissenschaften, 6020 Innsbruck, Austria*

<sup>†</sup>arfor.houwman@uibk.ac.at

Lanthanide atoms, such as erbium and dysprosium, feature unique properties compared to alkali atoms including a large spin manifold in their absolute ground state, complex collisional behaviour in the ultracold regime and long-range dipolar interactions. Precise control over the initial spin composition of the system - by applying a sequence of Rabi pulses with a laser tuned to a clock-like transition at 1299nm<sup>1</sup> - allows us to study spin-dependent scattering processes.

We explore the collisional properties of a variety of spin mixtures of erbium, observing multiple inter- and intra-spin scattering resonances. Some resonances feature a distinctive Fano shape, where we observe a remarkable suppression of losses, indicative of interference phenomena during the collision. We model the system with a multi-channel square-well model and find good agreement with the experimental data. By combining our high-fidelity spin preparation technique with additional confinement of the atoms in 3D optical lattices, we plan to further investigate those spin mixtures. This will pave the way for implementing advanced spin models in lattice systems.

---

<sup>1</sup>Claude, F., Lafforgue, L., Houwman, J. J. A., Mark, M. J., & Ferlaino, F. Physical Review Research 6(4), L042016 (2024).

Abstract number: P137  
Friday 14:00-15:30

## Photon statistics in a steady-state superradiant laser

Schäffer S. A.<sup>†1,2</sup>, Gentil N.<sup>2,3</sup>, Kristensen S. L.<sup>2,4</sup>, Müller J. H.<sup>2</sup>

<sup>1</sup>NNF Quantum Computing Programme (NQCP), Niels Bohr Institute, University of Copenhagen, Copenhagen, Denmark

<sup>2</sup>Niels Bohr Institute, University of Copenhagen, Copenhagen, Denmark

<sup>3</sup>Technical University of Eindhoven, Eindhoven, Netherlands

<sup>4</sup>Max-Planck-Institut für Quantenoptik, Garching, Germany

<sup>†</sup>schaffer@nbi.ku.dk

Narrow optical transitions in ensembles of atoms can be used to generate superradiant laser emission for robust atom-based reference lasers and clocks. Superradiance allows the emission of useful light intensities from transitions that are naturally narrow, and whose emission rates are exceedingly slow.

Inverting a collective ensemble will produce short superradiant bursts which give spectrally broad Fourier-limited linewidths. If one can instead achieve sustained emission from a collective state coupled to a bad optical cavity, this would produce Purcell-narrowed emission spectra<sup>1</sup>. The achievable linewidths can be in the mHz regime  $\Delta\nu = C\gamma$ , where  $C$  is the atom-cavity cooperativity and  $\gamma$  is the natural decay rate of the bare atomic transition. For bad cavities the cooperativity can be significantly lower than 1 leading to emission spectra orders of magnitude lower than the natural linewidth of the transition. Additionally, this regime will lead to a suppression of the spectral sensitivity to cavity noise, thus making such a laser robust to environmental effects such as thermal and mechanical vibrations in the mirror substrates and coatings.

Steady-state superradiance can be achieved by using cold atoms that are continuously fed through an optical cavity<sup>2,3</sup>, or by repumping atoms that reside inside an optical cavity volume<sup>4</sup>. Several experiments are now pursuing the realization of continuous superradiant emission from a narrow atomic transition, but so far, only quasi-continuous operation has been shown.

The onset-dynamics and collective nature of superradiant ensembles poses the questions whether the emission state is expected to be purely coherent, thermal or something else. The evolution of the photon statistics have been studied for pulsed emission<sup>5,6</sup> and in extended ensembles of Rb atoms<sup>7</sup>, but not in a coupling-symmetric Dicke picture as realized either by the ensemble dimensions  $L \ll \lambda$  or using cavity coupling. By repumping cold strontium-88 atoms we can achieve several ms of steady-state superradiant emission<sup>8</sup> on the intercombination line  $^1S_0 - ^3P_1$ . This allows us to measure the evolution of photon statistics during onset, steady-state and chaotic superradiance. We present the observed statistics and its consequences for the use of superradiant emission as a resource in light generation and fast state readout.

<sup>1</sup>D. Meiser, Jun Ye, D. R. Carlson, and M. J. Holland, *Physical Review Letters* **102**, 163601 (2009).

<sup>2</sup>H. Liu *et al.*, *Physical Review Letters* **125**, 253602 (2020).

<sup>3</sup>F. Famà *et al.*, *Physical Review A* **110**, 063721 (2024).

<sup>4</sup>M. A. Norcia and J. K. Thompson, *Physical Review X* **6**, 011025 (2016).

<sup>5</sup>C. Bach, F. Tebbenjohanns, C. Liedl, P. Schneeweiss, and A. Rauschenbeutel, *arXiv:2407.12549* (2024).

<sup>6</sup>G. Ferioli, I. Ferrier-Barbut, and A. Browaeys, *arXiv:2410.08652* (2024).

<sup>7</sup>G. Ferioli, *et al.*, *Physical Review Letters* **132**, 133601 (2024).

<sup>8</sup>S. L. Kristensen *et al.*, *Physical Review Letters* **130**, 223402 (2023).

Abstract number: P138  
Friday 14:00-15:30

## Paraxial quantum fluid of light in cold atomic cloud

Sukhman Kler Singh<sup>1</sup>, Devang Naik<sup>1</sup>, Simon Lepleux<sup>1</sup>, Quentin Schiebler<sup>1</sup>, Quentin Glorieux<sup>†1</sup>

<sup>1</sup>Laboratoire Kastler Brossel, Sorbonne Université, ENS, Collège de France, Paris, France

<sup>†</sup>quentin.glorieux@lkb.upmc.fr

The mean field evolution of a Bose-Einstein condensate (BEC) is described by the GPE which is a non linear version of the Schrödinger equation. The paraxial propagation of light in a  $\chi^{(3)}$  media is similarly described by a non linear Maxwell equation which can be formally mapped onto the GPE. Hence, one can define an effective mass and an interaction term for the photons, to describe them as a quantum fluid of light.

The time evolution of the matter wave is replaced by the spatial evolution in the propagation direction for the light. The dynamics in the transverse plane mimics one of a 2D Bose gas. In terms of hydrodynamical equations for photons, the fluid density is given by the intensity while the fluid velocity is given by the spatial-phase gradient.

The interaction strength can be tuned via the atomic density or laser detuning with respect to the atomic resonance. Furthermore, the photon-photon interactions can be enhanced using a coherent optical scheme such as electromagnetically induced transparency (EIT). Our group has previously implemented Bragg spectroscopy in a paraxial fluid of light and measured its Bogoliubov spectrum demonstrating the formal equivalence<sup>1</sup>. Tunability of the on site interactions coupled with the effective photon tunneling in the 2D transverse plane would allow for the engineering of a 2D many-body state for photons where the initial superfluid (coherent) photon state could be tuned for the realization of a Mott insulator for photons.

Here, we present progress towards realization of fluids of light in a cold atomic cloud. Particularly, the preliminary characterization of the non-linear phase acquired by the photon fluid in our cold atomic media.

<sup>1</sup>Fontaine, Q. and Bienaimé, T. and Pigeon, S. and Giacobino, E. and Bramati, A. and Glorieux, Q, *Phys. Rev. Lett.* **121**, 183604 (2018).



Abstract number: P139  
 Friday 14:00-15:30

## Spin squeezing in an array of atomic ensembles via Rydberg dressing

Moreau G. L.<sup>†1</sup>, Wahrman M. D.<sup>1</sup>, Lewis N. A.<sup>1</sup>, Rajagopal S. V.<sup>1,2</sup>, Schleier-Smith M.<sup>1</sup>

<sup>1</sup>Stanford University, California, USA

<sup>2</sup>University of Michigan, Michigan, USA

<sup>†</sup>moreauga@stanford.edu

State of the art atomic sensors of time and fields are fundamentally limited by the quantum projection noise. However, this limit can be overcome by introducing entanglement between the sensor's constituent atoms, a paradigmatic example of which is the squeezed spin state. The method of Rydberg dressing enables the building up of entanglement directly among ground-state atoms, as well as a high degree of optical control over the native Ising interactions. In this work, we prepared multiple squeezed spin states in an array of ensembles of cesium atoms via the local interactions induced by Rydberg dressing<sup>1</sup>. This was enabled by temporal control of the dressing light in the form of a stroboscopic dressing sequence consisting of shaped pulses to ensure adiabaticity, thereby increasing the coherence of the dressed interactions. The results pave the way towards applications in multiplexed atomic clocks and sensors benefiting from the use of local, optically controlled interactions to prepare multiple squeezed ensembles. We also describe progress towards leveraging coherent Rydberg dressing in an array of single atoms for applications in quantum sensing and simulation that benefit from combining optical control of Ising interactions with site-resolved imaging. Prospects include optimal control of metrologically useful entanglement via Hamiltonian engineering and exploration of non-equilibrium phases of the Floquet transverse-field Ising model.

<sup>1</sup>J. A. Hines *et al.*, *Phys. Rev. Lett.* **131**, 063401 (2023).

Abstract number: P140

Friday 14:00-15:30

## Progress towards a new search for time-variation of the proton-to-electron mass ratio with a molecular lattice clock

**Rodewald J.**<sup>†1</sup>, Cox J.<sup>1</sup>, Liu Q.<sup>1</sup>, Voges K.<sup>1</sup>, Lopez O.<sup>2</sup>, Manceau M.<sup>2</sup>, Darquie B.<sup>2</sup>, Sauer B.<sup>1</sup>, Tarbutt M.<sup>1</sup>

<sup>1</sup>Centre for Cold Matter, Blackett Laboratory, Imperial College London, Prince Consort Road, London SW7 2AZ UK

<sup>2</sup>Laboratoire de Physique des Lasers, CNRS, Université Sorbonne Paris Nord, F-93430, Villetaneuse, France

<sup>†</sup>j.rodewald@imperial.ac.uk

The search for time-variation of fundamental constants is a promising way to probe physics beyond the standard model<sup>1</sup>. In the frame of the QSNET project<sup>2</sup>, we are setting up a molecular lattice clock to test for time-variation of the proton-to-electron mass ratio. The clock will be based on the fundamental vibrational transition in Calcium Monofluoride (CaF) at a wavelength of around  $17\mu\text{m}$ . The transition is expected to have a linewidth of a few Hz and be largely insensitive to systematic DC Stark or Zeeman shifts. Additionally, the AC Stark shifts of the ground and excited states of the clock transition are expected to cancel for several wavelengths, potentially facilitating the trapping of the molecules in a magic wavelength lattice<sup>3</sup>. The frequency of the clock transition is currently known with an accuracy of several MHz. To narrow this down, we perform vibrational spectroscopy of CaF with a  $17\mu\text{m}$  quantum cascade laser (QCL)<sup>4</sup>. The frequency of the QCL is referenced to a stable low-finesse cavity as well as to absorption lines of the  $\nu_2$  fundamental vibration mode of N<sub>2</sub>O in the  $17\mu\text{m}$  region which we resolve with frequency modulation spectroscopy<sup>5</sup>.

<sup>1</sup>Safronova *et al.*, *Rev. Mod. Phys.* **90**, 025008 (2018)

<sup>2</sup>Barontini *et al.*, arXiv:2112.10618, (2021)

<sup>3</sup>Kajita, *J. Phys. Soc. Jpn.* **87**, 104301 (2018)

<sup>4</sup>Nguyen Van *et al.*, *Photonics* **6**, (2019)

<sup>5</sup>Wang, Rodewald *et al.*, *New J. Phys.* **27** 023038 (2025)

Abstract number: P141  
Friday 14:00-15:30

## Isotope shift spectroscopy in mercury vapors

Gravina S., Di Bernardo S., Castrillo A., Moretti L., Gianfrani L.<sup>†</sup>

Dipartimento di Matematica e Fisica, Università degli Studi della Campania "Luigi Vanvitelli", Caserta, Italy

<sup>†</sup>livio.gianfrani@unicampania.it

Precision spectroscopy of atomic systems is an invaluable tool to test fundamental physics, looking for potential signatures of phenomena beyond the Standard Model of elementary particles. In particular, isotope shift spectroscopy in heavy atoms offers a sensitive probe for possible new bosonic interactions between electrons and neutrons through the analysis of King plots, where at least two different atomic transitions are combined so that common nuclear and atomic uncertainties cancel out. As a unique feature, deviations from linearity of a King plot may be due higher-order nuclear structure effects but also to new physics<sup>1</sup>. In recent years, King-plot linearity has been tested in refined experiments using ionic<sup>2,3</sup> and neutral ytterbium<sup>4</sup>, as well as calcium ions<sup>5</sup>. An alternative to King plots uses the so-called chain-normalized isotope shifts, which are particularly useful to probe the occurrence of nuclear deformation contributions<sup>6</sup>. These studies may be conveniently extended to other atomic species with at least four bosonic isotopes, such as neutral mercury and cadmium<sup>7,8</sup>.

We recently performed accurate determinations of the absolute frequency of the  $6s^2\ ^1S_0 \rightarrow 6s6p\ ^3P_1$  intercombination transition for  $^{200}\text{Hg}$  and  $^{202}\text{Hg}$  at 253.7 nm, employing comb-locked, wavelength-modulated, Lamb-dip spectroscopy, a quite powerful technique that is briefly described hereafter.

The UV radiation is generated through a double stage of second harmonic generation in a pair of nonlinear crystals, starting from an external cavity diode laser (ECDL) emitting at 1014.8 nm<sup>9</sup>. The near-infrared emission frequency is tightly locked to the nearest tooth of an optical frequency comb synthesizer referenced to a GPS-disciplined Rb clock. The wavelength-modulation technique was implemented by dithering the offset frequency between the near-IR ECDL and the nearest comb-tooth. Such a dither propagates throughout the frequency chain, while a fine-tuning of the comb repetition rate is performed, thus allowing accurate UV frequency scans across the mercury intercombination transition. This technical effort allowed us to probe sub-Doppler features with high sensitivity in a miniature vapor cell at room temperature ( $\approx 298\text{ K}$ ). Absolute line center frequencies were determined for the isotopes  $^{200}\text{Hg}$  and  $^{202}\text{Hg}$ , with relative uncertainties of  $6.8 \times 10^{-12}$  and  $1.3 \times 10^{-11}$ , respectively<sup>10</sup>. Consequently, the  $^{200}\text{Hg}$ - $^{202}\text{Hg}$  isotope shift was determined with enhanced precision and accuracy compared to previous works.

Here, we present new spectroscopic measurements of the  $6s^2\ ^1S_0 \rightarrow 6s6p\ ^3P_1$  transition in bosonic mercury isotopes at a stabilized temperature of 270 K, aimed at further improving the accuracy of the isotope shifts for this spectral line. Since the vapor pressure is lowered by one order of magnitude, the uncertainty contribution from the collision-induced frequency shift is significantly reduced. We also report the results of a double-resonance experiment in an open three-level ladder scheme. This experiment may lead to novel isotope shift data for transitions between excited levels.

<sup>1</sup>J.C. Berengut and C. Delaunay, *Nature Reviews Physics* **7**, 119 (2025).

<sup>2</sup>I. Counts *et al.*, *Phys. Rev. Lett.* **125**, 123002 (2020).

<sup>3</sup>J. Hur *et al.*, *Phys. Rev. Lett.* **128**, 163201 (2022).

<sup>4</sup>N. L. Figueroa, J. C. Berengut, V. A. Dzuba, V. V. Flambaum, D. Budker, D. Antypas, *Phys. Rev. Lett.* **128**, 073001 (2022).

<sup>5</sup>C. Solaro, S. Meyer, K. Fisher, J. C. Berengut, E. Fuchs, M. Drewsen, *Phys. Rev. Lett.* **125**, 123003 (2020).

<sup>6</sup>M. Door *et al.*, *Phys. Rev. Lett.* **134**, 063002 (2025).

<sup>7</sup>J.S. Schelfhout and J.J. McFerran, *Phys. Rev. A* **105**, 022805 (2022).

<sup>8</sup>S. Hofsäss *et al.*, *Phys. Rev. Res.* **5**, 013043 (2023).

<sup>9</sup>C. Clivati, S. Gravina, A. Castrillo, G.A. Costanzo, F. Levi, L. Gianfrani, *Opt. Lett.* **45**, 3693 (2020).

<sup>10</sup>S. Gravina, N.A. Chishti, S. Di Bernardo, E. Fasci, A. Castrillo, A. Laliotis, L. Gianfrani, *Phys. Rev. Lett.*, **132**, 213001 (2024).

Abstract number: P142  
Friday 14:00-15:30

## Hyperfine Structure of the Aluminum Atom

Gómez-Fernández L.<sup>†</sup>, Robinson-Tait J., Eriksen A.S., Kjær J.K., Thomsen J.W.

NNF Quantum Computing Program, Niels Bohr Institute, Københavns Universitet, København, Danmark

<sup>†</sup>laura.fernandez@nbi.ku.dk

We are investigating laser cooling of  $^{27}\text{Al}$  ( $I = 5/2$ ). Aluminum was first laser cooled in 1995 by Roger W. McGowan, David M. Giltner and Siu Au Lee.<sup>1</sup> They addressed the cooling transition  $3p^2P_{3/2} F = 4 \rightarrow 3d^2D_{5/2} F = 5$  ( $\lambda = 309.27 \text{ nm}$ )<sup>2</sup> for aluminium, shown in Figure 1. The first measurement of the hyperfine structure was done in 1962 by Karl Börje S. Eriksson and H. Bengt S. Isberg.<sup>2</sup> However, this pioneering work could benefit from higher accuracy determination of the hyperfine A and B coefficients. These transitions are located in the visible and UV, implying additional challenge due to the scaling of the saturation intensity with  $\lambda^3$ , resulting in very high intensity requirements for effective excitation.

In contrast to many elements previously laser cooled, aluminum has a notably low vapor pressure, requiring oven temperatures around 1600 K to achieve sufficient atomic flux. This necessitates careful design of both the atomic oven and the vacuum chamber to ensure stable operation under such demanding thermal conditions. One of the upcoming challenges is the ground state distribution shown in Figure 1. The states  $(3p^2)P_{1/2}$  and  $(3p^2)P_{3/2}$  are only 0.01 nm away, resulting in a thermal spread along the whole hyperfine structure at oven temperatures of 1600K. The limitation of the population of the ground state of the cooling transition to 25% sets an upper limit to the efficiency of the cooling process. To increase the number of atoms that could undergo the cycling transition and therefore be cooled requires optical pumping. This process has already been done for another group III atom: Ga.<sup>3</sup>

To perform both cooling and optical pumping an accurate resolution of the hyperfine levels is required. We plan a series of high-precision spectroscopy experiments that would enable us to resolve the hyperfine structure and identify the key optical transitions. The results will be presented in the upcoming conference.

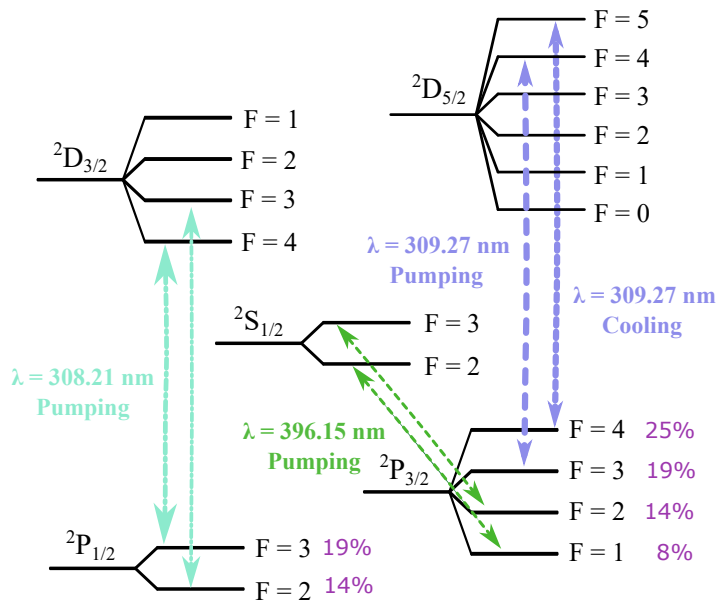


Figure 1: Aluminium hyperfine structure. Typical hyperfine splitting is of the order of 400-800 MHz

<sup>1</sup>Roger W. McGowan, David M. Giltner, and Siu Au Lee, *Optics letters* **Vol.20**, No. 24 (1995)

<sup>2</sup>Karl Börje S. Eriksson and H. Bengt S. Isberg *Arkiv för fysik* **Vol.23**, No. 47 (1962)

<sup>3</sup>Steven J. Rehse, Karen M. Bockel and Siu Au Lee, *Physical review* **Vol.69**, 063404 (2004)

Abstract number: P143  
 Friday 14:00-15:30

## Spectrally tailoring a clock laser for quantum state engineering and many-body physics in a 3D lattice clock

**Stefan Lannig<sup>†1</sup>, Lingfeng Yan<sup>1</sup>, William R. Milner<sup>1</sup>, Max N. Frankel<sup>1</sup>, Yu Hyun Lee<sup>1</sup>, Ben Lewis<sup>1</sup>,  
 Dahyeon Lee<sup>1</sup>, Kyungtae Kim<sup>1</sup>, Jun Ye<sup>1</sup>**

<sup>1</sup>*JILA, National Institute of Standards and Technology and University of Colorado and Department of Physics, University of Colorado, Boulder, CO 80309, USA*

<sup>†</sup>stefan.lannig@jila.colorado.edu

Highly stable lasers are a ubiquitous tool for investigating quantum systems. In optical lattice clocks these are essential to probe the ultranarrow optical transition of the atoms. Apart from frequency metrology, clock systems also provide a flexible testbed for investigating many-body interactions, which benefits from the resolution provided by the atomic clock transition. Here, for fast and accurate state engineering and system manipulation, lasers that extend the stability of the clock lasers from the sub-Hz to the kHz range are required.

To this end, we present a spectrally engineered laser that provides both, the long-term stability of cryogenic silicon cavities and the short-term (intermediate-to-high Fourier frequency) stability of a ULE cavity. Using our <sup>87</sup>Sr three-dimensional optical lattice clock as atomic spectrum analyzer, we certify the performance of this laser system in situ and demonstrate a cutting-edge single-qubit fidelity of 0.99964(3) when driving 3000 atoms simultaneously. Looking forward, we will apply this tool to study superexchange-driven spin squeezing on the clock transition and investigate collective photon-mediated dynamics of open many-body systems in the 3D lattice by effectively tuning the dipole moment of the clock transition.

Abstract number: P144

Friday 14:00-15:30

## High precision mid-infrared vibrational spectroscopy with cold molecules

**Hahn R.**<sup>†1</sup>, Bonifacio A.<sup>1</sup>, Saffre M.<sup>1</sup>, Dong W.<sup>1</sup>, Liu Y.<sup>1</sup>, Viel S.<sup>1</sup>, Ngo M. N.<sup>1</sup>, Lopez O.<sup>1</sup>, Cantin E.<sup>1</sup>, Amy-Klein A.<sup>1</sup>, Manceau M.<sup>1</sup>, Darquié B.<sup>1</sup>

<sup>1</sup> Laboratoire de Physique des Lasers, CNRS, Université Sorbonne Paris Nord, 93430 Villetaneuse, France

<sup>†</sup>raphael.hahn@univ-paris13.fr

There is an increasing demand for precise molecular spectroscopy, in particular in the mid-infrared (MIR) fingerprint window, to feed atmospheric models, to interpret astrophysical spectra or to test fundamental physics. I will present our efforts towards building new-generation mid-infrared spectrometers specifically designed for precision vibrational spectroscopy of complex polyatomic molecules in the gas phase. This includes amongst other things:

- producing gases of polyatomic species cooled to a few kelvins in cryogenic buffer-gas cells<sup>1</sup>,
- high-quality laser sources that are spectrally narrow, broadly tunable, stabilised and ultimately referenced to some of the world's best frequency standards<sup>23</sup>.
- exploring the opportunities offered by cutting-edge mid-IR photonics technologies: new detectors, new phase-, frequency- or amplitude-modulators, and new laser sources. This allows us to extend the wavelength range of our spectrometers around 6  $\mu\text{m}$ , 8-12  $\mu\text{m}$ , and 17  $\mu\text{m}$ <sup>4,5,6,7,8,9</sup>.

These developments are at the forefront of cold molecules research, frequency metrology, and photonics, and have allowed us to carry out sub-Doppler spectroscopy of a variety of species of atmospheric, astrophysical, metrological or fundamental interest and measure absolute frequencies with record 12 digit accuracies<sup>10,11</sup>. These measurements significantly enhance and refine molecular databases and are also steps toward testing fundamental physics in various ways. Current efforts include investigating potential variations in the electron-to-proton mass ratio and testing parity symmetry by measuring the tiny parity-violating energy differences between enantiomers of chiral molecules<sup>12</sup>.

<sup>1</sup>Tokunaga *et al.*, *New J Phys* **19**, 053006 (2017)

<sup>2</sup>Argence *et al.*, *Nature Photon* **9**, 456 (2015)

<sup>3</sup>Santagata *et al.*, *Optica* **6**, 411 (2019)

<sup>4</sup>Chomet *et al.*, *Appl Phys Lett* **122**, 231102 (2023)

<sup>5</sup>Dely *et al.*, *Opt Express* **31**, 30876 (2023)

<sup>6</sup>Manceau *et al.*, arXiv:2310.16460 (2023)

<sup>7</sup>Saemian *et al.*, *Nanophotonics* **13**, 10 (2024)

<sup>8</sup>Chomet *et al.*, *Optica* **11**, 1220 (2024)

<sup>9</sup>Wang *et al.*, *New J Phys* **27**, 023038 (2025)

<sup>10</sup>Tran *et al.*, *APL Photonics* (2024)

<sup>11</sup>Tran *et al.*, arXiv:250208201 (2025)

<sup>12</sup>Fiechter *et al.*, *J Phys Chem Lett* **13**, 42 (2022)

Abstract number: P145  
Friday 14:00-15:30

## Laser Cooling and Trapping of Silicon Atoms

Kjær J. K.<sup>†1</sup>, Robinson-Tait J.<sup>1</sup>, Eriksen A. S.<sup>1</sup>, Gómez-Fernández L.<sup>1</sup>, Thomsen J. W.<sup>4</sup>

<sup>1</sup>NNF Quantum Computer Programme, Niels Bohr Institute, University of Copenhagen, Denmark

<sup>†</sup>jacob.kibsgaard@nbi.ku.dk

Silicon is the backbone of the electronics and semiconductor industries due to its abundance and versatility. It is essential for manufacturing everything from transistors to solar cells and thus of huge interest to material scientists and engineers. Understanding the fundamental properties is therefore crucial for the development of new materials, however, the characterization of important optical transitions of silicon remain lacking. This is where laser cooling and trapping of silicon atoms provides a unique platform for high-precision spectroscopy - though there are significant experimental challenges.

The main laser cooling and re-pumping transitions are often located in the UV-B and UV-C spectral regions. The saturation intensity,  $I_{\text{sat}}$ , scales with  $\frac{1}{\lambda^3}$ , leading to very high intensity requirements for effective excitation.

$$I_{\text{sat}} = \frac{\pi \hbar c}{3 \lambda^3 \tau} \quad (1)$$

For example, the main cooling transition at 221.74 nm is well-known and has been measured experimentally, but the weak decay to the  $^1D_2$  metastable state (see Fig. 1) has never been directly observed (and is only calculated by multi-configuration Hartree-Fock numerical methods<sup>1</sup>).

We plan a series of high-precision spectroscopy experiments aimed at mapping out isotope shifts, identifying key optical transitions, and resolving hyperfine structures. The results of these studies will be presented at the 26<sup>th</sup> ICOLS. By utilizing the principal optical transitions of  $^{28}\text{Si}$ , we will investigate using laser cooling and trapping.

Furthermore, unlike many elements commonly used in laser cooling experiments, silicon presents unique challenges due to its exceptionally low vapor pressure. Oven temperatures exceeding 1500 K are necessary, which requires innovative vacuum chamber designs to maintain operational stability and prevent contamination under extreme thermal conditions.

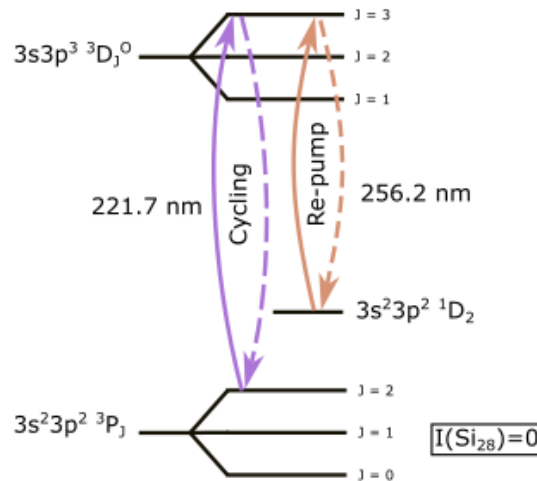


Figure 1: Principal transitions for  $^{28}\text{Si}$  used for laser cooling and trapping.

<sup>1</sup>C. Froese Fischer *et al.*, *ab initio mchf calculations* The mchf/mcdhf collection, (2009).

Abstract number: P146  
Friday 14:00-15:30

## Superfluid Fraction in an Interacting Spatially Modulated Bose-Einstein Condensate

**Wattellier S.<sup>1</sup>, Chauveau G.<sup>1</sup>, Rabec F.<sup>1</sup>, Brochier G.<sup>1</sup>, Nascimbene S.<sup>1</sup>, Dalibard J.<sup>1</sup>, Beugnon J.<sup>† 1</sup>**

<sup>1</sup>Laboratoire Kastler Brossel, Collège de France, CNRS, ENS-PSL University, Sorbonne University

<sup>†</sup>beugnon@lkb.ens.fr

At zero temperature, a Galilean-invariant Bose fluid is expected to be fully superfluid. In this work we investigate theoretically and experimentally the quenching of the superfluid density of a dilute Bose-Einstein condensate due to the breaking of translational (and thus Galilean) invariance by external 1D and 2D periodic potentials. Both Leggett's bounds fixed by the knowledge of the total density and the anisotropy of the sound velocity provide a consistent determination of the superfluid fraction in the case of a 1D separable density modulation<sup>1</sup>. In the case of a 2D non-separable density modulation, the value of the superfluid fraction, relying on the measurement of the compressibility and the speed of sound, is consistent with the computation of Leggett's bounds.

---

<sup>1</sup>G. Chauveau *et al.*, *Physical Review Letters* **130**, 22 (2023).



Abstract number: P147  
Friday 14:00-15:30

## False vacuum decay at finite temperatures in ferromagnetic superfluids

**Cominotti R.**<sup>†1</sup>, **Baroni C.**<sup>2</sup>, **Rogora C.**<sup>1</sup>, **Guarda G.**<sup>1</sup>, **Andreoni D.**<sup>1</sup>, **Lamporesi G.**<sup>1</sup>, **Ferrari G.**<sup>1</sup> and **Zenesini A.**<sup>1</sup>

<sup>1</sup> *Pitaevskii BEC Center, CNR-INO and Dipartimento di Fisica, Università di Trento, 38123 Trento, Italy, and Trento Institute for Fundamental Physics and Applications, INFN, 38123 Trento, Italy*

<sup>2</sup> *Institute for Quantum Optics and Quantum Information (IQOQI) and Institute for Experimental Physics, University of Innsbruck 6020 Innsbruck, Austria*

<sup>†</sup>riccardo.cominotti@ino.cnr.it

Classical systems can have multiple equilibrium states at different energies; the absolute ground state is a stable configuration, while the other local energy minima are metastable. The transition from the metastable state to the ground one is driven by thermal fluctuations, which both modify the energy landscape and introduce random local inhomogeneities that can trigger this transition. A prototypical example is a supercooled vapour. In quantum systems described by a field theory, quantum fluctuations can instead induce the macroscopic tunneling of the field from a metastable state (the false vacuum) to the ground state (true vacuum) through the many-body energy barrier<sup>1</sup>. The decay of a false vacuum, which is thought to manifest via the nucleation of spatially localized bubbles of true vacuum, is a fascinating phenomena for a rich variety of systems, ranging from condensed matter<sup>2</sup> to cosmology. Investigating the interplay between quantum and thermal fluctuations in the decay mechanism is particularly interesting and relevant, for instance, to advancing our understanding of phase transitions in the early universe<sup>3</sup>. Despite extensive theoretical and numerical efforts to estimate the relaxation rate of the metastable field, experimental studies on quantum systems have only recently become feasible on ultracold atomic platforms<sup>4</sup> and quantum annealers<sup>5</sup>. Here we present experimental evidence of false vacuum decay through the nucleation of spin bubbles in a metastable ferromagnetic superfluid, realized with a Bose-Bose mixture of ultracold sodium atoms. The effect of finite temperature on the decay rate is characterized, leveraging the tunability of our ultracold atomic platform. Our results find good agreement with numerical simulations and instanton theory, paving the way for the simulation of out-of-equilibrium phenomena in a highly controllable and tunable atomic system.

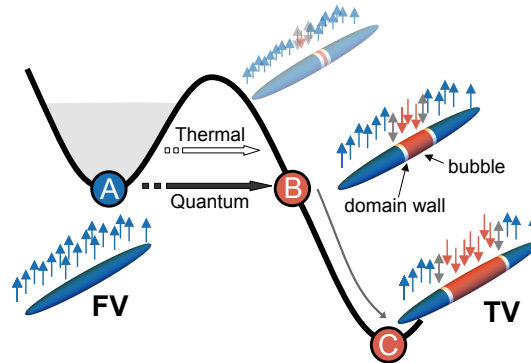


Figure 1: False vacuum decay process. Tunneling occurs from the false vacuum (A) to the resonant state (B), leading to bubble formation. Once formed, the bubble eventually expands into the true vacuum state (C). The presence of thermal fluctuations in the system (grey area) can accelerate the decay process.

<sup>1</sup>S. Coleman, *Phys. Rev. D*, **16**, 1248 (1977).

<sup>2</sup>G. Lagnese *et al.*, *Phys. Rev. B* **104**, L201106 (2021)

<sup>3</sup>M. Hindmarsh *et al.*, *SciPost Phys. Lect. Notes* **24** (2021)

<sup>4</sup>A. Zenesini *et al.*, *Nat. Phys.*, **20**, 558–563 (2024)

<sup>5</sup>J. Vodeb *et al.*, *Nature*, **21**, 386–392 (2025)

Abstract number: P148  
Friday 14:00-15:30

## Recent advances of PTB's transportable $\text{Al}^+$ ion clock

**Constantin Nauk<sup>†1,2</sup>, Joost Hinrichs<sup>1,2</sup>, Gayatri Sasidharan<sup>1,2</sup>, Vanessa Galbierz<sup>1</sup>, Benjamin Kraus<sup>1</sup>, Sofia Herbers<sup>1</sup>, Piet O. Schmidt<sup>1,2</sup>**

<sup>1</sup>Physikalisch-Technische Bundesanstalt, 38116 Braunschweig, Germany

<sup>2</sup>Leibniz Universität Hannover, Institut für Quantenoptik, 30167 Hannover, Germany

<sup>†</sup>constantin.nauk@ptb.de

Optical atomic clocks demonstrate exceptional fractional systematic and statistical frequency uncertainties on the order of  $10^{-18}$ , surpassing the respective uncertainties of caesium fountains<sup>1</sup>. This advancement opens new avenues for novel applications and encourages the redefinition of the SI second<sup>2</sup>, for which an agreement on reproducible frequency ratio measurements between different institutes is a key requirement. However, remote frequency comparisons of distant optical clocks via satellite link would artificially limit the achievable frequency stability<sup>3</sup>. Instead, one solution are frequency comparisons at local national metrology sites using transportable clock setups to infer frequency ratios and instabilities across the globe.

Moreover, transportable setups enable applications in relativistic geodesy, such as height measurements at the cm level<sup>4</sup>, since each frequency comparison is affected by the geopotential difference between two clocks.

To address these topics, we present a transportable clock setup based on the  $^1\text{S}_0 \rightarrow ^3\text{P}_0$  transition in  $^{27}\text{Al}^+$ , utilizing a co-trapped  $^{40}\text{Ca}^+$  ion to enable state detection and cooling through quantum logic spectroscopy<sup>5</sup> and sympathetic cooling.

All clock hardware is fully integrated in commercial 19" racks and is shown in Figure 1.

The physics package includes a multi-segmented chip ion trap in an aluminum/titanium composite vacuum system housed inside a mu-metal magnetic shield. A reference cavity provides pre-stabilization for the clock fundamental frequency to  $2 \times 10^{-16}$  at 1 s integration time<sup>6</sup>. The latter is frequency quadrupled using a single-pass fourth-harmonic setup to generate phase-stable clock light at 267.4 nm<sup>7</sup>. An additional dual-wavelength cubic resonator stabilizes the respective logic laser of each ion species<sup>8</sup>. The frequency-controlled cooling laser for  $^{40}\text{Ca}^+$  is integrated and combined with infrared repumpers and ultraviolet ionization lasers inside an optical drawer, mounted on a heavy-duty pull-out frame in the rack.

We detail the optimization of ion loading efficiency, Doppler cooling, and micromotion compensation. Additionally, we present characterization measurements, including secular motions and ion swap rates, to infer a background gas pressure range at the ion position in the low  $10^{-10}$  mbar range<sup>9</sup>. Finally, we demonstrate coherent manipulation on the  $^2\text{S}_{1/2} \rightarrow ^2\text{D}_{5/2}$  transition in  $^{40}\text{Ca}^+$ , required for quantum logic spectroscopy.

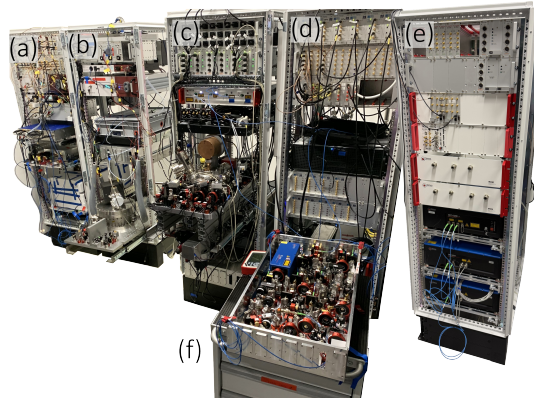


Figure 1: The transportable Aluminium ion clock setup. The hardware is mounted in five 19" racks, each measuring 1800 mm x 800 mm x 600 mm. From left to right, the racks house the clock laser (a), the combined logic lasers (b), the physics package (c), electronics (d) and a frequency comb (e). Optics are integrated using stable drawers as exemplarily shown by the  $^{40}\text{Ca}^+$  cooling laser system in the front (f).

<sup>1</sup>S. M. Brewer *et al.*, *Phys. Rev. Lett.* **123**, 033201 (2019).

<sup>2</sup>N. Dimarcq *et al.*, *Metrologia* **61**, 012001 (2024).

<sup>3</sup>F. Riedel *et al.*, *Metrologia* **57**, 045005 (2022).

<sup>4</sup>T. E. Mehlstäubler, G. Grosche, C. Lisdat, P. O. Schmidt and H. Denker, *Rep. Prog. Phys.* **81**, 064401 (2018).

<sup>5</sup>P. O. Schmidt, T. Rosenband, C. Langer, W. M. Itano, J. C. Bergquist and D. J. Wineland, *Science* **309**, 749-752 (2005).

<sup>6</sup>B. Kraus, S. Herbers, C. Nauk, U. Sterr, C. Lisdat, and Piet O. Schmidt, *Opt. Lett.* **50**, 658-661 (2025).

<sup>7</sup>B. Kraus, F. Dawel, S. Hannig, J. Kramer, C. Nauk, and P. O. Schmidt, *Opt. Express* **30**, 44992-45007 (2022).

<sup>8</sup>F. Dawel *et al.*, *Opt. Express* **32**, 7276-7288 (2024).

<sup>9</sup>A. M. Hankin *et al.*, *Phys. Rev. A* **100**, 033419 (2019).

Abstract number: P149  
Friday 14:00-15:30

## Photonic Interfaces for Telecommunication-band Quantum Networking with Neutral Atoms

G. Eirini Mandopoulou<sup>1†</sup>, Brandon Grinkemeyer<sup>1</sup>, Andrei Ruskuc<sup>1†</sup>, Sophie W. Ding<sup>2</sup>, Matthew Bilotta<sup>1</sup>, Michel Tao<sup>1</sup>, Danilo Shchepanovich<sup>1</sup>, Offek Tziperman<sup>1</sup>, Alexander S. Zibrov<sup>1</sup>, Marko Lončar<sup>2</sup>, Kiyoul Yang<sup>2</sup>, Vladan Vuletić<sup>3</sup>, Mikhail D. Lukin<sup>1</sup>,

<sup>1</sup>*Department of Physics, Harvard University, Cambridge, USA*

<sup>2</sup>*John A. Paulson School of Engineering and Applied Sciences, Harvard University, Cambridge, USA*

<sup>3</sup>*Department of Physics and Research Laboratory of Electronics, MIT, Cambridge, USA*

<sup>†</sup>gemandopoulou@g.harvard.edu, <sup>†</sup>aruskuc@fas.harvard.edu

Neutral atoms coupled to optical cavities are a well-developed platform for quantum networking and quantum information processing<sup>1</sup>. Combined with advances in programmable arrays of neutral atoms, this approach promises significant progress towards distributed quantum computing<sup>2,3</sup>. However, the performance of these platforms is critically dependent on both the construction and the geometry of the optical interface<sup>4,5</sup>. In this work, we present the fabrication of high-finesse optical microcavities compatible with neutral atom quantum computers. The micromirrors are produced through a two-step silicon etching process followed by thermal smoothing<sup>6</sup>. This scalable fabrication method yields hundreds of micromirrors with low radii of curvature and sub-angstrom surface roughness with minimal variation. These features allow for microcavities with small mode volumes and high quality factors, and can enable multiplexed cavity array architectures. Utilizing the fabricated micromirrors we introduce a novel dual-resonance Fabry–Pérot cavity design. Further, we report on progress towards cavity assisted atom-photon entanglement at telecom wavelengths with <sup>87</sup>Rb atoms trapped in optical tweezers. The demonstrated silicon microcavities provide a high-efficiency platform for interfacing neutral atom arrays with telecommunication-band photons, paving the way for scalable quantum networking technologies.

<sup>1</sup>B. Grinkemeyer *et al.*, *Science* **387**, 1301 (2025).

<sup>2</sup>D. Bluvstein *et al.*, *Nature* **626**, 775 (2024).

<sup>3</sup>C. Monroe *et al.*, *Phys. Rev. A* **89**, 022317 (2014).

<sup>4</sup>D. Hunger *et al.*, *New J. Phys.* **12**, 065038 (2010).

<sup>5</sup>P. L. Ocola *et al.*, *Phys. Rev. Lett.* **132**, 133001 (2024).

<sup>6</sup>G. Wachter *et al.*, *Light Sci. Appl.* **8**, 37 (2019).

Abstract number: P150  
Friday 14:00-15:30

## Evanescent light – matter interaction in an integrated MEMS – nanophotonic vapor cell

Riley P. S.<sup>†1,4</sup>, Hoang K. T.<sup>2,3</sup>, Shrestha R.<sup>2,3</sup>, Zektzer R.<sup>2,3</sup>, Westly D.<sup>3</sup>, Srinivasan K.<sup>2,3</sup>, Hummon M.<sup>4</sup>

<sup>1</sup> University of Colorado Boulder, USA

<sup>2</sup> Joint Quantum Institute, NIST/University of Maryland College Park, USA

<sup>3</sup> National Institute of Standards and Technology, Gaithersburg, USA

<sup>4</sup> National Institute of Standards and Technology, Boulder, USA

<sup>†</sup>Peter.riley@colorado.edu

Integrating atomic vapor cells and photonic integrated circuits (PICs) in a robust fashion is critical for the development of quantum devices. Making use of interactions between the evanescent field of the guided light and the atomic vapor, applications of warm atomic vapor – based devices include telecommunication band wavelength references<sup>1</sup>, gas sensing<sup>2</sup>, cavity quantum electrodynamics (cQED)<sup>3,4</sup> systems, and other applications in nonlinear and quantum optics<sup>5</sup>. Previous works have limited operational lifetime, temperature range, or manufacturability due to their use of epoxy<sup>1,4</sup>, larger glass-blown stems<sup>6</sup>, or glass cells connected to auxiliary vacuum systems<sup>7</sup> for integration. In this work we demonstrate a device that does not suffer from these drawbacks, a microfabricated rubidium atomic vapor cell directly bonded to a silicon nitride photonic chip. We perform evanescent field spectroscopy using a 60 micrometer-long air-clad waveguide device and observe Rb absorption features for operating temperatures as high as 300 °C.

The device consists of a silicon nitride PIC, a machined glass frame, and a glass lid that are anodically bonded together to form the completed vapor cell. Figure 1 shows evanescent absorption of 780 nm light by warm Rb vapor through a 60  $\mu$ m-long air-clad waveguide as a function of temperature, plotted next to absorption from a reference Rb vapor cell for comparison. Next steps include studying the interaction between the atomic vapor and nanophotonic microresonators to enable strong light-atom interactions for applications including cQED<sup>3,4,5,6</sup> that can be investigated in this platform.

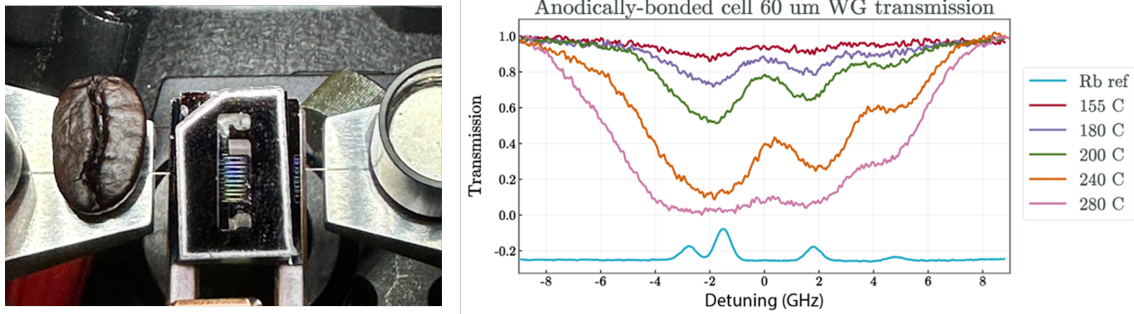


Figure 1: Device and results. (a) Photograph of 12 mm x 16 mm x 3.5 mm integrated PIC – vapor cell device. Lensed fibers are used to edge-coupled light onto the chip. (b) Evanescent absorption of 780 nm light by warm rubidium vapor in an integrated MEMS-nanophotonic vapor cell device. Multiple traces obtained with different device temperatures are shown. A reference spectrum free-space interrogation of a separate Rb cell is shown on the bottom in blue.

<sup>1</sup>R. Zektzer *et al*, *Laser & Photon Rev* **14**, 1900414 (2020).

<sup>2</sup>L. Tombez, E. J. Zhang, J. S. Orcutt, S. Kamlapurkar, and W. M. J. Green, *Optica* **4**, 1322-1325 (2017).

<sup>3</sup>H. Alaeian *et al.*, *Appl. Phys. B* **126**, 25 (2020).

<sup>4</sup>R. Zektzer *et al.*, *Optica* **11**, 1376-1384 (2024)

<sup>5</sup>Q. Glorieux, T. Aladjidi, P.D. Lett, and R. Kaiser, *New Journal of Physics* **25** 051201 (2023).

<sup>6</sup>R. Ritter, N. Gruhler, W. H. P. Pernice, H. Kübler, T. Pfau, and R. Löw, *New Journal of Physics* **18** 103031 (2016)

<sup>7</sup>S. E. McBride, C. M. Gentry, C. Holland, C. Bellew, K. R. Moore, A. Braun, arXiv:2409.05254, (2024).

Abstract number: P151  
Friday 14:00-15:30

## Cavity-Mediated Programmable Interactions for Quantum Metrology and Simulation

**Merrick Ho**<sup>†1</sup>, Avikar Periwal<sup>1</sup>, Philipp Kunkel<sup>1, 3</sup>, Jonathan Jeffrey<sup>2</sup>, Eric Cooper<sup>1</sup>, Ocean Zhou<sup>2</sup>, Prithvi Raj Datla<sup>1</sup>, Monika Schleier-Smith<sup>1, 3</sup>

<sup>1</sup>*Department of Physics, Stanford University, Stanford, CA, USA.*

<sup>2</sup>*Department of Applied Physics, Stanford University, Stanford, CA, USA.*

<sup>3</sup>*SLAC National Accelerator Laboratory, Menlo Park, CA, USA.*

<sup>†</sup>merrickh@stanford.edu

Quantum sensing and simulation benefit from fine control over long-range interactions. We leverage such control in an array of atomic ensembles coupled to an optical cavity<sup>1,2</sup> for applications in entanglement-enhanced multiparameter sensing and in simulating topological physics. We demonstrate quantum-enhanced sensing of spatially patterned fields using a scheme that employs cavity-mediated interactions both to generate squeezing and to subsequently amplify the signal in a spatial mode of interest, facilitating detection of the entangled state. We further demonstrate simultaneous sensing of conjugate observables with precision beyond the standard quantum limit, by entangling an array of sensor ensembles with an array of ancilla ensembles. Crucial to our protocol is the use of interaction-based readout to access nonlocal observables forming a “quantum-mechanics free” subsystem. The capability of accessing nonlocal observables via coupling to a delocalized cavity mode additionally offers a powerful tool for probing topological physics. As a proof of principle, we employ the cavity as a nonlocal interferometer for probing topological edge states in a bosonic Su-Schrieffer-Heeger (SSH) model, composed of magnons that hop between sites of the array of spin ensembles. We benchmark the realization of the SSH model by probing its topological invariant, the Zak phase, and by observing edge-state oscillations. We further demonstrate tunability of the on-site interactions and apply cavity-based nonlocal interferometry to probe the influence of interactions on the edge-mode dynamics. As direct extensions, we present prospects for introducing complex coupling terms and engineering flat bands. In parallel, we are constructing a new near-concentric cavity with the goal of accessing a more strongly interacting regime for quantum simulations. We outline our plans for the new apparatus, where we aim to trap an array of single atoms, while improving our scheme for implementing interactions and cavity cooperativity by two orders of magnitude.

<sup>1</sup>Periwal, A. *et al.*, *Nature* **600**, 630-635 (2021).

<sup>2</sup>Cooper, E.S., Kunkel, P., Periwal, A., Schleier-Smith, M. H., *Nat. Phys.* **20**, 770-775 (2024).

Abstract number: P152  
Friday 14:00-15:30

## Exploring noise-induced Fano coherence in a hot vapor atomic gas

**Donati L.**<sup>†1,2</sup>, **Bruno N.**<sup>1,2</sup>, **Gherardini S.**<sup>1,2</sup>, **Cataliotti F. S.**<sup>1,2,3</sup>

<sup>1</sup>National Institute of Optics, CNR, Firenze, Italy

<sup>2</sup>European Laboratory for Non-linear Spectroscopy, Sesto Fiorentino (FI), Italy

<sup>3</sup>Dipartimento di Fisica e Astronomia, University of Florence, Sesto Fiorentino (FI), Italy

<sup>†</sup>ludovica.donati@cnr.it

In multi-level quantum systems, coherent superposition states can unexpectedly arise from interactions with the continuum of modes associated with incoherent processes, such as spontaneous emission and incoherent pumping<sup>1,2</sup>. This type of coherence, known as *noise-induced Fano coherence*, tend to disappear when the incoherent source vanishes. The formation of Fano coherence between internal states generated by “noisy” conditions has particular significance for systems in contact with thermal reservoirs, as photovoltaic devices, photodetectors or quantum heat engines, since their performance could see improvements<sup>3,4</sup>. We propose a V-type three-level quantum system realized in the hyperfine structure of hot <sup>87</sup>Rb atoms, as depicted in Figure 1. The objective is the detection of spatial anisotropy in the fluorescence spectrum of the atomic system driven by an incoherent field, thereby confirming the existence of noise-induced Fano coherences, as explained by Dodin *et al.*<sup>5</sup>. This will offer the first observation and new insights into quantum coherence phenomena arising from non-coherent excitation in a multi-level atomic system, potentially paving the way for the development of novel high-efficiency devices.

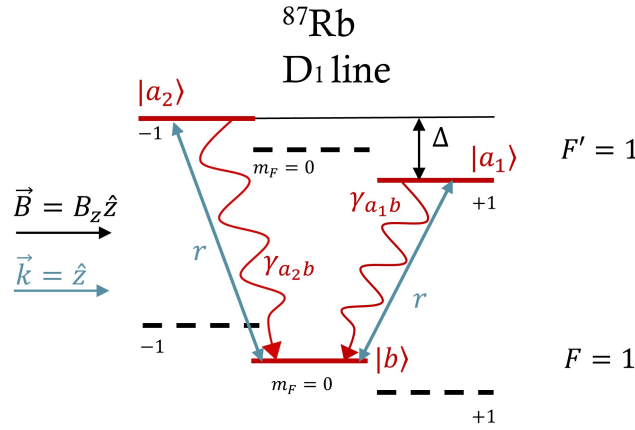


Figure 1: V-type three level system in the <sup>87</sup>Rb D<sub>1</sub> transition hyperfine structure. The system is driven by an incoherent source, with pumping rate  $r$ , close to the transition frequencies. Rates  $\gamma_{a_1b}$ ,  $\gamma_{a_2b}$  are the decay rates. A uniform magnetic field  $\vec{B} = B_z \hat{z}$  is applied along  $\hat{z}$  axis.

<sup>1</sup>Dodin A., Tscherbul T. V., and Brumer P., *J. Chem. Phys.* **144**, 244108 (2016).

<sup>2</sup>Koyu S., Dodin A., Brumer P., and Tscherbul T. V., *Phys. Rev. Res.* **3**, 013295 (2021).

<sup>3</sup>Scully M. O., Chapin K. R., Dorfman K. E., and Svidzinsky A. A., *Proc. Natl. Acad. Sci. U.S.A.* **108**, 15097 (2011).

<sup>4</sup>Svidzinsky A. A., Dorfman K. E., and Scully M. O., *Phys. Rev. A* **84**, 053818 (2011).

<sup>5</sup>Dodin A., Tscherbul T. V., Alicki R., Vutha A., and Brumer P., *Phys. Rev. A* **97**, 013421 (2018).

Abstract number: P153  
Friday 14:00-15:30

## Ultra-wideband search for axionlike dark matter using precision spectroscopy of octupole-enhanced nuclei in a crystal

**Fan M.<sup>†</sup>, Nima B., Radak A., Alonso-Álvarez G., Vutha A.**  
University of Toronto, 60 St. George Street, Toronto ON M5S 1A7, Canada  
<sup>†</sup>mingyu.fan@utoronto.ca

Most of the matter in the universe is in the form of dark matter<sup>1</sup>. However, the nature of dark matter remains unknown and dark matter has never been observed to interact with normal matter in laboratory experiments. Ultralight axionlike particles (ALPs) are a class of dark matter models that are consistent with astrophysical constraints<sup>2</sup>, and produce measurable signatures in the form of oscillating violations of discrete symmetries in nuclei<sup>3</sup>.

In this work we search for oscillating parity (P)-odd time-reversal (T)-odd nuclear moments of  $^{153}\text{Eu}^{3+}$  ions that are doped in a yttrium orthosilicate crystal. The  $^{153}\text{Eu}$  nucleus is octupole-shaped, leading to a collective enhancement of hardonic P, T-odd interactions<sup>4</sup>. In addition, the Eu ions are strongly polarized by the neighboring ions in the crystal by incorporating them in noncentrosymmetric crystal sites. The P, T-odd moments in the nucleus interact with the electron gradient density to shift the energies of the nuclear spin states. Therefore, the wavelike ALPs can interact with the Eu nuclei to induce an oscillating P, T-odd nuclear moment, which in turn produce oscillations in the nuclear spin state energy levels of the Eu ion.

We measure the energy splitting between two nuclear spin levels of the  $^7\text{F}_0$  electronic state of  $\text{Eu}^{3+}$  to search for ALP fields coupling to the gluons in the Eu nuclei. In particular, two sub-ensembles of Eu ions that are polarized in opposite directions in the crystal are probed simultaneously, which cancels out the magnetic field fluctuations and kept the sensitivity to the nuclear P, T-odd moments. A frequency analysis of the differential signal between the two sub-ensembles with opposite ALP sensitivities is used to place an experimental constraint on the ALP-gluon coupling across 10 orders of ALP masses, see Fig. 1. The result surpasses the previous constraint from a P, T-odd moment measurement using  $\text{HfF}^+$ <sup>5</sup>, and improves upon the best limit from neutron electric dipole moment measurements<sup>6,7</sup> in some ranges of ALP masses.

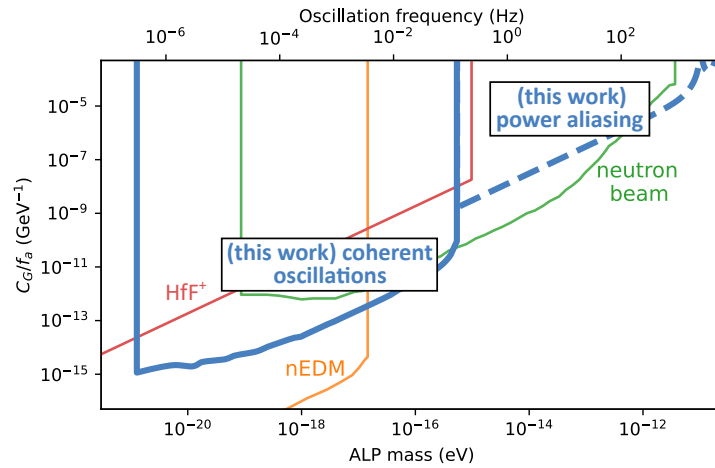


Figure 1: 95% confidence exclusion range on the ALP-gluon coupling from this work enclosed in blue lines. The area enclosed by the blue solid line (labeled as “coherent oscillations”) is the constraint from a spectral analysis of the measured energy level splittings. The area enclosed by the blue dashed line (labeled as “power aliasing”) is excluded by analyzing aliased power into the experiment bandwidth from ALP-induced oscillations that are faster than the experiment cycle frequency. Other constraints from molecular and nuclear P, T-odd moments in this range of ALP masses are also shown.

<sup>1</sup>Planck Collaboration: Aghanim, N. *et al.*, *Astronomy & Astrophysics* **641**, A6 (2020).

<sup>2</sup>Ferreira, E. G. M., *The Astronomy and Astrophysics Review* **29**, 7 (2021).

<sup>3</sup>Stadnik, Y. V and Flambaum, V. V., *Phys. Rev. D* **89**, 043522 (2014).

<sup>4</sup>Flambaum, V. V. and Feldmeier, H., *Phys. Rev. C* **101**, 015502 (2020).

<sup>5</sup>Roussy, T. S. *et al.*, *Phys. Rev. Lett.* **126**, 171301 (2021).

<sup>6</sup>Schulthess, I. *et al.*, *Phys. Rev. Lett.* **129**, 191801 (2022).

<sup>7</sup>Abel, C. *et al.*, *Phys. Rev. X* **7**, 041034 (2014)



Abstract number: P154  
Friday 14:00-15:30

## Advancing Anti-Matter-Wave Interferometry: Design and Implementation of Techniques for Gravity Measurements on Positronium Atoms

**Vinelli G.**<sup>†1,2,3</sup>, Bayo M.<sup>5,6</sup>, Castelli F.<sup>6,7</sup>, Ferragut R.<sup>5,6</sup>, Romé M.<sup>6,7</sup>, Sacerdoti M.<sup>5</sup>, Salvi L.<sup>1,3,4</sup>, Toso V.<sup>6,7</sup>, Giammarchi M.<sup>6</sup>, Rosi G.<sup>3</sup>, Triggiani F.<sup>6</sup>, Tino G. M.<sup>1,3,4,8</sup>

<sup>1</sup>Dipartimento di Fisica e Astronomia, Università di Firenze, Via Sansone 1, 50019 Florence, Italy

<sup>2</sup>Agenzia Spaziale Italiana, Via del Politecnico snc, 00133 Roma, Italy

<sup>3</sup>INFN, Sezione di Firenze, Via Sansone 1, 50019 Florence, Italy

<sup>4</sup>LENS, Università di Firenze, Via Nello Carrara 1, 50019 Sesto Fiorentino, Italy

<sup>5</sup>L-NESS and Dipartimento di Fisica, Politecnico di Milano, Via Anzani 42, 22100 Como, Italy

<sup>6</sup>INFN, Sezione di Milano, Via Celoria 16, 20133 Milano, Italy

<sup>7</sup>Dipartimento di Fisica, Università degli Studi di Milano, Via Celoria 16, 20133 Milano, Italy

<sup>8</sup>Istituto Nazionale di Ottica del Consiglio Nazionale delle Ricerche (CNR-INO), 50019 Sesto Fiorentino, Italy

<sup>†</sup>giuseppe.vinelli@unifi.it

The QUPLAS (QUantum interferometry and gravitation with Positrons and LASers) experiment aims to test fundamental physical laws with antimatter by measuring the **positronium (Ps) fall in the Earth's gravitational field**. Such measurement would represent a test of the **Einstein Equivalence Principle and the CPT symmetry** and is further motivated by the need for a deeper understanding of antimatter behavior in a gravitational field.

The setup and techniques of the experiment involve three phases of production, preparation, and interference of the positronium beam. I will present the design and simulation of a **high-power (200 kW) enhancement cavity for photodetachment** of the positronium negative ion, along with the **Single Photon Large Momentum Transfer (LMT) Mach-Zehnder interferometer**<sup>1</sup>, used to probe the influence of Earth's gravitational field via the phase shift of the Ps wavefunction:  $\Delta\phi = k_{\text{eff}}gT^2$ . Simulations using OSCAR (optical), Ansys (thermal), show that thermal effects on the cavity mirrors are negligible and a circulating power of  $\sim 200$  kW is achievable.

By simulating the interferometer, it was possible to estimate its efficiency, contrast and signal acquisition times as well as the size, shape and power of the laser pulses.

These results, along with the current status of the experimental implementation and test of the cavity (maximum 60 kW achieved due to technical factors), will be reported.

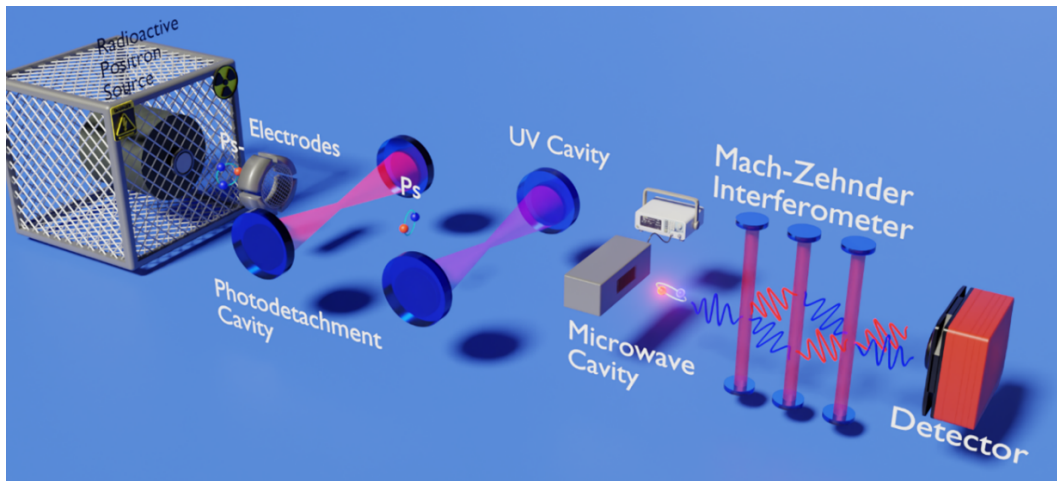


Figure 1: Schematic diagram of the experimental setup showing the above mentioned high-power (200 kW) enhancement cavity for photodetachment of the positronium negative ion and the large momentum transfer Mach-Zehnder interferometer.

<sup>1</sup>G Vinelli *et al.*, *Class. Quantum Grav.* **40** 205024 (2023).



Abstract number: P155

Friday 14:00-15:30

## Progress on measuring the $|\alpha/\beta|$ transition polarizability ratio in the one photon Rb 5S - 6S transition

Lindsay M. D.<sup>†1,2</sup>, Ayachitula R.<sup>2</sup>, Anderson M. D.<sup>2</sup>, Mangani N. A.<sup>2</sup>, Baklarz A. E.<sup>2</sup>, Murray C. M.<sup>2</sup>,  
Knize A. R.<sup>2</sup>, Knize R. J.<sup>2</sup>

<sup>1</sup>Lindsay Enterprises LLC, USAF Academy, CO, USA

<sup>2</sup>United States Air Force Academy, USAF Academy, CO, USA

<sup>†</sup>mark.lindsay@afacademy.af.edu

Using a laser induced fluorescence spectroscopy scheme with a hyperfine pumped collimated Rb atomic beam, we have measured the dc Stark induced one photon Rb 5S - 6S transition at 497 nm, both for  $\Delta F = 0$  and for the much weaker  $\Delta F = \pm 1$ . We excite the 6S state and use a large Si photodiode to measure the 780 nm 5P - 5S cycling transition fluorescence from the previously emptied hyperfine state, which is populated (for the most part) only by the 497 nm transition. We have measured for the first time the ratio of the atomic scalar and vector transition polarizabilities  $\alpha$  corresponding to  $\Delta F = 0$ , and  $\beta$  corresponding to  $\Delta F = \pm 1$ , of the Rb 6S state. We measure their ratio to be  $|\alpha/\beta| = 33(3)$ . We compare this to theoretical calculations. We are working to measure the even weaker zero electric field M1 transition amplitude of the 5S - 6S transition, by implementing an optical build-up traveling wave cavity for the 497 nm laser. This will ultimately allow tests of the Dirac negative energy states.

Abstract number: P156  
Friday 14:00-15:30

## Quantum-enhanced sensing with spin-dependent squeezing

**Bond L. J.**<sup>†1,2</sup>, **Shankar A.**<sup>3</sup>, **Tan T. R.**<sup>4</sup>, **Safavi-Naini A.**<sup>1,2</sup>

<sup>1</sup>*University of Amsterdam, the Netherlands*

<sup>2</sup>*QuSoft, the Netherlands*

<sup>3</sup>*Indian Institute of Technology Madras, India*

<sup>4</sup>*University of Sydney, Australia*

<sup>†</sup>l.j.bond@uva.nl

Parameter sensing plays a fundamental role in science and engineering. When sensing an unknown displacement, bosonic squeezed states are exponentially more sensitive than classical (coherent) states, due to the exponential reduction in variance of either  $x$  or  $p$ . This comes at the cost of exponentially increased variance in the other quadrature, which makes squeezed states unsuitable for the simultaneous sensing of both  $x$  and  $p$ . Here, we reveal that spin-dependent squeezing can be used for the simultaneous sensing of  $x$  and  $p$ . We propose explicit protocols that can be readily implemented in trapped ion platforms. Our work overcomes previous requirements of phase-locking and/or two-mode squeezing and therefore makes a significant step towards quantum-enhanced multi-parameter displacement sensing, with applications ranging from fundamental physics to advanced quantum technologies.

Abstract number: P157  
Friday 14:00-15:30

## Towards a squeezed interferometer with strontium atoms in a high-finesse cavity

**Mancini C.**<sup>†1, 2</sup>, **Mariani T.**<sup>3</sup>, **Pappalardo A.**<sup>4</sup>, **Rosi G.**<sup>4</sup>, **Salvi L.**<sup>4</sup>, **Vendemiati M.**<sup>3</sup>, **Vezio P.**<sup>4</sup>, **Vinelli G.**<sup>4</sup>,  
**Tino G.M.**<sup>4, 5</sup>

<sup>1</sup>*Scuola Superiore Meridionale, Largo San Marcellino 10, 80138 Napoli (NA), Italy*

<sup>2</sup>*INFN Sezione di Napoli, Complesso Universitario di Monte S. Angelo, Via Cinthia Edificio 6, I-80126 Napoli (NA), Italy*

<sup>3</sup>*Dipartimento di Ingegneria Industriale, Università di Firenze, Via Santa Marta 3, 50139 Firenze (FI), Italy*

<sup>4</sup>*Dipartimento di Fisica e Astronomia and LENS, Università di Firenze, INFN Sezione di Firenze, via Sansone 1, I-50019  
Sesto Fiorentino (FI), Italy*

<sup>5</sup>*Istituto Nazionale di Ottica del Consiglio Nazionale delle Ricerche (CNR-INO), 50019 Sesto Fiorentino, Italy*

<sup>†</sup>christian.mancini@na.infn.it

The lowest uncertainty achievable in atom interferometers with  $N$  uncorrelated atoms is due to the standard quantum limit (SQL), for which the smallest interferometric phase resolution is  $1/\sqrt{N}$ . Introducing entanglement among atoms can surpass the SQL, and the spin squeezing technique is very promising in this context<sup>1</sup>. Various approaches have been proposed and used to generate these squeezed states, among them the quantum non-demolition measurement enhanced by optical cavities is one of the most successful. The cavity resonance frequency experiences a state dependent shift from each individual atom. Thus the ground and excited state population are determined in a non-destructive way by measuring the total shift in resonance frequency<sup>2</sup>. Recent squeezing experiments with Yb and Sr atoms have shown significant progress in optical clocks, but overcoming the SQL in interferometers with free-falling atoms remains a challenge.

In this presentation, I will illustrate our proposal<sup>3</sup> and our experimental efforts towards the generation of squeezed states with Sr atoms. Our approach is based on exploiting the enhanced atom-light interaction obtained in a piezoelectrically-tunable, high-finesse optical cavity in a ring bow-tie configuration. In such cavities, even small perturbations to their mechanical properties can compromise stability and severely limit the tunability of the resonance frequency, which is crucial for generating squeezed states.

Our new cavity (see Fig. 1) has been designed, and its performance has been assessed through a finite element analysis, in which a stiffness-wise optimization was carried out while accounting for a wide range of noise sources, including improper optical and opto-mechanical settings, mechanical vibrations transmitted to the cavity, self-weight deformations, temperature fluctuations, and electromagnetic interferences. With this design, mechanical resonances at acoustic frequencies have been significantly reduced. The cavity was then fabricated with a particular high-performance ceramic called Shapal Hi-M Soft. It is a hybrid composite material consisting of aluminum nitride and boron nitride. It has high thermal conductivity, high mechanical strength, excellent electrical insulation, ultra-high purity. The cavity is decoupled from the vacuum chamber thanks to springs of Kalrez, which act as a low-pass filter and avoid vibrations. I will illustrate the experimental apparatus that has been realised towards this goal and show some preliminary measurement results.

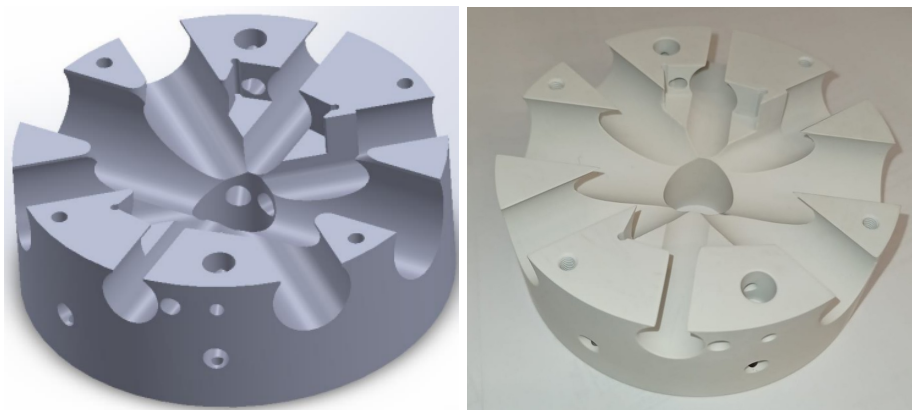


Figure 1: Design of the new cavity (left) and its realization in Shapal (right).

<sup>1</sup>M. Kitagawa, M. Ueda, *Phys. Rev. A* **47**, 5138 (1993).

<sup>2</sup>B.K. Malia, Y. Wu, J. Martínez-Rincón, M.A. Kasevich, *Nature* **612**, 661-665 (2022).

<sup>3</sup>L. Salvi, N. Poli, V. Vuletić and G. M. Tino, *Phys. Rev. Lett.* **120**, 033601 (2018).

Abstract number: P158

Friday 14:00-15:30

## Towards non-destructive microwave detection of magnetically guided ultracold atoms

**T. Xia<sup>1</sup>, D. O. Sabulsky<sup>1</sup>, L. A. Sidorenkov<sup>1</sup>, C. L. Garrido Alzar<sup>†1</sup>**

<sup>1</sup>*LTE, Observatoire de Paris, Université PSL, CNRS, Sorbonne Université, LNE, 61 avenue de l'Observatoire, 75014 Paris, France*

<sup>†</sup>carlos.garrido@obspm.fr

The present research study targets the demonstration of high-bandwidth, microwave non-destructive quantum state detection of magnetically guided <sup>87</sup>Rb ultracold atoms. The atoms are confined in magnetic potentials generated by micro-fabricated wires on an atom chip. The detection principle is based on the measurement of a reflected microwave signal sent to a horn antenna, illuminating the atomic ensemble under non-resonant condition with respect to the clock hyperfine ground state transition.

The achievable demonstrated measurement bandwidth can be as high as 30 kHz, with less than 1% of induced decoherence<sup>1</sup>. The microwave detection solution allows for state-sensitive differential population measurement, between the two F=1 and F=2 hyperfine ground states and between Zeeman states inside a given ground state. As demonstrated in preliminary Ramsey sequences with free-falling atoms, this technique can be very useful for atom interferometry. In particular, it allows one to foresee compact implementations of quantum sensors using an atom chip platform for applications such as inertial sensing and fundamental physics in space.<sup>2</sup>

---

<sup>1</sup>Dubosclard, W., Kim, S. & Garrido Alzar, C.L. Nondestructive microwave detection of a coherent quantum dynamics in cold atoms. *Commun Phys* 4, 35 (2021).

<sup>2</sup>This project has received funding from the European Defence Fund (EDF) under grant agreement 101103417 EDF-2021-DIS-RDIS-ADEQUADE. Funded by the European Union. Views and opinions expressed are however those of the author(s) only and do not necessarily reflect those of the European Union or the European Commission. Neither the European Union nor the granting authority can be held responsible for them. This work was partially supported by the “Sophie Germain” programme, funded by the French Ministry for Europe and Foreign Affairs and the UK Department for Science, Innovation and Technology.

Abstract number: P159  
Friday 14:00-15:30

## Towards a strong coupling regime in Waveguide QED using slow-mode photonic crystal waveguide and cold Rb atoms

Sukanya Mahapatra<sup>†1</sup>, Anaïs Chochon<sup>1</sup>, Idriss Douss<sup>1</sup>, Valère Sautel<sup>2</sup>, Adrien Bouscal<sup>1</sup>, Jérémy Berroir<sup>1</sup>, Tridib Ray<sup>1</sup>, Malik Kemiche<sup>3</sup>, Kamel Bencheikh<sup>2</sup>, Juan Ariel Levenson<sup>2</sup>, Nikos Fayard<sup>4</sup>, Christophe Sauvan<sup>4</sup>, Jean-Jacques Greffet<sup>4</sup>, Alban Urvoy<sup>1</sup>, Julien Laurat<sup>1</sup>

<sup>1</sup>Laboratoire Kastler Brossel, Sorbonne Université, CNRS, ENS-PSL, Collège de France, 75005 Paris, France

<sup>2</sup>Centre de Nanosciences et de Nanotechnologies, CNRS, Université Paris-Saclay, 91120 Palaiseau, France

<sup>3</sup>IMEP-LAHC, Univ. Grenoble Alpes, Univ. Savoie Mont Blanc, CNRS, Grenoble INP, 38000 Grenoble, France

<sup>4</sup>Laboratoire Charles Fabry, Université Paris-Saclay, IOGS, CNRS, F-91127 Palaiseau, France

<sup>†</sup>sukanya.mahapatra@lkb.upmc.fr

Strong light-matter interaction at the quantum level serves as a fundamental building block for quantum technologies, a highly sought-after field of research. In this context, nanophotonic platforms have emerged as more promising compared to free-space systems. Among various nanophotonic platforms, waveguide quantum electrodynamics (waveguide QED) stands out as it offers a higher figure of merit due to the transversely tight confinement of the propagating mode and improved scalability, as it can accommodate a large number of emitters in its vicinity. In this regard, optical nanofibers have opened up new possibilities for quantum networking, quantum nonlinear optics, and quantum many-body physics<sup>1</sup>.

Our objective is to enhance the efficiency of light-matter interaction on the level of single photon using a photonic crystal (PhC) waveguide. We have developed a slow-mode PhC half-W1 waveguide with improved figures of merit compared to an optical nanofiber<sup>2</sup>. Its asymmetric geometry offers two key advantages: enhanced optical access for efficient atom transport and greater flexibility for dispersion engineering (figure 1a). The structure is designed for tight transverse confinement of the guided mode, achieving a high group index ( $\sim 28$ ) over a 9 nm bandwidth, enabling slow-light propagation while mitigating nanofabrication imperfections (figures ?? and 1c). The fabrication has been successfully implemented on a high-refractive-index material, GaInP. We estimated the optimal distance and potential of the two-color dipole trap from the waveguide surface using our in-house Python package, Nanotrappy<sup>3</sup>. The calculated Purcell factor is two orders of magnitude higher than that of an optical nanofiber<sup>2</sup>. I will describe our current work on integrating the waveguide chip into the vacuum system and developing a tighter hybrid dipole trap using Laguerre-Gauss modes to minimize light reflection from the waveguide edge during atom transport<sup>4</sup>.

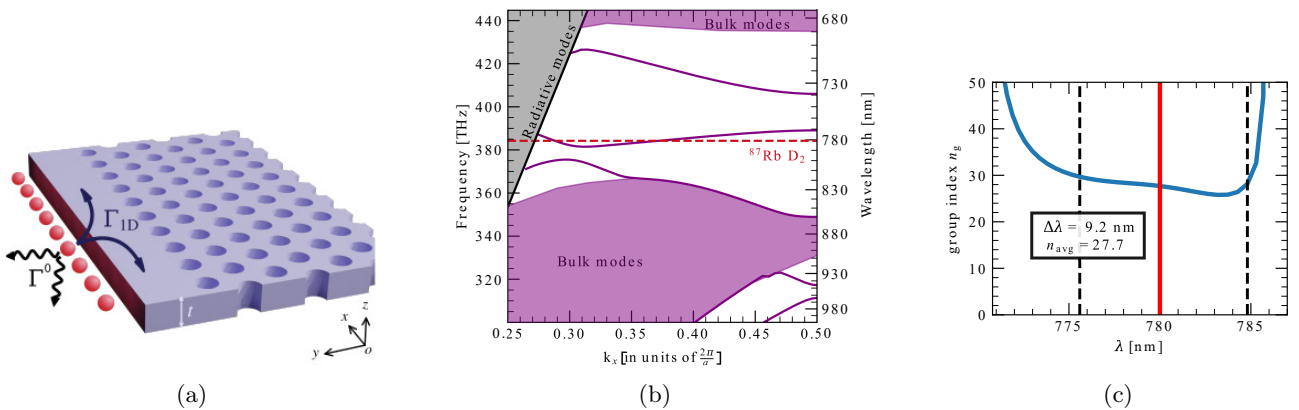


Figure 1: (a) Schematic diagram of the slow mode PhC half W1 waveguide with trapped atoms in its vicinity. (b) Simulated band diagram of the half W1 waveguide. The  $D_2$  transition of  $^{87}\text{Rb}$  (red dotted line) crosses the linear part of the band which indicates a slow-mode region. (c) The calculated group index is constant over a larger bandwidth (indicated by black vertical dotted lines).

<sup>1</sup>N. V. Corzo, J. Raskop, A. Chandra, A. S. Sheremet, B. Gouraud and J. Laurat, *Nature*, **566**, 7744 (2019).

<sup>2</sup>A. Bouscal *et al.*, *New J. Phys.* **26**, 023026 (2024).

<sup>3</sup>J. Berroir, A. Bouscal, A. Urvoy, T. Ray and J. Laurat, *Phys. Rev. Research* **4**, 013079 (2022).

<sup>4</sup>J. B. Béguin, J. Laurat, X. Luan, A. P. Burgers, Z. Qin and H. J. Kimble, *PNAS* **42**, 117 (2020).

**Abstract number: P160**  
**Friday 14:00-15:30**

## Dissipative spin manipulation in a SU(N)-symmetric Fermi gas

Meyroneinc A.<sup>1</sup>, Guesdon P.<sup>1</sup>, Pasquiou B.<sup>1</sup>, Laburthe-Tolra B.<sup>1</sup>, Robert-de-Saint-Vincent M.<sup>1</sup>

<sup>1</sup>Laboratoire de Physique de Lasers, CNRS, Université Sorbonne Paris Nord

Strontium-87 is an alkaline-earth atom with a nuclear spin of  $I=9/2$  that exhibits SU(N) symmetric spin interactions. This type of interaction leads to exotic physics in strongly correlated systems under the influence of effective antiferromagnetic interactions. To engineer such a system, we can use dissipative mechanisms to produce correlated states, which have potential implications for quantum simulation or sensing.

Our team has developed schemes that enable the characterization of the collective spin of alkaline-earth atomic ensembles. Given the large atomic spin  $I=9/2$ , a standard set of measurements of spin projections along three directions of space (x,y,z) does not perform a complete characterization of the state. We have developed a method to coherently and freely manipulate the spins in their wide Hilbert space, that enables implementing complete measurement sets<sup>1</sup>.

Methods relying on Hamiltonian dynamics for creating correlations are challenging to implement because of the requirement for low losses and stable gases. An alternative approach is to use dissipation techniques to favor spin correlation<sup>2</sup>. The idea is to induce spin-selective two-body losses using a photoassociation laser. The two-body losses will be spin-selective due to Pauli's exclusion principle, and only pairs of atoms in a singlet spin state will be affected. The remaining atoms will align their spins along the same axis, driving the system into strongly correlated Dicke states. These states are highly sensitive to phase changes and have a great metrological interest.

To achieve this, we first need to locate the photoassociation lines on the intercombination lines (1S0-3P1) of <sup>87</sup>Sr, which has never been done before. Following this, we intend to demonstrate the creation of correlated states with and without a lattice and characterize their properties like spin fluctuations, correlations, and metrological interest.

Additionally, our system also provides the possibility to investigate losses in higher-dimensional Hilbert space, opening the way to new possibilities. For example, we intend to study two- or three-body losses in the SU(3) manifold and understand the different regimes, the dynamics, and the possible dark states<sup>3,4</sup>.

<sup>1</sup>Husain Ahmed, et al. Coherent control over the high-dimensional space of the nuclear spin of alkaline-earth atoms.  
<https://doi.org/10.48550/arXiv.2501.01731>

<sup>2</sup>Foss-Feig, J. Daley, et al. Steady-State Many-Body Entanglement of Hot Reactive Fermions. *Phys. Rev. Lett.* **109**, 230501 (2012).  
<https://doi.org/10.1103/PhysRevLett.109.230501>

<sup>3</sup>L. Rosso, L. Mazza and A. Biella Eightfold way to dark states in SU(3) cold gases with two-body losses.  
<https://doi.org/10.1103/PhysRevA.105.L051302>.

<sup>4</sup>A. Marché et al. SU(3) Fermi-Hubbard gas with three-body losses: symmetries and dark states.  
<https://doi.org/10.48550/arXiv.2503.17217>

Abstract number: P161

Friday 14:00-15:30

## Saturated-absorption Cavity Ring-down (SCAR) Spectroscopy: Exploring the limits of Sensitivity and Precision for Molecular Detection

Bartalini S.<sup>1,2</sup>, Delli Santi M. G.<sup>3</sup>, Galli I.<sup>1,4</sup>, Detti A.<sup>1,2</sup>, Montori A.<sup>1,2</sup>, Aiello R.<sup>3</sup>, Maddaloni P.<sup>3</sup>, Mazzotti D.<sup>1,4</sup>, De Natale P.<sup>†1</sup>

<sup>1</sup>National Institute of Optics, CNR, Sesto Fiorentino (FI), Italy

<sup>2</sup>ppqSense, srl, Viale Ariosto 492/B 50019 Sesto Fiorentino (FI), Italy

<sup>3</sup>National Institute of Optics, CNR, Via Campi Flegrei, 34 - Comprensorio A.Olivetti, 80078 Pozzuoli (NA), Italy

<sup>4</sup>LENS - European Laboratory for Non-Linear Spectroscopy, Via Carrara, 1 - 50019 Sesto Fiorentino, Italy

<sup>†</sup>paolo.denatale@cnr.it

Saturated Absorption Cavity Ringdown (SCAR) technique has achieved unprecedented sensitivity in molecular detection, reaching parts-per-quadrillion levels for radiocarbon dioxide ( $^{14}\text{CO}_2$ )<sup>1,2</sup>. This milestone is attributed to the effective implementation of SCAR and the ultra-low noise operation of mid-infrared quantum cascade lasers (QCLs). Technological advancements have consistently improved upon these remarkable capabilities, unlocking new avenues for key applications. Recent advancements have focused on optimizing the noise spectral density of QCLs and improving the overall stability of the setup, aiming to push sensitivity limits beyond the classical regime.

By combining the SCAR technique in the Lamb-dip regime with the buffer gas cooling method, we have also demonstrated absolute frequency metrology of ro-vibrational molecular spectra at 1 kHz level accuracy<sup>3</sup>. This technique has significant implications for applications requiring the highest sensitivity, such as environmental monitoring and, in particular, the precise measurement of radiocarbon levels in atmospheric samples. It will be shown that state-of-the-art SCAR spectrometers can already achieve a sensitivity, for  $^{14}\text{CO}_2$ , better than 1 part-per-quadrillion, moving further the best results ever achieved by laser molecular spectroscopy. These advancements position SCAR as a transformative tool for climate science, archaeology, and nuclear safety<sup>4,5</sup>, aligning with global initiatives focused on controlling greenhouse gas emissions.

<sup>1</sup>Giusfredi, G., Bartalini, S., Borri, S., Cancio, P., Galli, I., Mazzotti, D., and De Natale, P., Saturated absorption cavity ring-down spectroscopy, *Physical review letters* **104**(11), 110801 (2010).

<sup>2</sup>Galli, I., Bartalini, S., Borri, S., Cancio, P., Mazzotti, D., De Natale, P., and Giusfredi, G., Molecular gas sensing below parts per trillion: radiocarbon-dioxide optical detection, *Physical Review Letters* **107**(27), 270802 (2011).

<sup>3</sup>Aiello, R., Di Sarno, V., Delli Santi, M. G., De Rosa, M., Ricciardi, I., De Natale, P., Santamaria, L., Giusfredi, G., and Maddaloni, P., Absolute frequency metrology of buffer-gas-cooled molecular spectra at 1 kHz accuracy level, *Nature Communications* **13**(1), 7016 (2022).

<sup>4</sup>Delli Santi, M. G., Bartalini, S., Cancio, P., Galli, I., Giusfredi, G., Haraldsson, C., Mazzotti, D., Pesonen, A., and De Natale, P., Biogenic fraction determination in fuel blends by laser-based  $^{14}\text{CO}_2$  detection, *Advanced Photonics Research* **2**(3), 2000069 (2021).

<sup>5</sup>Delli Santi, M. G., Insero, G., Bartalini, S., Cancio, P., Carcione, F., Galli, I., Giusfredi, G., Mazzotti, D., Bulgheroni, A., Martinez Ferri, A. I., *et al.*, Precise radiocarbon determination in radioactive waste by a laser-based spectroscopic technique, *Proceedings of the National Academy of Sciences* **119**(28), e2122122119 (2022).

Abstract number: P162

Friday 14:00-15:30

# The Anderson Transition in a Symplectic Two-Dimensional Ultracold Gas

**Hutchinson D. A. W.**<sup>†1,2</sup>, Arabahmadi E.<sup>1</sup>, Schumayer D.<sup>3</sup>, Hoogerland M.<sup>4</sup>, Grémaud B.<sup>2,5</sup>, Miniatura C.<sup>2,6</sup>

<sup>1</sup>Dodd-Walls Centre, University of Otago, New Zealand

<sup>2</sup>Centre for Quantum Technologies, National University of Singapore, Singapore

<sup>3</sup>University of Sydney, Australia

<sup>4</sup>Dodd-Walls Centre, University of Auckland, New Zealand

<sup>5</sup>Aix Marseille Univ, Université de Toulon, CNRS, CPT, IPhU, AMUtech, Marseille, France

<sup>6</sup>Université Côte d'Azur, CNRS, Institut de Physique de Nice, Nice, France

<sup>†</sup>david.hutchinson@otago.ac.nz

The wave-nature of electrons is responsible for the long mean free path in regular lattices because of destructive interference from back-scattered waves. This leads to the high conductivity of metals. In disordered systems, interference can suppress transport in all directions leading to insulating behaviour, (Anderson Localisation).

In one-dimension (1D) in the thermodynamic limit, however weak the disorder, all single particle states are localised, and the system is an insulator. In three-dimensions (3D), states with low energy can be localised, whilst those with higher momenta and energy can be extended. There then exists a quantum phase transition depending upon the location of the Fermi Surface relative to the Mobility Edge, the boundary between localised and extended states. Two-dimensions (2D) represents the marginal dimension in which the system asymptotically approaches the metallic phase as the strength of disorder approaches zero such that, again, for any finite disorder, the states are always localised and the system an insulator, but the localisation length can be very large.

Direct observation of the localisation of matter waves in 2D, particularly in ultracold atomic gases, had remained elusive. Using a geometry based upon a circular source region of atoms and a similar drain region, connected by a 2D channel containing a series of optical “spike” potentials representing the disorder, we were able to observe, the characteristic exponential decay of atom density, and hence conclude that we had observed Anderson Localisation in a 2D ultracold atom system.

For continuous phase transitions, such as the Anderson transition, there exists a single parameter that diverges exponentially at the transition point, determined by a critical exponent unique to the specific universality class. For time-reversal and spin-rotational symmetries (orthogonal symmetry class) an Anderson transition occurs for a finite level of disorder in three (and higher) dimensions, below which the system is a conductor and above which it is an insulator. In 1D, as stated above, any disorder, however weak, always localises states, and (2D), for weakening disorder the localisation length gets longer and longer, but again for large enough systems, the states are always localised, and the system is an insulator.

Spin-orbit coupling breaks the spin rotational symmetry, e.g., leads to the splitting of the sodium D-line. Such reduction of symmetry yields a system in the symplectic symmetry class and permits the development of a well-defined Anderson transition even in 2D. In the symplectic class the critical exponent was first accurately evaluated by Slevin's group. More recently, in a Letter published in Physical Review Research, we have shown how the critical exponent can be extracted from experimentally available momentum-space signatures. Both our group, and that of Slevin, have also characterised the temporal and finite-size properties of the symplectic 2D system around the phase transition.

This investigation has raised several questions regarding the nature of this novel metal-insulator phase transition in a 2D system and has implications for other fields including electron transport in Si MOSFETs.

We present results from our recent work both experimentally observing Anderson Localisation in a two-dimensional ultracold atomic gas within the orthogonal symmetry class and theoretically investigating the Anderson Transition in a 2D symplectic system with spin-orbit coupling.



Abstract number: P163  
Friday 14:00-15:30

# Measurement validation and cycle slip detection on a single optical frequency comb

Burden A.<sup>†1,2</sup>, Griffin P.<sup>1</sup>, Riis E.<sup>1</sup>, Tunesi J.<sup>2</sup>, Margolis H.S.<sup>2</sup>

<sup>1</sup>University of Strathclyde, Glasgow, Scotland

<sup>2</sup>National Physical Laboratory, Teddington, England

<sup>†</sup>alexander.burden@strath.ac.uk

Stable, accurate, and traceable frequency reference signals are critical for the academic and industrial development of precision timekeeping technologies, with applications in telecommunications, navigation, finance, and the energy sector. We will present how the deployment of a UTC(NPL) steered caesium beam clock, an optical frequency comb (OFC) and an ultrastable laser (USL), at the University of Strathclyde, enables the provision of test and evaluation services for these emerging technologies, while also providing accessible and trusted optical frequency signals to support next-generation optical clock development.

To ensure and maintain trust in the results produced, ongoing validation of frequency and phase measurements is important, as a single cycle slip within an hour of measurement can cause a bias on the measured frequency on the order of  $10^{-18}$ , if undetected and unaccounted for. The ideal validation is an out-of-loop secondary comb measurement used to verify each data point<sup>1</sup>; however, this is often unfeasible or unpractical. Alternatives involve counting several known optical frequency ratios, which requires access to several stable frequency standards, using multiple independent tracking oscillators to detect cycle slips<sup>2</sup> or employing redundant counting<sup>3</sup>, which can both increase experimental complexity.

Using the experimental setup seen in Figure 1, we will show how frequency errors are introduced in relation to the SNR of the different comb signals. Ensuring consistent SNR over a given threshold may be unrealistic in some cases, so a validation scheme implemented by monitoring the SNR signals in real time will be presented. This is going to be employed to detect likely cycle slip events in both the counting and locking electronics, that otherwise may be missed in alternative schemes. The effectiveness of the technique is verified using a second frequency comb.

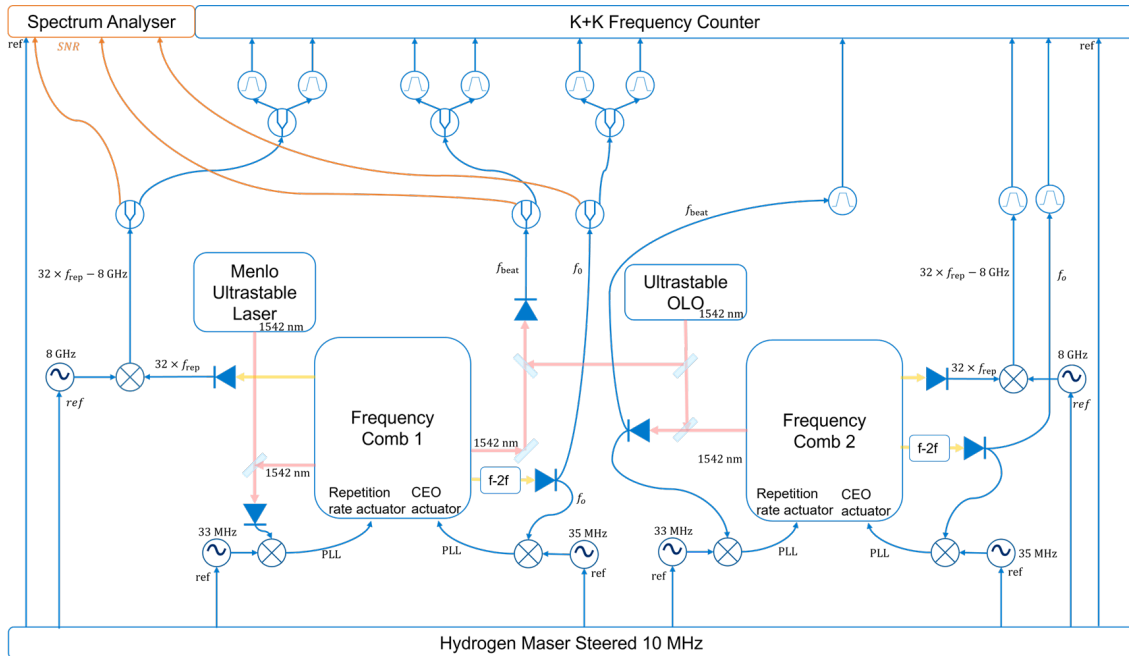


Figure 1: SNR monitoring and dual comb validation experimental setup in Teddington.

<sup>1</sup>L.A.M Johnson, P. Gill and H.S. Margolis, *Metrologia* **52**, 62 (2015).

<sup>2</sup>M. Risaro, P. Savio, M. Pizzocaro, F. Levi, D. Calonico and C. Clivati, *Phys. Rev. Appl.* **18**, 064010 (2022).

<sup>3</sup>T. Udem, J. Reichert, T.W. Hänsch and M. Kourogi, *Opt. Lett.* **23**, 1387-1389 (1998).

Abstract number: P164  
Friday 14:00-15:30

## Development of a high-bandwidth atom interferometer for gravity sensing

Mendes M. I. F.<sup>1</sup>, Naniyil V.<sup>1</sup>, Pietrzyk M. E.<sup>1</sup>, Kinge S.<sup>2</sup>, Wilkinson P.<sup>3</sup>, Holynski M.<sup>1</sup>, Smith V. A.<sup>4</sup>,  
Lien Y.-H.<sup>†1</sup>

<sup>1</sup>*School of Physics and Astronomy, University of Birmingham, Birmingham, UK*

<sup>2</sup>*Materials Engineering, Toyota Motor Europe, Hoge Wei 33, Zaventem 1930, Brussels, Belgium*

<sup>3</sup>*British Geological Survey, Keyworth, Nottingham, UK*

<sup>4</sup>*British Geological Survey, Space Geodesy Facility, Herstmonceux, UK*

<sup>†</sup>y.lien@bham.ac.uk

Atom interferometry has rapidly progressed since its birth and attracted huge interests for its applications in fundamental research, including test of weak equivalent principle<sup>1</sup>, quantum superposition<sup>2</sup>, gravitational wave and dark energy detectors<sup>3</sup>, determination of fundamental constants<sup>4 5</sup>, to name a few. Atom interferometry has rapidly progressed since its birth and attracted huge interest for its applications in fundamental research, including tests of weak equivalent principle, demonstration of spatial entanglement, gravitational wave and dark energy detectors, and determination of fundamental constants, to name a few. In the past decade, people have worked tirelessly to demonstrate its potential in real-world applications, for example, the detection of urban underground structures<sup>6</sup>, magma monitoring<sup>7</sup>, and marine and airborne gravity surveys<sup>8 9</sup>, in the recent surge of interest in quantum technology.

The quantum sensing group at the University of Birmingham in collaboration with Toyota Motor Europe has been developing a high-bandwidth absolute gravimeter for mobile platforms such as vehicles since 2019. The high-bandwidth quantum gravimeter utilises laser cooling and trapping techniques to prepare <sup>87</sup>Rb atoms into specific quantum states. Later, a technique of Raman atom interferometry is used to manipulate the quantum states of atoms to measure local gravity. The designed sensitivity of the gravimeter is 10<sup>-7</sup>g/√Hz at a bandwidth of 100 Hz. The latest progress will be reported at the conference.

<sup>1</sup>P. Asenbaum, C. Overstreet, M. Kim, J. Curti, and M. A. Kasevich, *Phys. Rev. Lett.* **125**, 191101 (2020).

<sup>2</sup>T. Kovachy *et al.*, *Nature* **528**, 530 (2015).

<sup>3</sup>B. Canuel, *et al.*, *Classical Quant. Grav.* **37**, 225017 (2020).

<sup>4</sup>G. Rosi, F. Sorrentino, L. Cacciapuoti, M. Prevedelli, and G. M. Tino, *Nature* **510**, 518 (2014).

<sup>5</sup>L. Morel, Z. Yao, P. Cladé, and S. Guellati-Khélifa, *Nature* **588**, 61 (2020).

<sup>6</sup>B. Stray, *et al.*, *Nature* **602**, 590 (2022).

<sup>7</sup>L. Antoni-Micollier, *et al.*, *Geophys. Res. Lett.* **49**, e2022GL097814 (2022).

<sup>8</sup>Y. Bidel, *et al.*, *Nat. Commun.* **9**, 627 (2018).

<sup>9</sup>Y. Bidel, *et al.*, *J. Geophys. Res. Solid Earth* **128**, e2022JB025921 (2023).

Abstract number: P165  
Friday 14:00-15:30

## Spin- and Momentum-Correlated Atom Pairs Mediated by Photon Exchange and Seeded by Vacuum Fluctuations

**Fricke J. F.<sup>1</sup>, Finger F.<sup>1</sup>, Rosa-Medina R.<sup>1</sup>, Reiter N.<sup>1</sup>, Montalti N.<sup>1</sup>, Christodoulou P.<sup>1</sup>, Donner T.<sup>1</sup>, Esslinger T.<sup>†1</sup>**

<sup>1</sup>*Institute for Quantum Electronics and Quantum Center, ETH Zürich, 8093 Zürich, Switzerland*

<sup>†</sup>esslinger@phys.ethz.ch

Quantum correlations among the constituents of many-body systems determine their fundamental properties. With their pristine control over external and internal degrees of freedom, Quantum gases offer a versatile platform to manipulate and detect such correlations at a microscopic level. Here, we report on observing correlated atomic pairs in specific spin and momentum modes. Our implementation relies on Raman scattering between different spin levels of a spinor Bose-Einstein condensate induced by the interplay of a running-wave transverse laser and the vacuum field of an optical cavity. Far-detuned from Raman resonance, a four-photon process gives rise to collectively-enhanced spin-mixing dynamics. We investigate the statistics of the produced pairs and explore their non-classical character through noise correlations in momentum space. Our results demonstrate a new platform for the fast generation of correlated pairs in a quantum gas and provide prospects for matter-wave interferometry using entangled motional states.

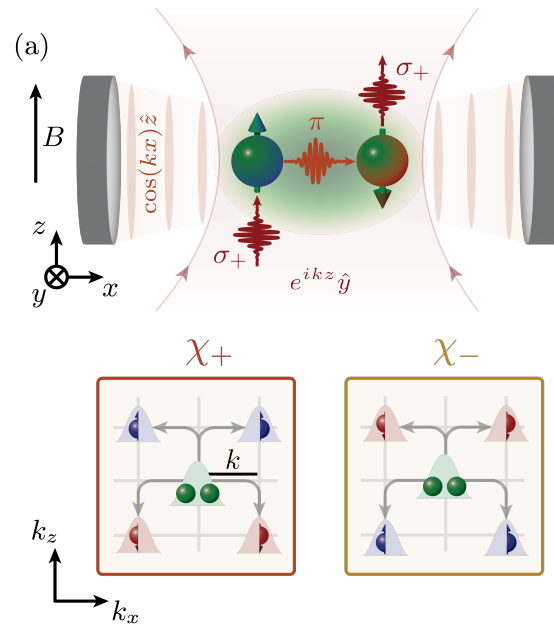


Figure 1: (a) Microscopic pair-production mechanism. Two  $m = 0$  atoms in the BEC (green) are converted into a pair of  $m = +1$  (blue) and  $m = -1$  (red) via two Raman processes involving absorption and emission of a  $\sigma_+$  drive photon and a shared virtual cavity  $\pi$ -photon.

Abstract number: P166

Friday 14:00-15:30

## Ultra-cold Hg atoms for sensing fundamental physics

Witkowski M.<sup>1</sup>, Nandi I.<sup>1</sup>, Sahu A.<sup>1</sup>, Linek A.<sup>1</sup>, Zawada M.<sup>1</sup>, Ciuryło R.<sup>†1</sup>

<sup>1</sup>*Institute of Physics, Faculty of Physics, Astronomy and Informatics, Nicolaus Copernicus University, Toruń, Poland*

<sup>†</sup>rciurylo@umk.pl

We are developing a molecular sensor based on ultra-cold Hg for the study of fundamental interactions. Our experimental system allows implementation of optical Feshbach resonances in ultra-cold collisions of Hg-Hg or Hg-alkali atoms<sup>1,2</sup>. One of our goals is construction of an Hg<sub>2</sub> optical molecular clock<sup>3,4</sup>. Such a tool has the potential to obtain the new level of accuracy and precision in study of fundamental interactions.

Possible new hadron-hadron interactions beyond Standard Model will be studied with Hg<sub>2</sub> molecule, one of the heaviest two-atom system. The choice of the Hg-Hg system is dictated by the relatively good characterization of interaction between mercury atoms<sup>5</sup>. Further mitigation of the impact of theoretical imperfections will be reached thanks to quantum defect theory<sup>6</sup> and measurements of rovibronic bound states near the dissociation threshold within the ground electronic configuration<sup>7</sup>. Such an approach has emerged as a promising method for probing new interactions<sup>8</sup>.

Key step for this study is development of the proper optical dipole trap. In case of Hg atoms it is especially challenging because the polarizability of mercury atoms is significantly smaller than the polarizabilities of other commonly trapped and cooled atoms. Molecular structure of Hg<sub>2</sub> will be determined with help of one- and two-color photoassociations involving various isotopologues of Hg<sub>2</sub>.

<sup>1</sup>M. Witkowski, B. Nagórny, R. Munoz-Rodriguez, R. Ciuryło, P. S. Żuchowski, S. Bylicki, M. Piotrowski, P. Morzyński, M. Zawada, *Opt. Express* **25**, 3165 (2017).

<sup>2</sup>M. Borkowski, R. Munoz Rodriguez, M. B. Kosicki, R. Ciuryło, P. S. Żuchowski, *Phys. Rev. A* **96**, 063411 (2017).

<sup>3</sup>M. Borkowski, *Phys. Rev. Lett.* **120**, 083202 (2018).

<sup>4</sup>S. S. Kondov, C. H. Lee, K. H. Leung, C. Liedl, I. Majewska, R. Moszynski, T. Zelevinsky, *Nat. Phys.* **15**, 1118 (2019).

<sup>5</sup>M. Krośnicki, M. Strojecki, T. Urbańczyk, A. Pashov, J. Koperski, *Phys. Rep.* **591**, 1 (2015).

<sup>6</sup>F. H. Mies, "A multichannel quantum defect analysis of diatomic predissociation and inelastic atomic scattering", *J. Chem. Phys.* **80**, 2514 (1984).

<sup>7</sup>M. Kitagawa, K. Enomoto, K. Kasa, Y. Takahashi, R. Ciuryło, P. Naidon, P. S. Julienne, *Phys. Rev. A* **77**, 012719 (2008).

<sup>8</sup>M. Borkowski, A. A. Buchachenko, R. Ciuryło, P. S. Julienne, H. Yamada, Y. Kikuchi, Y. Takasu, Y. Takahashi, *Sci. Rep.* **9**, 14807 (2019).

Abstract number: P167  
 Friday 14:00-15:30

## Isotopic effect on optical clock transition affected by cold atoms collisions

Bala R.<sup>1</sup>, Linek A.<sup>1</sup>, Witkowski M.<sup>1</sup>, Żuchowski P.<sup>1</sup>, Julienne P. S.<sup>1,2</sup>, Zawada M.<sup>1</sup>, Ciuryło R.<sup>†1</sup>

<sup>1</sup>*Institute of Physics, Faculty of Physics, Astronomy and Informatics, Nicolaus Copernicus University, Toruń, Poland*

<sup>2</sup>*Joint Quantum Institute, University of Maryland and NIST, College Park, MD 20742, USA*

<sup>†</sup>rciurylo@umk.pl

We consider the Hg clock transition<sup>1</sup> perturbed by elastic collisions with cold Rb atoms in their ground electronic state as a case study for variation of collisional width and shift of clock transition with respect to reduced mass of colliding partners. The experimental system for the study of Hg-Rb ultra-cold collisions is under development and is capable to provide basic information about interaction potentials and scattering properties at ultra-low collision energies<sup>2,3</sup>. In this study, the Born-Oppenheimer effective interaction potentials are modeled by including the leading long-range van der Waals coefficients. Unfortunately, the s-wave scattering lengths describing the basic scattering properties at ultralow energies are not known for Hg-Rb system. Nevertheless, our study shows possible range of variation of collisional width and shift when isotopic compositions of colliding atoms and hence, the reduced mass changed. Calculations were carried out in the range of temperatures from 1 nK to 1 K. We confront the full quantum scattering calculations<sup>4</sup> with approximations based on s-wave scattering lengths<sup>5,6</sup> and the semi-classical approximation<sup>7</sup> for collisional widths and shifts. We show that the shape resonances in excited and ground scattering states lead to a significant variations of collisional line shape parameters with the change of the reduced mass of colliding atoms. We also indicate the possible influence of inelasticity of collisions on obtained results.

<sup>1</sup>H. Hachisu, K. Miyagishi, S. G. Porsev, A. Derevianko, V. D. Ovsiannikov, V. G. Pal'chikov, M. Takamoto, H. Katori, *Phys. Rev. Lett.* **100**, 053001 (2008).

<sup>2</sup>M. Witkowski, B. Nagórny, R. Munoz-Rodriguez, R. Ciuryło, P. S. Żuchowski, S. Bylicki, M. Piotrowski, P. Morzyński, M. Zawada, *Opt. Express* **25**, 3165 (2017).

<sup>3</sup>M. Borkowski, R. Munoz Rodriguez, M. B. Kosicki, R. Ciuryło, P. S. Żuchowski, *Phys. Rev. A* **96**, 063411 (2017).

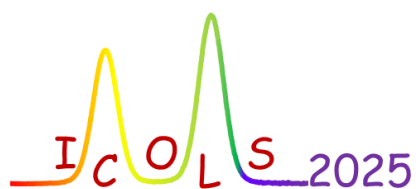
<sup>4</sup>P. S. Julienne, F. H. Mies, *Phys. Rev. A* **34**, 3792 (1986).

<sup>5</sup>P. J. Leo, P. S. Julienne, F. H. Mies, C. J. Williams, *Phys. Rev. Lett.* **86**, 3743 (2001).

<sup>6</sup>S. J. J. M. F. Kokkelmans, B. J. Verhaar, K. Gibble, D. J. Heinzen, *Phys. Rev. A* **56**, R4389 (1997).

<sup>7</sup>N. Allard, J. Kielkopf, *Rev. Mod. Phys.* **54**, 1103 (1982).

*Authors index*



# Index of contributions

## Hot topic contributions

HT1	36
HT2	37
HT3	38
HT4	39
HT5	40
HT6	41
HT7	42
HT8	43
HT9	44

## Invited contributions

I1	6
I2	7
I3	8
I4	9
I5	10
I6	11
I7	12
I8	13
I9	14
I10	15
I11	16
I12	17
I13	18
I14	19
I15	20
I16	21
I17	22
I18	23
I19	24
I20	25
I21	26
I22	27
I23	28
I24	29
I25	30
I26	31
I27	32
I28	33
I29	34

## Poster contributions

P1	46
P2	47
P3	48
P4	49
P5	50
P6	51
P7	52
P8	53
P9	54
P10	55
P11	56
P12	57
P13	58
P14	59
P15	60
P16	61
P17	62
P18	63
P19	64
P20	65
P21	66
P22	67

P23	68
P24	69
P25	70
P26	71
P27	72
P28	73
P29	74
P30	75
P31	76
P32	77
P33	78
P34	79
P35	80
P36	81
P37	82
P38	83
P39	84
P40	85
P41	86
P42	87
P43	88
P44	89
P45	90
P46	91
P47	92
P48	93
P49	94
P50	95
P51	96
P52	97
P53	98
P54	99
P55	100
P56	101
P57	102
P58	103
P59	104
P60	105
P61	107
P62	108
P63	109
P64	110
P65	111
P66	112
P67	113
P68	114
P69	115
P70	116
P71	117
P72	118
P73	119
P74	120
P75	121
P76	122
P77	123
P78	124
P79	125
P80	126
P81	127
P82	128
P83	129
P84	130
P85	131

P86	132
P87	133
P88	134
P89	135
P90	136
P91	137
P92	138
P93	139
P94	140
P95	141
P96	142
P97	143
P98	144
P99	145
P100	146
P101	147
P102	148
P103	149
P104	150
P105	151
P106	152
P107	153
P108	154
P109	155
P110	156
P111	157
P112	158
P113	159
P114	160
P115	161
P116	162
P117	163
P118	164
P119	165
P120	167
P121	168
P122	169
P123	170
P124	171
P125	172
P126	173

P127	174
P128	175
P129	176
P130	177
P131	178
P132	179
P133	180
P134	181
P135	182
P136	183
P137	184
P138	185
P139	186
P140	187
P141	188
P142	189
P143	190
P144	191
P145	192
P146	193
P147	194
P148	195
P149	196
P150	197
P151	198
P152	199
P153	200
P154	201
P155	202
P156	203
P157	204
P158	205
P159	206
P160	207
P161	208
P162	209
P163	210
P164	211
P165	212
P166	213
P167	214



# Alphabetical index of presenting authors

Abraham J. J. - <b>P73</b> .....	<b>119</b>	Filin D. - <b>P31</b> .....	<b>76</b>
Ackerman Z. E. D. - <b>P27</b> .....	<b>72</b>	Fouka K. - <b>P22</b> .....	<b>67</b>
Ajayakumar A. - <b>P51</b> .....	<b>96</b>	Franke-Arnold S.- <b>I16</b> .....	<b>21</b>
Arndt M. - <b>I6</b> .....	<b>11</b>	Fricke J. F. - <b>P165</b> .....	<b>212</b>
Arnold A. S. - <b>P48</b> .....	<b>93</b>		
Athanasakis-Kaklamanakis M. - <b>P20</b> .....	<b>65</b>	Gaaloul N. - <b>P130</b> .....	<b>177</b>
Aude Craik D. P. L. - <b>HT1</b> .....	<b>36</b>	Gajda M. - <b>P56</b> .....	<b>101</b>
		Gao K. - <b>P115</b> .....	<b>161</b>
Baruzzo M. - <b>P24</b> .....	<b>69</b>	Gaudout S. - <b>P119</b> .....	<b>165</b>
Battelier B. - <b>P66</b> .....	<b>112</b>	Gauguet A. - <b>P25</b> .....	<b>70</b>
Baur D. - <b>P99</b> .....	<b>145</b>	Gavryusev V. - <b>P45</b> .....	<b>90</b>
Beck H. - <b>P134</b> .....	<b>181</b>	Giardini V. - <b>P71</b> .....	<b>117</b>
Bednarski B. - <b>P6</b> .....	<b>51</b>	Goti I. - <b>P133</b> .....	<b>180</b>
Beller T. - <b>P131</b> .....	<b>178</b>	Gozzelino M. - <b>P97</b> .....	<b>143</b>
Biagioni G. - <b>P46</b> .....	<b>91</b>	Gravina S. - <b>P141</b> .....	<b>188</b>
Blondel C. - <b>P15</b> .....	<b>60</b>	Gómez-Fernández L. - <b>P142</b> .....	<b>189</b>
Blume D. - <b>P77</b> .....	<b>123</b>		
Bohr E. A. - <b>HT2</b> .....	<b>37</b>	Hahn R. - <b>P144</b> .....	<b>191</b>
Bond L. J. - <b>P156</b> .....	<b>203</b>	Hangst J. S. - <b>I12</b> .....	<b>17</b>
Bouloufa-Maafa N. - <b>HT3</b> .....	<b>38</b>	Heier J. - <b>P70</b> .....	<b>116</b>
Burden A. - <b>P163</b> .....	<b>210</b>	Heizenreder B. - <b>P2</b> .....	<b>47</b>
Butery E. - <b>P12</b> .....	<b>57</b>	Herrera-Sancho O. A. - <b>P80</b> .....	<b>126</b>
		Hillberry L. E. - <b>P122</b> .....	<b>169</b>
Cacciapuoti L. - <b>HT7</b> .....	<b>42</b>	Ho M. - <b>P151</b> .....	<b>198</b>
Castrillo A. - <b>P84</b> .....	<b>130</b>	Hollberg L. H. - <b>HT9</b> .....	<b>44</b>
Chakraborty A. - <b>P21</b> .....	<b>66</b>	Houwman J. J. A. - <b>P136</b> .....	<b>183</b>
Chen S. - <b>P38</b> .....	<b>83</b>	Huang D.-Y. - <b>P92</b> .....	<b>138</b>
Chen Y. - <b>P16</b> .....	<b>61</b>	Huang M.-Z. - <b>P113</b> .....	<b>159</b>
Cheuk L. - <b>I21</b> .....	<b>26</b>	Humphreys B. - <b>P94</b> .....	<b>140</b>
Cimmino R. T. - <b>P63</b> .....	<b>109</b>	Hutchinson D. A. W. - <b>P162</b> .....	<b>209</b>
Ciuryło R. - <b>P166</b> .....	<b>213</b>		
Ciuryło R. - <b>P167</b> .....	<b>214</b>	Jenkins R. - <b>P82</b> .....	<b>128</b>
Cline J. R. K. - <b>P72</b> .....	<b>118</b>	Jiang J. - <b>P114</b> .....	<b>160</b>
Cominotti R. - <b>P147</b> .....	<b>194</b>	Jiang M. - <b>P107</b> .....	<b>153</b>
Corgier R. - <b>P127</b> .....	<b>174</b>	Jyoti A. - <b>P58</b> .....	<b>103</b>
Cornell E. - <b>I1</b> .....	<b>6</b>		
Cornish S. L.- <b>I20</b> .....	<b>25</b>	Kang S. - <b>P100</b> .....	<b>146</b>
Cui J.-M. - <b>P50</b> .....	<b>95</b>	Ketterle W.- <b>I17</b> .....	<b>22</b>
Curtis E. A. - <b>P47</b> .....	<b>92</b>	Kjær J. K. - <b>P145</b> .....	<b>192</b>
Cygan A. - <b>P14</b> .....	<b>59</b>	Koch C. - <b>I18</b> .....	<b>23</b>
		Kocik R. R. - <b>P102</b> .....	<b>148</b>
de Léséleuc S. - <b>P18</b> .....	<b>63</b>	Kristensen S. L. - <b>P42</b> .....	<b>87</b>
De Natale P. - <b>P161</b> .....	<b>208</b>	Kwong C.C. - <b>P44</b> .....	<b>89</b>
De Natale P. - <b>P96</b> .....	<b>142</b>		
DeMille D. - <b>I2</b> .....	<b>7</b>	Landru M. - <b>P34</b> .....	<b>79</b>
Dinesan H. - <b>P79</b> .....	<b>125</b>	Lannig S. - <b>P143</b> .....	<b>190</b>
Donati L. - <b>P152</b> .....	<b>199</b>	Lecomte M. - <b>P78</b> .....	<b>124</b>
Dubois L. - <b>P55</b> .....	<b>100</b>	Lee S. - <b>P89</b> .....	<b>135</b>
		Lee S.-B. - <b>P64</b> .....	<b>110</b>
Eikema K. - <b>I11</b> .....	<b>16</b>	Lei J.-Y. - <b>P28</b> .....	<b>73</b>
Eriksen A. S. - <b>P129</b> .....	<b>176</b>	Lien Y.-H. - <b>P164</b> .....	<b>211</b>
		Lienhard V. - <b>P110</b> .....	<b>156</b>
Fabre A. - <b>P36</b> .....	<b>81</b>	Lindsay M. D. - <b>P155</b> .....	<b>202</b>
Famà F. - <b>P60</b> .....	<b>105</b>	Lisak D. - <b>I8</b> .....	<b>13</b>
Fan M. - <b>P153</b> .....	<b>200</b>	Liu J. - <b>P29</b> .....	<b>74</b>
Fang S.-C. - <b>P68</b> .....	<b>114</b>	Lombardi P. - <b>P123</b> .....	<b>170</b>
Favier M. - <b>P95</b> .....	<b>141</b>	Luo W. - <b>P37</b> .....	<b>82</b>

Mahapatra S. - <b>P159</b> .....	206	Robinson-Tait J. - <b>P128</b> .....	175
Mamat B. - <b>P108</b> .....	154	Rodewald J. - <b>P140</b> .....	187
Mancini C. - <b>P157</b> .....	204	Roe T. H. - <b>P83</b> .....	129
Mandopoulou G. E. - <b>P149</b> .....	196	Rosa-Medina R. - <b>P13</b> .....	58
Manzoor S. - <b>P69</b> .....	115	Roschinski S. - <b>P91</b> .....	137
Marchesini M. - <b>P85</b> .....	131		
Marinelli M. - <b>P106</b> .....	152	Safavi-Naini A. - <b>I24</b> .....	29
Martín F. - <b>I22</b> .....	27	Salvatierra J. P. - <b>P117</b> .....	163
Martinez-Lahuerta V. J. - <b>P111</b> .....	157	Sanner C. - <b>P132</b> .....	179
Masuda T. - <b>P43</b> .....	88	Schioppo M. - <b>P54</b> .....	99
Mehlstäubler T. - <b>I3</b> .....	8	Schmid F. - <b>P124</b> .....	171
Merkt F. - <b>I14</b> .....	19	Schäffer S. A. - <b>P137</b> .....	184
Meyroneinc A. - <b>P160</b> .....	207	Senellart-Mardon P. - <b>I15</b> .....	20
Milani G. - <b>P81</b> .....	127	Sias C. - <b>P7</b> .....	52
Miller C. - <b>P101</b> .....	147	Singh S. K. - <b>P138</b> .....	185
Mishra D. K. - <b>P3</b> .....	48	Sowiński T. - <b>P135</b> .....	182
Mondal S. - <b>P4</b> .....	49	Spreeuw R. J. C. - <b>P104</b> .....	150
Moreau G. L. - <b>P139</b> .....	186	Sun X. - <b>P98</b> .....	144
Morsch O. - <b>P33</b> .....	78		
Mouhanna H. - <b>P11</b> .....	56	Tang Z. M. - <b>P61</b> .....	107
Mukherjee R. - <b>P39</b> .....	84	Thariq M. - <b>P88</b> .....	134
Mun J. - <b>P32</b> .....	77		
Müller H. - <b>I4</b> .....	9		
Nascimbene S. - <b>I26</b> .....	31	Valencia G. - <b>P41</b> .....	86
Natale G. - <b>P109</b> .....	155	Valtolina G. - <b>P93</b> .....	139
Nauk C. - <b>P148</b> .....	195	van Druten K. - <b>HT8</b> .....	43
Nosske I. - <b>P57</b> .....	102	Vinelli G. - <b>P154</b> .....	201
Oghittu L. - <b>P76</b> .....	122		
Pal M. - <b>P75</b> .....	121	Wang J. - <b>P19</b> .....	64
Pargoire Y. - <b>P125</b> .....	172	Wattellier S. - <b>P146</b> .....	193
Park S. E. - <b>P35</b> .....	80	Will S. - <b>I19</b> .....	24
Park Y.-H. - <b>P52</b> .....	97	Wilson J. D. - <b>P116</b> .....	162
Parke A. L. - <b>P53</b> .....	98	Wineland D. - <b>I23</b> .....	28
Peik E. - <b>I10</b> .....	15	Wirth V. - <b>P65</b> .....	111
Pelini J. - <b>P90</b> .....	136	Wolf F. - <b>P5</b> .....	50
Piest B. - <b>P74</b> .....	120	Wolf N. - <b>P49</b> .....	94
Piqué N. - <b>I7</b> .....	12	Wright S. C. - <b>HT6</b> .....	41
Poli N. - <b>P112</b> .....	158	Wunderlich Ch. - <b>P120</b> .....	167
Politi C. - <b>HT5</b> .....	40		
Preston A. - <b>P105</b> .....	151		
Pupic A. - <b>P59</b> .....	104		
Qiao M. - <b>P17</b> .....	62	Xia T. - <b>P158</b> .....	205
Qiu L. - <b>P67</b> .....	113		
Quensen M. - <b>P40</b> .....	85		
Rapol U. D. - <b>HT4</b> .....	39	Yadav P. - <b>P8</b> .....	53
Rasel E. M. - <b>P9</b> .....	54	Yamamoto S. - <b>P87</b> .....	133
Rattanasakuldilok W. - <b>P86</b> .....	132	Yao X. C. - <b>I27</b> .....	32
Rey A. M. - <b>I25</b> .....	30	Yao Z. - <b>P30</b> .....	75
Richard J. - <b>P26</b> .....	71	Ye J. - <b>I9</b> .....	14
Riley P. S. - <b>P150</b> .....	197	Yoshioka K. - <b>I13</b> .....	18
Roati G. - <b>I28</b> .....	33	Young D. J. - <b>P1</b> .....	46
Robalo Pereira C. - <b>P23</b> .....	68		
Robert P. - <b>P118</b> .....	164		
		Zaheer A. - <b>P10</b> .....	55
		Zhan M.-S. - <b>I5</b> .....	10
		Zhang C. - <b>P121</b> .....	168
		Zhang T. - <b>P62</b> .....	108
		Zhao B. - <b>I29</b> .....	34
		Zhou X. - <b>P103</b> .....	149
		Zhuang J. - <b>P126</b> .....	173

## Index of invited contributions

<b>Arndt M.</b> -I6 : <i>From Schrödinger kittens to UV spectroscopy</i> .....	<b>11</b>
<b>Cheuk L.</b> -I21 : <i>Quantum Many-Body Physics with Molecular Tweezer Arrays: From Magnon Dynamics to Spin-Squeezing</i> .....	<b>26</b>
<b>Cornell E.</b> -I1 : <i>Bose-Einstein Condensation: Exactly as I planned and not at all as I thought</i> .....	<b>6</b>
<b>Cornish S. L.</b> -I20 : <i>Dipolar interactions between ultracold RbCs molecules in magic-wavelength traps and optical tweezers</i> .....	<b>25</b>
<b>DeMille D.</b> -I2 : <i>Searches for new CP-violating physics using cold and ultracold molecules</i> .....	<b>7</b>
<b>Eikema K.</b> -I11 : <i>Alpha and helion particle charge radius difference determination with quantum-degenerate helium</i> .....	<b>16</b>
<b>Franke-Arnold S.</b> -I16 : <i>Polarisation textures of light and atoms</i> .....	<b>21</b>
<b>Hangst J. S.</b> - I12: <i>Spectroscopy of Antihydrogen: The ALPHA experiment at CERN</i> .....	<b>17</b>
<b>Ketterle W.</b> -I17 : <i>How one, two and many atoms scatter light</i> .....	<b>22</b>
<b>Koch C.</b> -I18 : <i>Quantum resonances in cold collisions</i> .	<b>23</b>
<b>Lisak D.</b> - I8: <i>High-accuracy molecular spectroscopy exploiting resonant frequencies of an optical cavity</i> .....	<b>13</b>
<b>Martín F.</b> -I22 : <i>Attosecond molecular science</i> .....	<b>27</b>
<b>Mehlstäubler T.</b> -I3 : <i>Precision Spectroscopy in Ion Coulomb Crystals and Search for New Physics</i>	<b>8</b>
<b>Merkt F.</b> - I14: <i>Precision spectroscopy of few-body atoms and molecules</i> .....	<b>19</b>
<b>Müller H.</b> -I4 : <i>Cavity-based, lattice-held atom interferometry as a new tool for precision measurement and inertial sensing</i> .....	<b>9</b>
<b>Nascimbene S.</b> -I26 : <i>Exploring quantum Hall physics with ultracold dysprosium atoms</i> .....	<b>31</b>
<b>Peik E.</b> -I10 : <i>Nuclear laser spectroscopy of the 8.4 eV transition in Th-229</i> .....	<b>15</b>
<b>Piqué N.</b> -I7 : <i>Frequency comb interferometry</i> .....	<b>12</b>
<b>Rey A. M.</b> -I25 : <i>New frontiers in quantum simulation and sensing via photon mediated interactions</i> .	<b>30</b>
<b>Roati G.</b> -I28 : <i>Vortex dynamics in strongly interacting Fermi superfluids</i> .....	<b>33</b>
<b>Safavi-Naini A.</b> -I24 : <i>New pathway to universal quantum computing and entanglement generation</i> .....	<b>29</b>
<b>Senellart-Mardon P.</b> -I15 : <i>Revisiting and exploiting spontaneous emission with solid-state artificial atoms</i> .....	<b>20</b>
<b>Will S.</b> -I19 : <i>Bose-Einstein condensation of dipolar molecules</i> .....	<b>24</b>
<b>Wineland D.</b> -I23 : <i>Quantum Computers and Raising Schrödinger's Cat</i> .....	<b>28</b>
<b>Yao X. C.</b> -I27 : <i>Correlations in homogeneous fermionic Hubbard gases: Coherence and Magnetism</i> .	<b>32</b>
<b>Ye J.</b> -I9 : <i>Scaling quantum systems for clock and fundamental physics</i> .....	<b>14</b>
<b>Yoshioka K.</b> - I13: <i>Laser cooling of positronium with a chirped laser pulse train</i> .....	<b>18</b>
<b>Zhan M.-S.</b> -I5 : <i>Cold atom interferometry in space</i>	<b>10</b>
<b>Zhao B.</b> -I29 : <i>Creation of ultracold triatomic molecules</i>	<b>34</b>

## Index of hot topic contributions

<b>Aude Craik D. P. L.</b> -HT1 : <i>Searching for new physics by measuring isotope shifts and parity violation in trapped ions</i> .....	36
<b>Bohr E. A.</b> -HT2 : <i>Observation of three and four-body interactions between momentum states in a high-finesse cavity</i> .....	37
<b>Bouloufa-Maafa N.</b> -HT3 : <i>Ionization threshold of Rb<sub>2</sub> molecule measured by the electric field-dependent Rydberg-state spectroscopy</i> .	38
<b>Cacciapuoti L.</b> -HT7 : <i>ACES in orbit</i> .....	42
<b>Hollberg L. H.</b> -HT9 : <i>Dynamic Imaging Magnetic Fields with Yb Fluorescence</i> .....	44
<b>Politi C.</b> -HT5 : <i>Two-photon cooling of calcium atoms</i> .....	40
<b>Rapol U. D.</b> -HT4 : <i>Investigating Quantum Diffusion and Localization in Atom-Optics Kicked Rotor Systems</i> .....	39
<b>Wright S. C.</b> -HT6 : <i>Magneto-optical trapping of aluminium monofluoride</i> .....	41
<b>van Druten K.</b> -HT8 : <i>Measurement of the g factor of ground-state <sup>87</sup>Sr at the parts-per-million level using co-trapped ultracold atoms</i> .....	43

# Index of poster contributions

- Abraham J. J. -P73 : Development of a Compact Cold Atom Interferometric Rotation Sensor ... [119](#)
- Ackerman Z. E. D. -P27 : Quantum Gates with Trapped Ions and Optical Tweezers ..... [72](#)
- Ajayakumar A. -P51 : High resolution laser spectroscopy towards exotic lanthanide and actinide isotopes for nuclear physics ..... [96](#)
- Arnold A. S. -P48 : Single-beam grating-chip 3D and 1D optical lattices ..... [93](#)
- Athanasakis-Kaklamanakis M. -P20 : Towards a measurement of the electron's electric dipole moment with molecules in a lattice ..... [65](#)
- Baruzzo M. -P24 : Measurement of Ground-State Hyperfine Splitting in Muonic Hydrogen: The FAMU Experiment ..... [69](#)
- Battelier B. -P66 : All optical ultracold atoms in microgravity ..... [112](#)
- Baur D. -P99 : Bandstructure of a coupled BEC-cavity system: effects of dissipation and geometry [145](#)
- Beck H. -P134 : Status of the Laser System for Cold Atom Experiments in BECCAL onboard the ISS ..... [181](#)
- Bednarski B. -P6 : Cavity-enhanced spectroscopy of  $H_2$  in a deep cryogenic regime ..... [51](#)
- Beller T. -P131 : Programmable Arrays of Rydberg Ytterbium Atoms for Quantum Computing [178](#)
- Biagioni G. -P46 : Collective light scattering in ordered 1D chains of dysprosium atoms ..... [91](#)
- Blondel C. -P15 : The quantum offset of velocity imaging-measured electron energies ..... [60](#)
- Blume D. -P77 : Laser-pulse induced helium trimer dynamics ..... [123](#)
- Bond L. J. -P156 : Quantum-enhanced sensing with spin-dependent squeezing ..... [203](#)
- Burden A. -P163 : Measurement validation and cycle slip detection on a single optical frequency comb ..... [210](#)
- Butery E. -P12 : Spectroscopic measurements of the Rydberg-surface Casimir-Polder interaction [57](#)
- Castrillo A. -P84 : Comb-locked cavity ring-down spectroscopy: combining high precision with ultra-high detection sensitivity in molecular interrogation ..... [130](#)
- Chakraborty A. -P21 : Probing Nuclear Spin-Dependent Parity-Violation in  $^{133}\text{Cs}$  Using Relativistic Coupled-Cluster Theory ..... [66](#)
- Chen S. -P38 : Excited-state magnetic properties of carbon-like calcium  $\text{Ca}^{14+}$  ..... [83](#)
- Chen Y. -P16 : Experimental Demonstration of Tunable Spin-Phonon Coupling in Trapped Ions via Optical Tweezers ..... [61](#)
- Cimmino R. T. -P63 : A dual-species optical tweezer array of Na and Cs Rydberg atoms ..... [109](#)
- Ciuryło R. -P166 : Ultra-cold Hg atoms for sensing fundamental physics ..... [213](#)
- Ciuryło R. -P167 : Isotopic effect on optical clock transition affected by cold atoms collisions [214](#)
- Cline J. R. K. -P72 : Towards scalable trapped-ion quantum computing ..... [118](#)
- Cominotti R. -P147 : False vacuum decay at finite temperatures in ferromagnetic superfluids [194](#)
- Corgier R. -P127 : Squeezing-enhanced accurate differential sensing under large phase noise ... [174](#)
- Cui J.-M. -P50 : Trapped-Ion Electric Noise Spectrum Analyzer Assisted by Optical Tweezers ..... [95](#)
- Curtis E. A. -P47 : A highly accurate  $^{171}\text{Yb}^+$  ion optical clock at NPL for metrology and tests of fundamental physics ..... [92](#)
- Cygan A. -P14 : Heterodyne cavity ring-down spectroscopy exploiting eigenmode frequencies for high-fidelity measurements ..... [59](#)
- De Natale P. -P161 : Saturated-absorption Cavity Ring-down (SCAR) Spectroscopy: Exploring the limits of Sensitivity and Precision for Molecular Detection ..... [208](#)
- De Natale P. -P96 : Mid infrared semiconductor lasers between classical and quantum operation regime [142](#)
- Dinesan H. -P79 : A portable, cost-efficient microwave spectrometer and its application to Matrix isolation spectroscopy for searching physics beyond the standard model ..... [125](#)
- Donati L. -P152 : Exploring noise-induced Fano coherence in a hot vapor atomic gas ..... [199](#)
- Dubois L. -P55 : A cavity-microscope for micrometer-scale control of atom-photon interactions ..... [100](#)
- Eriksen A. S. -P129 : Optical Cooling and Trapping of Germanium ..... [176](#)
- Fabre A. -P36 : Microscopy of density-wave ordering in strongly interacting Fermi gases ..... [81](#)
- Famà F. -P60 : Silicon Nitride microresonators for narrowband entangled photon-pair generation . [105](#)
- Fan M. -P153 : Ultra-wideband search for axionlike dark matter using precision spectroscopy of octupole-enhanced nuclei in a crystal ..... [200](#)
- Fang S.-C. -P68 : Measuring External Electric Fields Using Stark and Zeeman Effects in Rydberg-EIT Vapor Cells ..... [114](#)
- Favier M. -P95 : Improving optical lattice clock stability with Dick-noise-free architectures ..... [141](#)
- Filin D. -P31 : Calculation of polarizabilities of low-lying states of silver ..... [76](#)
- Fouka K. -P22 : Multilevel Electromagnetically Induced Transparency Cooling ..... [67](#)
- Fricke J. F. -P165 : Spin- and Momentum-Correlated Atom Pairs Mediated by Photon Exchange and Seeded by Vacuum Fluctuations ..... [212](#)
- Gaaloul N. -P130 : Quantum Sensing in Space for Fundamental Physics and Earth Observation . [177](#)
- Gajda M. -P56 : Bell correlations with multicomponent Bose-Einstein condensates ..... [101](#)
- Gao K. -P115 : Precision Spectroscopy and Nuclear Structure Parameters in  $^7\text{Li}^+$  ion ..... [161](#)
- Gaudout S. -P119 : Probing the local dispersion of  $k$ -vectors in situ with a Bose-Einstein Condensate ..... [165](#)
- Gauguet A. -P25 : Optimal Floquet state engineering for large scale atom interferometers ..... [70](#)
- Gavryusev V. -P45 : Optimal control in phase space applied to minimal-time transfer of thermal atoms in optical traps ..... [90](#)

- Giardini V. -P71 : Single Strontium Atoms in Optical Tweezer Arrays for Quantum Simulation . 117
- Goti I. -P133 : Operation of Yb optical lattice clock at sub- $\mu$ K atomic temperature and international clock comparisons ..... 180
- Gozzelino M. -P97 : Exploiting the light-shift for laser stabilization in atomic clocks ..... 143
- Gravina S. -P141 : Isotope shift spectroscopy in mercury vapors ..... 188
- Gómez-Fernández L. -P142 : Hyperfine Structure of the Aluminum Atom ..... 189
- Hahn R. -P144 : High precision mid-infrared vibrational spectroscopy with cold molecules ..... 191
- Heier J. -P70 : Collisions in a quantum gas of bosonic  $^{23}\text{Na}^{39}\text{K}$  molecules ..... 116
- Heizenreder B. -P2 : Towards continuous spectroscopy and superradiance in a strontium cavity QED system ..... 47
- Herrera-Sancho O. A. -P80 : A High-Resolution Ion Microscope to Spatially Observe Ion-Rydberg Interaction ..... 126
- Hillberry L. E. -P122 : High phasespace density of YO molecules ..... 169
- Ho M. -P151 : Cavity-Mediated Programmable Interactions for Quantum Metrology and Simulation ..... 198
- Houwman J. J. A. -P136 : Fano-shaped Feshbach resonances in ultracold dipolar spin mixtures . 183
- Huang D.-Y. -P92 : Ultrafast high-fidelity state readout of single neutral atom ..... 138
- Huang M.-Z. -P113 : Entropy transport between strongly interacting superfluids ..... 159
- Humphreys B. -P94 : Zeeman-Sisyphus Deceleration of CaF Molecules ..... 140
- Hutchinson D. A. W. -P162 : The Anderson Transition in a Symplectic Two-Dimensional Ultracold Gas ..... 209
- Jenkins R. -P82 : Measuring the Electron's Electric Dipole Moment Using Ultracold YbF Molecules 128
- Jiang J. -P114 : High-resolution spectroscopy of  $^{173}\text{Yb}^+$  ions ..... 160
- Jiang M. -P107 : Robust, rapid laser autolocking with compact radio frequency generators for laser pulse sequencing in field-deployable atom interferometers ..... 153
- Jyoti A. -P58 : Magic Wavelengths for  $^{85}\text{Rb}$  and  $^{133}\text{Cs}$  atoms based Active Optical Clocks in Visible-Near Infrared Spectrum ..... 103
- Kang S. -P100 : Laser frequency reference with a micro-fabricated Rubidium vapor cell for Doppler-free saturated absorption spectroscopy 146
- Kjær J. K. -P145 : Laser Cooling and Trapping of Silicon Atoms ..... 192
- Kocik R. R. -P102 : Sub-nanosecond 780 nm pulse generation from a continuous wave laser for ultrafast hyperfine-resolved Rydberg excitation 148
- Kristensen S. L. -P42 : Precision spectroscopy of  $^{88}\text{Sr}$  with direct readout of the  $^3\text{P}_n$  metastable states 87
- Kwong C.C. -P44 : Measurement of 477 nm magic wavelength for strontium clock transition .. 89
- Landru M. -P34 : Multi-species cold-atom interferometry for inertial measurements .. 79
- Lannig S. -P143 : Spectrally tailoring a clock laser for quantum state engineering and many-body physics in a 3D lattice clock ..... 190
- Lecomte M. -P78 : Production and stabilization of a spin mixture of ultracold dipolar Bose gases .. 124
- Lee S.-B. -P64 : Uncertainty evaluation of KRISS-AGRb-1 and development status of new atomic gravimeter toward the accuracy of below  $10\text{ nm/s}^2$  ..... 110
- Lee S. -P89 : Highly Stable Compact Optical Frequency Standard based on Modulation Transfer Spectroscopy on the  $^{87}\text{Rb D}_2$  Line ..... 135
- Lei J.-Y. -P28 : Measuring G with atom interferometry 73
- Lien Y.-H. -P164 : Development of a high-bandwidth atom interferometer for gravity sensing ... 211
- Lienhard V. -P110 : Generation of motional squeezed states for neutral atoms in optical tweezers 156
- Liu J. -P29 : Test of the gravitational redshift with single-photon-based atomic clock interferometers ..... 74
- Lombardi P. -P123 : A new machine for many-body physics investigation with dipolar quantum gases ..... 170
- Luo W. -P37 : A  $^{171}\text{Yb}$ - $^{173}\text{Yb}$  cold-atom comagnetometer ..... 82
- Mahapatra S. -P159 : Towards a strong coupling regime in Waveguide QED using slow-mode photonic crystal waveguide and cold Rb atoms 206
- Mamat B. -P108 : Mitigating Residual Electric Field Noise to Enhance the Coherence of Rydberg Atoms ..... 154
- Mancini C. -P157 : Towards a squeezed interferometer with strontium atoms in a high-finesse cavity . 204
- Mandopoulou G. E. -P149 : Photonic Interfaces for Telecommunication-band Quantum Networking with Neutral Atoms ..... 196
- Manzoor S. -P69 : Precision spectroscopy and frequency determination of the hyperfine components of the P(63) 4-4 transition of molecular iodine near 652 nm ..... 115
- Marchesini M. -P85 : Ultra-Cold Atoms Interferometry for Space Applications ..... 131
- Marinelli M. -P106 : Ultrafast imaging of ytterbium tweezer arrays ..... 152
- Martinez-Lahuerta V. J. -P111 : Robust Bragg diffraction for atom interferometers using optimal control theory ..... 157
- Masuda T. -P43 : Laser spectroscopy of the Th229 nuclear clock transition ..... 88
- Meyroneinc A. -P160 : Dissipative spin manipulation in a SU(N)-symmetric Fermi gas ..... 207
- Milani G. -P81 : Progress on cold-atoms based quantum atomic clocks at Leonardo Innovation Hub 127
- Miller C. -P101 : Exploring spin-motion models with a quantum gas of polar molecules ..... 147
- Mishra D. K. -P3 : Enhanced Sensitivity of Coherent Anti-Stokes Raman Spectroscopy via SU(1,1) Interferometry ..... 48
- Mondal S. -P4 : 3D-Printed Optical Cavity for Laser Stabilization. .... 49
- Moreau G. L. -P139 : Spin squeezing in an array of



- atomic ensembles via Rydberg dressing ... 186
- Morsch O. -P33 : Spatially resolved Rydberg Doppler thermometry of a cold gas ..... 78
- Mouhanna H. -P11 : High resolution spectroscopy of molecules confined in gas cells of sub-wavelength thickness ..... 56
- Mukherjee R. -P39 : Enhancement of Kerr Nonlinearity in Quantum Dot Molecules Via Tunneling Mechanism ..... 84
- Mun J. -P32 : Qubit control based on various transition lines of  $^{171}\text{Yb}$  atoms in optical tweezers ... 77
- Natale G. -P109 : Mode synchronization in a quantum gas with cavity-mediated interactions ..... 155
- Nauk C. -P148 : Recent advances of PTB's transportable  $\text{Al}^+$  ion clock ..... 195
- Nosske I. -P57 : Transportable strontium optical lattice clock for geodesy at the few-cm height level 102
- Oghittu L. -P76 : Confinement induced resonances in alkali – alkaline earth atom mixtures ..... 122
- Pal M. -P75 : Performance Comparison of Dual Comb Spectrometers with MHz and GHz Repetition Rate ..... 121
- Pargoire Y. -P125 : Continuous-wave superradiant laser based on a continuous cold atomic beam . 172
- Park S. E. -P35 : Improvement of Short-Term Stability in a Compact Laser-Cooled Rb Atomic Clock . 80
- Park Y.-H. -P52 : Cavity design simulation to reduce cavity-related errors in atomic fountain clocks 97
- Parke A. L. -P53 : Long optical cavity storage time and active RAM cancellation towards frequency stabilisation at  $1 \times 10^{-18}$  ..... 98
- Pelini J. -P90 : Exploiting high-sensitivity and resolution in cavity-enhanced photoacoustic sensors ..... 136
- Piest B. -P74 : Implementation of Delta-Kick squeezing in an atom interferometer ..... 120
- Poli N. -P112 : Progress towards atom interferometry using large momentum transfer UV transitions in ultra-cold cadmium ..... 158
- Preston A. -P105 : A compact quantum inertial sensor using atom interferometry ..... 151
- Pupic A. -P59 : Towards a spin-squeezing-enhanced atom interferometer in an optical cavity .. 104
- Qiao M. -P17 : Realization of a doped quantum antiferromagnet with dipolar tunnelings in a Rydberg tweezer array ..... 62
- Qiu L. -P67 : A High-Data-Rate Fermionic Quantum Simulator in Optical Lattices ..... 113
- Quensen M. -P40 : Hong-Ou-Mandel interference of more than 10 indistinguishable atoms ..... 85
- Rasel E. M. -P9 : Second-long light-pulse interferometry at pKs ..... 54
- Rattanasakuldilok W. -P86 : Ultracold caesium radioisotopes and isomers for nuclear magnetic octupole moment studies ..... 132
- Richard J. -P26 : Absolute Quantum Gravimetry in the Field ..... 71
- Riley P. S. -P150 : Evanescent light – matter interaction in an integrated MEMS – nanophotonic vapor cell ..... 197
- Robalo Pereira C. -P23 : Optical tweezer optimisation for trapped-ion quantum simulation ..... 68
- Robert P. -P118 : Optically dressed three-level coherence in neutral bosonic alkaline-earth-like species ..... 164
- Robinson-Tait J. -P128 : The Spectroscopic Investigation of Carbon Clusters in a Thermal Source ..... 175
- Rodewald J. -P140 : Progress towards a new search for time-variation of the proton-to-electron mass ratio with a molecular lattice clock ..... 187
- Roe T. H. -P83 : A Momentum State Quantum Computer ..... 129
- Rosa-Medina R. -P13 : Developing a quantum gas microscope with programmable lattices ..... 58
- Roschinski S. -P91 : Towards entanglement generation in a cavity coupled atomic array ..... 137
- Salvatierra J. P. -P117 : Current Advances in the Strontium Optical Lattice Clock and Development of a Cavity-Enhanced System at INRiM ..... 163
- Sanner C. -P132 : Zero-contrast clock interferometry .. 179
- Schioppo M. -P54 : Ultrastable lasers at NPL with fractional frequency instability below  $10^{-16}$  . 99
- Schmid F. -P124 : Quantum logic spectroscopy of the hydrogen molecular ion ..... 171
- Schäffer S. A. -P137 : Photon statistics in a steady-state superradiant laser ..... 184
- Sias C. -P7 : Metastable two-dimensional Coulomb crystals ..... 52
- Singh S. K. -P138 : Paraxial quantum fluid of light in cold atomic cloud ..... 185
- Sowiński T. -P135 : Three-component few-fermion mixtures in one-dimensional geometry .... 182
- Spreeuw R. J. C. -P104 : Parallel rearrangement of single atoms with an SLM for quantum simulation ..... 150
- Sun X. -P98 : High-precision optical frequency measurements: supporting UK industry and academia at NPL ..... 144
- Tang Z. M. -P61 : Study on the clock-line sideband cooling of Yb atoms ..... 107
- Thariq M. -P88 : How to Generate XUV Frequency Combs Without Enhancement Resonators? ... 134
- Valencia G. -P41 : Towards quantum limited milligram scale optomechanics ..... 86
- Valtolina G. -P93 : Towards a quantum gas with multiple long-range interactions ..... 139
- Vinelli G. -P154 : Advancing Anti-Matter-Wave Interferometry: Design and Implementation of Techniques for Gravity Measurements on Positronium Atoms ..... 201
- Wang J. -P19 : Precision spectroscopy of CO for gas metrology ..... 64
- Wattellier S. -P146 : Superfluid Fraction in an Interacting Spatially Modulated Bose-Einstein Condensate ..... 193
- Wilson J. D. -P116 : Universal gate set for optical lattice based atom interferometry ..... 162
- Wirth V. -P65 : Precision Spectroscopy of the Fine-Structure in the  $a^3\Sigma_u^+(\nu=0)$  and  $c^3\Sigma_g^+(\nu=4)$  States of the Helium Dimer ..... 111
- Wolf F. -P5 : Quantum logic control of transition metal and molecular ions ..... 50
- Wolf N. -P49 : Bose-Einstein Condensation of Photons in Variable Potentials ..... 94

- Wunderlich Ch.** -P120 : *Fast, robust and laser-free universal entangling gates for trapped-ion quantum computing* ..... 167
- Xia T.** -P158 : *Towards non-destructive microwave detection of magnetically guided ultracold atoms* ..... 205
- Yadav P.** -P8 : *High precision measurement of atom number in a mesoscopic cold atomic ensemble using fluorescence imaging* ..... 53
- Yamamoto S.** -P87 : *First observation of Muonium  $1S$ - $2S$   $F=0 \rightarrow F'=0$  transition at J-PARC* 133
- Yao Z.** -P30 : *Microwave spectroscopy of ultracold sodium least-bound molecular states* ..... 75
- Young D. J.** -P1 : *Exploring correlated hopping along a synthetic dimension in a strontium cavity QED system* ..... 46
- Zaheer A.** -P10 : *Discrete time crystals with bouncing potassium Bose-Einstein condensates* ..... 55
- Zhang C.** -P121 : *Investigation of isotope shifts and Stark shifts in the strontium Rydberg state via  $5s^2\ ^1S_0 \rightarrow 5s5p\ ^1P_1^0 \rightarrow 5p_{1/2}5p_{1/2} \rightarrow 4d_{3/2}n\ell_j$  ( $n^* = 39.4$ )* . 168
- Zhang T.** -P62 : *ECNU Yb optical lattice clocks with both instability and systematic uncertainty below  $5 \times 10^{-18}$*  ..... 108
- Zhou X.** -P103 : *Realizing a spatially correlated lattice interferometer* ..... 149
- Zhuang J.** -P126 : *Probing the interaction energy of two  $^{85}\text{Rb}$  atoms in an optical tweezer via spin-motion coupling* ..... 173
- de Léséleuc S.** -P18 : *Measurement and feedforward correction of the fast phase noise of lasers* . 63





UNIVERSITÀ  
DEGLI STUDI  
FIRENZE

Dipartimento  
di Fisica e  
Astronomia